INELASTIC DESIGN AND EXPERIMENTAL TESTING OF COMPACT AND NONCOMPACT STEEL GIRDER BRIDGES

Prepared For
MISSOURI DEPARTMENT OF TRANSPORTATION

By
Michael G. Barker
Bryan A. Hartnagel
Charles G. Schilling
Burl E. Dishongh

April 1997

in cooperation with
U.S. Department of Transportation
Federal Highway Administration

TECHNICAL REPORT STANDARD TITLE PAGE

1. Report No.	2. Government Accession No.	3. Recipient's Catalog No.
MCHRP 97 – 4		

4. Title and Subtitle	5. Report Date
Longitudinal Restraint Response of Existing Bridge Bearings	May 1997
	6. Performing Organization Code

7. Author(s)	8. Performing Organization Report No.
M.G. Barker and B.A. Hartnagel	

9. Performing Organization Name and Address	10. Work Unit No.
University of Missouri – Columbia Civil Engineering Department E2509 Engineering Building East Columbia, MO 65211	11. Contract or Grant No. SPR 1997 57

12. Sponsoring Agency Name and Address	13. Type of Report and Period Covered
Missouri Department of Transportation 105 West Capital Avenue P.O. Box 270 Jefferson City, MO 65102	14. Sponsoring Agency Code

15. Supplementary Notes

16. Abstract

Sixteen Type D bridge bearings were cyclically tested to determine the bearing response to vertical and simulated longitudinal loads. The purpose of the tests is to examine the load-deformation characteristics and energy dissipation capabilities of bearings that have been in service for many years. The results are to be used to determine if existing in-place bearings may be utilized in seismic retrofitting of earthquake susceptible bridges.

The bearings were cycled 1.75 in. each direction 40 times in the "as received" state. After this initial test, another 40 cycle test was conducted. The desired friction force-deformation hysteretic loops were determined from the net horizontal force-deformation test results. The cycles were applied in a sinusoidal manner in deflection control with a 4 second period to simulate dynamic demand on the bearing.

A coulomb (dry) friction coefficient was calculated for each bearing. Although the bearing responses were not rectangular (due to deterioration in the bearings), an approximate coefficient of friction was determined.

Four of the bearings were tested statically to failure to examine the limit state response. The ultimate limit tests produced horizontal load-deformation data. The horizontal force was applied slowly in deflection control (8 in. in 6 minutes) while acquiring data until failure. The modes of failure were slipping over the anchor rods and separation of the bearing pin from the seat. The ultimate bearing tests showed that all four bearings were able to move over 5 inches longitudinally prior instability.

17. Key Words	18. Distribution Statement
Bearings, Bridges, and Dynamic Testing	No Restrictions

19. Security Classif. (of this report)	20. Security Classif. (of this page)	21. No. of Pages	22. Price
Unclassified	Unclassified	51	

Form DOT F 1700.7 (8-69)

ABSTRACT

Inelastic design of steel girder bridges offers the potential for significant cost savings because it accounts for the true strength of the bridge, which is often considerably above that predicted by the elastic or pseudo-plastic procedures used in present bridge specifications. However, current inelastic design procedures are only applicable to bridges comprising compact sections. The objectives of this research are to (1) propose new comprehensive and practical inelastic design procedures that allow compact and noncompact sections, (2) experimentally verify inelastic limit state behavior with large-scale continuous span tests of composite girders, and (3) examine the moment-rotation behavior of compact and noncompact pier sections.

The inelastic behavior of composite and noncomposite steel girder bridges subject to highway loadings, and limit states related to this behavior, are discussed. In single continuous-span girders, local yielding at various locations causes plastic rotations at these locations and results in inelastic redistribution of moments. The plastic rotations cause permanent moments and deflections that remain after the loading has been removed. These moments are called redistribution moments or automoments. In multigirder continuous-span bridges, local yielding causes inelastic redistribution of moments in both the longitudinal and lateral directions.

The strength and permanent-deflection limit states used in the LRFD inelastic design bridge specifications are summarized, and new simplified inelastic procedures that satisfy these limit states are proposed. Shakedown is appropriately used to define strength under moving loads. The permanent-deflection limit state can be satisfied either by limiting positive-bending stresses after inelastic redistribution of moments or by limiting calculated permanent deflections directly. The simplified procedures proposed to satisfy the two limit states apply to both compact and noncompact sections. They utilize elastic moment envelopes and do not require successive loadings, iterative procedures, or simultaneous equations. Corresponding provisions and commentary that could be incorporated into the LRFD bridge specifications are presented.

Experimental testing of continuous span girders and girder components were conducted to verify inelastic design limits and investigate inelastic behavior. A compact three span composite girder and a noncompact two-span composite girder were tested subjected to simulated moving

truck loads. Experimental results are compared to design limit states, along with discussion on general inelastic behavior.

Various girder components were tested to develop and verify moment-inelastic rotation relations. A total of six composite and noncomposite, compact and noncompact girder components were tested. One component test was subjected to simulated moving loads to examine slip between the concrete deck and the steel beam.

The results from the tests performed in this project support the development and verify the procedures of the proposed LRFD inelastic design provisions for bridges comprising noncompact girders. The limit state design levels were satisfied and the overall behavior of the girders met expectations.

ACKNOWLEDGMENTS

The authors gratefully acknowledge the sponsors of this work. These include the National Science Foundation, the American Iron and Steel Institute, the American Institute of Steel Construction, the Missouri Transportation Department, Bethlehem Steel, Nucor-Yamato Steel, US Steel, the University of Missouri - Columbia College of Engineering, St. Louis Screw & Bolt Co., Delong's Inc., and Stupp Bros. Inc.

Also deserving thanks are undergraduate and graduate students who worked on this project including: David C. Weber, Kara C. Unterreiner, Derek A. White, Paul C. Boenisch and Keith A. Hutton. The project could not have been a success without the excellent services of the University of Missouri - Columbia research technicians: Clyde H. Cassil, Rick J. Wells, Richard L. Oberto and Orral "Rex" S. Gish.

TABLE OF CONTENTS

LIST OF TABLES

LIST OF FIGURES

CHAPTER ONE

INELASTIC DESIGN AND TESTING OF STEEL GIRDER BRIDGES

1.1 INTRODUCTION

For many years, research on the inelastic behavior of buildings was conducted in the United States and abroad (ASCE 1971 and Beedle 1958). This research showed that the full strength of structures, especially statically indeterminate structures, can only be determined by considering inelastic behavior. Suitable procedures for calculating this strength for buildings were developed and included in the American Institute of Steel Construction (AISC) specifications (AISC 1993). As a result, plastic-design methods for buildings are now well established. Although the basic principles on which these methods are based apply to bridges as well as buildings, two significant differences must be considered when applying the methods to bridges. First, buildings can be safely designed for static loads, but bridges must be designed for moving loads. Second, buildings can generally utilize compact members while bridges often utilize noncompact girders with slender webs. Because of these differences, the plastic-design procedures for buildings are not sufficient for bridges.

The increase in strength provided by inelastic behavior was first incorporated into the American Association of State Highway and Transportation Officials (AASHTO) specifications for highway bridges in a limited empirical way. Specifically, two simple provisions were incorporated into the Load Factor Design (LFD) specifications (AASHTO 1973). First, the elastic moment caused at a compact section by the design loads was permitted to equal the plastic-moment capacity of the section rather than being limited to the yield-moment capacity. Second, 10% of the peak negative elastic moments in continuous-span girders were permitted to be shifted to positive-bending regions before the bending strengths at these locations were checked. This second provision was intended to account, in an approximate way, for the redistribution of moments that actually occurs due to inelastic action.

Comprehensive inelastic design procedures were first permitted for highway bridges with the adoption of guide specifications for Alternate Load Factor Design (ALFD) in 1986 (AASHTO 1986). These design procedures, which were originally called autostress design procedures, are applicable only to compact sections. They specify a strength check by the plastic-design mechanism method at Maximum Load and a permanent-deflection check by inelastic procedures at Overload. In this latter check, yielding is allowed to occur at peak negative-moment locations (piers) and the resulting redistribution moments (automoments) are calculated. The stresses in positive-bending regions due to the combined applied and redistribution moments are limited to 95% and 80% of the yield stress in composite and noncomposite girders, respectively. These same stress limits are imposed at both the positive- and negative-bending locations in the LFD specifications (AASHTO 1992) and are assumed to prevent objectionable permanent deflections. In 1994, the inelastic design procedures from the ALFD guide specifications (AASHTO 1986) were incorporated into the new AASHTO Load and Resistance Factor Design (LRFD) bridge specifications (AASHTO 1994) with minor modifications and additions.

In 1993, inelastic rating procedures were proposed for highway bridges (Galambos et. al. 1993). These procedures utilize the same rating vehicles and load and resistance factors as the alternative load factor rating procedures adopted in 1989 guide specifications (AASHTO 1989), but define the strength limit state as either shakedown (deflection stability) or a specified maximum permanent deflection.

1.2 OBJECTIVES

Research advances on structural behavior in bridge design clearly indicate the need for generalized inelastic design procedures which include all possible girder cross-sectional shapes, both compact and noncompact. Inelastic design offers the potential for significant cost savings because they account for the true strength of the bridge, which is often considerably above that predicted by the elastic or pseudo-plastic procedures used in present bridge specifications. The objectives of this research are to (1) propose new comprehensive and practical inelastic design procedures that allow compact and noncompact sections, (2) experimentally verify inelastic limit state behavior with large-scale continuous span tests of composite girders, and (3) examine the moment-rotation behavior of compact and noncompact pier sections.

1.3 REPORT ORGANIZATION

Chapter 3 contains the background and basis for present and proposed inelastic design provisions. It is a clear and detailed account of past research and engineering practice and current inelastic design capabilities. The chapter presents the development of the proposed LRFD inelastic design provisions included in the Appendix. A quick reference to the proposed procedures in found in Section 3.5.

Chapter 3 describes the inelastic behavior of highway bridges under moving loads including (a) the formation and significance of redistribution moments and permanent deflections, (b) shakedown related to sequential loading and/or dynamic yielding, and (c) methods of calculating redistribution moments, ultimate strength, and shakedown. Procedures for calculating redistribution moments and permanent deflections are described. The mechanism method of calculating ultimate strength, and the related concepts of effective plastic moment and rotation capacity, are discussed. Simplified procedures for checking shakedown in bridges are developed. Present, and proposed new, procedures for satisfying the strength and permanent-deflection limit states are described. Unlike the present inelastic procedures, the proposed new inelastic procedures apply to both compact and noncompact sections. They are simpler than the present procedures. Corresponding provisions and commentary suitable for inclusion in the LRFD bridge specifications are included in the Appendix.

Chapters 4 and 5 design bridges comprising compact and noncompact sections according to current and proposed inelastic provisions, respectively. The chapters compare current LRFD inelastic design, LFD elastic design with or without the 10% redistribution of negative pier moments, LRFD elastic design with or without 10% redistribution of negative pier moments, and proposed LRFD inelastic design methods. A quick reference to these comparisons are found in Table 4.2 for the compact girder and Table 5.2 for the noncompact girder.

Chapters 4 and 5 describe the modeling and testing of compact and noncompact continuous girders. The compact girder (Chapter 4) was a three-span composite girder and the noncompact girder (Chapter 5) was a two-span composite girder. Both girders were subjected to simulated moving truck loads from elastic loading to collapse. Experimental results are compared to design limit states, along with discussion on general inelastic behavior.

Various girder components were tested to develop and verify moment-inelastic rotation relations. Chapter 4 contains details of four components tests, three composite and one

noncomposite similar to the compact bridge girder section, and in Chapter 5 are two component tests, one composite and one noncomposite, similar to the noncompact girder section. One component test presented in Chapter 4 subjected the specimen to simulated moving loads to examine slip between the concrete deck and the steel beam.

Chapter 2 presents the summary and conclusions of this research. It discusses the comparison of current and proposed bridge design provisions. The experimental verification of proposed inelastic design procedures are summarized.

The Appendix contains the proposed LRFD inelastic design provisions that are meant to replace Section 6.10.11 of the current LRFD Bridge Design Specifications.

CHAPTER TWO

SUMMARY AND CONCLUSIONS

2.1 INTRODUCTION

Inelastic steel bridge design procedures account for the reserve strength inherent in multiple-span steel girder bridges by allowing redistribution of negative pier region elastic moments to adjacent positive moment regions. The redistribution causes slight inelastic rotation at the interior pier sections, residual moments in the beam, and some permanent residual deflection. After the redistribution, the structure achieves shakedown: deformations stabilize and future loads are resisted elastically.

The AASHTO Alternate Load Factor Design (ALFD) method allows inelastic design for bridges comprising compact sections. ALFD is incorporated in the AASHTO Load and Resistance Factor Design (LRFD) Bridge Design Specification for inelastic design of steel girder bridges.

Inelastic design procedures allow the designer flexibility and the possibility of more economical designs by decreasing member sizes and eliminating cover plates and flange transitions at negative moment regions. However, current provisions apply only to compact steel bridges. Expanding inelastic design provisions to include noncompact sections is desirable because of the wide use of plate girders with thin webs. Previous research has shown that noncompact girders have predictable moment-rotation behavior that can be incorporated into inelastic design provisions. However, even though the analytical tools exist, large-scale testing is necessary to validate theoretical engineering practice.

The objectives of this research were to (1) propose new comprehensive and practical inelastic design procedures that allow compact and noncompact sections, (2) experimentally verify inelastic limit state behavior with large-scale continuous span tests of

composite girders, and (3) examine the moment-rotation behavior of compact and noncompact pier sections.

2.2 INELASTIC DESIGN PROVISIONS

Currently, bridges can be designed by several methods according to AASHTO. The Load Factor Design (LFD) method can be employed to design bridges using elastic limits with (compact) or without (noncompact) non-linear redistribution of negative pier moments. The Load and Resistance Factor Design (LRFD) method can be used to design bridges using elastic limits with (compact) or without (noncompact) non-linear redistribution of negative pier moments or by inelastic design provisions. The Alternate Load Factor Design (ALFD) provisions, the forerunner of inelastic design, have been incorporated into the current LRFD inelastic design method. This research proposes LRFD inelastic design provisions (located in Appendix) meant to replace the current LRFD inelastic design sections. The proposed provisions allow the use of compact and noncompact girder sections. The proposed LRFD inelastic design provisions are also greatly simplified compared to current inelastic design methods. The justification for inelastic design, the background to address inelastic design concerns, and the simplified formulation are presented in Chapter 3.

In comparing the proposed inelastic design provisions to the current elastic and inelastic methods, the following conclusions can be made.

For bridges comprising compact shapes (shown in Table 4.2):

- The Service II limit controlled for LRFD methods and the Overload controlled for the LFD method (both serviceability limit states).
- The proposed LRFD inelastic design and the current LRFD inelastic design methods both result in the same design load. The Service II limit for the two methods are near identical, although the proposed method has simplified the procedures greatly.
- The LFD and the LRFD with the redistribution of moments are slightly less. However, with bridges comprising compact sections, the designs should not differ greatly since the LFD and the LRFD with the

redistribution of moments accounts for the ability of the girder to redistribute the pier moments with some inelastic action.

The proposed LRFD inelastic design procedures require the same amount of engineering effort than the other elastic methods and they are less work than the current LRFD inelastic design procedures. The simplified provisions have removed iterative procedures and/or graphical solutions that have plagued past inelastic design efforts.

For bridges comprising noncompact shapes (shown in Table 5.2):

The Service II limit state controlled for the proposed LRFD inelastic design, but the Strength I (Maximum Load for LFD) controlled for the remaining methods. The elastic methods limit the stress at the pier to $0.95F_y$ subject to factored loads while the proposed LRFD inelastic method has no stress limit at the pier and allows redistribution.

The elastic methods (LFD and LRFD) have much lower capacities than the proposed LRFD inelastic design method. The ability to redistribute large negative pier moments, coupled with section capacities exceeding the yield moment, results in an efficient structure used to its limit state capacity. Elastic methods don't account for either component of this reserve strength.

For bridges comprising noncompact sections, the proposed LRFD inelastic design methods should have significantly higher design capacities than bridges that are forced to remain elastic at factored loads. The available stress remaining for live load is small and, when the total stress must remain elastic, the truck capacity is low compared to an inelastic method that allows some of this live load stress to be redistributed to other areas.

The proposed LRFD inelastic design procedures require the same amount of engineering effort that the other elastic methods require. The simplified provisions have removed iterative procedures and/or graphical solutions that have plagued past inelastic design efforts.

2.3 IMPACT OF PROPOSED LRFD INELASTIC DESIGN PROVISIONS

Inelastic design procedures, currently limited to bridges comprising compact sections, offer the potential for significant cost savings by accounting for a better estimate of the true strength and behavior of the bridge. Inelastic limits can show a significant increase of capacity over that predicted by conventional elastic or pseudo-plastic procedures used in present bridge specifications. Bridge safety is not compromised because, after the structure has experienced several passes of the design limit loads, future loads are resisted elastically. Furthermore, inelastic techniques permit greater design flexibility such as optimizing material use as is done in plastic design procedures, eliminating cover plates and flange transitions, and quantifying the redistribution characteristics for more consistent safety considerations.

The Appendix contains proposed LRFD inelastic design provisions to replace the current LRFD inelastic design sections. The proposed provisions allow the use of compact and noncompact girder sections, unlike current procedures that are limited to compact sections. Limiting noncompact sections to the yield capacity with no redistribution of force effects unnecessarily ignores the reserve strength of the girder.

The proposed LRFD inelastic design provisions are also greatly simplified compared to current inelastic design methods. Engineers need no longer compare a "moment-inelastic rotation" curve with a "continuity relation" to determine an "inelastic rotation" and a "residual moment." The simplified procedures are no more difficult than current elastic provisions (although one can also use more refined analyses) and lend themselves easily to computerization.

2.4 EXPERIMENTAL VERIFICATION

Experimental testing of continuous span girders and girder components were conducted to verify inelastic design limits and investigate inelastic behavior. Chapters 4 and 5 describe the modeling and testing of compact and noncompact continuous girders. The compact girder (Chapter 4) was a three-span composite girder and the noncompact girder (Chapter 5) was a two-span composite girder. Both girders were subjected to

simulated moving truck loads from low elastic loading to collapse. Experimental results are compared to design limit states, along with discussion on general inelastic behavior.

Various girder components were tested to develop and verify moment-inelastic rotation relations. Chapter 4 contains details of four components tests, three composite and one noncomposite, similar to the compact bridge girder section. In Chapter 5 are two component tests, one composite and one noncomposite, similar to the noncompact girder section. One component test presented in Chapter 4 subjected the specimen to simulated moving loads to examine slip between the concrete deck and the steel beam.

2.4.1 Compact Girder Tests

The one-half scale three-span continuous composite girder was subjected to simulated moving HS20 loading. The girder was designed and modeled to represent an interior girder of the current LRFD inelastic design bridge in the design comparisons above. Figures 4.8 and 4.16 are photos of the test structure during testing. After the simulated moving load tests, the girder was subjected to modeled ultimate loading to determine the load-deflection characteristics. Chapter 4 presents experimental results at the design limit states, during inelastic loading, and during the collapse test. The following conclusions can be made:

The behavior of the model behaved according to elastic structural theory. The elastic deflections and stresses (strains) matched well with that predicted.

The measured Service II load level stresses (strains) met the Service II stress criteria. The fatigue stresses also met design criteria.

The compact pier section redistributed moments and there were permanent residual deflections approximately according to predictions, especially when considering small inelastic rotations at the positive moment region. The current and proposed LRFD inelastic design provisions refer the engineer to ways of incorporating the positive moment region in analyses if deformations are important.

The plastic collapse test showed great ductility prior to collapse. The total deflection being approximately 1/33 of the span length.

Strength I loads did not control the design. However, the experimental and the theoretical collapse loads were within 1%. This means the girder could withstand the theoretical Strength I loading.

The pier section suffered moment unloading during the collapse test. This is in accordance with the design specification for a section which is compact yet not ultra-compact.

During the pier section moment unloading, the positive moment region had significant moment loading due to the redistribution of moments from the pier section. The positive region eventually failed by concrete crushing.

The girder components were tested to develop and verify moment-inelastic rotation relations. They were tested in a double cantilever manner to model the pier section of a continuous span girder. Chapter 4 contains moment-inelastic rotation relations for the four girder components. The experimental results are compared to the current LRFD inelastic design moment-inelastic rotation relations. The following conclusions can be made:

The experimental moment-inelastic rotation relation met or exceeded that predicted by the current LRFD inelastic design relation. Also the design relation modeled the test results well in magnitude and behavior.

The noncomposite component had ultra-compact flanges and web. The section was able to maintain the plastic moment capacity well into the inelastic range.

The other components had ultra-compact flanges, but only compact webs. Therefore, by theory, the moment should have, and did, decrease with increasing inelastic rotation. The slope of the moment unloading was near identical to that predicted by the current LRFD inelastic design provisions.

The girder component that was tested subjected to simulated moving loads did not show any indication of slip between the concrete deck and the

steel beam. This puts some concern to rest related to stiffness and strength degradation during strain reversals at the interface.

2.4.2 Noncompact Girder Tests

The one-third scale two-span continuous composite girder was subjected to (adjusted) simulated moving HS20 loading. The girder was designed and modeled to represent an interior girder of the proposed LRFD inelastic design bridge in the design comparisons above. Figures 5.8 and 5.14 are photos of the structure during testing. During large simulated moving load tests, the girder suffered plastic collapse. Chapter 5 presents experimental results at the design limit states and during inelastic loading. The following conclusions can be made:

The behavior of the model behaved according to elastic structural theory. The elastic deflections and stresses (strains) matched well with that predicted.

The measured Service II load level stresses (strains) nearly met (within 12%) the Service II stress criteria. This bridge was a very efficient design where both the pier and positive moment region were at design limits. Thus, the 12% overstress is deemed adequate, especially considering design philosophy. The fatigue stresses met design criteria.

The noncompact pier section redistributed moments and there were permanent residual deflections approximately according to predictions, although the simplified proposed LRFD inelastic design procedures do not require the determination of deflections. The current and proposed LRFD inelastic design provisions refer the engineer to ways of calculating deformations if deemed important.

The experimental moment at the Service II and Strength I levels exceeded the predicted. The proposed LRFD inelastic design provisions use a M_{pe} at each limit state and there is no need to relate moment to inelastic rotation. M_{pe} depends on the web and flange slenderness ratios.

The girder obtained shakedown above the theoretical incremental collapse level. The pier section maintained higher than predicted moments at large rotations.

The girder resisted well above theoretical collapse loads during the last cycle of loads. Again, the pier section maintained higher than predicted moments at large rotations.

Rotations at the limit states were within the boundaries necessary for redistribution according to Chapter 3.

The girder components were tested to develop and verify moment-inelastic rotation relations. They were tested in a double cantilever manner to model the pier section of a continuous span girder. Chapter 5 contains moment-inelastic rotation relations for the two girder components. The experimental results are compared to the proposed LRFD inelastic design effective moment capacities at the different limit states. The following conclusions can be made:

The experimental moment-inelastic rotation relations met or exceeded the effective plastic moments predicted by the proposed LRFD inelastic design procedures.

The noncomposite component had ultra-compact flanges and web. The section was able to maintain the plastic moment capacity well into the inelastic range.

The composite component had ultra-compact flanges, but noncompact webs. Therefore, by theory, the moment should have, and did, decrease with increasing inelastic rotation. However, the moment exceeded the expectations from the design predictions.

2.5 SUMMARY

Inelastic design procedures allow the designer flexibility and the possibility of more economical designs by decreasing member sizes and eliminating cover plates and flange transitions at negative moment regions. Expanding inelastic design provisions to include noncompact sections is desirable because of the wide use of plate girders with thin webs.

The proposed LRFD inelastic design procedures in the Appendix allow the use of compact and noncompact girder sections. The proposed LRFD inelastic design provisions are also greatly simplified compared to current inelastic design methods. They are also no harder than the LFD or LRFD methods when using the 10% redistribution of pier moments. The tests performed in this project support the development and verify the procedures of the proposed inelastic design provisions for bridges comprising noncompact girders. The limit state design levels were satisfied and the overall behavior of the girders were good.

CHAPTER THREE

INELASTIC DESIGN PROCEDURES AND SPECIFICATIONS

3.1 INTRODUCTION

The present report describes the inelastic behavior of highway bridges under moving loads including (a) the formation and significance of redistribution moments and permanent deflections, (b) shakedown related to sequential loading and/or dynamic yielding, and (c) methods of calculating redistribution moments, ultimate strength, and shakedown. The unified autostress (Schilling 1989, 1991 and 1993), residual-deformation (Dishongh 1990 and 1992, and Dishongh and Galambos 1992), and beam-line methods (Carskaddan et. al. 1982, Disque 1964 and Haaijer et. al. 1987) of calculating redistribution moments and permanent deflections are described. The mechanism method of calculating ultimate strength, and the related concepts of effective plastic moment and rotation capacity, are discussed. Simplified procedures for checking shakedown in bridges are developed. Present, and proposed new, procedures for satisfying the strength and permanent-deflection limit states are described. Unlike the present inelastic procedures, the proposed new inelastic procedures apply to both compact and noncompact sections. They are simpler than the present procedures. Corresponding provisions and commentary suitable for inclusion in the LRFD bridge specifications are included.

3.2 INELASTIC BEHAVIOR

3.2.1 Single Girders

3.2.1.1 Simple Spans

3.2.1.1.1 Noncomposite Sections

Load-Deflection Relationship

A typical load-deflection curve for a steel simple-span beam or girder loaded by a concentrated load at midspan is shown in Figure 3.1. Due to residual stresses, yielding starts below the load P_y, corresponding to the theoretical yield moment. This yielding causes plastic deflection, which adds to

the theoretical elastic deflection to produce the actual total deflection as shown. The loading continues to increase to a maximum value P_{max}, which may be larger or smaller than the load P_p, corresponding to the theoretical plastic moment, M_p. If the section is compact, P_{max} significantly exceeds P_p due to strain hardening and the curve remains above P_p over a considerable range of deflection. If the section is noncompact, P_{max} usually remains below P_p throughout the loading. The slope of the descending portion of the curve depends on the slenderness of the flange and web and on the spacing of lateral supports for the compression flange. The descending curve continues indefinitely as local buckling causes major distortions of the cross section and/or lateral buckling causes large permanent lateral deflections, but cracking or fracture does not occur.

If the load is fully removed after yielding has started, the resulting unloading curve is usually parallel to the elastic loading curve as indicated by the light line in Figure 3.1 (If the imposed deflection is high enough to cause large permanent distortions of the cross section this may not be true). A permanent deflection, but no moment, remains after all load is removed. If load is applied again one or more times, no additional yielding will occurs, and the loading will follow up and down the original unloading curve unless the original maximum applied load is exceeded. If the original load is exceeded, the additional load follows the solid curve, which is a continuation of the original loading curve, and unloading from this higher load again follows a line parallel with the original elastic loading curve.

Dynamic Yielding Effects

The preceding discussion is based on the assumption that the loading is applied at a very slow rate in the inelastic range, or that the deflection and load are allowed to stabilize after each load or deflection increment in this range. If a deflection increment is rapidly applied and then held constant in the inelastic range, the load will at first exceed the theoretical value indicated by the curve in Figure 3.1, but will gradually decrease to the theoretical value as it stabilizes after a few minutes. This behavior occurs because yielding (inelastic straining) does not occur instantaneously, but instead requires a small amount of time.

Moment-Rotation Relationship

The moment-rotation relationship for the simple-span beam or girder is shown in Figure 3.2, again for the stabilized yield condition. The total rotation is equal to the sum of the slopes at the two ends of the member (inflection points) and is composed of elastic and plastic components. Elastic

rotation occurs along the entire length of the member; the total elastic rotation for a prismatic member is equal to

$$\Theta_e = \frac{PL^2}{8EI} \tag{3.1}$$

where P is the midspan load, L is the span length, I is the moment of inertia, and E is the modulus of elasticity.

The plastic rotation, in contrast, is concentrated in a short yield region at midspan and is usually determined by subtracting the calculated elastic rotation from the measured total rotation in a test. If the load is fully removed in the inelastic range, the unloading curve for total rotation is again parallel with the elastic loading curve and a permanent rotation remains. On the plastic-rotation plot, this unloading corresponds to a vertical line at a plastic rotation equal to the permanent rotation. Thus, the plastic rotation caused by a given load is equal to the permanent rotation that remains after the load has been removed. No additional plastic rotation occurs unless a higher load is applied later.

The shape of the ascending portion of a plastic-rotation curve is controlled by the spread of yielding through the cross section and along the length of the member. This depends on the initial pattern of residual stresses and on the proportions (ratio of flange area to web area, etc.) of the cross section. The shape of the descending portion depends primarily on the compression-flange slenderness, web slenderness, and compression-flange bracing spacing. The behavior of a simple-span member under distributed load is similar to that under a concentrated load, but the plastic rotation is spread over a longer yield region.

Although plastic rotation actually occurs over a finite yield length, it is usually assumed to occur at a single cross section (infinitesimal length) under the load to simplify calculation procedures for plastic design (ASCE 1971 and Beedle 1958). Thus, the member is assumed to be elastic over its entire length and to have all of the plastic rotation concentrated in a single angular discontinuity. This discontinuity is equivalent to the angular discontinuity created by cutting the ends of two beams slightly off square and then welding them together end to end. Thus, plastic rotations caused by yielding have the same effect on subsequent structural behavior as angular discontinuities (kinks) that could be built into a member by slight angular mismatches at splices.

3.2.1.1.2Composite Sections

Positive Bending

The inelastic behavior of composite beams and girders in positive bending is similar to that discussed earlier for noncomposite members, but there are some significant differences. For composite sections, yielding starts in the bottom (tension) flange at a load below that corresponding to the yield moment as a result of residual stresses. As the loading continues, yielding progresses through the bottom flange, web, and top flange and eventually causes tension cracking of the lower portion of the concrete slab. The load-deflection and moment-rotation curves continue to rise during this stage until a failure load is eventually reached when the concrete in the top portion of the slab suddenly crushes.

The curves do not include descending portions similar to those for noncomposite sections because most of the steel section is in tension; therefore, local and lateral buckling do not occur. As a result of strain hardening, the failure moment, M_{max}, usually exceeds M_p. The difference depends on the proportions of the cross section and can be as high as 35% (Ansourian 1982 and Rotter and Ansourian 1979). The shape factor, M_p/M_y, for composite sections in positive bending is usually considerably larger (it ranges up to 1.50) than that of noncomposite sections (it is usually less than 1.15); therefore, yielding usually starts at a much lower percentage of M_p and there is a large rounded portion of the load-deflection and moment-rotation curves between M_y and M_p.

Unloading in the inelastic range follows a line parallel with the original elastic loading curve on the load-deflection and moment-rotation plots unless the applied load exceeds that required to cause tension cracking in the slab. A permanent deflection and rotation, but no moment, remains after all load is removed. Thus, the unloading behavior is essentially the same as that for noncomposite sections.

If load is applied to the steel section before the slab has hardened, this section behaves as a noncomposite section. Any yielding that occurs during this stage causes a permanent angular discontinuity that remains in the composite member after the slab has hardened, but the composite section is not otherwise affected. The dynamic yield effects discussed for noncomposite sections also apply to composite sections.

Negative Bending

Simple-span composite beams and girders are not normally loaded in negative bending, but inelastic behavior under such loading is discussed here because it simulates behavior in negative-

bending regions of continuous spans. A typical moment-rotation curve for a simple-span composite member loaded in negative bending by a concentrated load at midspan is shown in Figure 3.3.

The slope of the initial portion of the curve is defined by the stiffness of the uncracked composite section. When cracking of the concrete slab occurs, the curve shifts (Carskaddan 1991) to a new position as shown in the figure. If the moment is held constant during cracking, a horizontal shift occurs; if the rotation is held constant a vertical shift occurs. In either case, the new position falls on the curve for the cracked section (steel section plus deck reinforcement). Like the uncracked-section curve, the cracked-section curve passes through the origin.

Subsequently, the composite member behaves as a noncomposite member as discussed previously, and the unloading curve is parallel with the initial elastic line for the steel section plus rebars. The permanent rotation, Θ_r, that remains after fully unloading from a moment above the cracking moment is the plastic rotation for that moment as shown in the figure. Thus, cracking of the slab does not contribute to the plastic rotation(Carskaddan 1991).

The effect of load applied to the steel section before the slab has hardened is the same as that discussed previously for composite sections in positive bending. Any yielding that occurs during this stage causes a permanent angular discontinuity that remains in the composite member after the slab has hardened, but the composite section is not otherwise affected.

3.2.1.2 Continuous Spans

Positive- and negative-bending regions between points of contraflexure in continuous spans behave like simple spans in developing plastic rotations. For example, a simple span loaded in negative bending by a concentrated load at midspan simulates the negative bending region near a pier; the midspan load simulates the pier reaction and the simple supports simulate adjacent points of contraflexure. When simple spans are joined together into a continuous span, however, permanent moments, as well as permanent deflections, occur as a result of yielding at any cross section. Since these permanent moments develop automatically they are often called automoments (Grubb 1985, Haaijer et. al. 1970, 1987 1993); alternatively they are called redistribution moments because they are caused by a redistribution of the elastic moments (AASHTO 1994). The latter term will be used in this report.

3.2.1.2.1 Redistribution Moments

Due to Yielding at Piers

The development of redistribution moments due to yielding at the pier of a two-span girder is illustrated in Figure 3.4. As discussed previously, the yielding causes a permanent angular discontinuity that can be simulated by cutting the ends of two beams slightly off square and then welding them together end to end as illustrated in an exaggerated manner in the figure. When the spliced beam is placed on the abutments and held down against the pier (either by a downward reaction at the pier or by deadweight), redistribution moments occur along the beam as illustrated.

If the amount of the plastic rotation is known, the magnitude of the resulting redistribution moments and permanent deflections can be calculated by classical methods of indeterminate analysis as illustrated conceptually for a three-span girder in Figure 3.5. In these methods, the continuous span is treated as a series of simple spans and the end moments necessary to restore continuity are determined. The end moment required to cause a given end rotation depends on the stiffness of the adjacent span. Thus, the magnitude of the redistribution moments depends on the magnitude of the plastic rotation and on the stiffness properties of the girder.

Redistribution moments are held in equilibrium by the reactions at piers and abutments. Therefore, the redistribution moments must peak at pier locations and vary linearly between reactions. If yielding and plastic rotations occur at more than one pier, the redistribution moments caused by the plastic rotation at each pier can be calculated separately and summed to get the total redistribution moments. Subsequent loading may cause additional yielding and thereby modify the redistribution moments.

Due to Yielding Within a Span

Yielding at peak-moment and splice locations within a span also causes plastic rotations and redistribution moments. In Figure 3.6, the development of such redistribution moments is illustrated for yielding at midspan of Span 1 of a three-span girder. Again, the plastic rotation is assumed to be concentrated in an angular discontinuity and the continuous span is conceptually separated into three simple spans. This angular discontinuity causes end slopes defined by

$$S = \frac{aR}{L} \tag{3.2}$$

where S is the slope at one end of the span, a is the distance from the angular discontinuity, R, to the opposite end, and L is the span length. The redistribution moments and permanent deflections caused by the known plastic rotation can again be calculated with classical methods of indeterminate analysis by determining the end moments necessary to restore continuity.

These redistribution moments, which are held in equilibrium by the reactions, must again peak at pier locations and vary linearly between reactions. Redistribution moments caused by yielding at other locations within the span, and within other spans, can be calculated individually and combined with redistribution moments due to yielding at piers to get the total redistribution moments for the girder. Yielding at any span or pier location causes redistribution moments throughout the girder.

3.2.1.2.2 Relationships Defining Moments and Deflections

As a continuous-span girder is progressively loaded, the distribution of moments along the span remains constant until yielding starts at any location. As the loading continues, the distribution of moments changes because of the resulting plastic rotation (angular discontinuity) at the yield location. Specifically, the moment at that location increases at a slower rate than it did in the elastic range. This amounts to a shifting of moment from the yield location to other adjacent locations. In continuous-span bridge girders, yielding usually starts first at piers and shifts moment from negative- to positive-bending regions.

The correct moments for any loading are equal to the algebraic sum of elastic moments caused by the applied loads and the redistribution moments caused by yielding during this loading or some previous loading. If the same loading is repeated, no additional yielding or changes in redistribution moments or permanent deflections occur. A higher loading, however, causes additional yielding and changes the redistribution moments and permanent deflections. A different distribution of loads may or may not cause additional yielding and changes in redistribution moments.

The redistribution moments and permanent deflections for a continuous-span girder are uniquely defined if the plastic rotations at all yield locations are known as explained earlier. To fully define the inelastic behavior of the girder, however, it is necessary to determine the plastic rotations caused at all yield locations by a given loading. Two relationships are available to define these plastic rotations: a continuity relationship and a rotation relationship. These two relationships provide enough simultaneous equations to uniquely define the moments and plastic rotations throughout the girder. As

mentioned previously, all plastic rotations are assumed to be concentrated in angular discontinuities and the rest of the girder is assumed to be fully elastic.

The continuity relationship interrelates the plastic rotations and total moments (elastic moments due to applied loads plus redistribution moments) along the girder and depends on the distribution of stiffness along the girder. It provides one equation at each pier location. The rotation relationship is the plastic-rotation curve discussed previously. The ascending portion of this curve depends primarily on the proportions of the cross section (ratio of flange area to web area, etc.) and the descending portion depends primarily on the compression-flange slenderness, web slenderness, and compression-flange bracing spacing. The rotation relationship provides one equation at each yield location.

3.2.1.3 Ultimate Strength

Theoretical ultimate strength is reached when the moment at a critical location can no longer be shifted to other locations; for an interior span this occurs when the effective-plastic-moment capacity is reached at three locations defining a mechanism (ASCE 1971 and Beedle 1958). The theoretical ultimate strength represents the maximum loading that can theoretically be applied to the girder if strain hardening is ignored. Because of strain hardening, however, the actual ultimate strength (maximum loading) may be higher if the critical sections are sufficiently compact.

Large plastic rotations may occur at some yield locations as the loading is increased and moment is shifted to other locations. While these plastic rotations are occurring, the corresponding moments vary as defined by the appropriate plastic-rotation curves discussed earlier. In continuous-span bridge girders, pier sections are usually required to sustain such large plastic rotations to reach ultimate strength. If the sections are noncompact, the plastic rotations may be well into the descending portions of the curves so that the effective-plastic-moment capacities at those locations may be well below the full theoretical plastic moments. Peak positive-bending locations may also sustain significant plastic rotations, but if such sections are composite they sustain the plastic rotations without a decrease in moment capacity as discussed earlier.

3.2.2 Multigirder Systems

3.2.2.1 Theoretical Behavior

The inelastic redistribution of moments discussed above occurs longitudinally within a single continuous-span steel girder. Inelastic redistribution of moments can also occur laterally among the

individual steel girders of multigirder bridges. This can occur in both simple-span and continuous-span bridges and provides a reserve strength that is not normally accounted for in design or rating (Barker and Galambos 1992).

The development of inelastic lateral redistribution of moments can be illustrated by considering a four-lane simple-span bridge consisting of six identical girders and loaded by a single vehicle in an outer lane. The elastic moments caused in the individual girders by this type of loading vary from a maximum in the exterior girder under the load to a much smaller moment in the other exterior girder. The actual distribution of moments among the girders depends on the ratio of the longitudinal stiffness of the girders to the lateral stiffness of the slab and diaphragms or cross frames.

As the loading is increased, the distribution of moments among the girders remains constant until yielding starts in the exterior girder. Thereafter, the exterior girder takes a smaller fraction of any additional loading because of its reduced stiffness. Consequently, the lateral distribution of moment becomes more uniform. After the moment in the exterior girder reaches its maximum-moment capacity, all additional loading must be carried by the other girders.

If the exterior girder is compact, the moment it carries will remain constant while the other girders continue to take additional moment. If the exterior girder is noncompact, the moment it carries may decrease in conformance with its rotation curve as the other girders continue to take additional moment. The ultimate strength is reached when plastic hinges form in all girders.

For continuous spans, inelastic redistribution of moments usually occurs in both the longitudinal and lateral directions. Continuity and rotation relationships apply at all yield locations in the girders, and redistribution moments, plastic rotations, and permanent deflections develop as previously discussed. However, the deflections of the individual girders are now interrelated by elastic bending of the slab and diaphragms or cross frames in the lateral direction. In effect, this means that the loading carried by each girder, which is a given in the analysis of a single girder, changes with respect to both total magnitude and distribution along the length as plastic hinges develop in the girders.

3.2.2.2 Application to Design

The importance of inelastic lateral redistribution of moments depends primarily on the lateral position of the loading. For loading with a large lateral eccentricity, such as loading only in the outside lane of a multilane bridge, considerable additional load can be applied after a mechanism forms in the

first girder. For loading distributed laterally in such a way that the elastic moments are the same in all girders, there is no reserve strength because all girders form mechanisms at the same loading.

In design specifications (AASHTO 1992 and 1994), the same loadings are usually specified for all design lanes. Specified lane loads are usually assumed to be distributed uniformly across the lane widths, but concentrated truck loads are usually placed near the edges of the lanes. Furthermore, the deck overhang may not be sufficient to provide equal dead-load moments in all girders. Under such loadings, the elastic moments are usually not the same in all girders. (Such moments are not actually calculated in the design process because specified lateral-distribution factors are used to determine the loadings on individual girders). Because the elastic moments are not the same in all girders, inelastic lateral redistribution is expected to provide a significant reserve strength for typical bridge designs.

Researchers have been studying this reserve strength and exploring different ways of accounting for it in design. Eyre and Galambos (1973) and Barker (1990 and 1992) investigated the grid method for directly determining the ultimate strength of multigirder systems; inelastic finite element analyses could also be used for this purpose (Hall and Kostem 1981 and Kostem 1984). Heins and Kuo (1973 and 1975) developed inelastic lateral-distribution factors for use at ultimate load. Ghosn and Moses (1991 and 1993), and Frangopol and Nakib (1991), developed redundancy factors that reflect the reserve strengths for different multigirder systems and could be incorporated into the LRFD format for bridge design. As yet, however, none of these approaches has been incorporated into bridge design specifications.

3.2.3 Shakedown

3.2.3.1 Due to Sequential Loading

3.2.3.1.1 Classical Theory

Incremental collapse and shakedown have been extensively studied, especially in connection with plastic-design requirements for buildings (ASCE 1971 and Beedle 1958). Studies of continuous-span girders were conducted by Eyre and Galambos (1970 and 1973), Grundy (1976 and 1983), Gurley (1981 and 1982), Fukumoto and Yoshida (1969), Toridis and Wen (1966), and others (Eyre and Galambos 1969). Incremental collapse occurs in a continuous-span girder when a sequence of loads causes progressive increases in permanent deflections without limit. Shakedown, also called

deflection stability, occurs when permanent deflections stabilize after a finite number of loading cycles and all subsequent behavior is fully elastic.

Studies (ASCE 1971) have shown that shakedown occurs in a structure that satisfies classical plastic-design assumptions if a pattern of redistribution moments can be found such that the algebraic sum of these moments, and the elastic moments due to any loading in the sequence, is not numerically larger than the plastic-moment capacity at any location. The main plastic-design assumption related to shakedown is that all sections must have moment-rotation curves that can be satisfactorily approximated by a sloping straight line to the plastic moment followed by a horizontal line extending sufficiently to allow the development of the required redistribution moments. Compact noncomposite sections satisfy this requirement.

As a result of strain hardening, which is ignored in the assumed rotation curve, actual compact structures always reach shakedown at higher loads than predicted by the classical theory (ASCE 1971). Incremental collapse does not occur in simple spans since redistribution moments cannot develop in such spans. Consequently, the spans behave elastically (based on the assumed rotation curve) until a particular loading in the sequence causes the applied moment to exceed the plastic-moment capacity at some location and theoretically collapse under that loading.

Tests to determine shakedown for a sequence of loadings are usually performed in the following way (ASCE 1971 and Beedle 1958). Each loading in the sequence consists of a set of concentrated and/or distributed loads applied in specified directions at specified locations, and all individual loads in all sets in the sequence are interrelated by specified ratios. The magnitude of a sequence is defined by a single factor that applies to all individual loads in the sequence.

In the test, a sequence of loadings with a low factor is applied first and repeated; the permanent deflections generally increase each loading cycle, but by a successively smaller amount. If the permanent deflections finally stabilize, shakedown has been achieved for that factor. Then the process is repeated with progressively higher factors until a factor is reached for which the permanent deflections do not stabilize.

3.2.3.1.2 Compact Bridge Girders

Recently, incremental collapse and shakedown in highway bridges have been extensively studied by Barker (1990 and 1995), Barker and Galambos (1992), Weber (1994), and others (Galambos et. al. 1993). For simplicity, this behavior will first be illustrated by considering a

symmetrical three-span compact noncomposite girder, which satisfies the classical plastic-design assumptions. Later, the somewhat more complex behavior of noncompact girders will be discussed.

Figure 3.7 shows how incremental collapse or shakedown can occur in the compact girder as a result of repeated passages of heavy trucks across the bridge. In the figure, the passage of two trucks with a constant spacing is represented by placing a set of two concentrated loads successively at different critical locations on the bridge.

The elastic moments that occur throughout the girder when the live loads are in any particular position do not change as redistribution moments develop and are modified by repeated passages of these loads. Also, yielding is assumed to occur only when the elastic moment combined with the redistribution moment at any section exceeds the plastic-moment capacity. Thus, the small amount of yielding that occurs between the yield moment and the plastic moment is neglected in line with classical plastic-design assumptions.

The live loads first straddle Pier 1 and, in combination with the dead load, are assumed to cause a negative elastic moment exceeding the negative plastic-moment capacity at that pier. The resulting plastic rotation causes the shown redistribution moments; at the pier, the algebraic sum of the negative elastic moment and the positive redistribution moment equals the negative plastic-moment capacity. Next, the live loads are placed midway between the two piers to cause the maximum possible positive moments in Span 2, but it is assumed that the resulting positive elastic moment combined with the positive redistribution moment from the plastic rotation at Pier 1 does not exceed the positive plastic-moment capacity at critical locations so that no change in plastic rotation or redistribution moments occurs.

The live loads are then advanced to straddle Pier 2 and due to symmetry cause the same negative elastic moment at that pier as was originally caused at Pier 1. The negative elastic moment caused by the dead and live loads combined with the negative redistribution moment due to the plastic rotation at Pier 1 exceeds the negative plastic-moment capacity of the section so that plastic rotation occurs at that pier. As shown, the resulting positive redistribution moment at Pier 2 is higher than the original positive redistribution moment at Pier 1 due to the plastic rotation at Pier 1 by an amount equal the negative redistribution moment at Pier 2 due to the plastic rotation at Pier 1. The total redistribution moment at that stage, and at subsequent stages, is equal to the sum of the redistribution moments due to plastic rotations (Θ_{p1} and Θ_{p2}) at Piers 1 and 2.

The live loads are now returned to straddle Pier 1 and cause additional plastic rotation and a higher positive redistribution moment at that pier. The positive redistribution moment at Pier 1 due to plastic rotation at Pier 1 must increase because it is now equal to the negative elastic moment combined with the negative redistribution moment at Pier 1 due to the plastic rotation at Pier 2, which was zero when the live loads first straddled Pier 1, minus the negative plastic-rotation capacity.

As this sequence of loadings proceeds, the plastic rotations at the two piers, and the resulting redistribution moments, continue to increase but at a slower rate until they stabilize at the final redistribution moments shown. If the final positive redistribution moment combined with the maximum positive elastic moment when the live loads are placed between the piers does not exceed the positive plastic-moment capacity at that location, shakedown has occurred. Otherwise, incremental collapse occurs because the positive-bending section cannot sustain any more moment shifted from negative-bending regions through the formation of the redistribution moments.

3.2.3.1.3Noncompact Bridge Girders

The simple bilinear plastic-rotation curve assumed in classical plastic-design theory is not appropriate for typical composite noncompact bridge girders. At piers, the maximum moment for such girders is usually limited to the yield-moment, rather than the plastic-moment capacity, and the amount of plastic rotation that occurs before unloading is much smaller than for noncomposite compact sections. In positive-bending regions, the composite sections are usually compact because of the location of the neutral axis, but such sections sustain considerable plastic rotations between the yield and plastic moments as described previously. Consequently, it is not appropriate to assume that the rotation curve for such sections is elastic to the plastic moment as is done in classical plastic-design theory.

Even with these differences in the rotation curves, however, incremental collapse or shakedown develops in much the same way for noncompact bridge girders as was discussed for compact bridge girders. The actual development of the permanent deflection and redistribution moments, as a sequence of loadings is applied, can be traced mathematically by the unified autostress method (Schilling 1989, 1991 and 1993) or the residual-deformation method (Dishongh 1990 and 1992 and Dishongh and Galambos 1992) mentioned earlier. Again, a sequence of loadings causes incremental collapse when a positive-bending section cannot sustain any more moment shifted from negative-

bending regions through the formation of redistribution moments, and shakedown occurs if all positive-bending sections can take more moment.

The following differences in shakedown behavior, however, occur between compact and noncompact girders. At each pier in noncompact girders, the algebraic sum of the negative elastic moment and the positive redistribution moments due plastic rotations at all yield locations cannot exceed the positive yield-moment capacity of the cracked section and may need to be limited to an even lower value if the plastic rotation at the pier is large enough to fall on the unloading portion of the rotation curve. Also, yielding will usually occur in positive-bending regions and influence the development of redistribution moments and permanent deflections. Specifically, each plastic rotation in a positive-bending region causes redistribution moments throughout the girder and thereby adds to, or subtracts from, the maximum elastic moment at each pier.

Shakedown will occur in a composite noncompact girder if the algebraic sum the elastic moment and all redistribution moments does not exceed the plastic-moment capacity at each positive-bending section and the effective plastic-moment capacity at each negative-bending section. This effective plastic-moment capacity depends on the plastic rotation expected to occur at shakedown (after the permanent deflections due to a sequence of loadings have stabilized) and does not exceed the yield-moment capacity. It will be discussed in more detail later. The elastic moment referred to above is the maximum that can occur at the section being checked for any position of live loads; thus, it can be obtained from the elastic moment envelope.

3.2.3.2 Due to Dynamic Yielding

3.2.3.2.1 Theoretical Behavior

Time is required to cause yielding (inelastic straining) of steel elements as mentioned previously. This dynamic yielding effect can cause progressive increases in permanent deflections similar to those discussed above for continuous-span girders under sequential loadings. The progressive increases due to dynamic yielding, however, can occur in simple spans as well as continuous spans. In continuous spans, they can occur in combination with progressive increases in permanent deflections due to sequential loading (Ho 1972). Thus, dynamic yielding effects can increase the number of loading cycles required to achieve shakedown or cause incremental collapse in continuous spans under sequential loadings.

Dynamic yielding affects the development of permanent deflections in the following way. If a stationary heavy truck on a simple-span girder bridge causes a midspan moment above the yield-moment capacity, but below the plastic-moment capacity, the resulting permanent deflection can be predicted theoretically as described previously. If the same truck travels across the bridge at a fast speed it will cause higher elastic stresses due to impact but may cause smaller permanent deflections because the full permanent deflection does not have time to develop before the truck has left the bridge. To isolate the effect of dynamic yielding, consider fast passages of a similar, but lighter, truck that causes the same elastic stresses as the stationary truck. The first passage will cause considerably smaller permanent deflections than the stationary truck. Each subsequent passage of the lighter truck at the same speed will cause an additional increment of permanent deflection until the total reaches the value theoretically predicted for the stationary truck.

The magnitude of the permanent-deflection increment caused by each passage depends on the speed and weight of the truck, but cannot be predicted theoretically at present. Experimental observations, however, show that the increment is usually largest for the first passage and decreases progressively for subsequent passages. Presumably, this is because the difference between the actual and full permanent deflections decreases with each passage and approaches zero asymptotically.

If a stationary heavy truck on a simple-span girder bridge causes a moment above the plastic-moment capacity (or maximum-moment capacity if strain hardening causes this capacity to be significantly above the plastic-moment capacity), the girder will collapse. If a similar lighter truck that causes the same elastic stresses as the stationary truck travels across the bridge at a fast speed, the bridge probably will not collapse, but will sustain significant permanent deflection. Subsequent passages of this truck will cause additional increments of permanent deflection and eventual collapse of the bridge. Thus, increases in permanent deflections due to dynamic yielding, as well as sequential loading, can result in either shakedown or incremental collapse.

3.2.3.2.2 Experimental Behavior

The AASHO road tests (HRB 1962a and 1962b) provided experimental evidence of the effects of dynamic yielding consistent with the theoretical behavior described above. Ten composite and noncomposite steel beam bridges with simple spans of 50 feet were subjected to many passages of trucks traveling at speeds between 20 and 50 mph. The bridges were one lane wide and utilized three parallel beams. Most of the bridges were subjected to about 500,000 truck passages, but tests of some

were terminated earlier when excessive permanent deflections occurred within a few hundred passages. The mean measured dynamic strains caused in the beams of a particular bridge by a particular truck remained approximately constant over the life of the test, but the stresses caused by individual passages varied considerably about this mean.

Tests of four bridges (1B, 2A, 4A, 4B) were stopped because excessive permanent deflections of more than 3 inches developed within 26 to 235 passages of the regular truck plus 131 to 188 passages of lighter trucks. One of these bridges (1B) was also unintentionally subjected to 2 passages of a considerably heavier truck. This group of bridges illustrates incremental collapse; the permanent deflections did not stabilize and were expected to continue without limit. Even for these cases, however, many passages were required to produce large permanent deflections.

The ratios of the total measured strains (dead load plus the moving regular truck) to the measured static yield strain for the three bridges not subjected to the unintended overloads ranged from 1.19 to 1.27 and averaged 1.22. The corresponding ratio was only 1.03 for the overloaded bridge, but a similar ratio based on the overload truck, rather than the regular truck, was 1.19. It was estimated (HRB 1962b) that the dynamic yield stress or strain for the loading rate associated with the moving trucks was 10% above the static yield stress or strain. Hence, the ratios of measured total strain to estimated dynamic yield strain for the three bridges ranged from 1.08 to 1.15 and averaged 1.11.

The measured total strains (dead load plus the moving regular truck) were generally below the measured static yield strains in the other bridges (1A, 2B, 3A, 3B, 9A, 9B). For these bridges, some permanent deflections occurred as a result of residual stresses, but were relatively small and eventually stabilized. Specifically (HRB 1962b), "the permanent set increased rapidly during the initial phases of the regular test traffic, but the bridges became almost stable after a few hundred trips." Thus, the behavior of this group illustrates shakedown.

"The only exception (in the preceding group) was noncomposite bridge 3A which continued to deform at a moderately rapid rate throughout the first 50,000 trips of vehicles" (HRB 1962b). The test of this bridge was stopped by an accident after 392,000 passages when the permanent deflection was about 3 inches. The measured total strains in two out of three of the beams in this bridge were above the measured static yield strain.

After approximately 500,000 passages of the regular test truck had been applied to each of the bridges in the preceding group, the weight of the truck was periodically increased and 30 or fewer

passages were applied at each new weight. Typically, the first passage at a new weight caused an additional permanent deflection increment and subsequent passages at that weight caused progressively smaller additional increments. This is consistent with the theoretical behavior described previously.

3.2.3.3 Alternating Plasticity

Another type of deflection instability that has been studied in connection with plastic-design requirements is alternating plasticity, which occurs when a section is subjected to repeated reversals of moments large enough to cause yielding in both directions (ASCE 1971). A stable hysteresis loop forms if such yielding occurs, but repeated load applications will eventually cause failure by low-cycle fatigue.

It has been shown, however, that significant alternating plasticity does not occur if the range of alternating moments does not exceed twice the yield-moment capacity of the section (ASCE 1971). Instead, the behavior will remain essentially elastic if this limit is not exceeded. In highway bridges, the limit is rarely, if ever, exceeded. Therefore, alternating plasticity need not be considered in the inelastic design of such bridges; it is of concern mainly in earthquake design of buildings.

3.3 CALCULATION PROCEDURES

This section describes procedures for calculating redistribution moments, permanent deflections, ultimate strengths, and shakedown for beams and girders subjected to loadings sufficient to cause yielding at one or more locations. First, inelastic procedures for simple spans are briefly outlined. Then, three alternative procedures for calculating the moments and permanent deflections caused in continuous spans by any given loading are described: the unified autostress method (Schilling 1989, 1991 and 1993), the residual-deformation method (Dishongh 1990 and 1992 and Dishongh and Galambos 1992), and the beam-line method (Carskaddan et. al. 1982, Disque 1964 and Haaijer et. al. 1987).

All three of these methods utilize the continuity and rotation relationships mentioned earlier. The three methods do not directly determine ultimate strength, but will not provide a solution if the loading being checked exceeds the ultimate strength. Thus, the methods can be used to check whether a specified maximum loading exceeds the ultimate strength of a trial design. They can also be used to check whether permanent deflections will stabilize under repeated passages of specified maximum truck loadings.

The mechanism method (ASCE 1971 and Beedle 1958) of determining ultimate strength is described next. This method does not permit calculation of the moments and permanent deflections caused by a given loading, but gives the magnitudes of the loads that will theoretically cause collapse for any assumed mechanism. Finally, a simple method of checking shakedown for highway bridges is explained.

3.3.1 Simple-Span Calculations

3.3.1.1 Permanent Deflections

Yielding does not cause any redistribution of moments in simple spans because they are statically determinate. Consequently, the moments caused by a given loading can be calculated by elastic procedures even after yielding occurs. The amount of plastic rotation caused by yielding at any location can be determined directly from the appropriate plastic-rotation curve since the corresponding moment at that location is known.

The permanent deflection resulting from yielding at one or more locations can then be determined by assuming that the plastic rotations are concentrated in angular discontinuities and the rest of the member is fully elastic. The three-moment method (Gaylord and Gaylord 1979) discussed under the heading Unified Autostress Method, and the conjugate-beam method (Gutkowski 1990) discussed under Residual-Deformation Method, could be used for this calculation. Other elastic analysis methods could also be used.

The preceding discussion applies specifically to simple-span cases, such as composite girders, where significant yielding occurs below the maximum-moment capacity, M_{max}. If it is assumed that no yielding occurs below M_{max}, as is often done with noncomposite compact beams, no permanent deflections occur.

3.3.1.2 Ultimate Strength

Since no redistribution of moments occurs in simple spans, the theoretical ultimate strength is reached when the moment at any location equals the maximum-moment capacity at that location. The plastic hinge at the yield location and the two simple supports constitute a mechanism. Depending on the compactness of the critical section, the maximum-moment capacity may be larger or smaller than the plastic-moment capacity. For example, the actual ultimate strength of a composite girder may exceed the theoretical ultimate strength by as much as 35% as mentioned earlier (Ansourian 1982 and

Rotter and Ansourian 1979). If the critical section is noncompact, in contrast, the maximum-moment capacity may be limited to the yield-moment capacity or less.

At ultimate load, however, the section will never be on the descending portion of the plastic-rotation curve because redistribution of moments does not occur in simple spans. Therefore, the moment never needs to be limited to a value less than the maximum-moment capacity of the critical section.

Incremental collapse due to sequential loadings does not occur in simple-span beams and girders so that shakedown never needs to be checked for such girders.

3.3.2 Unified Autostress Method

The unified autostress method is described briefly in this section and in more detail elsewhere (Schilling 1989, 1991 and 1993). It was developed specifically to calculate the redistribution moments and permanent deflections in a continuous-span girder due to a given loading sufficient to cause yielding. By substituting an elastic moment envelope for the elastic moment diagram for the given loading, however, the unified autostress method can also be used to calculate the redistribution moments and permanent deflections due to the combination of stationary and moving loads that define the elastic moment envelope. In other words, the method will predict the final redistribution moments and permanent deflections that remain after live loads are successively placed at all possible positions to simulate passage of one or more trucks across the bridge.

A solution is obtained by conceptually cutting the continuous span into simple spans as illustrated in Figures 3.5 and 3.6 and then calculating the end moments necessary to restore continuity with all plastic rotations (angular discontinuities) in place. The unknown inelastic quantities are the redistribution moments at all piers and the plastic rotations at all yield locations. A unique solution is achieved by satisfying a continuity relationship at each pier and a rotation relationship at each yield location. The number of these relationships matches the number of unknowns. Once the inelastic unknowns have been determined, the elastic moments, redistribution moments, elastic deflections, and permanent deflections throughout the girder can be determined by well-known elastic analytical methods.

3.3.2.1 Continuity Relationship

The continuity relationship interrelates the moments at all pier locations and the plastic rotations at all yield locations; it depends on the stiffness properties of the girder. The total moment at each pier is equal to the algebraic sum of the elastic moment and the redistribution moments due to plastic rotations at all yield locations. Thus, the total moment at Pier 1 can be expressed as

$$M_1C = M_1E + (M_1P_1)(RP_1) + (M_1P_2)(RP_2) + (M_1S_1)(RS_1) + \cdots + (M_1P_n)(RP_n) \quad (3.3)$$

In this equation, M_1C is the total (continuity) moment at Pier 1, RP_1 is the plastic rotation at Pier 1, M_1P_1 is the redistribution moment at Pier 1 due to a unit plastic rotation at Pier 1, M_1P_2 is the redistribution moment at Pier 1 due to a unit plastic rotation at Pier 2, RS_1 is the plastic rotation at a point in Span 1, M_1S_1 is the redistribution moment at Pier 1 due to a unit plastic rotation at that point in Span 1. Other parameters are defined in a comparable way.

The elastic moment M_1E at Pier 1 can be taken as either the elastic moment due to a specified loading or the maximum moment at Pier 1 from an elastic moment envelope for combined dead and live loads including impact. The first case gives the solution for the specified loading, and the second case gives the final solution for a combination of stationary dead loads and a sequence of live loads successively placed at different positions until the permanent deflections stabilize. The plastic rotations due to yielding at any number of different locations can be included in Equation 3.3. For the first case, the plastic rotations could be caused either by the specified loading or some previous loading.

The redistribution moments due to unit plastic rotations (M_1P_1, M_1S_1, and similar terms) are called redistribution-moment coefficients. The actual redistribution moments can be expressed as the products of these coefficients and the corresponding plastic rotations because redistribution moments are proportional to plastic rotations. The redistribution-moment coefficients are stiffness properties of the girder. The references (Schilling 1989, 1991 and 1993) illustrate how they can be determined by the three-moment method of analysis, but other methods of indeterminate analysis could be used instead. The redistribution-moment-coefficient approach facilitates computation of the inelastic unknowns, especially for the most-general cases where an iterative procedure is required.

3.3.2.2 Rotation Relationship

The rotation relationship used in the unified autostress method relates the total moment at a section to the plastic rotation at that section. The total moment is the algebraic sum of all redistribution

moments and the elastic moment either for a specified loading or from an elastic moment envelope. At piers, for example, the total moment is M_nC from Equation 3.3.

The plastic rotation is the permanent rotation that remains after a simple-span beam or girder has been loaded into the inelastic range and then unloaded. As mentioned earlier and illustrated in Figure 3.2, it is usually determined by subtracting the elastic rotation from the total rotation in a test, but sophisticated computer modeling has recently been developed to generate such curves analytically (Barth et. al. 1994, White et. al. 1994 and White and Dutta 1992a, 1992b).

The ascending portion of the curve is controlled by the spread of yielding through the cross section and depends on the proportions of the cross section, such as the ratios of web area to tension and compression flange areas. The descending portion of the curve is controlled by local and/or lateral buckling and depends on the slenderness ratios of the compression flange and web and the spacing of lateral supports. As mentioned earlier, tensile cracking of the slab of a composite section in negative bending does not affect the plastic rotation (Carskaddan 1991).

If rotation curves are available for the particular sections being used in a beam or girder, they should be utilized in the analysis. However, such curves are rarely available to bridge engineers. Therefore, typical approximate curves for certain categories of beams and girders are presented under the heading Typical Rotation Curves. Appropriate curves from any other source can be used equally as well in the unified autostress method. It is anticipated that better typical curves that more precisely account for various pertinent factors will be developed in the future. The exact shape of the rotation curve generally does not have a large effect on the inelastic analysis; therefore, simplified representations of such curves are appropriate for design purposes.

3.3.2.3 Computational Procedures

Although a sufficient number of continuity and rotation relationships are available to provide a unique solution as described earlier, various factors discussed below can complicate the process. Therefore, an iterative procedure described elsewhere (Schilling 1989, 1991 and 1993) was used to apply the unified autostress method to cases involving all of these complications. Redistribution-moment coefficients were used to define stiffness properties in this procedure. A direct solution without simultaneous equations, however, can be obtained for two-span girders without yielding in positive bending.

The locations of the peak positive moments in continuous spans usually shift as the loading increases in the inelastic range; therefore, positive-bending yield locations generally are not known for a given loading and several locations must be tried in the analytical procedure. To permit a direct solution by simultaneous equations, all rotation relationships must be defined by single mathematical expressions. Solutions for bilinear curves, trilinear curves, or curves defined by a series of coordinates, require different computational procedures. Loadings applied before and after the slab has hardened also complicate computational procedures as discussed elsewhere (Schilling 1989, 1991 and 1993). Variations in stiffness (EI) along the span cause minor complications; such variations can be conveniently defined by the redistribution-moment coefficients mentioned earlier.

3.3.3 Residual-Deformation Method

Residual-deformation method (Dishongh 1990 and 1992 and Dishongh and Galambos 1992) is similar to the unified autostress method. It utilizes the same continuity and rotation relationships to determine the plastic rotations, redistribution moments, and permanent deflections due to inelastic behavior in continuous-span beams and girders. These quantities can be determined for either (a) a given distribution of stationary loads or (b) a combination of stationary dead loads and moving live loads that define a particular elastic moment envelope. The latter case gives the final plastic rotations, redistribution moments, and permanent deflections that will remain after the moving loads are repeatedly placed at different locations until shakedown occurs.

The conjugate-beam method (Gutkowski 1990) is used in the residual-deformation method to develop equations interrelating the plastic rotations and redistribution moments that remain after all loading is removed. These equations are similar to the continuity equations utilized in the unified autostress method, which were developed by using the three-moment method of analysis. A distributed loading corresponding to the M/EI diagram for the redistribution moments, and concentrated loads corresponding to the plastic rotations (angular discontinuities), are applied to the conjugate beam.

The resulting shear at any point on the conjugate beam corresponds to the slope at that point in the real girder, and the moment at any point in the conjugate beam corresponds to the permanent deflection at that point in the real girder. The Newmark method of numerical integration (Gaylord and Gaylord 1979 and Newmark 1942) is useful in applying the conjugate-beam method to girders with varying stiffnesses along their lengths. To facilitate inelastic ratings based on specified limiting

permanent deflections, equations interrelating such deflections with the corresponding plastic rotations and redistribution moments were derived for some simple cases.

3.3.4 Beam-Line Method

The beam-line method was developed (Carskaddan et. al. 1982, Disque 1964 and Haaijer et. al. 1987) long before the unified autostress method and the residual-deformation method, but is really a special case of these two more general methods. The first application of the method to bridges was in calculating redistribution moments at Overload in Alternate Load Factor Design procedures (AASHTO 1986 and 1991 and Haaijer et. al. 1987). Specifically, the redistribution moments due to yielding at the pier of a two-span beam were calculated. It was assumed that no positive-bending yielding occurs in this case.

The beam-line chart shown in Figure 3.8 applies to this simple case. A continuity relationship that defines the stiffness characteristics of the beam, and a rotation relationship that defines plastic-rotation characteristics of the cross section at the pier, are plotted in the figure. These are the same relationships that are used in the unified autostress and residual-deformation methods. For this simple case, the correct redistribution moment, and corresponding plastic rotation, are defined by the intersection of the two lines. Thus, no iterations are required for the solution.

When there is more than one pier, however, the redistribution moments caused at one pier by the critical loading for that pier (usually loads straddling the pier) are changed when this loading is moved to another pier to cause the maximum yielding at that location. Consequently, iterations are required to get the final stabilized redistribution moments. Yielding in positive-bending regions causes further complications (Carskaddan 1984). Therefore, the beam-line method is most useful for calculating redistribution moments due to yielding at the pier in two-span beams, and the two general methods are more suitable when positive-bending yielding is involved and/or there are more than two spans.

3.3.5 Typical Rotation Curves

3.3.5.1 Negative Bending

3.3.5.1.1 Ascending Portion

Autostress-Design Curve

Typical curves that conservatively represent the ascending portions of the plastic-rotation relationships for composite and noncomposite compact sections were developed (Carskaddan 1980, Grubb and Carskaddan 1979 and 1982, and Haaijer et. al. 1987) from available experimental results for use in autostress (ALFD) design procedures (Grubb 1987 and AASHTO 1986 and 1991). Originally, moment was normalized by dividing by the plastic-moment capacity, but it was later decided (Carskaddan and Grubb 1991) that it would be more appropriate to divide by the maximum-moment capacity especially for unsymmetrical sections.

Separate curves were originally proposed for composite and noncomposite sections (Haaijer et. al. 1987), but it was later concluded (Carskaddan and Grubb 1991) that the noncomposite curve should be used for both because concrete cracking does not affect plastic rotations as discussed previously. Although this curve was developed specifically for compact sections, which were the only sections originally permitted in autostress design, it is also appropriate for noncompact sections because the ascending portion of plastic-rotation curves is not significantly affected by local or lateral buckling.

The original curve, and two simplified approximations of this curve, are plotted in Figure 3.9. Mathematical equations defining the approximations are shown on the plot. The first is a higher order curve developed for use in a study of exploratory autostress designs (Schilling 1986), in the figure, it is indistinguishable from the original autostress curve. The second is a straight-line representation included in the LRFD bridge specifications (AASHTO 1994). This simple straight-line representation is suitable for most applications in which plastic rotation below the maximum moment is considered.

Inelastic-Rating Curve

In their proposed inelastic rating procedure, Galambos and his associates (1993) use a simple bilinear total-rotation curve (Figure B6 of the reference) consisting of an ascending straight line to the maximum moment followed by a descending, or horizontal, straight line. According to that representation, no plastic rotation occurs until the maximum moment is exceeded. This is the

assumption normally made in the plastic design of buildings (AISC 1993). The effect of the small amount of yielding, and resulting plastic rotation, that occurs below the maximum moment is usually counteracted by the beneficial effect of strain hardening (Dishongh and Galambos 1992), which is normally neglected in the plastic design of buildings. Thus, it is reasonable to assume elastic behavior to the maximum moment in most building applications. Since the shape of the ascending portion of the rotation curve for typical bridge members in negative bending (shown in Figure 3.9) is similar to that of typical building members, it is also appropriate to assume elastic behavior to the maximum moment for most bridge applications.

3.3.5.1.2Descending Portion

Compact Sections

After reaching the maximum moment, the rotation curve for compact sections can be assumed to remain at that moment through a plastic rotation of approximately three times the elastic rotation at the plastic moment, which is usually enough to reach the collapse load of a continuous-span girder (AISC 1993). Therefore, it is usually unnecessary to define the descending portion of the rotation curve for compact sections in negative bending. If such a descending curve is needed, however, the noncompact-section curve described in the next section and defined by Equations 3.8 to 3.10 can be utilized since it is expressed in terms of M_{pe}, which is a function of the web and compression-flange slenderness ratios. M_{pe} is the effective-plastic-moment capacity of the section as defined under the heading Mechanism Method. M_{pe} equals M_p when the unloading portion of this curve is horizontal.

Noncompact Sections

Two proposed curves that approximate the descending portion of the rotation relationship for noncompact sections are plotted in Figure 3.10. These curves are applicable if the compression-flange bracing requirements for inelastic design (AASHTO 1991 and 1994) are satisfied. Both curves start with zero plastic rotation at the maximum moment M_{max}, to be consistent with the assumption of elastic action to M_{max}.

The curved line represents the lower bound for three tests specifically conducted to define the plastic rotation of noncompact sections for use in autostress design procedures (Schilling 1985 and 1988). The straight line was developed (Kubo and Galambos 1988) from these three tests and results from other sources (Holtz and Kulak 1975 and Ohtake and Iwamuro 1982). The equation defining this

line was originally formulated (Kubo and Galambos 1988) in terms of the total rotation, but was modified in the present study to provide a more convenient equation defining the plastic rotation directly.

The original formulation was

$$\frac{M}{M_p} = \frac{M_{max}}{M_p} + k\left(\frac{\Theta}{\Theta_{ep}} - \frac{M_{max}}{M_p}\right) \tag{3.4}$$

The following expressions were inserted into Equation 3.4 to get the new formation shown in Figure 3.10:

$$\Theta = \Theta_e + \Theta_p \tag{3.5}$$

$$\frac{\Theta_e}{\Theta_{ep}} = \frac{M}{M_p} \tag{3.6}$$

$$\Theta_{ep} = \frac{M_p L}{2EI} \tag{3.7}$$

Equation 3.7 defines the elastic rotation at M_p for a simple span of length L and loaded by a concentrated load simulating the reaction at a pier.

In preceding equations, M is the moment, M_p is the plastic-moment capacity of the section, M_{max} is the maximum-moment capacity of the section, which may be less than M_p due to local buckling, θ is the total rotation, θ_e is the elastic rotation, θ_p is the plastic rotation, θ_{ep} is the elastic rotation corresponding to M_p and given by Equation 3.7, L the distance between adjacent points of contraflexure, I is the average moment of inertia in that region, and E is the modulus of elasticity. For girders that are nonprismatic within L, Equation 3.7 provides an approximate value of θ_{ep}; an exact value can be determined by an elastic deflection analysis that accounts for the variation of stiffness along the span.

As shown in the figure, the new rotation formulation is:

$$\frac{M}{M_{max}} = 1 + a\Theta_p \tag{3.8}$$

where a is the slope and is defined by:

$$a = \left(\frac{k}{1-k}\right)\left(\frac{2EI}{LM_{max}}\right) \tag{3.9}$$

In the original development (Kubo and Galambos 1988), it was suggested that a value of -0.1 be used for k. Later, in utilizing the original formulation for inelastic rating (Galambos et. al. 1993), it was suggested that k be defined by the following relationship:

$$k = \frac{(M_{pe}/M_p) - (M_{max}/M_p)}{4 - (M_{max}/M_p)} \tag{3.10}$$

where:

M_{pe} = effective-plastic-moment capacity of the section as defined under the heading Mechanism Method.

Ultracompact-Compression-Flange Sections

Plastic-rotation curves are plotted in Figure 3.11 for sections with ultracompact compression flanges and noncompact webs with different web slenderness ratios, D/t (Schilling 1991 and 1993). D is the web depth and t is the web thickness. These curves were developed from test results (Schilling 1990 and Shilling and Marcos 1988) that showed ultracompact flanges provide a considerable improvement in rotation characteristics even when used with noncompact webs.

Compression flanges are considered to be ultracompact when they satisfy the following requirement (Schilling 1989):

$$\frac{b}{2t_f} \le \frac{49.5}{\sqrt{F_y}} = 7.0 \text{ for 50 ksi steel} \tag{3.11}$$

where:

b = compression-flange width,

t_f = compression-flange thickness, and

F_y = yield stress (KSI).

The rotation curves in Figure 3.11 are applicable only if the compression-flange bracing requirements for inelastic design (AASHTO 1991 and 1994) are satisfied and a transverse stiffener is placed within a distance not exceeding one-half of the web depth on each side of the yield (pier) location (Schilling 1990 and Shilling and Marcos 1988). If this stiffener is placed on one side of the web only, it must be welded to the compression flange.

The descending portions of the rotation curves in Figure 3.11 represent a family of downward sloping parallel lines. Each curve in the family is defined by:

$$M/M_{max} = 1.00 - 0.0092(R - RL) \quad (3.12)$$

where:

R = plastic rotation corresponding to a moment M,

M_{max} = maximum-moment capacity of the section, and

RL = limiting plastic rotation at which the sloping line intersects the horizontal line corresponding to $M/M_{max} = 1$.

The following values of RL for different web slenderness ratios were derived from the test results (Schilling 1990 and Shilling and Marcos 1988), values for other slenderness ratios can be obtained by interpolation.

D/t	RL, (mrad)
80	65.1
100	45.2
120	30.8
140	20.2
160	10.7
163	9.3

The test results (Schilling 1990 and Shilling and Marcos 1988) showed that M_{max} can be taken as equal to the plastic-moment capacity, M_p, for web slenderness ratios up to 134 and can be obtained from the following equation for ratios between 134 and 170 (Eyre and Galambos 1970 and 1973).

$$\frac{M_{max}}{M_p} = 1.41 - \frac{0.00306D}{t} \quad (3.13)$$

Alternatively, M_{max} could be determined from the formulas for flexural resistance given in Articles 6.10.5.6 and 6.10.6.3.1 of the LRFD bridge specifications (AASHTO 1994).

3.3.5.2 Positive Bending

3.3.5.2.1Noncomposite Sections

For noncomposite sections, the rotation curves discussed previously for negative bending also apply to positive bending. Specifically the ascending portion of the curve can be assumed to remain elastic to the maximum moment, or one of the plastic-rotation curves in Figure 3.9 can be used if it is desired to consider the small effect of yielding at lower moments. For compact noncomposite sections,

the maximum-moment capacity is the plastic-moment capacity and the rotation curve can be assumed to remain horizontal thereafter. For noncompact noncomposite sections, the maximum-moment capacity is less than the plastic-moment capacity as defined previously and the plastic-rotation curves in Figures 3.10 and 3.11 are applicable.

3.3.5.2.2 Composite Sections

Autostress-Design Curve

Composite sections in positive bending are usually compact so that $M_{max} = M_p$. Such sections sustain a large amount of plastic rotation between the yield and plastic moments as discussed earlier. The plastic-rotation curves continue to rise after yielding starts and generally do not have a descending portion; failure usually results from crushing of the concrete in the top portion of the slab. This behavior can be represented by the curved line in Figure 12, which was developed (Schilling 1989, 1991 and 1993) from experimental data (Vasseghi and Frank 1987) specifically for use in the unified autostress method.

Inelastic-Rating Curve

A straight-line approximation of the rotation curve was proposed for use in the inelastic rating of bridges (Galambos et. al. 1993) and is based on earlier studies by Rotter and Ansourian (1979 and 1982). This approximation is defined by the equation in Figure 3.12, which depends on M_y/M_p and other parameters. Therefore, it was necessary to assume typical values of these parameters to allow a line representing this approximation to be plotted on the shown axes. The following typical values were assumed: M_p/M_y=1.3, k=0.0725, and Θ_{ep}=0.0167.

The equation actually proposed for inelastic rating was in a somewhat different form than the equation in the figure. Specifically, the total-rotation relationship defined by Equation 3.4, but with M_y substituted for M_{max}, was actually proposed (Galambos et. al. 1993). In the present study, Equations 3.5 and 3.6 plus the following equation were inserted into this total-rotation equation to get the equation in the figure, which defines the plastic rotation directly:

$$\Theta_{ep} = \frac{2M_pL}{3EI} \tag{3.14}$$

This equation defines the elastic rotation at M_p for a simple span of length L and loaded by a uniform loading; this rotation is 1/3 higher than that caused by a concentrated load that produces the

same moment. It is conservative and appropriate to use this equation, rather than Equation 3.7, because the rotation in positive bending results from a combination of distributed and concentrated loads (AASHTO 1994). For girders that are nonprismatic within L, Equation 3.14 provides an approximate value of θ_{cp} if I is taken as the average within L, but an exact value can be determined by an elastic deflection analysis that accounts for the variation of stiffness along the span.

The resulting plastic-rotation equation is

$$\frac{M}{M_p} = \frac{M_y}{M_p} + c\Theta_p \tag{3.15}$$

where:

M_y = total dead-and live-load moment that causes first yielding in the bottom flange as defined in Article 6.10.5.1.2 of the LRFD bridge specifications (AASHTO 1994).

Thus, M_y depends on the percentage of the total moment applied before and after the slab has hardened.

The slope, c, is defined by

$$c = \left(\frac{k}{1-k}\right)\left(\frac{3EI}{2LM_p}\right) \tag{3.16}$$

$$k = \frac{1-(M_y/M_p)}{1+A-(M_y/M_p)} \tag{3.17}$$

$$A = 1.6\left(\frac{0.41f_cA_g}{F_yA_s} - 1.6\right) \tag{3.18}$$

where:

f_c = compressive strength of the concrete,

F_y = yield stress of the steel section,

A_s = cross-sectional area of the steel section, and

A_g = gross area, which equals the effective width of the slab times the total depth of the composite section.

The relationship for A was developed by Rotter and Ansourian (1979 and 1982), who also proposed a relationship defining the cross-sectional proportions necessary to assure that premature

concrete crushing will not prevent the composite section from reaching its plastic-moment capacity. A modified version of this relationship is included in Article 6.10.5.2.2b of the LRFD bridge specifications (AASHTO 1994) and assures that the curves in Figure 3.12 will reach M_p.

3.3.6 Mechanism Method

3.3.6.1 Classical Theory

3.3.6.1.1 Basic Approach

The ultimate strength of a beam, girder, or frame is the maximum proportional loading it can sustain. Proportional loading means a set of individual concentrated and/or distributed loads applied in specified directions at specified locations and interrelated by specified ratios. The magnitude of the proportional loading is defined by a single factor that applies to all individual loads.

In a beam or girder subjected to downward loads only, three or more real and/or plastic hinges are required to form a mechanism as illustrated in Figure 3.13. Plastic hinges are shown as open circles in the figure and real hinges are shown as filled circles. Three-hinge mechanisms generally govern, but mechanisms consisting of four or more hinges are theoretically possible if there are changes in cross section within the girder. There are splices at the $-M_{p1}$ locations in the four-hinge mechanisms shown in the figure.

Valid three-hinge mechanisms consist of two negative-bending hinges with a positive-bending hinge between. The negative-bending hinges occur at piers, abutments, or splice locations. The invalid three-hinge mechanisms shown at the bottom of the figure are not valid because support from adjacent portions of the girder, or from piers, prevents free downward or upward movement at all hinge locations.

The strength of each mechanism (proportional loading that causes the mechanism) can be determined by isolating the mechanism from the rest of the structure and assuming that the moment at each plastic-hinge location is equal to the plastic-moment capacity at that location as illustrated in Figure 3.13. There are two different methods of calculating the magnitude of the proportional loading required to cause the assumed plastic moments: the virtual-work method and the statical method. Only loads and reactions applied within the mechanism need to be considered.

3.3.6.1.2 Virtual-Work Method

In the virtual-work method, a virtual deflection, Δ, is imposed at a central hinge and causes plastic rotations at all hinges and deflections of all individual loads. The total work caused by the individual loads moving through these different deflections is equated to the total internal work caused by the individual hinge moments rotating through different angles. The individual deflections and rotations are expressed as a function of Δ, which cancels out when the external and internal work are equated. In relating individual deflections and rotations to Δ, member segments between hinges are assumed to remain straight since only mechanism movements are being considered.

3.3.6.1.3 Statical Method

The statical method, which is sometimes considered to be a separate method from the mechanism method (ASCE 1971 and Beedle 1958 and Gaylord and Gaylord 1979), was utilized in the example illustrating ALFD procedures for bridges (AASHTO 1986 and 1991) and in other autostress designs (Grubb 1985 and 1989, Hourigan and Holt 1987 and Loveall 1986). In this method, two moment diagrams are combined in such a way that the moments at plastic hinge locations equal the plastic-moment capacities of the sections at these locations. The method can be applied to both three-hinge mechanisms and higher order mechanisms, but is simpler when applied to three-hinge mechanisms as described below.

For three-hinge mechanisms, the first moment diagram is for the plastic hinges at one or both ends of the mechanism. The second moment diagram defines the elastic simple-span moments for all loads applied within the mechanism; these moments are of the opposite sign to the moments in the first diagram. The second moment diagram can be increased or decreased by applying the same factor to all loads. The factor defining the strength of this particular mechanism results in combined moments (first and second moment diagrams) that just equal the plastic-moment capacity at the central hinge. The second moment diagram does not depend on stiffness variations along the length because it defines simple-span moments.

3.3.6.1.4 Selection of Mechanisms

To determine the ultimate strength of the girder, all possible mechanisms must be checked. The lowest strength (proportional loading) for any individual mechanism is the ultimate strength of the girder. All potential plastic-hinge locations for all possible positions of movable live loads must be

considered in selecting possible mechanisms. All pier locations, splice locations, cover-plate ends, and peak-moment locations are potential plastic-hinge locations.

For concentrated loads, peak-moment locations occur only at such loads and at piers. For distributed loads, peak-moment locations must be determined from the moment diagrams for the proportional loading under consideration. Elastic moment diagrams suggest approximate locations of peak moments, but do not indicate the exact locations because inelastic behavior causes a redistribution of the elastic moments.

Often peak-moment locations fall between two known hinge locations; for example, the peak positive-bending moment falls between the two known hinge locations at adjacent piers. In this case, the peak-moment location can easily be determined from the moment diagrams used to calculate the strength of the mechanism by the statical method. If the plastic-moment capacities at the two ends of the mechanism are equal and the mechanism is symmetrically loaded, the peak-moment location is at midlength.

Although use of the mechanism method for simple bridge cases is straightforward (AASHTO 1991, Grubb 1985 and 1989, Hourigan and Holt 1987 and Loveall 1986), it can be tricky to identify all possible mechanisms for more complex cases involving multiple unsymmetric spans, many splices, and many possible load positions.

3.3.6.2 Rotation Capacity

3.3.6.2.1 Significance

Considerable inelastic redistribution of moments is required to develop the moment diagrams assumed in calculating the strength of a mechanism. Specifically, the first plastic hinge to form sustains plastic rotation as moment is shifted to the other plastic hinges. Similarly, plastic rotation occurs in the second hinge to form as moment is shifted to the third hinge. The amount of plastic rotation required at any hinge to form the mechanism is called the required rotation capacity (Schilling and Marcos 1988) or hinge angle (ASCE 1971). The actual rotation capacity provided by the section at each hinge location must not be less than the required capacity at that location.

3.3.6.2.2Actual

Compact Sections

Compact sections that satisfy classical plastic-design assumptions have total-rotation curves similar to the top curve in Figure 3.14. The rotation curve rises above the plastic moment, remains above that moment until a large amount of rotation has been imposed, and then decreases below the plastic moment if additional rotation is imposed. The plastic rotation over which the curve remains above M_p is the actual rotation capacity of the section. If the required rotation capacity for a particular plastic hinge in a continuous-span girder does not exceed the actual rotation capacity at that location, the hinge moment can be conservatively taken as the full plastic moment in plastic-design calculations. Experience and trial designs have shown that compact sections usually provide more rotation capacity than is required for beam and girder applications (ASCE 1971, Beedle 1958, and Gaylord and Gaylord 1979).

Noncompact Sections

Noncompact sections have lower rotation curves similar to the curve illustrated in Figure 3.14. Typically such curves do not reach the plastic moment and start decreasing at lower rotations than the curve for compact sections. As illustrated in the figure, however, combinations of effective plastic moments, and corresponding rotation capacities, can be defined in a manner similar to that of the full plastic moment and corresponding rotation capacity. Specifically, the rotation capacity for a given effective plastic moment, M_{pc}, is the plastic rotation over which the moment exceeds M_{pc}. The effective plastic moment can be used in place of the full plastic moment in plastic-design procedures, such as the mechanism method, provided that required rotation capacity for the section does not exceed the rotation capacity corresponding to that effective plastic moment.

3.3.6.2.3Required

For a Given Girder

If classical plastic-design assumptions are applicable, the required rotation for each plastic hinge in a mechanism can be calculated as illustrated in Figure 3.15. First, the moment diagram corresponding to the ultimate strength of the mechanism is developed. The portion of the diagram within the mechanism is determined by the statical method explained previously. The portions to the left and right of the mechanism are determined by treating these portions as elastic members subjected

to the applied loads and to the appropriate plastic moments at ends connecting to the mechanism. Vertical loads may also need to be applied to the ends of the elastic members to simulate the shear that can be transmitted through plastic hinges.

It is then assumed that the entire girder is elastic except for plastic rotations (angular discontinuities) at all plastic hinges except the last to form. Continuity (no angular discontinuity) is assumed to exist at the last hinge just prior to the formation of the mechanism. Next, the plastic rotations at the hinges are calculated for the known moment diagram by using any convenient method of elastic deflection analysis. The slope-deflection and dummy-load methods are often recommended for building applications (Beedle 1958 and Gaylord and Gaylord 1979) and the dummy-load method has been used in bridge applications (Axhag 1995).

Consider, for example, calculation of the plastic rotations at B and D in Figure 3.15 if the hinge at C forms last. The portion of the girder between B and D behaves as a simple span subject to the known moment diagram, which results from the applied concentrated and uniform load and from negative moments equal to M_p at the ends. Therefore, the end slopes at B and D can be calculated elastically. Similarly, the portion of the girder between A and B behaves as a simple beam loaded by the uniform load and a negative end moment at B equal to M_p. Again, the end slope at B can be calculated elastically. The difference between the two end slopes at B is equal to the angular discontinuity there. The portion of the girder between D and F behaves as a continuous span loaded by the uniform load and a negative moment equal to M_p at D. The difference between the end slopes at D is the angular discontinuity there. If it is not known which plastic hinge will be the last to form, trial calculations must be made with each plastic hinge in the mechanism assumed to be the last to form. The correct hinge is the one that results in the largest deflections (Beedle 1958 and Gaylord and Gaylord 1979).

For noncompact sections, the correct required rotation capacity, θ_{pr}, cannot be calculated by substituting M_{pc} for M_p in the procedures discussed above. If this were done the calculated angular discontinuities at plastic hinges would generally not satisfy the appropriate rotation relationships for those sections. In other words, a point defined by the corresponding values of M_{pc} and θ_{pr} would generally not fall on the rotation curve for the section. This is not a problem for compact sections because it is assumed that the rotation remains constant at M_p after yielding starts; thus, the corresponding values of M_p and θ_{pr} fall on the assumed rotation curve.

The correct required rotation for any case, however, can be obtained from methods, such as the unified autostress method and the residual-deformation method, that satisfy both the continuity and rotation relationships. Alternatively, conservative values of θ_{pr} can be obtained by calculating θ_{pr} for the M_p, rather than M_{pc}, in the procedures discussed earlier; this will result in a higher θ_{pr}.

For Typical Bridges

Required rotation capacities rarely need to be calculated in designing actual structures by plastic-design procedures (ASCE 1971, Beedle 1958, and Gaylord and Gaylord 1979). Instead, experience and trial designs have been used to establish a practical upper bound for the required rotation capacity of certain classes of structures. For example, experience and trial designs have shown that the rotation capacity provided by compact sections exceeds the required rotation capacity for typical building beams and frames (Beedle 1958 and Gaylord and Gaylord 1979). Therefore, required rotation capacities need not be calculated for such structures.

At the time autostress (ALFD) procedures were first developed (Haaijer et. al. 1987), the compactness requirements for plastic design of buildings (AISC 1978) were more restrictive (slenderness limits were lower) than present compactness requirements for buildings (AISC 1993) and bridges (AASHTO 1994). At that time, it was assumed that sections satisfying these earlier plastic-design compactness requirements provide sufficient rotation capacity for bridge applications (Haaijer et. al. 1987). The assumption that these earlier compactness requirements provide sufficient rotation capacity for bridges has been retained in present inelastic bridge design specifications (AASHTO 1991 and 1994).

For bridge sections that do not satisfy these compactness requirements, however, it would be helpful to establish a practical upper-bound required rotation capacity for bridge applications. Such an upper bound could then be used in developing appropriate M_{pc} formulations for bridges as described in the next section. Since it is often efficient to use noncompact sections at piers, the required rotation capacity at such locations is particularly needed.

A limited amount of information is available on required rotation capacities for negative-bending sections in bridge beams and girders designed by inelastic procedures. Specifically, 50 preliminary autostress designs were made for a range of design parameters (Schilling 1986); the noncompact-section rotation curve shown in Figure 3.10 was used for the pier sections in most of these designs. The plastic rotations at pier sections in the Maximum Load check ranged up to 29 mrad

(1 mrad = 0.001 radian), but were usually considerably less. Also, the required rotation capacity for the pier section of a two-span continuous bridge analyzed in a previous autostress study (Carskaddan 1976) was reported to be 11 mrad. These data suggest that 30 mrad would be a suitable upper-bound value of the required rotation capacity for negative-bending sections in bridges. Further trial design studies, however, would be desirable to better establish this value.

3.3.6.3 Effective-Plastic-Moment Capacity

3.3.6.3.1From AASHTO Equations

Development and Usage

Empirical relationships were developed in autostress studies (Carskaddan et. al. 1982, Grubb and Carskaddan 1981 and Haaijer et. al. 1987) to define the effective-plastic-moment capacity of negative-bending sections in bridges. These relationships were incorporated into inelastic bridge design specifications (AASHTO 1991 and 1994). Specifically, the following equations define effective yield stresses for the steel flanges and web as a function of their slenderness ratios:

$$F_{yec} = 0.0845E(2t_c / b_c)^2 \leq F_{yc} \tag{3.19}$$

$$F_{yew} = 5.28E(t_w / 2D_{cp})^2 \leq F_{yw} \tag{3.20}$$

$$F_{yet} = F_{yec} \leq F_{yt} \tag{3.21}$$

where:

t_c = compression flange thickness,

b_c = compression-flange width,

t_w = web thickness,

D_{cp} = depth of web in compression at the plastic moment,

E = modulus of elasticity,

F_y = actual yield stress,

F_{ye} = effective yield stress, and

the subscripts c, t, and w denote the compression flange, tension flange, and web.

These effective yield stresses can then be used to calculate the corresponding effective plastic moment, M_{pe}, in the same way that the full plastic moment is calculated. If rebars are included in the

section the full yield stress is used for these rebars. The empirical relationship applies the effective yield stress for the compression flange to both flanges even though the tension flange is not subject to local buckling (Carskaddan et. al. 1982, Grubb and Carskaddan 1981 and Haaijer et. al. 1987).

By letting F_{ye} equal F_y in Equations 319 and 320, the following limiting slenderness ratios can be derived:

$$\left(\frac{b_c}{2t_c}\right)_L = 0.291\sqrt{\frac{E}{F_y}} \tag{3.22}$$

$$\left(\frac{2D_{cp}}{t_w}\right)_L = 2.30\sqrt{\frac{E}{F_y}} \tag{3.23}$$

If the actual slenderness ratios do not exceed these limiting ratios, the section is fully effective and M_{pe} equals M_p. These limiting ratios correspond to the 1978 compactness requirements for plastic design of buildings (AISC 1978), which were in effect at the time the effective-plastic-moment relationships were developed (Carskaddan et. al. 1982, Grubb and Carskaddan 1981 and Haaijer et. al. 1987).

Limits of Applicability

In the inelastic bridge specifications (AASHTO 1991 and 1994), applicability of the effective-plastic-rotation relationships defined by Equations 3.19 to 3.21 are specifically limited to compact sections as defined by the following slenderness limits:

$$\left(\frac{b_c}{2t_c}\right)_L = 0.382\sqrt{\frac{E}{F_y}} \tag{3.24}$$

$$\left(\frac{2D_{cp}}{t_w}\right)_L = 3.76\sqrt{\frac{E}{F_y}} \tag{3.25}$$

Thus, the AASHTO M_{pe} equations (Equations 3.19 to 3.21) are applicable only between the limits defined by Equations 3.22 and 3.23 and the limits defined by Equations 3.24 and 3.25.

Studies (Carskaddan et. al. 1982, Grubb and Carskaddan 1981 and Haaijer et. al. 1987) of a considerable amount of experimental data showed that within these limits of applicability, the actual rotation capacities corresponding to the AASHTO M_{pe} exceed 60 mrad. Subsequent studies (Schilling 1985, 1988 and 1990, and Schilling and Morocos 1988) showed that the actual rotation capacities corresponding to M_{pe} may be considerably less if Equations 3.19 to 3.21 are applied beyond the range

of applicability defined by Equations 3.24 and 3.25. Specifically, the actual rotation capacities corresponding to the AASHTO M_{pc} ranged from 34 to 70 mrad for noncompact sections (Schilling 1985 and 1988) and sections with ultracompact flanges and noncompact webs (Schilling 1990 and Schilling and Morocos 1988). These results suggest that the AASHTO M_{pc} can be safely applied beyond the present limits of applicability since the corresponding actual rotation capacities exceed the 30 mrad required rotation capacity suggested earlier for bridges.

If the AASHTO M_{pc} equations are applied to noncompact sections, however, M_{pc} should not be permitted to exceed M_{max} as defined by appropriate specification equations. Generally, the M_{pc} equation will not give values higher than M_{max}, but there is no theoretical assurance of that since the M_{pc} equations are empirical.

3.3.6.3.2From Typical Rotation Curve

As an alternative to the empirical equations, M_{pc} can be taken as the moment corresponding to a plastic rotation equal to the required rotation capacity on the rotation curve assumed for the section under consideration. As indicated earlier, 30 mrad is a reasonable required rotation capacity for use the mechanism method.

3.3.7 Shakedown Check

Shakedown can be checked by either (a) calculating the shakedown loading for the girder, that is the largest sequential loading that will result in shakedown in that girder, or (b) calculating whether a given sequential loading will achieve shakedown in a given girder. The latter calculation is somewhat simpler and is generally sufficient for design purposes. As explained earlier, the magnitude of the sequential loading is defined by a single factor that applies to all individual loads in the sequence.

There are two basic methods of making either of the calculations mentioned above: permanent-deflection analysis or assumed redistribution moments. Permanent-deflection analysis requires considerably more work than assuming redistribution moments, but provides the final permanent deflections and plastic rotations for the given sequential loading. In contrast, the method of assuming redistribution moments indicates whether a given sequential loading will achieve shakedown, but does not provide the resulting permanent deflections and plastic rotations. The two methods are discussed separately below.

3.3.7.1 Permanent-Deflection Analysis

3.3.7.1.1 Check a Given Loading

The two methods described earlier for calculating redistribution moments and permanent deflections, the unified autostress method and the residual-deformation method, can be used to make a shakedown check. Specifically, shakedown will occur for a given sequential loading if a solution can be found for the elastic moment envelope corresponding to the given sequential loading. Otherwise, iterative procedures used in the analysis will not converge, or simultaneous equations used in the analysis will not provide a feasible solution.

3.3.7.1.2 Determine the Shakedown Loading

To determine the shakedown loading for a given girder, that is the highest sequential loading that results in shakedown, progressively larger sequential loadings must be analyzed until a loading is found that does not provide a solution. This process usually requires a considerable amount of work since each individual analysis often requires iterations.

3.3.7.2 Assumed Redistribution Moments

3.3.7.2.1 Check a Given Loading

Moment Check at All Sections

Shakedown can be checked for a given sequential loading by simply assuming the redistribution moments as illustrated in Figure 3.16 and checking that the algebraic sum of these redistribution moments and the elastic moment envelope does not exceed the effective-plastic-moment capacity at any location. Thus, the following equation must be satisfied at all locations:

$$|M_{pe}| \geq |M_e + M_r| \tag{3.26}$$

where:

M_e = moment from the elastic moment envelope for combined dead and live load plus impact,

M_{pe} = effective-plastic-moment capacity, and

M_r = is the redistribution moment.

For composite girders, the moments for loads applied before and after the slab has hardened should be combined into a single moment envelope defining M_e. The correct signs must be assigned to the moments in the equation.

If the Equation 3.26 is not satisfied at a particular positive-bending location, the girder cross section can be changed either at that location or at adjacent pier locations to satisfy the deficiency. Similarly, if the check shows that particular positive-bending regions are over-designed, changes can be made either at those locations or at adjacent pier locations to improve the economy of the girder. If the equation is not satisfied at splice locations in negative-bending regions the splice locations must be moved.

Redistribution-Moment Diagram

The positive redistribution moment at each pier should be assumed to be equal to the absolute difference between the negative elastic moment envelope and the negative effective-plastic-moment capacity at the pier. This is the smallest M_r that satisfies Equation 3.26 at the pier; a larger M_r would satisfy Equation 3.26 at the pier, but would make it harder to satisfy that equation in positive-bending regions.

Since the redistribution moments must vary linearly between reactions as discussed earlier, the full redistribution moment diagram can be obtained by connecting the pier moments by straight lines and extending these lines from the first and last piers to the zero moments at adjacent abutments. These redistribution moments are the assumed final redistribution moments caused by all yielding at positive- and negative-bending locations due to the loadings defined by the elastic moment envelope.

Effective Plastic Moment

It is conservative to use M_{pe} values based on the required rotation capacity of 30 mrad suggested for mechanism checks because the plastic rotations occurring at shakedown are less than those required to form a mechanism. Therefore, either the M_{pe} defined by Equations 3.19 to 3.21 or the M_{pe} corresponding to a plastic rotation of 30 mrad on a typical rotation curve is appropriate for composite or noncomposite sections in negative bending and for noncomposite sections in positive bending. For composite sections in positive bending, however, M_{pe} equals M_p if the web is compact, which is usually the case because of the location of the neutral axis. Such sections provide an adequate rotation capacity for the shakedown check as discussed earlier.

It would eventually be desirable to determine a required rotation capacity specifically for use in shakedown checks. This could be done by calculating the final rotations at piers in trial inelastic designs covering a practical range of bridge parameters. Either the unified autostress method or the residual-deformation method should be used in these trial designs to properly account for the effects of positive-bending yielding, especially in composite sections. Also, the elastic moment envelopes for the factored dead and live loads specified for the strength limit state in the LRFD bridge specifications (AASHTO 1994) should be used in such calculations. It is expected that the required capacity determined in this way will be less than 30 mrad.

3.3.7.2.2Determine the Shakedown Loading

The shakedown loading for a given girder can be determined in the following way. First, express the elastic moment envelope and all pier redistribution moments as a function of the factor defining the magnitude of the sequential loading. In developing expressions for the pier redistribution moments these moments should again be assumed to be equal to the absolute difference between the negative elastic moment envelope and the negative effective-plastic-moment capacity at the pier.

Next, each potential yield location except pier locations must be investigated to determine the highest loading factor that will satisfy Equation 3.26 at that location. The resulting equation at each location depends on the variation of stiffness along the girder, which controls the elastic moment envelope, and involves the M_{pe} at that location and at adjacent pier locations. Each equation is sufficient to define the loading factor for the location; and the lowest factor for any location defines the shakedown loading for the given girder.

3.4 LIMIT STATES

3.4.1 Strength

3.4.1.1 LRFD Bridge Specifications

3.4.1.1.1Dead and Live Loading

In the LRFD bridge specifications (AASHTO 1994), the same loading consisting of dead load plus a combination of truck (or design tandem) and lane live load plus a dynamic allowance (impact) is used in the strength-limit-state check for both elastic and inelastic designs. The live loads are applied to all design lanes, and a multiple-presence factor that depends on the number of loaded lanes is applied to

these live loads. The truck has the same weight and configuration as the HS20 truck used in previous AASHTO bridge specifications (AASHTO 1992).

One truck per lane is applied in calculating positive moments. Two trucks per lane spaced at least 50 feet apart (front to rear) are used to calculate negative moments, but the moments thus calculated (including the moments for the lane loading) are multiplied by a factor of 0.9 to get the design live load moments.

The live-load moment determined from these specified unfactored loads is intended (AASHTO 1994 and Kulicki and Mertz 1991) to approximate the elastic moment caused by "a group of vehicles routinely permitted on highways of various states under grandfather exclusions of weight laws." For simple spans, the maximum moments that will occur during the assumed 75-year life of the bridge as a result of heavy traffic are predicted to be about 25% higher than those for the specified unfactored live loading (Nowak 1995). This value of 25% is the mean value predicted from statistical data on highway traffic; for 50% of the bridges in the United States, the maximum moments will be higher. For one-lane bridges, these maximum moments for a 75-year life result from the single heaviest truck that passes over the bridge during this life (Nowak 1993 and 1995 and Nowak and Hong 1991). For a two-lane bridge, these maximum moments for a 75-year life result from two trucks placed side by side, each having a weight about 85% of the heaviest truck for the 75-year life.

For the strength-limit-state (Strength I) check, a factor of 1.75 is applied to the specified live loading described above. This factor, together with other load and resistance factors, is intended to provide a reliability index, β, of 3.5 (AASHTO 1994), which assures that the probability of failure due to the maximum moments that occur during the 75-year life is acceptably low.

3.4.1.1.2Elastic Design

In elastic design (AASHTO 1994), the strength-limit-state check requires that the elastic moments caused at all locations by the specified loading (loadings described above times appropriate load factors) shall not exceed the maximum-moment capacities at these locations. The maximum-moment capacities generally range from the yield-moment capacity to the plastic-moment capacity; equations defining this maximum-moment capacity are given for various types of sections. This method of checking the strength limit state does not assess the true ultimate strength of continuous-span girders, which may be considerably higher than the allowed strength due to inelastic redistribution of moments.

3.4.1.1.3Inelastic Design

In inelastic design, the strength-limit-state check requires that the specified loading shall not cause a mechanism. This can be checked by either the mechanism method or the unified autostress method (AASHTO 1994). The effective plastic moment defined by Equations 3.19 to 3.21 is used in the mechanism check. All possible mechanisms must be checked as explained previously under the heading Mechanism Method. The inelastic design procedures are limited to steels with yield stresses not exceeding 50 ksi and to compact sections as defined by specified slenderness limits that apply to both elastic and inelastic design. These inelastic procedures assess the true ultimate strength of continuous-span girders, but do not consider the effects of moving loads.

3.4.1.1.4Load Combinations

Although the basic strength check (Strength I) includes only the factored dead, live, and impact loads described previously, load combinations that also include wind and/or temperature gradient may need to be considered as specified in Article 3.3.4 (AASHTO 1994).

Wind

The specifications (Article 4.6.2.7) give an approximate method of calculating the lateral wind moments in the flanges of exterior girders. For inelastic designs or elastic designs involving compact sections, however, the stresses caused by these wind moments cannot be combined with elastic stresses due to dead and live loads to check strength. This is true because compact sections are designed to sustain the plastic moment, which theoretically causes yielding of the entire cross section.

Instead of combining elastic stresses due to wind and other loads, therefore, it is assumed that the lateral wind moment is carried by a fully yielded width at each edge of the loaded flange, and that only the remaining portion of the cross section is available to carry vertical loads. This remaining portion is used in calculating the maximum-moment capacity of sections being checked for wind in combination with vertical loadings. LRFD Equation 6.10.5.7.1-1 defines the reduced width of flange available for carrying vertical loadings (AASHTO 1994).

Temperature Gradient

The LRFD bridge specifications (AASHTO 1994) do not require that temperature gradients be included in the load combinations that must be checked for steel beams and girders. Specifically, they state the following in Commentary Article C3.12.3: "If experience has shown that neglecting temperature gradient in the design of a given type of structure has not led to structural distress, the

Owner may choose to exclude temperature gradient. Multi-beam bridges are an example of a type of structure for which judgment and past experience should be considered."

3.4.1.2 Inelastic Rating Procedures

Shakedown was recommended as the appropriate limit state for the strength check in the proposed inelastic rating procedures (Galambos et. al. 1993). A computer program based on inelastic grid analysis (Barker 1990 and Barker and Galambos 1992) was developed to check this limit, but is applicable only to noncomposite compact sections. In the computer program, design trucks are repeatedly passed across the bridge in appropriate positions within the design lanes until the permanent deflections stabilize (Galambos et. al. 1993). A complete inelastic grid analysis is performed for each longitudinal position of the trucks and the resulting redistribution moments and plastic rotations for each position are input as starting values for the next position.

3.4.1.3 Proposed New Procedures for Inelastic Design

3.4.1.3.1 Justification

As explained earlier, repeated applications of a sequence of loadings to a continuous-span girder, such as a truck moving across a bridge several times, can theoretically cause incremental collapse even if none of the individual loadings in the sequence causes a mechanism. Thus, the ultimate strength of the girder as defined by the mechanism method considering all possible mechanisms for the sequence of loadings is higher than the shakedown loading. Studies suggest that the difference usually does not exceed 15% for continuous spans (ASCE 1971).

Several factors, however, tend to reduce the risk of incremental collapse in actual bridges. Tests have shown that shakedown almost always occurs at higher sequential loadings than predicted by theory because of strain hardening (ASCE 1971). These results are for static tests in which loads and deflections were allowed to stabilize after each loading in the sequence. Because of the dynamic yielding behavior discussed earlier, only a small amount of the yielding theoretically predicted for a given truck will occur during a single passage of that truck across the bridge. This is true even if the truck moves at a relatively slow speed since several minutes is required to fully stabilize loads and deflections after a load application in the inelastic range. Thus, higher loadings than theoretically predicted, and many repetitions of these loadings, are required to produce incremental collapse in bridges.

In spite of these mitigating factors, incremental collapse should not be ignored when moving loads are involved. Consequently, shakedown is the most appropriate limit for defining the true strength of a bridge as stated in the development of inelastic rating procedures for bridges (Galambos et. al. 1993). Shakedown also has the major advantage that it is much easier to determine than ultimate strength calculated by the mechanism method. In checking shakedown by the assumed-redistribution-moments method, the entire girder is checked in one simple operation; no simultaneous equations or iterative procedures are required. In the mechanism method, in contrast, all possible mechanisms must be individually identified and checked. This can be tricky and involves considerable work if there are many splices and/or unsymmetric spans as discussed earlier. For these reasons it is proposed that shakedown be used as the strength limit for the inelastic design of bridges.

3.4.1.3.2Implementation

To implement the proposed strength limit for inelastic design, the specifications should specify that one of the following two alternative requirements shall be satisfied for the factored strength loadings presently specified (AASHTO 1994), which are the appropriate loadings for a shakedown check.

Simplified Approach

The first alternative requirement is that the following equation be satisfied at all locations:

$$|\phi_{sd} M_{pc}| \geq |M_e + M_r| \tag{3.27}$$

where:

M_e = moment from the elastic moment envelope for dead and live loading plus impact,

M_r = redistribution moment established as explained below,

M_{pc} = effective-plastic-moment capacity of the section for bending in the same direction as M_e, and

ϕ_{sd} = resistance factor for shakedown.

The correct signs must be assigned to the moments in this equation. For composite girders, the moments for loads applied before and after the slab has hardened should be combined into a single moment envelope defining M_e.

M_{pe} should be based on a required rotation capacity of 30 mrad. For composite and noncomposite sections in negative bending and noncomposite sections in positive bending, therefore, M_{pe} can be either calculated from Equations 3.19 to 3.21 or taken as the moment corresponding to a plastic rotation of 30 mrad on a typical rotation curve for the section. For composite sections in positive bending, M_{pe} equals M_p if the web is compact, which is usually the case because of the location of the neutral axis. Such sections provide an adequate rotation capacity as discussed earlier.

For the special case of pier sections having an ultracompact compression flange:

$$\frac{M_{pe}}{M_{max}} = 1.0 \text{ for } \frac{2D_{cp}}{t} \le 120\sqrt{\frac{50}{F_{yc}}} \tag{3.28}$$

$$\frac{M_{pe}}{M_{max}} = 1.56 - 0.00462\left(\frac{2D_{cp}}{t}\right) \text{ for } \frac{2D_{cp}}{t} > 120\sqrt{\frac{50}{F_{yc}}} \tag{3.29}$$

where:

M_{max} = maximum-moment capacity of the section as defined by Equation 3.13 or by appropriate specification formulas,

D_{cp} = depth of the web in compression at the plastic moment,

t = web thickness, and

F_{yc} = yield stress of the compression flange in ksi.

Equations 3.28 and 3.29 define the moment corresponding to a plastic rotation of 30 mrad in Figure 3.11.

Equation 3.29 is applicable to web slenderness ratios not exceeding the maximum permitted without a longitudinal stiffener in Article 6.10.5.3.2b of the LRFD bridge specifications (AASHTO 1994). Also, a transverse stiffener must be placed a distance one-half the web depth on each side of the pier and if these stiffeners are placed on only one side of the web they must be welded to the compression flange.

In developing Equation 3.29, the results in Figure 3.11, which applies specifically to symmetrical sections of 50-ksi steel, were generalized to also apply to unsymmetric sections and other steels. First, $2D_{cp}$, the depth of the web in compression at the plastic moment, was substituted for D. Next, the $2D_{cp}/t$ values of 120, 140, and 160 corresponding to three curves were multiplied by the square root of $50/F_{yc}$ to express them as a function of the yield stress of the compression flange. This is

consistent with the widely accepted assumption that limiting slenderness ratios are inversely proportional to the square root of the yield stress. Finally, the M_{pe}/M_{max} values corresponding to 30 mrad were calculated for each curve and a straight line defining these values as a function of the slenderness parameter was fit to the results.

At each pier, the redistribution moment should be taken as

$$M_r = \phi_{sd} M_{pe} - M_e \geq 0 \qquad (3.30)$$

Again the correct sign must be used for M_e, and M_{pe} is for bending in the same direction as M_e. Normally, M_e and M_{pe} are negative and M_r is positive. If M_{pe} is numerically larger than M_e, no redistribution of moment occurs and M_r is zero; this means that the pier section is over-designed for this limit state. The full redistribution-moment diagram can be obtained by connecting the pier redistribution moments with straight lines and extending these lines from the first and last piers to the zero moments at adjacent abutments.

It is proposed that the resistance factor, ϕ_{sd}, be taken as 1.10 since many truck passages would be required to cause incremental collapse and ample visual warning would be provided by the progressively increasing permanent deflections before actual failure. Furthermore, the specified loading for this limit state is based on the single maximum moments expected to occur during the life of the bridge. Therefore, the additional loading cycles required to develop large permanent deflections would be of progressively smaller magnitudes. Also, inelastic lateral redistribution of moments provides an additional reserve strength not accounted for in this single-girder check.

Rigorous Approach

The second alternative requirement is that the beam or girder be analyzed for the specified factored loading by either the unified autostress method (Schilling 1989, 1991 and 1993) or the residual-deformation method (Dishongh 1990 and 1992 and Dishongh and Galambos 1992) and that a feasible solution be found. If the specified loading exceeds the shakedown loading a feasible solution cannot be found. The elastic moment envelope should be used in either of these analyses. For composite girders, the moments for loads applied before and after the slab has hardened should be combined into a single moment envelope defining M_e.

The typical rotation curves discussed under the heading Typical Rotation Curves should be used in the analysis by either method, but these curves should be scaled upward by the resistance

factor, ϕ_{sd}, to be consistent with the first alternative requirement. Specifically, the moments corresponding to the plastic rotations at all points on the curve should be increased by the factor of 1.10.

3.4.1.3.3Load Combinations

Wind

In checking the shakedown limit for load combinations that include wind, it should be assumed that all vertical loadings are carried by the reduced cross sections remaining after widths of wind-loaded flanges are assigned to carry the lateral wind moments defined in LRFD Article 4.6.2.7 (AASHTO 1994). LRFD Equation 6.10.5.7.1-1 defines the reduced width of flange available to carry vertical loadings.

Specifically, the reduced section should be used in calculating the effective-plastic-moment capacity, M_{pe}, or the maximum-moment capacity, M_{max}, of the section for given effective or actual yield stresses. M_{pe} or M_{max} calculated in that way should be used in Equations 3.27 and 3.30 and also in defining rotation curves for use in the unified autostress or residual-deformation methods. However, slenderness ratios used in Equation 3.19, or to satisfy compactness requirements, should be based on the full flange width. Also, stiffnesses used in calculating the elastic moment envelope should be based on the full cross section.

Temperature Gradient

As mentioned previously, the LRFD bridge specifications(AASHTO 1994) do not require that temperature gradients be included in the load combinations that must be checked for steel beams and girders. However, the moments caused by temperature gradients can be considered by simply including them in the elastic moment envelopes used in the check. A temperature gradient through the depth of a simple-span girder causes bowing, but no moments. In continuous-span girders, piers restrain the bowing and cause elastic moments that vary linearly between reactions like redistribution moments. These moments, like redistribution moments, can be determined by calculating the pier reactions necessary to force the unrestrained bowed girder onto the piers (Axhag 1995).

3.4.2 Permanent Deflection

3.4.2.1 LRFD Bridge Specifications

3.4.2.1.1Purpose

Control of permanent deflection is a service limit state intended (AASHTO 1994) "to prevent objectionable permanent deflections due to expected severe traffic loadings which would impair rideability." It corresponds to the overload check in previous AASHTO bridge specifications (AASHTO 1992). This check was first introduced into the specifications when load-factor design (LFD) was adopted in 1973 for steel bridges (AASHTO 1973). It applied only to load-factor design. A check of permanent deflections was not required for allowable-stress design (ASD), which was permitted in the same specifications and had been in effect for many years (AASHTO 1973 and 1994). Development of the LFD provisions including overload requirements is described in an AISI bulletin (Vincent 1969).

Although objectionable permanent deflections had not occurred in bridges designed by allowable-stress procedures, it was thought that permanent-deflection limits were needed for load-factor design because it utilized the plastic-moment capacity for compact sections and was expected to permit modest reductions in section sizes with corresponding increases in the stresses caused by actual traffic. For example, the average steel-weight reduction provided by LFD was 10.6% in 18 trial designs comparing LFD and ASD procedures (Vincent 1969). It was also thought that permanent-deflection criteria were needed to establish weight limits for overweight permit vehicles.

3.4.2.1.2Dead and Live Loading

The original overload check involved a loading of D+(5/3)L(1+I), where D is the dead load, L is the service live load (usually either an HS20 truck or lane load), and I is the impact. This factored live load was intended (AASHTO 1973) to represent overloads "that can be allowed on a structure on infrequent occasions without causing permanent damage." Thus, it is an appropriate limit for overweight permits that can be granted routinely.

The factor of 5/3 applied to service live loads in all lanes was said (Schilling 1989 and Wright and Walker 1971) to be "approximately equivalent to a double live load in one lane of a multilane bridge with no other vehicle on the structure." A maximum loading of

1.25[D+(5/3)L(1+I)] was used in checking strength; (AASHTO 1973) thus, the overload was 80% of the maximum design load.

In the LRFD bridge specifications (AASHTO 1994), the live-load factor for the permanent-deflection check is 1.3 for both elastic and inelastic design. This factored live load (Service II) is 74% of the maximum design loading (Strength I) used in the strength check, which provides a reliability factor of about 3.5. As noted previously, the maximum live loading expected during the life of the bridge is about 25% above the specified unfactored loading (Nowak 1995); this percent applies specifically to simple spans. Thus, the factored live loading specified for the permanent-deflection check is slightly higher (1.30 vs. 1.25) than the maximum loading expected during the life of the bridge. The live-load factor is used with resistance factors of 1.00 since that is the factor normally used for service limit states (AASHTO 1994). Load combinations including wind or temperature gradient need not be considered for the permanent-deflection service limit state.

3.4.2.1.3Elastic Design

In the original overload check (AASHTO 1973), the elastic stresses caused by the specified loading were limited to 95% of the yield stress for composite sections and 80% of the yield stress for noncomposite sections. These limiting stresses were developed (Vincent 1969) from the results of the AASHO road tests (HRB 1962a and 1962b). The permanent deflections were less than 1 inch within the 50-foot simple span for two composite beams subjected to measured stresses 81 to 88% of the yield stress and for three noncomposite beams subjected to measured stresses 75 to 79% of the yield stress. The permanent deflection was 3.4 inches within the 50-foot span for one noncomposite beam subjected to measured stresses 90% of the yield stress. All of these permanent deflections are the final values after about 500,000 load cycles. No attempt was made to determine the actual magnitude of permanent deflections that would be objectionable with respect to riding quality.

In the LRFD bridge specifications (AASHTO 1994), the elastic stresses in both positive- and negative-bending regions are limited to these same percentages of the yield stress: 95% for composite sections and 80% for noncomposite sections. The 95% limit applies to negative-bending composite sections consisting of the steel section plus longitudinal rebars.

3.4.2.1.4Inelastic Design

For inelastic design, the LRFD bridge specifications (AASHTO 1994), and the guide specifications for ALFD (AASHTO 1991), permit yielding at pier locations under the specified loading,

but limit the stresses in positive-bending regions after inelastic redistribution of moments to the same percentages of the yield stress as for elastic design. Thus, the yielding permitted at piers is limited by the positive-bending stress limit. The pier yielding shifts moment from piers to positive-bending regions.

The inelastic redistribution of moments is calculated by the beam-line (Carskaddan et. al. 1982, Disque 1964 and Haaijer et. al. 1987), unified autostress (Schilling 1989, 1991 and 1993), or residual-deformation method (Dishongh 1990 and 1992 and Dishongh and Galambos 1992) using one of the rotation curves in Figure 3.9 to define the ascending portion of the plastic-rotation curve for pier sections. Specifically, the positive redistribution moments due to the specified loading that causes maximum moments at the piers (live loads straddling the pier) are combined with positive applied moments due to the specified loading that causes maximum positive moments (live loads within the span) (Schilling 1986 and 1989). Positive stresses due these combined moments are limited to 95% or 80% of the yield stress.

For more than two continuous spans, the redistribution moments caused by live loading straddling one pier may be changed when the live loading is moved to straddle the next pier. Consequently, it is specified (AASHTO 1994) that "the two spans adjacent to each interior support shall be successively loaded until the resulting redistribution moments converge within acceptable limits." Simultaneous equations or iterative procedures are usually required to calculate redistribution moments for each successive loading when there are more than two continuous spans.

3.4.2.1.5Reliability

In developing the LRFD bridge specifications (AASHTO 1994), no attempt was made to assess the reliability factor, β, associated with the permanent-deflection limit state, or the probability that this limit state will be violated. However, the specified permanent-deflection check is considered to be very conservative for the following reasons:

- Numerous field measurements have shown that the actual stresses in bridges under traffic loading are almost always well below those calculated by normal design procedures (Moses et. al. 1987 and Schilling 1989 and 1990). Many factors contribute to this difference including: (a) unintended composite action, (b) contributions to strength from nonstructural elements, such as parapets, (c) unintended partial end fixity at abutments, (d)

catenary tension forces due to "frozen" joints or rigid end supports, (e) longitudinal distribution of moment, and (f) direct transfer of load through the slab to the supports.

- The moments caused by the specified factored live loading approximate the maximum moments expected during the life of the bridge (Nowak 1995). Because of dynamic yielding effects, many loading cycles (truck passages) would be required to develop the full theoretical permanent deflections; this effect was illustrated in the AASHO road tests (HRB 1962a and 1962b). The moments caused by these additional load cycles must be lower than the maximum since bridges are subjected to a continuous spectrum of moments of varying magnitudes and the specified loadings correspond to the maximum of these.
- The specified limiting stresses (95% and 80% of yield stress) are considered to be conservative, especially for noncomposite sections, since numerous static beam tests have shown that permanent deflections caused by yielding below the yield moment are usually small enough to be neglected (ASCE 1971 and Beedle 1958). This suggests that the yield stress, rather than 80 to 95% of the yield stress, would be an appropriate limit for the permanent-deflection check.
- The consequences of violating the permanent-deflection limit state are much smaller than the consequences of violating the strength limit state. Therefore, a considerable lower reliability factor is justified for the permanent-deflection check.
- Little or no evidence of objectionable permanent deflections in steel bridges subjected to normal traffic loading for many years has been reported. This includes many bridges designed for lower loadings than are now specified. Many steel bridges are now older than 50 years and a few are approaching 100 years old.

3.4.2.2 Inelastic Rating Procedures

The serviceability limit state in the proposed inelastic rating procedures (Galamobos et. al. 1993) is based on a permanent-deflection limit specified by the rating authority. In calculating the live loading corresponding to this limit, a total-rotation curve that is linear to the maximum-moment capacity is used for pier sections. Thus, the small amount of permanent deflection that occurs below the plastic moment in compact sections, and below the yield moment in noncompact sections, is

neglected. This is consistent with assumptions made in the plastic design of buildings (ASCE 1971, AISC 1993 and Beedle 1958), and simplifies calculations of permanent deflections.

3.4.2.3 Proposed New Procedures for Inelastic Design

Two alternative computational limits are proposed to check the permanent-deflection limit state and assure that objectionable permanent deflections will not occur. Both utilize the factored loadings presently specified for the permanent-deflection check (AASHTO 1994). The first alternative is to limit the positive-bending stresses after inelastic redistribution of moments. The second is to limit the maximum calculated permanent deflection to a specified maximum value. The first alternative is simpler and more conservative than the second. The two alternative limits are discussed in detail under separate headings.

3.4.2.3.1 Positive-Bending-Stress Limit

Proposed Limit

In the first alternative, positive-bending stresses are limited to a percentage of the yield stress after inelastic redistribution of moments has occurred due to yielding at pier sections. The present limits of 95 and 80% of the yield stress are conservatively proposed for composite and noncomposite sections, respectively. In this approach, no check of stresses is required at pier sections. Thus, this alternative is the same as the permanent-deflection limit in present inelastic design procedures (AASHTO 1991 and 1994). However, two changes in the computational procedures used to check this limit are proposed to greatly simplify the process; these are described in the next section.

In the future it may be appropriate to change the 95% and 80% stress limits to 100% of the yield stress for both types of sections if sufficient data can be assembled to justify such a change. Numerous steel beam and girder tests conducted over the years have shown that some yielding occurs below the yield moment, but that the resulting permanent deflection is small. Perhaps such experimental results could be used to justify changing the positive-bending limits to 100% of the yield stress for both composite and noncomposite sections.

New Computational Procedures

The first proposed change in computational procedures is to use a pier-section total-rotation curve that is linear to an effective plastic moment, M_{pe}, and then remains horizontal for a sufficient rotation to allow inelastic redistribution of moments. M_{pe} is equal to M_p for compact sections and is

equal to, or less than, M_y for noncompact sections. Thus, the small amount of permanent deflection that occurs below the plastic moment for compact sections, and below the yield moment for noncompact sections, is neglected. This is consistent with proposed inelastic rating procedures for bridges (Galambos et. al. 1993) and with plastic-design procedures for buildings (ASCE 1971, AISC 1993 and Beedle 1958). It is further justified by the conservative aspects of the permanent-deflection check that were discussed previously under the heading LRFD Bridge Specifications.

It is suggested that M_{pe} for noncompact sections be based on a required plastic-rotation capacity of 9 mrad. This is conservative for the permanent-deflection limit state because the loading specified for this limit state almost always causes plastic rotations that fall on the ascending portion of the presently used rotation curve (AASHTO 1991 and 1994), which reaches M_p at about 6 mrad. This suggests that the required rotation capacity is usually below 6 mrad. Furthermore, the plastic rotation at the pier at overload is only 4.1 mrad in the design example in the ALFD guide specifications (AASHTO 1991). Thus, it may be possible to show through trial designs that a required rotation capacity less than 9 mrad would be adequate for the permanent-deflection check and could be used in the future.

The M/M_{max} corresponding to 9 mrad on the lower-bound rotation curve shown in Figure 3.10 for noncompact sections is about 0.8. Therefore, in the permanent-deflection check, M_{pe} can be taken as $0.8M_{max}$ for noncompact sections. M_{pe} can be taken as M_{max} for sections having an ultracompact compression flange since Figure 3.11 shows that M/M_{max} equals 1.0 when the plastic rotation is less than 9 mrad regardless of the web slenderness. M_{max} can be obtained from appropriate specification formulas and is usually equal to M_y.

The second proposed change in computational procedures is to use the elastic moment envelope instead of the moment diagrams for particular live-load positions (such loads straddling the pier) in the permanent-deflection check. This approach is similar to the approach proposed for the strength check and gives the final permanent deflections that occur after a sequence of loadings, such as repeated truck passages, has been applied. Thus, the analyses for the successive loadings that are presently specified (AASHTO 1994) for more than two continuous spans are not required.

Implementation

With the two changes discussed above the permanent-deflection check can be made in the following way, which is similar to the computational procedure proposed for the strength check. First,

calculate the elastic moment envelope for the specified factored loading including dead load, live load, and impact. For composite girders, elastic moment envelopes must be developed separately for loads applied before and after the slab has hardened because positive-bending stresses, rather than moments, are limited in this check. The elastic moment envelope for loads applied before the slab has hardened, of course, is merely the moment diagram for dead load applied to the steel girder.

Next, determine the final redistribution moments for the specified loadings. The redistribution moments at piers are defined by the following equation:

$$M_r = M_{pe} - M_e \geq 0 \qquad (3.31)$$

where:

M_e = moment from the elastic moment envelope, and

M_{pe} = effective plastic moment defined under the heading New Computational Procedures.

The correct signs must be assigned to the moments. For composite sections, M_e is the sum of the moments applied before and after the slab has hardened. If M_{pe} is numerically larger than M_e no redistribution of moments occurs and M_r is zero. The full redistribution moment diagram can be obtained by connecting these pier moments with straight lines and extending these lines from the first and last piers to the zero moments at adjacent abutments.

Equation 3.31 defines the moment at each pier during inelastic redistribution of moments because M_{pe} remains constant after yielding starts according to the assumed rotation curve. Thus, the continuity and rotation relationships are both satisfied by a moment equal to M_{pe}. The ϕ_{ad} factor of 1.1 was not applied in this case because it is assumed that the specified load factor combined with a ϕ factor of 1.0 provides the desired level of reliability.

Finally, check that the following equation is satisfied at all positive-bending locations:

$$\alpha F_y \geq f_e + f_r \qquad (3.32)$$

where:

f_e = maximum stress in the steel flange for the moment from the elastic moment envelope,

f_r = maximum stress in the steel flange for the redistribution moment, and

α = 0.95 for composite sections and 0.80 for noncomposite sections.

For composite sections, f_e is the sum of the flange stresses caused by moments applied before and after the slab has hardened and f_r is the flange stress caused by the redistribution moment applied to the composite section. Normally, f_e and f_r have the same signs.

Although the final permanent deflections and plastic rotations associated with this limit state are not required for a design check, they can be calculated from the redistribution-moment diagram by elastic procedures since it is assumed that the entire girder is elastic except for the plastic rotations at pier locations. Specifically, the continuous-span girder can be treated as a series of simple-span girders with the pier redistribution moments applied at their ends. The resulting deflections are the permanent deflections for the specified loadings. The difference between the end slopes of the adjacent simple spans at any pier represents the angular discontinuity or plastic rotation at that location.

The calculated permanent deflections can be added to the dead-load camber if desired. However, the calculated permanent deflections are generally small and actual permanent deflections are expected to be even smaller due to various conservative assumptions made in the calculation procedures and discussed under the heading LRFD Bridge Specifications. A full-scale bridge designed to permit inelastic redistribution of negative moments under the overload condition specified in the ALFD guide specifications (AASHTO 1986) sustained only very small permanent deflections when tested under heavy loadings (Roeder and Eltvik 1985).

Advantages

The proposed procedure provides a very simple way of checking the permanent-deflection limit state. No successive loadings, iterative procedure, or simultaneous equations are required. The procedure is conservative because of various conservative assumptions normally made in the design process as discussed previously.

3.4.2.3.2 Permanent-Deflection Limit

Proposed Limit

In the second proposed alternative procedure for satisfying the permanent-deflection limit state, a permissible permanent deflection is specified and compared with actual permanent deflections calculated for the specified loading by the unified autostress (Schilling 1989, 1991 and 1993) or residual-deformation method (Dishongh 1990 and 1992 and Dishongh and Galambos 1992). Both of these methods permit positive-bending yielding, which is prohibited in the first alternative method. The

typical rotation curves described under the heading Typical Rotation Curves for negative- and positive-bending sections should be used in these methods; the ϕ factor used in the strength-limit-state check is not required because ϕ should be taken as 1.0 for service limit states (AASHTO 1994).

It is usually appropriate to define deflection limits as a fraction of the span length (AASHTO 1992 and 1994). For the permanent-deflection limit state, it is proposed that the maximum permanent deflection calculated within a span of length, L, be limited to L/300. This is the limit above which deflections become visually noticeable (Galambos and Ellingwood 1986) and was suggested to be the highest limit suitable for inelastic rating (Galambos et. al. 1993). L/600 was suggested as an alternative, more conservative, limit for inelastic rating. It corresponds to the maximum permanent deflections observed in the AASHO road tests (HRB 1962a and 1962b) for beams subjected to stresses not exceeding the 95% and 80% stress limits as discussed earlier. Since the choice of the specified limit has a major influence on the permanent-deflection check, and hence on the economy of the design, a limit based specifically on riding quality should be developed in the future.

As discussed for the first alternative limit, the calculated permanent deflection could be added to the dead-load camber, but the amount that actually develops in the bridge is expected to be considerably less than the calculated amount.

Advantages

Although this alternative limit is much more complicated to calculate than the first alternative, especially for more than two continuous spans, it has the advantage that it directly limits the parameter that controls performance at this limit state.

3.4.3 Constructibility

In Article 6.10.10.2.1, the LRFD bridge specifications (AASHTO 1994) limit the moments caused during various construction stages by factored construction loadings to the yield moment. This provision applies regardless of whether the bridges are designed by elastic or inelastic procedures. Therefore, the inelastic design procedures developed in the present report to check the strength and permanent-deflection limit states are not required in checking constructibility.

3.4.4 Fatigue

It is sometimes questioned whether yielding permitted in the inelastic design of bridges adversely affects fatigue life. This question is discussed below. As explained earlier, the yielding

permitted at piers, and other locations, eventually causes redistribution moments that assure elastic behavior during subsequent loadings of the same, or lesser, magnitude. Furthermore, the amount of yielding that can occur at these locations is restricted by the elastic behavior of the remaining structure. In this respect, the yielding is similar to that occurring in the webs of hybrid beams (ASCE-AASHO 1968), or even in bridges designed by elastic procedures as a result of residual stresses or of moments above the yield moment for compact sections. In all of these cases, localized yielding is restricted by the elastic portions of the structure so that elastic behavior eventually develops.

Such yielding modifies the original residual stresses that occur in most steel members; usually, it lowers the peak residual stresses (Schilling 1984). However, it does not change the stress range caused at a point by the passage of a given truck across the bridge, but merely shifts the stress range by changing the magnitude of the constant superimposed residual stress. Since stress range is the main stress parameter controlling fatigue life, such a shift does not normally change the fatigue life significantly, although there are exceptions that rarely apply to the cases under discussion (Schilling 1984). Furthermore, tests have confirmed that the fatigue lives of hybrid beams are not reduced by restricted local yielding of the web (Frost and Schilling 1964).

Because of this evidence, the effects on fatigue behavior of restricted local yielding in the webs of hybrid beams, and in elastically designed homogeneous beams, are not considered in the bridge specifications (AASHTO 1994 and ASCE-AASHO 1968). It is reasonable to also neglect the effects on fatigue behavior of the same kind of restricted local yielding in inelastically designed beams and girders.

3.5 SPECIFICATIONS AND COMMENTARY

The proposed simplified inelastic bridge design procedures could be incorporated into the LRFD bridge specifications (AASHTO 1994) by (a) substituting the following version of Article 6.10.11 for the present version, (b) defining ϕ_{sd} as equal to 1.10 in Article 6.5.4.2, (c) adding the new references cited in the new commentary, and (d) adding definitions of new terms like shakedown. The notation and terminology in these new specification provisions match those in the present specifications and differ slightly from those in the rest of this report. In line with the specification format, references are cited by author and year.

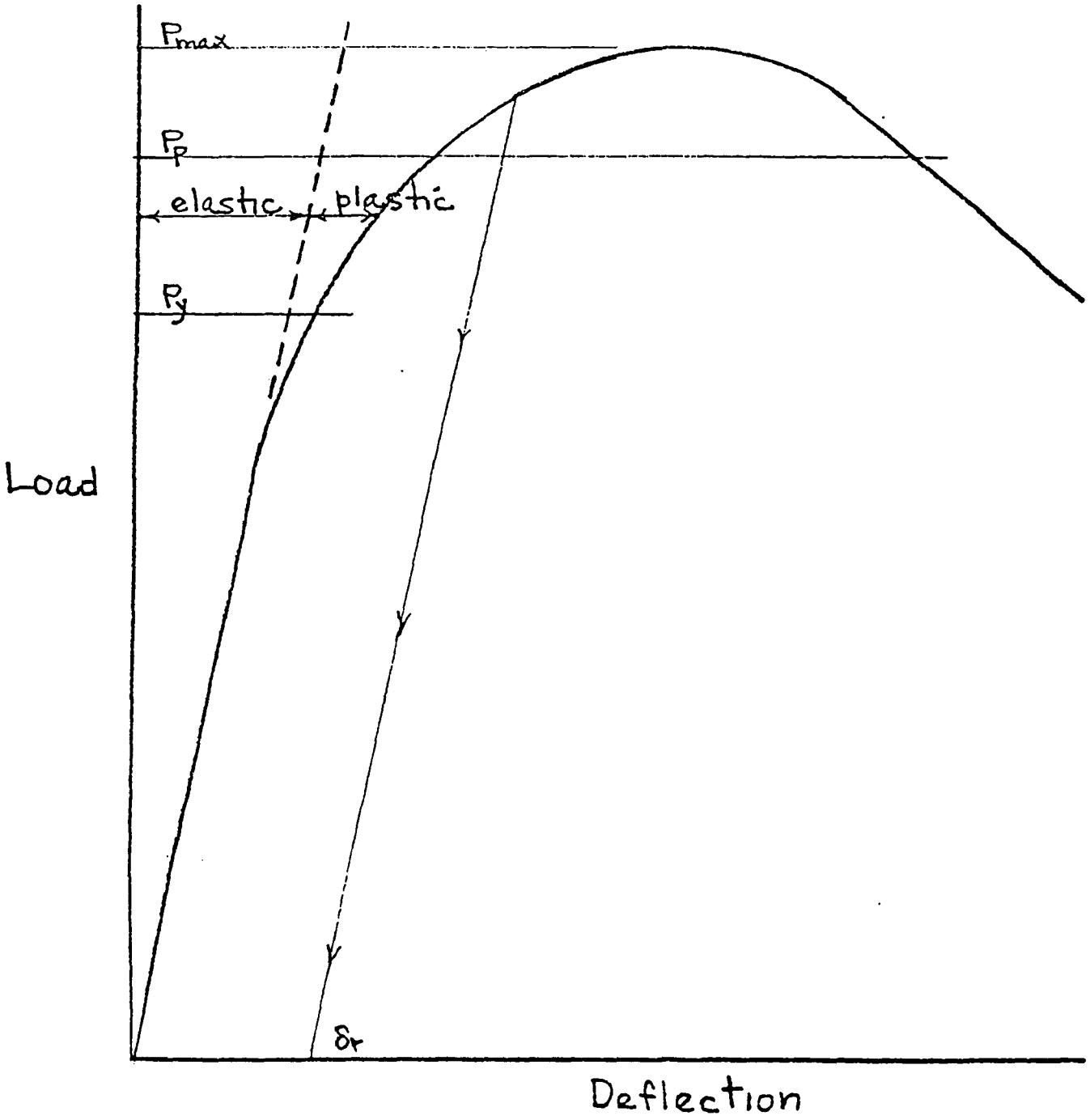

Figure 3.1 Typical Load-Deflection Curve

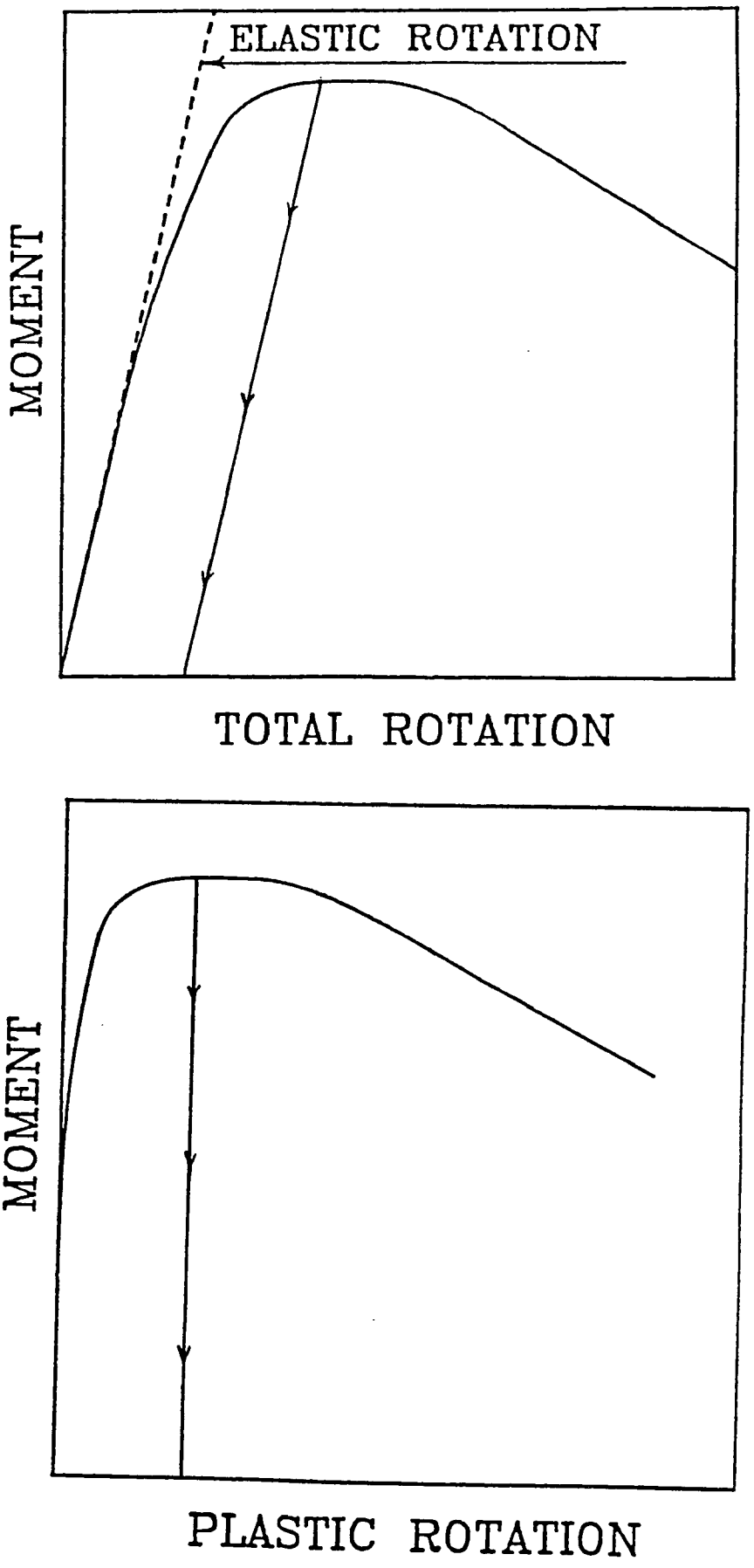

Figure 3.2 Relationship Between Total Rotation and Plastic Rotation

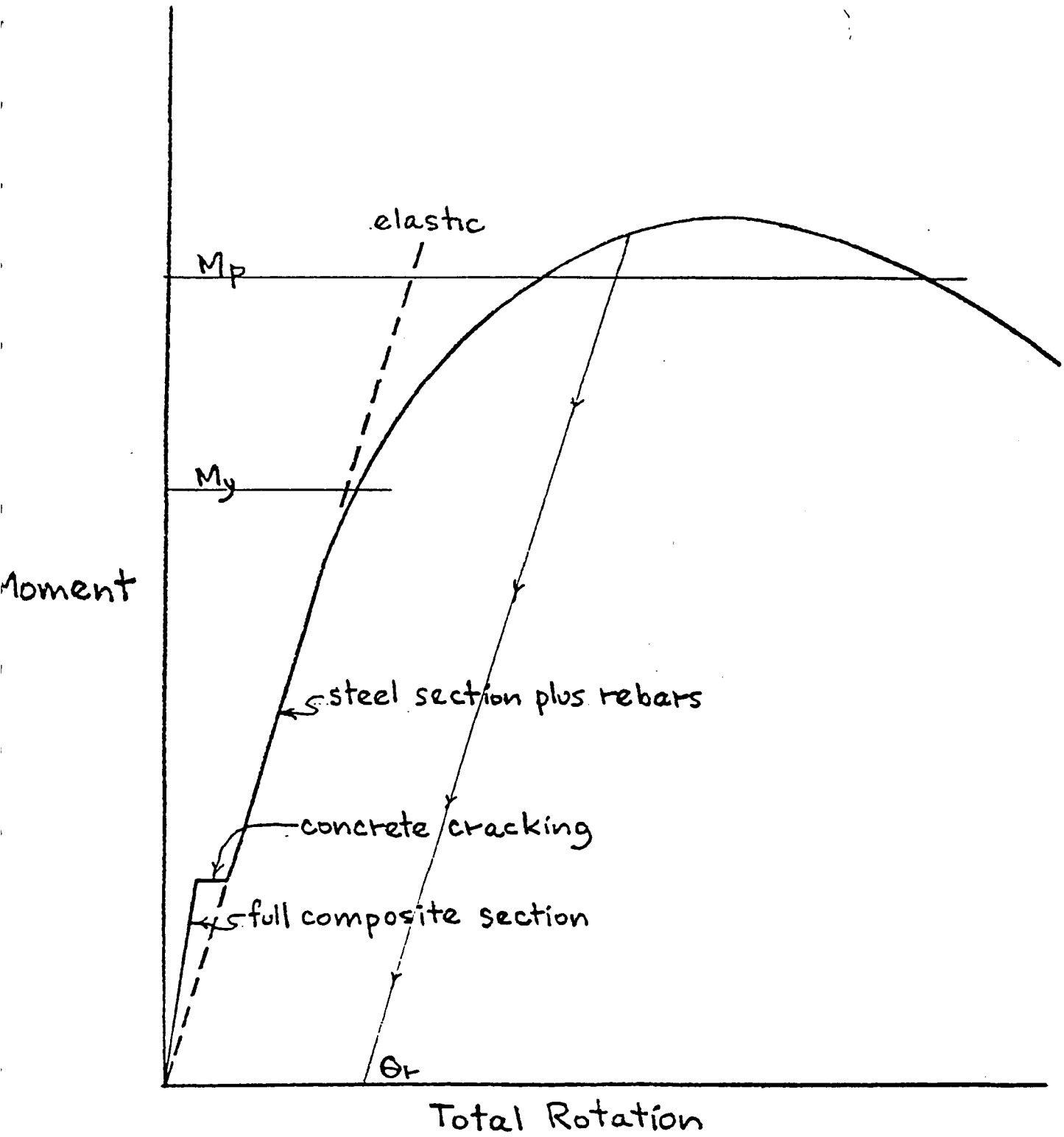

Figure 3.3 Typical Rotation Curve for Composite Section in Negative Bending

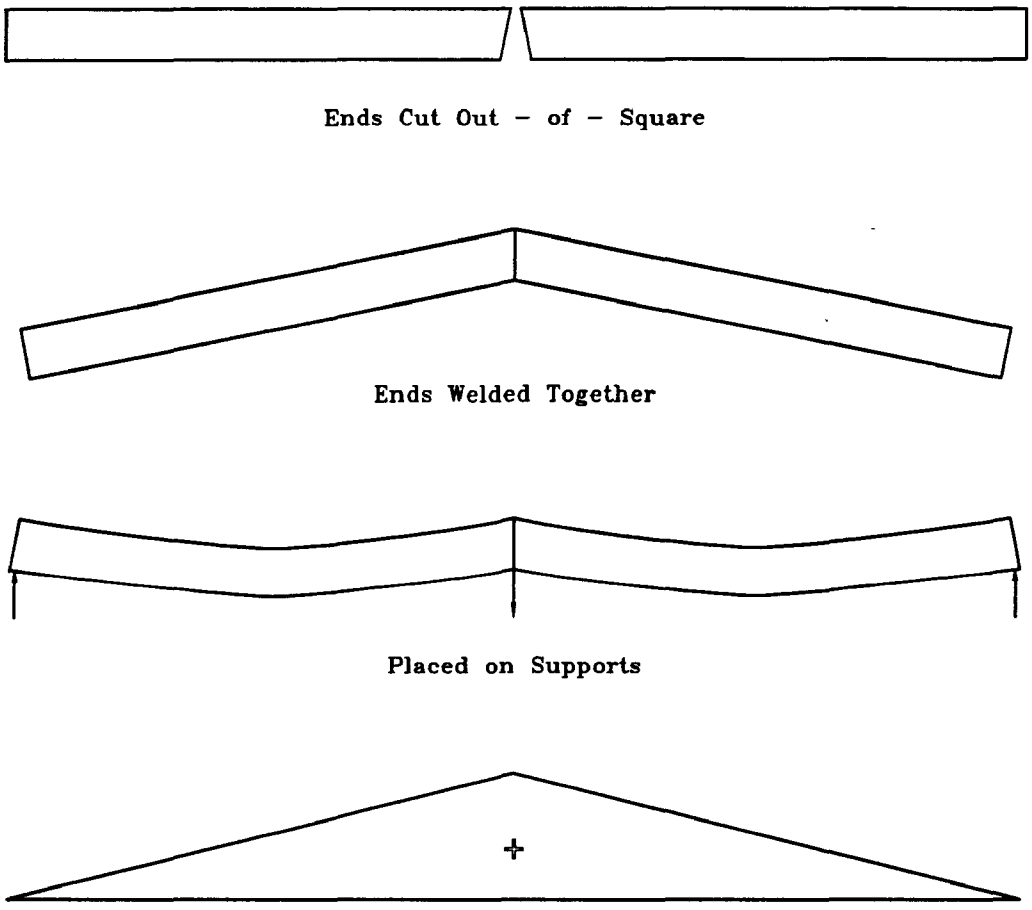

Figure 3.4 Plastic-Rotation Analogy

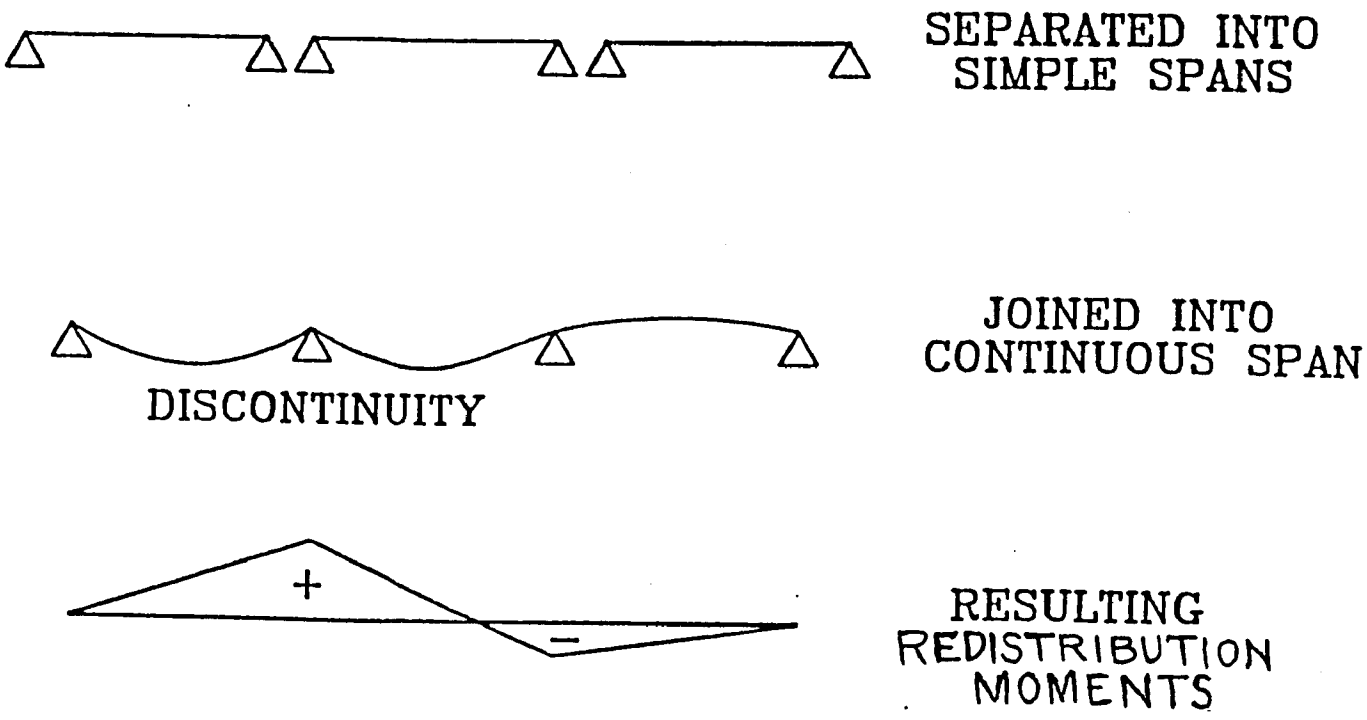

Figure 3.5 Redistribution Moments Due to Discontinuity at Pier 1

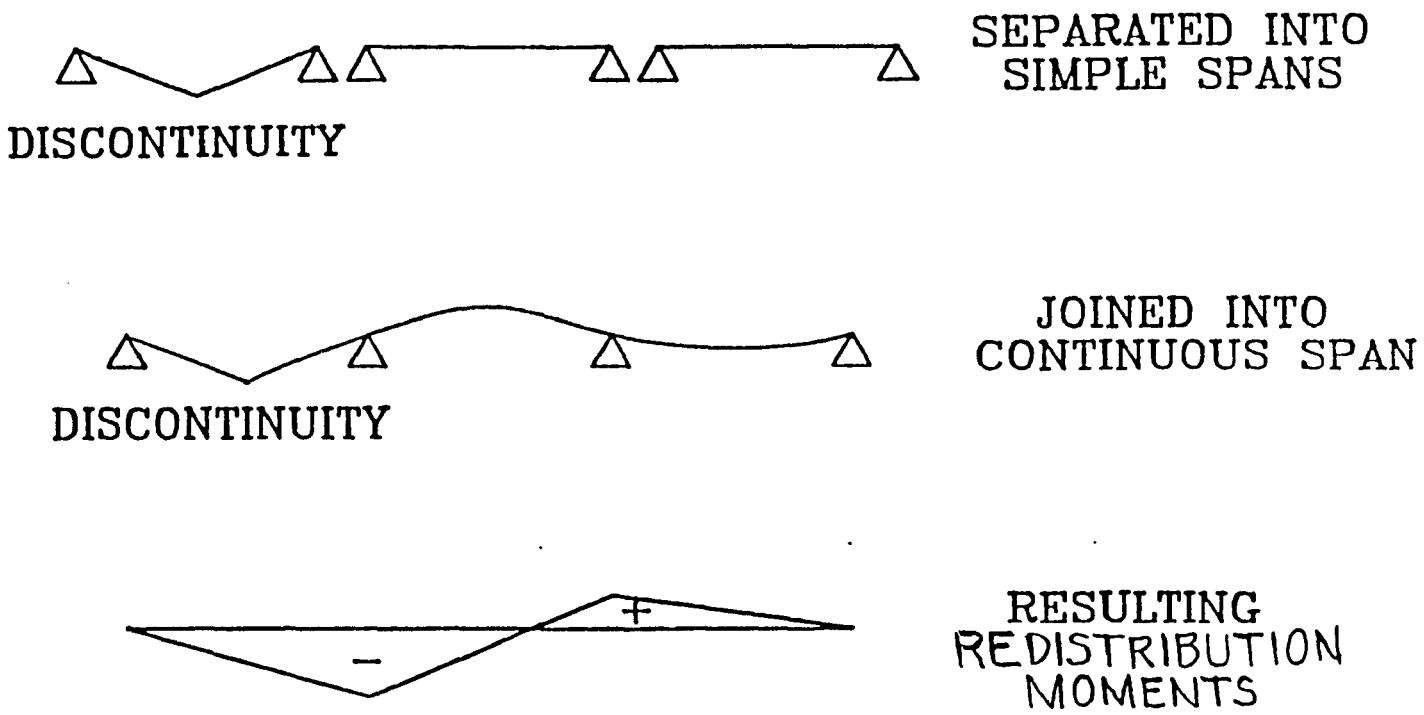

Figure 3.6 Redistribution Moments Due to Discontinuity in Span 1

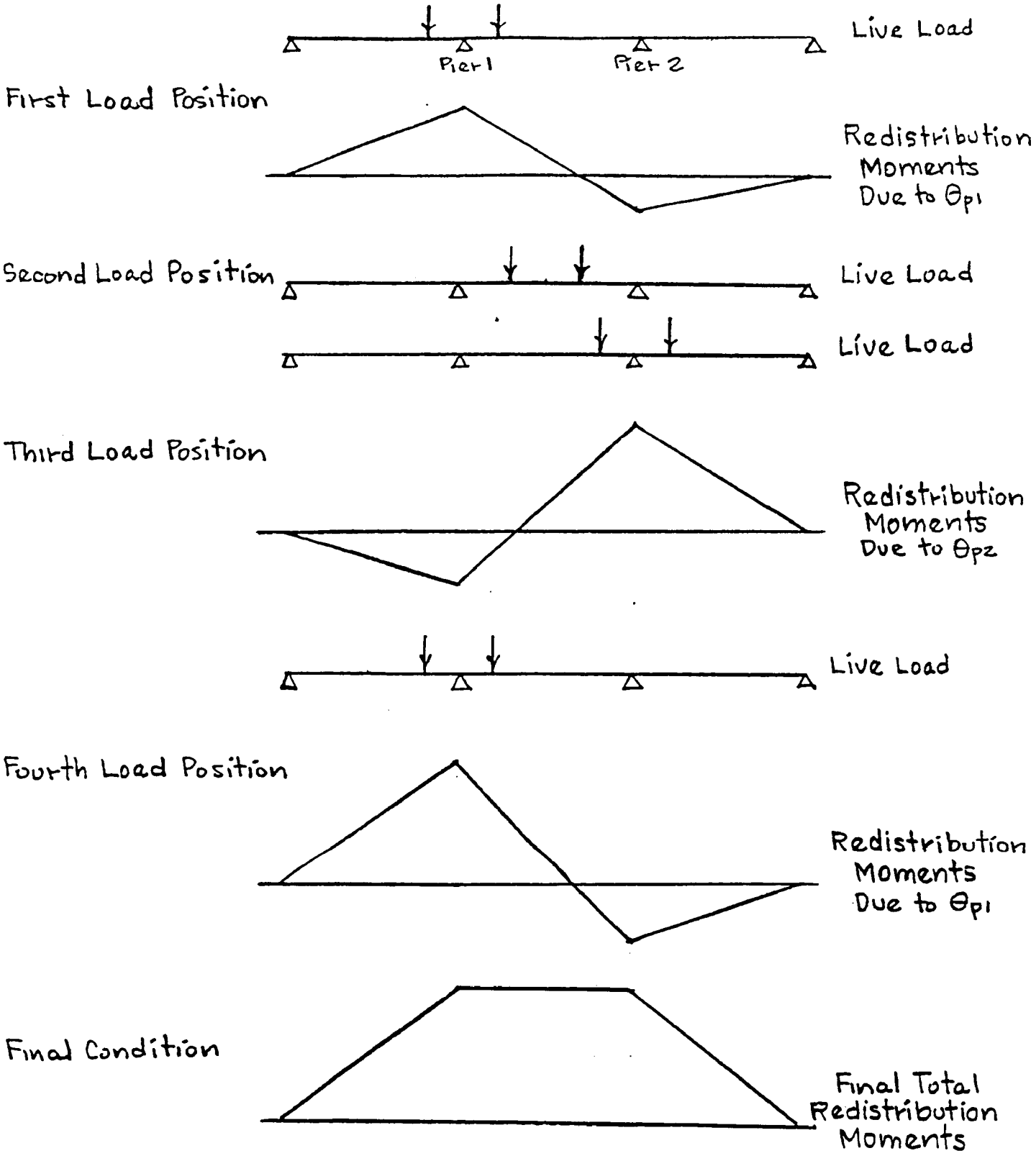

Figure 3.7 Redistribution Moments for Sequential Loading

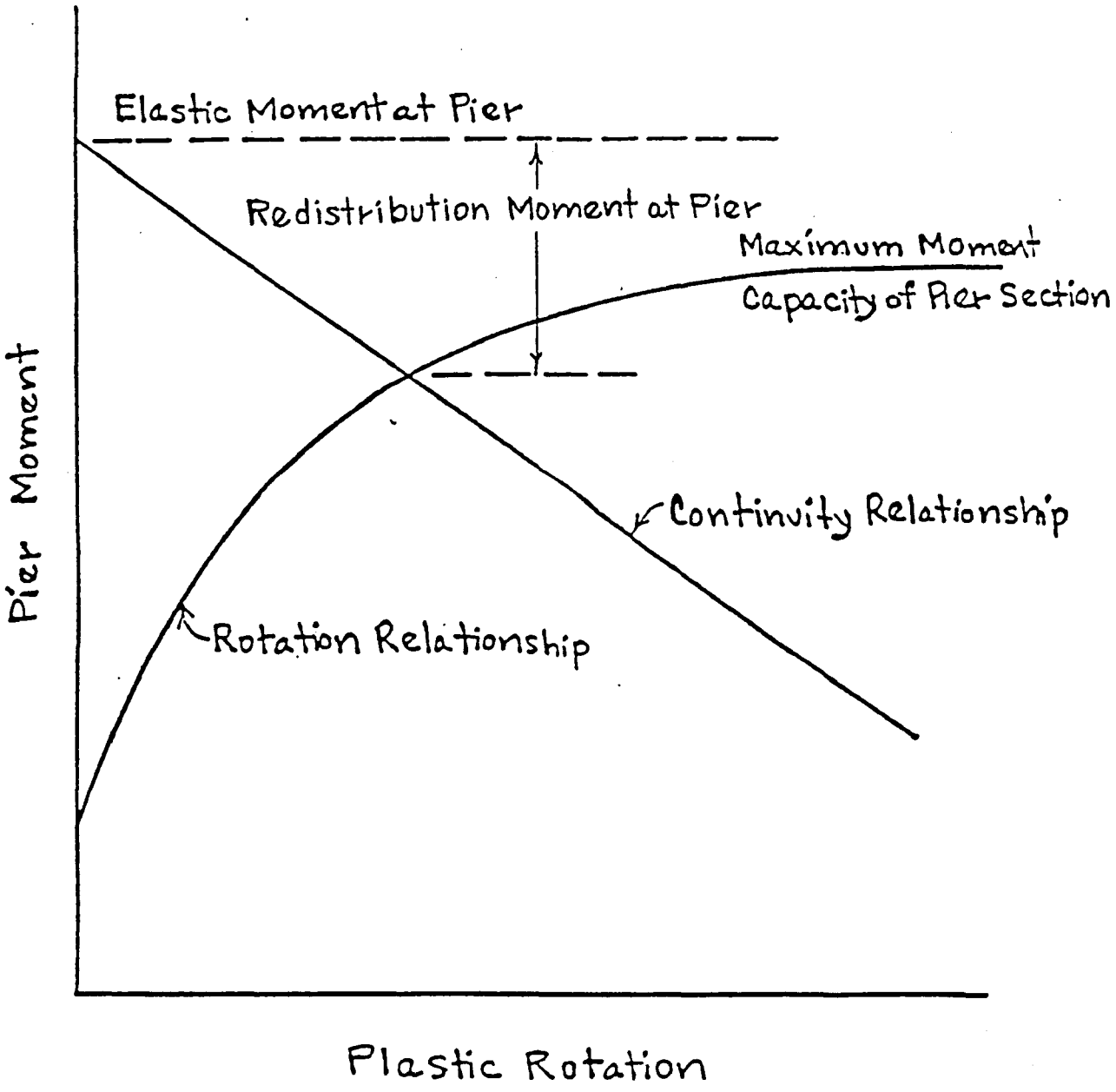

Figure 3.8 Beam Line Chart

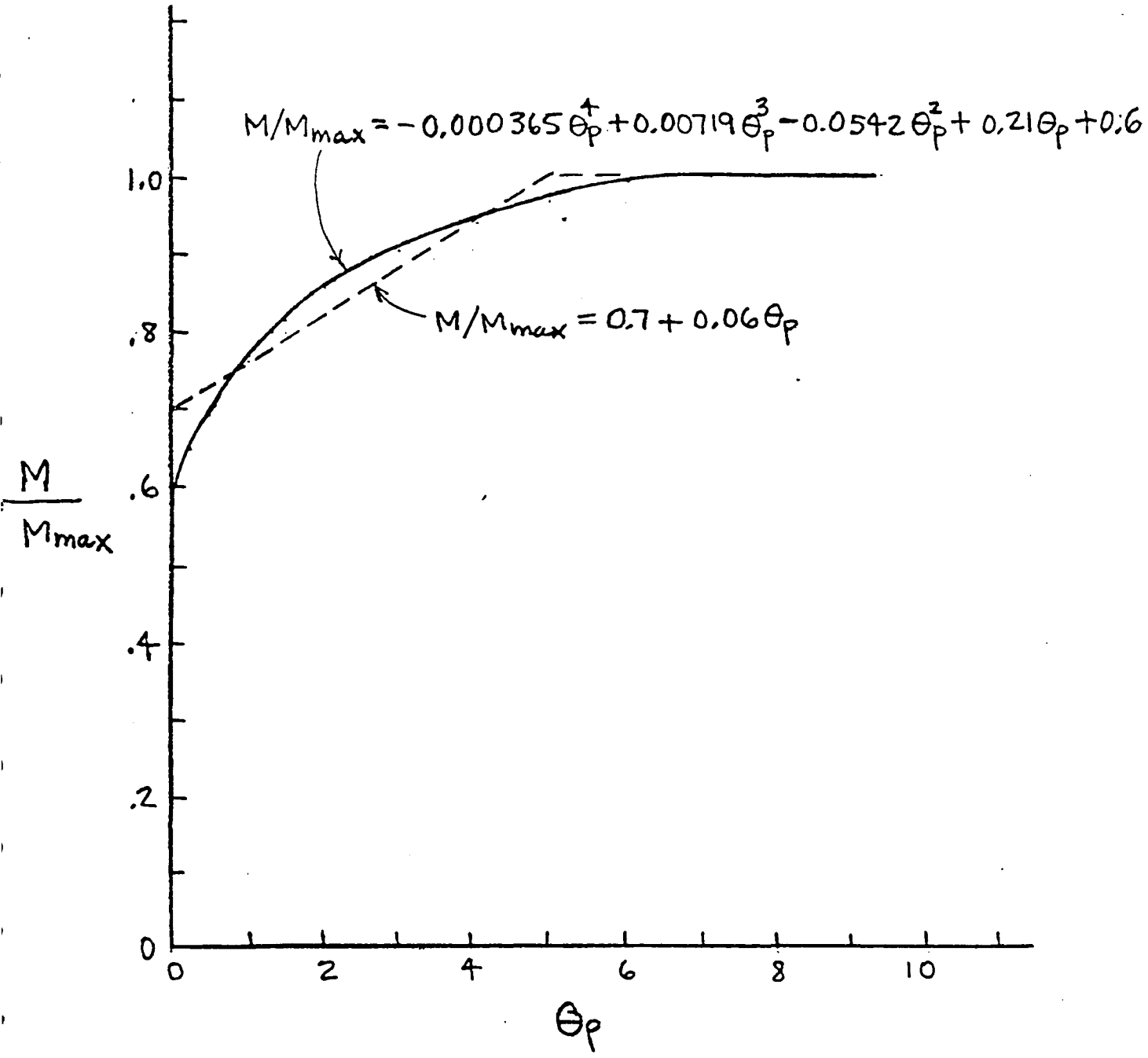

Figure 3.9 Ascending Portion of Rotation Curve for Negative-Bending Sections

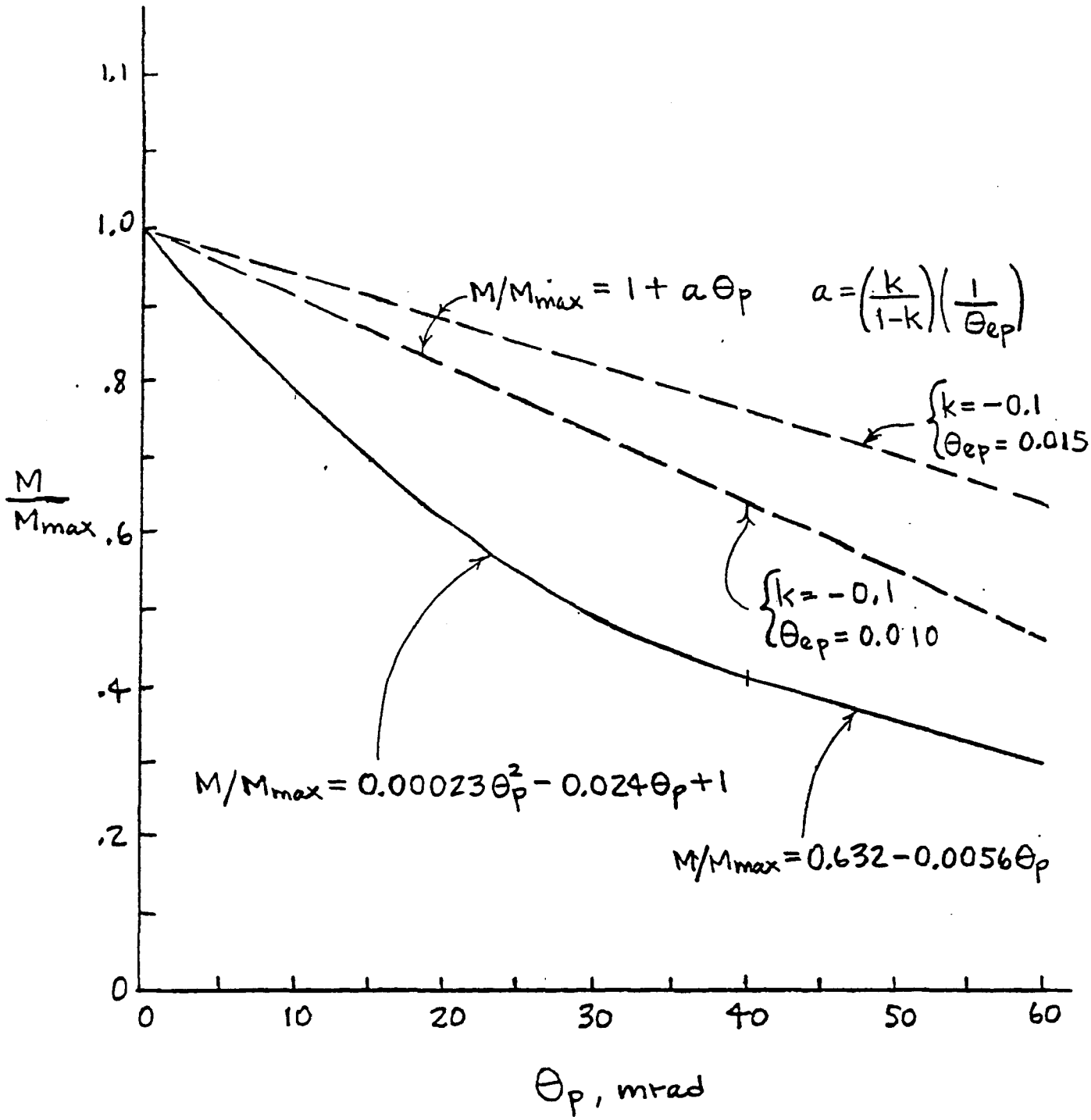

Figure 3.10 Plastic-Rotation Curves for Noncompact Sections in Negative Bending

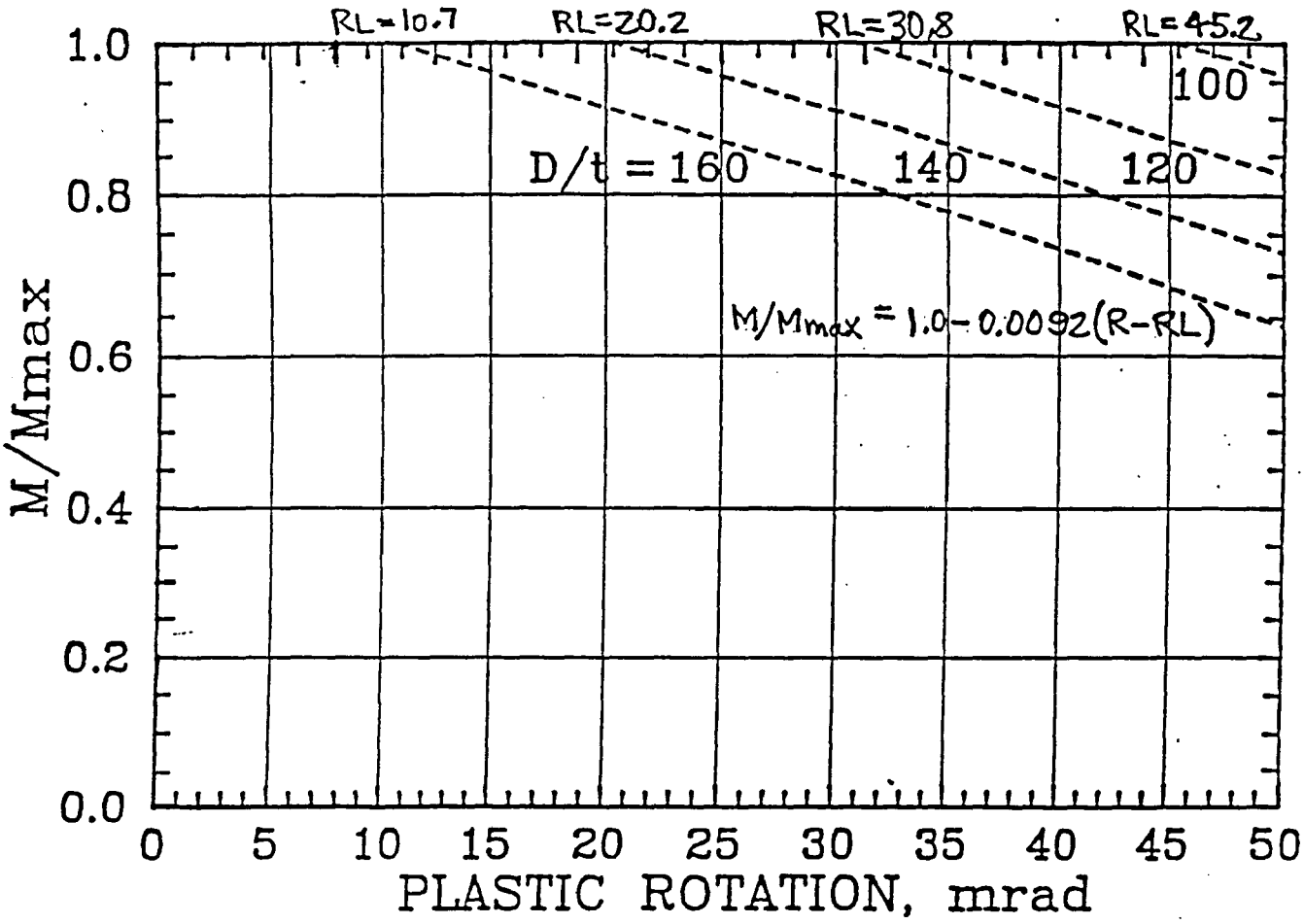

Figure 3.11 Plastic-Rotation Curves for Ultracompact-Flange Sections in Negative Bending

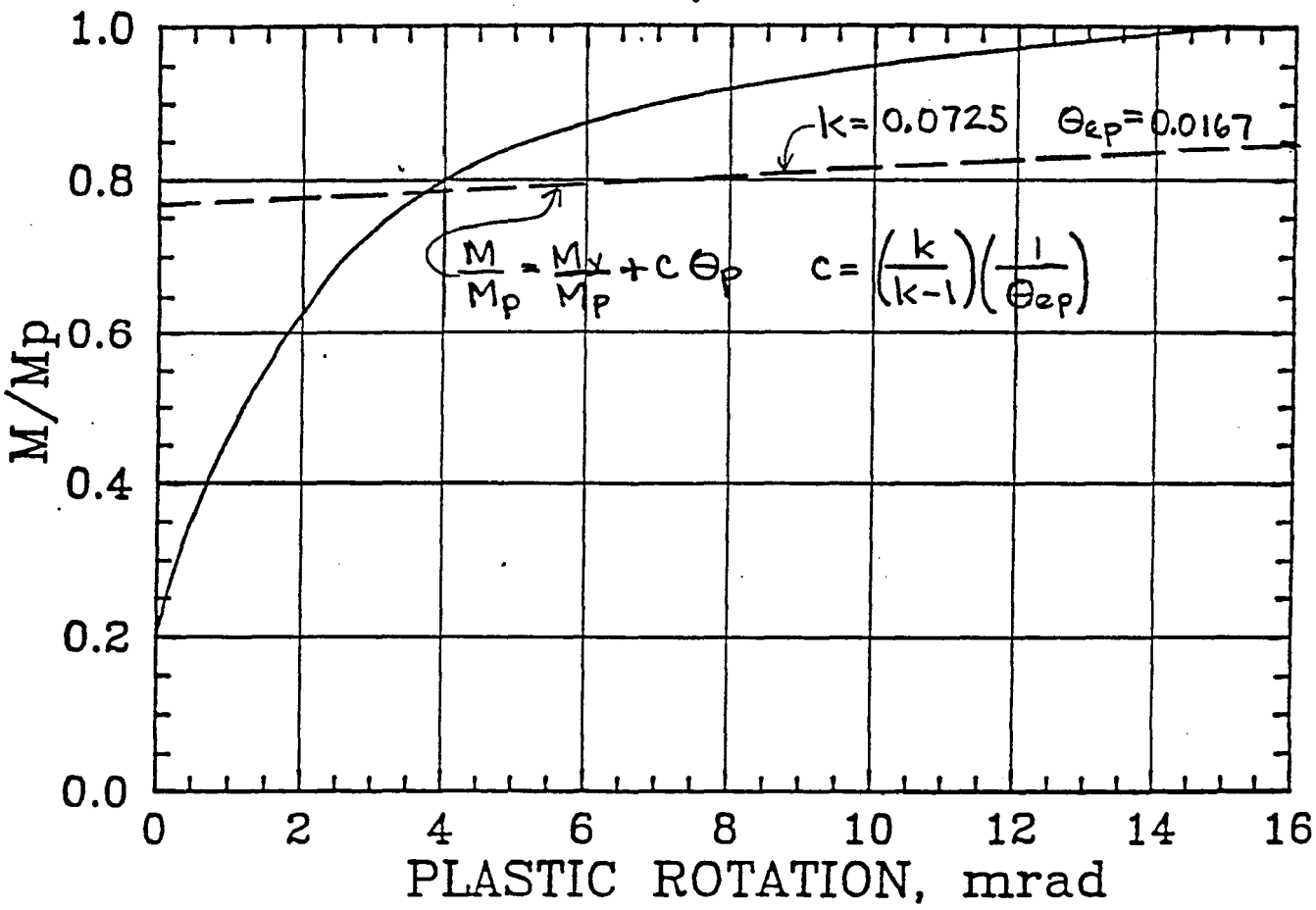

Figure 3.12 Plastic-Rotation Curves for Compact Composite Sections in Positive Bending

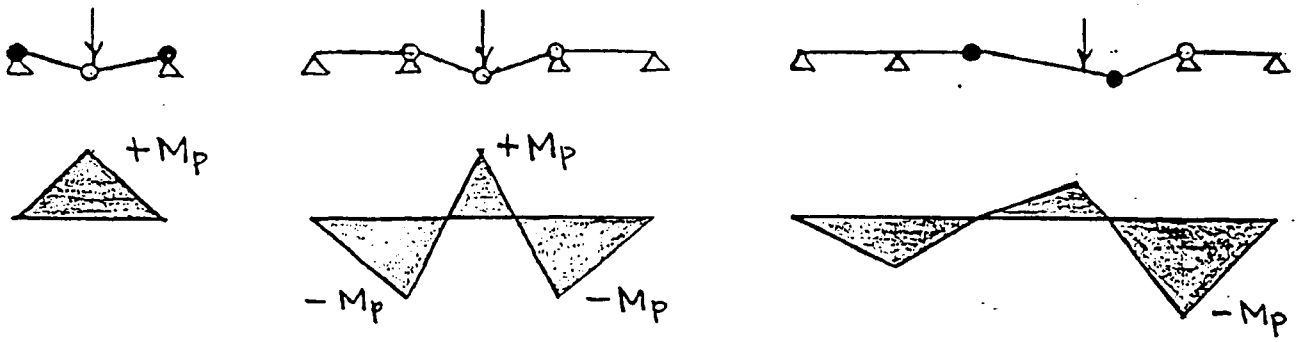

Valid Three-Hinge Mechanisms

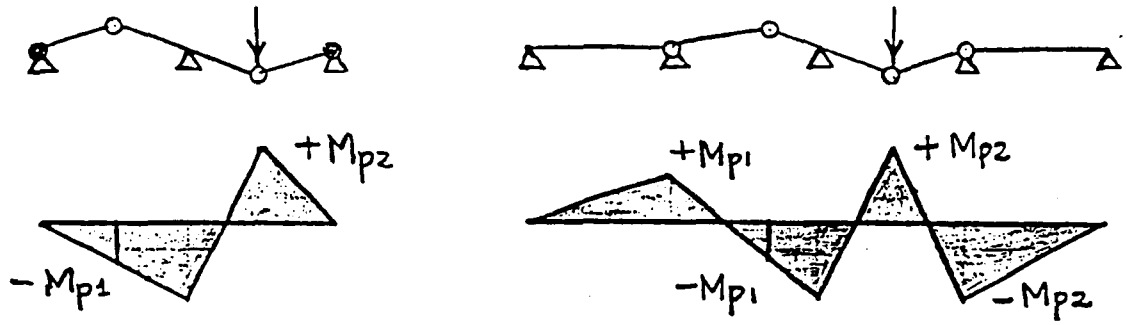

Valid Four-Hinge Mechanisms

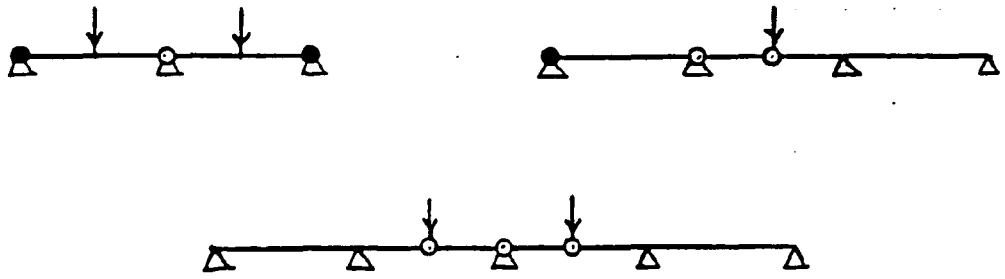

Invalid Three-Hinge Mechanisms

Figure 3.13 Valid and Invalid Mechanisms

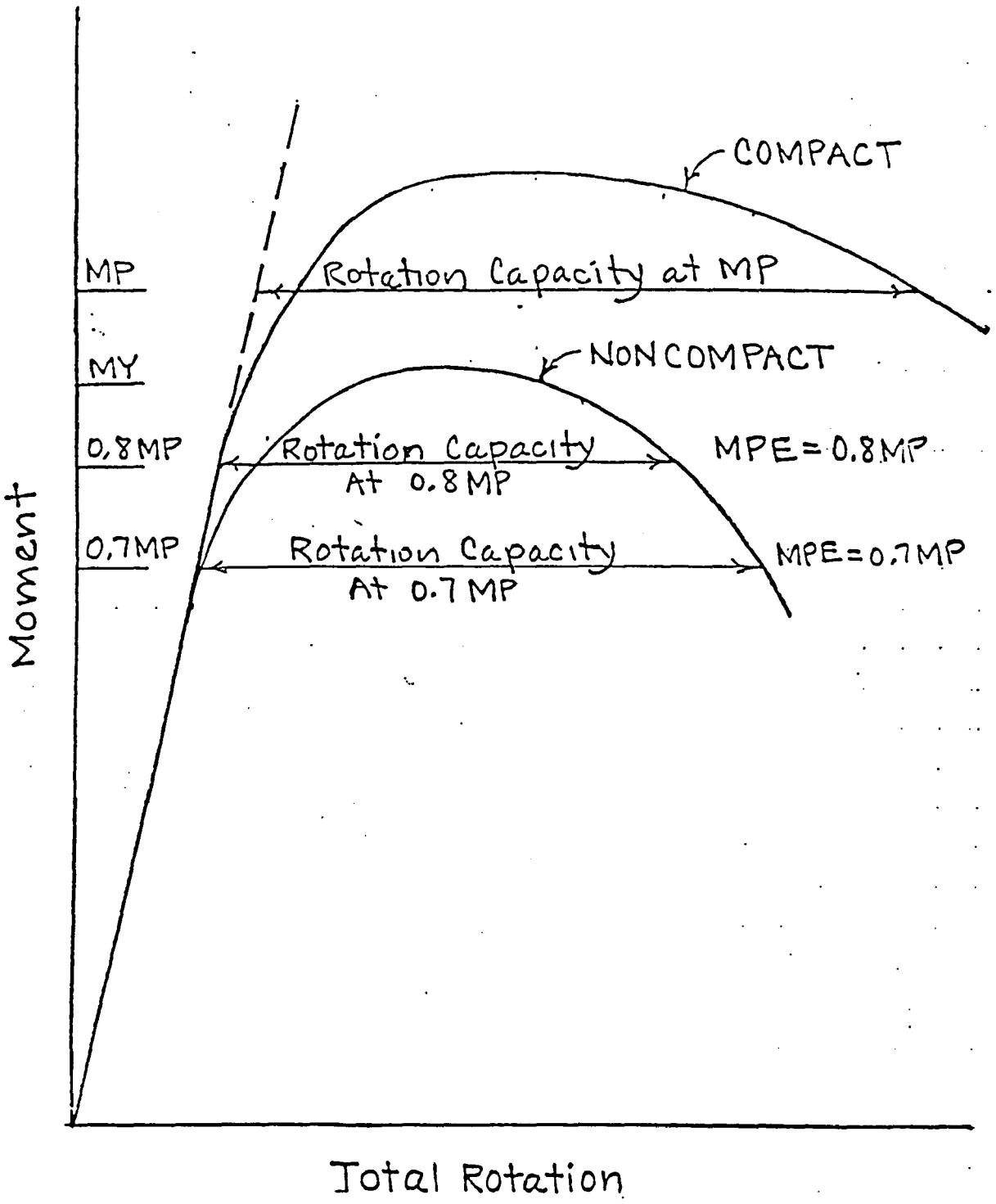

Figure 3.14 Typical Rotation curves for Compact and Noncompact Sections

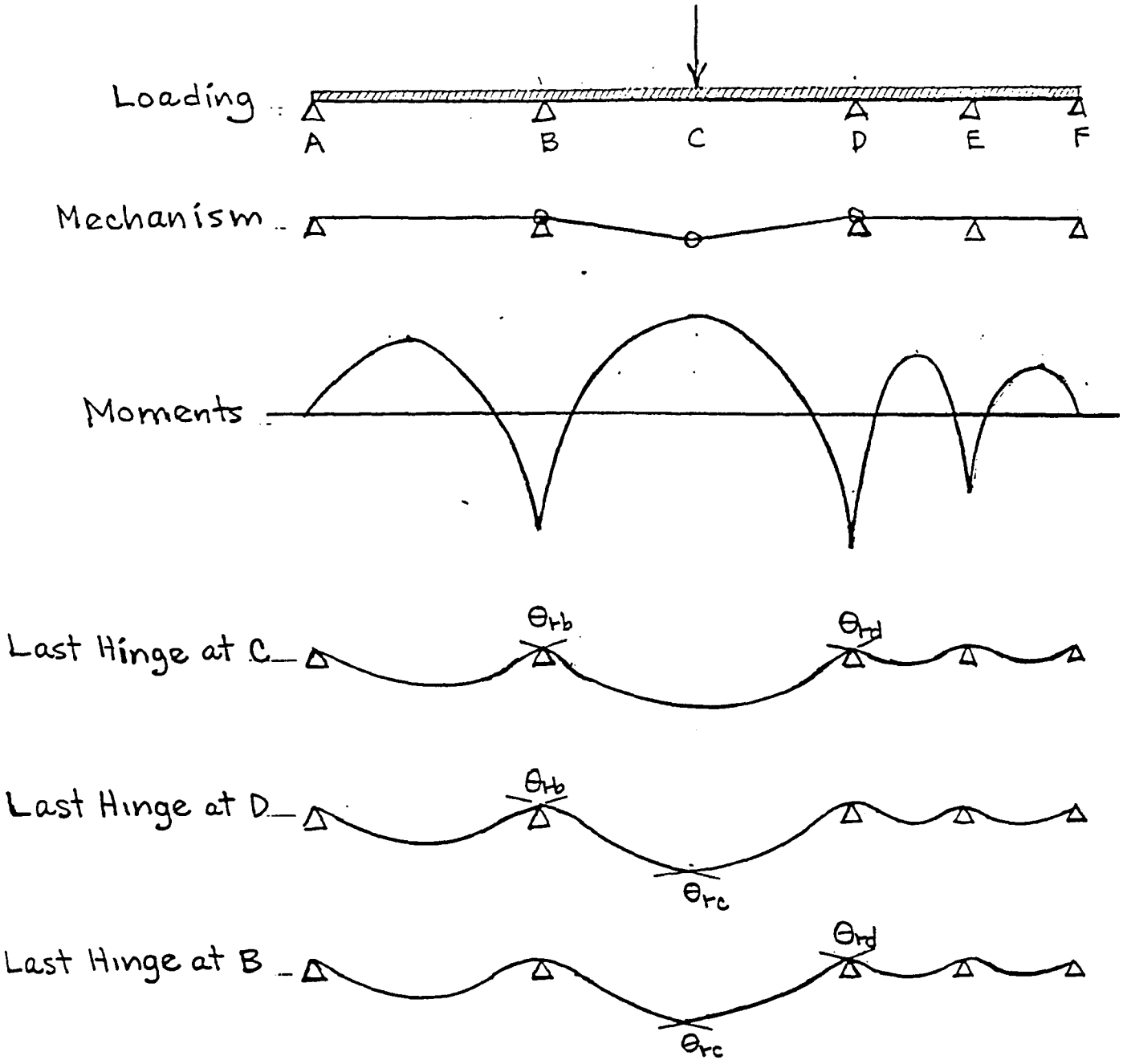

Figure 3.15 Calculation of Required Rotation Capacity

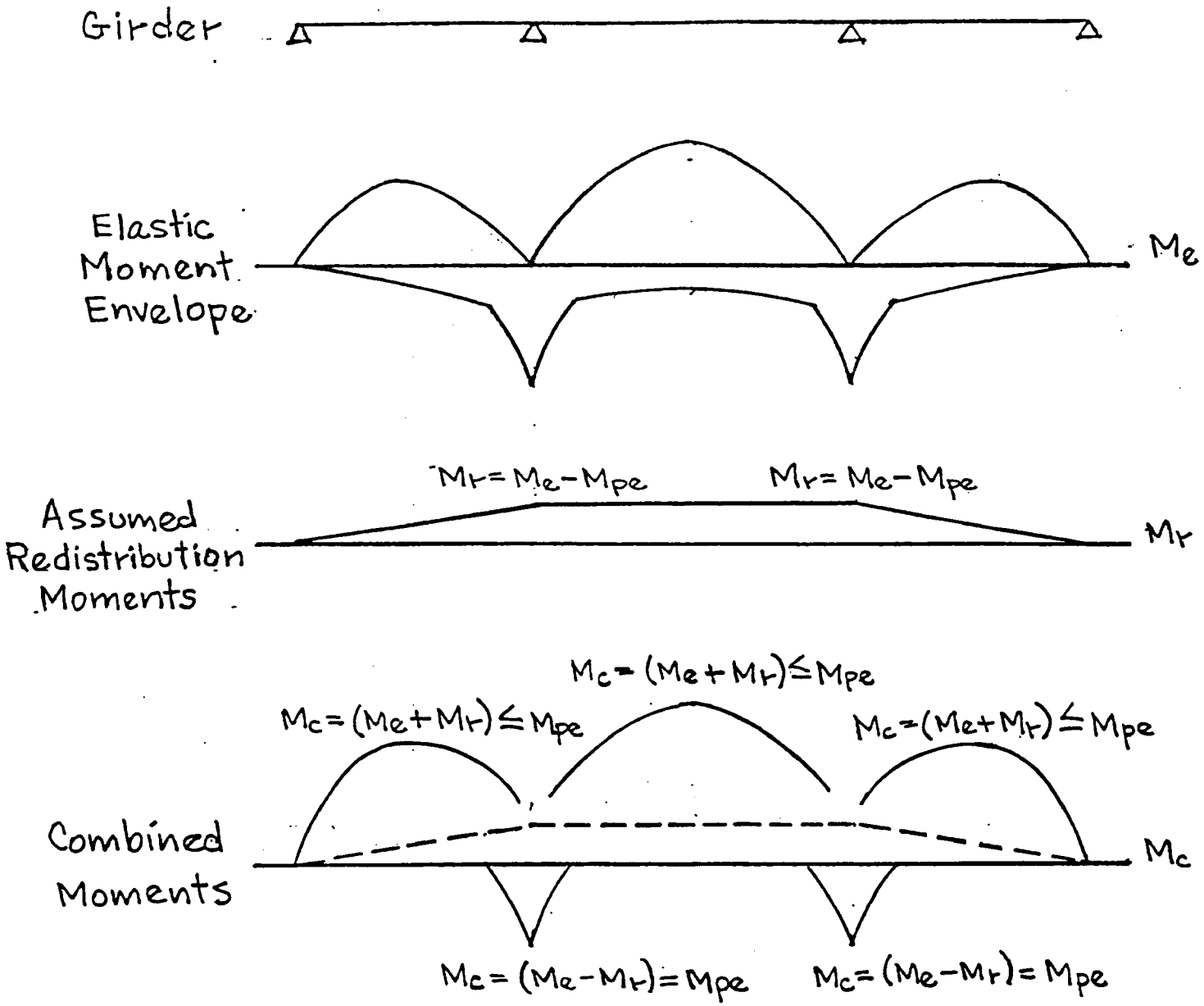

Figure 3.16 Shakedown Check

CHAPTER FOUR

GIRDER BRIDGES COMPRISING COMPACT SECTIONS

4.1 INTRODUCTION

This chapter presents design provisions for steel girder bridges comprising compact sections. The chapter is divided into two major themes: design and experimental verification. The presentation of material is summarized herein due to length. The original and detailed information can be found in Weber (1994), Unterreiner (1995) and Hartnagel (1997).

Currently, compact bridges can be designed by several methods according to AASHTO. The Load Factor Design (LFD - AASHTO 1992) method can be employed to design bridges using elastic limits with or without non-linear redistribution (assumed up to 10%) of negative pier moments. The Load and Resistance Factor Design (LRFD - AASHTO 1994) method can be used to design bridges using elastic limits with or without non-linear redistribution (assumed up to 10%) of negative pier moments or by inelastic design provisions. This report also presents proposed LRFD inelastic design provisions (Appendix) meant to replace the current LRFD inelastic design provisions. Alternate Load Factor Design (ALFD - AASHTO 1986) provisions have been, more or less, incorporated into the above mentioned inelastic design methods and are mentioned herein for discussion only.

In the first part of this chapter, a bridge is designed according to the current LRFD inelastic design provisions. This design is compared to the LFD with assumed redistribution of moments, the LRFD elastic with assumed redistribution of moments, and the proposed LRFD inelastic design provisions. The design comparisons are summarized in Table 4.2. The table shows the benefits of using inelastic design procedures.

The second part of this chapter is devoted to experimental testing of a one-half scale model of an interior girder from the bridge designed by the current LRFD inelastic design method. The tests consisted of a three-span composite girder subjected to modeled moving truck loads to examine the inelastic behavior of bridge girders and girder component tests to establish and verify

moment-inelastic rotation relations. This chapter examines the behavior at the design limit states and the general elastic and inelastic behavior through collapse of the test specimens.

4.2 DESIGN PROVISIONS

4.2.1 Current LRFD Design and Test Girder Prototype Design

4.2.1.1 General

ALFD inelastic design procedures (AASHTO 1986) specify requirements at service load levels (normal traffic), overload levels (occasional heavy vehicle), and maximum load levels (one-time maximum vehicle). Inelastic LRFD provisions (AASHTO 1994) specify these limits as Service I, Service II, and Strength I, respectively. The LRFD procedures also have a separate fatigue limit loading. Following are the LRFD load levels at the respective limits:

Fatigue $D + 0.75L(1+I)$, (4.1a)

Service I $D + 1.00L(1+I)$, (4.1b)

Service II $D + 1.30L(1+I)$, and (4.1c)

Strength I $1.25DC + 1.50DW + 1.75L(1+I)$, (4.1d)

where,

D = dead load,

L = live load with lateral distribution factor,

I = impact factor (33%),

DC = component dead load (slab, beam and barrier curbs), and

DW = wearing surface.

Fatigue and Service I limits are for fatigue and deflection checks. For inelastic design at the Service II limit state, after interior pier elastic moments are redistributed to adjacent positive moment regions, the design requirement is a limited stress at positive moment regions. At the Strength I level, a mechanism must not form with the application of the factored loads.

4.2.1.2 Prototype Bridge Design

A three-span, 60ft-76ft-60ft, two-lane prototype bridge was designed according to the LRFD bridge design specifications using the inelastic design provisions (AASHTO 1994). Four

W30x108 rolled beam girders with 1.0 in headed studs at a nominal spacing of 12 in were selected. A girder spacing of 10 ft was used to support the 36 ft wide roadway. Yield strength of the steel was 50 ksi. The deck was 8 in thick with 4000 psi compressive strength concrete and Grade 60 reinforcing steel. A future wearing surface of 12 psf (about 1 in of asphalt) and a barrier rail weighing 305 plf (a standard 16 in concrete barrier curb) were considered as composite dead load. The bridge was designed assuming unshored construction. Also, the LRFD HS20 design vehicle and a 640 plf lane load was used for determining live load effects. Following is a brief description of the Service II and Strength I limit design procedures (Weber 1994). Section properties for the prototype design are shown in Table 4.1.

4.2.1.3 Loads

The dead load of the steel girder and the concrete deck, component dead load DC, is applied to the non-composite section. This is a result of unshored construction. A non-prismatic elastic analysis was used to determine the moments caused on the structure from the non-composite dead load. Moments from the component dead load, DC, are 270 k-ft for the exterior positive moment region and 280 k-ft for the interior positive moment region. The interior support moments are -530 k-ft. Moments for the future wearing surface and barrier curbs, DW, are 71 k-ft and 80 k-ft for the positive moment regions (exterior and interior) and -120 k-ft for the interior support. Weight of the barrier rails and a future wearing surface, DW, is applied to the composite section with a modular ratio of $3n = 24$ to take into account for creep and shrinkage of the concrete.

Live loads and impact are applied to the composite section with a modular ratio of $n = 8$ for the positive moment region. At the interior support the structural resistance was the steel section plus the contribution of the longitudinal reinforcing steel in the concrete deck. All moments and shears were computed using a non-prismatic elastic analysis. Positive moments were based on the 640 plf lane load and the HS20 truck with 33% impact included only on the truck. Negative moments were based on 90% of both the lane load and two trucks spaced 50 feet apart from front to rear with impact included only on the trucks (LRFD, 3.6.1.3.1). The LRFD revised distribution factors (LRFD, 4.6.2.2) are used to estimate the amount of live load moment and shear that is applied to each girder. The live load moments for the girder were 890 k-ft and

990 k-ft for the positive moment regions (exterior and interior) and -720 k-ft for the interior support region. Moment envelopes are shown in Figure 4.2.

4.2.1.4 Design Limit States

4.2.1.4.1Service II Limit State

The Service II check ensures that occasional overload vehicles equal to 1.30L(1+I) will not cause excessive deformations. Elastic overload moments at the piers are shifted through residual moments, M_{rd}, that occur at the pier due to inelastic pier rotations, θ_p. The residual moment is the difference between the elastic moment and the actual moment at the pier section. Due to inelastic action, the girder develops a residual moment field (self-equilibrating) that is locked in the structure and adds to other applied moments. The pier sections resist bending according to the following relationship (AASHTO 1994).

$$M = M_p\left[0.7 - 60.0\theta_p\right] \le 1.0 \text{ where } -0.008 \le \theta_p \le 0 \text{ radians, and} \qquad (4.2)$$

M = actual moment in accordance to continuity and moment-rotation behavior,

θ_p = plastic rotation at pier in radians (negative), and

M_p = section plastic moment capacity.

For this design, residual moments were related to the pier rotation by an inelastic conjugate beam analysis developed by Dishongh (1990 and 1992). The moments at the piers due to inelastic rotations at the piers, M_a and M_b, and the residual moment, M_{rd}, are:

$$M_a = \frac{\frac{EI\theta_P}{L}}{\left[\frac{-A}{3} - \frac{1}{2} + \frac{\frac{B}{6}+\frac{1}{4}}{B+1}\right]}, \quad M_b = \frac{-M_a}{2B+2}, \quad M_{rd} = M_a + M_b, \qquad (4.3a, 4.3b, 4.3c)$$

where

A and B are ratios of the two outer span lengths to the center span length 18.3/23.2 = 0.79.

At the pier section, the applied Service II moment, [D + 1.30L(1+I)] (Equation 4.1c), plus the residual moment (Equation 4.3c) is equal to the actual moment defined by the moment rotation relation (Equation 4.2) for composite pier sections:

$$[D + 1.30L(1+I)] + M_{rd} = M_P[0.7 - 60(\theta_P)] \quad (4.4)$$

Solving Equation 4.4 for the plastic rotation at the pier section yields θ_p = -0.00083 radians. The residual moment was found as M_{rd} = 34 k-ft at the two pier sections and throughout the middle span. The residual moment field is symmetric due to the symmetric bridge design.

For the Service II criteria, center span centerline stresses were found to be maximum. LRFD states that the applied stresses must be less than or equal to 0.95 of the flange yield stress, F_y, for composite, homogeneous sections in positive bending. The maximum Service II stress is determined by superposition of stresses where the live load moment stress component is equal to the elastic moment plus the redistributed residual moment. The total stress was calculated as 47.9 ksi which is approximately equal to the requirement of 0.95 F_y = 47.5 ksi (Weber 1994).

4.2.1.4.2 Strength I Limit State

To satisfy the ultimate strength requirement, a plastic collapse mechanism must not form with the application of Strength I factored loads. LRFD inelastic provisions use an effective plastic moment, M_{pe}, at the negative moment pier hinge sections. The effective plastic moment accounts for moment unloading at large inelastic rotations. The mechanism check was carried out by applying the factored dead loads [1.25DC + 1.50DW], moving the factored design truck [1.75L(1+I)] over the entire beam in tenth point increments, and calculating the plastic collapse load factors for all truck positions (Weber 1994). The critical mechanism, using M_{pe} at the pier sections, was the maximum positive center span loading configuration. The plastic collapse load factor was found to be 1.38: the structure can withstand 38% more factored live loads than caused by the Strength I factored design live loads. Thus, Strength I requirements did not control the design.

4.2.2 LFD Design Using 10% Redistribution of Pier Moments

To compare the current LRFD inelastic design to past practice, the same geometry bridge with the same sections was used to determine the design capacity using the Load Factor Design provisions (AASHTO 1992). LFD has two limits: Overload and Maximum load. The Overload case controlled the design. The Overload limit is a limited stress at all sections of 0.95F_y subject to D+5/3L(1+I). The dead loads are identical to the previous design. The live loads used in LFD differ from the LRFD specs. Figure 4.3 shows the 5/3L(1+I) moment envelopes for an equivalent

HS18.1 loading. Redistributing 10% of the negative pier moments to the positive moment region as is allowed for compact shapes, the resultant stress at the pier section is 47.5 ksi (=0.95F_y) and it is 45.9 ksi at the positive moment region (Hartnagel 1997). Thus, the LFD HS18.1 design load is less than the capacity of the current LRFD inelastic design specifications. Design loads for this particular bridge structure are shown in Table 4.2.

4.2.3 LRFD Elastic Design Using 10% Redistribution of Pier Moments

To compare the current LRFD inelastic design to the LRFD elastic design, the same geometry bridge with the same sections was used to determine the design (AASHTO 1994). LRFD has two design limits: Service II and Strength I. The Service II case controlled the design. The Service II limit is a limited stress at all sections of 0.95F_y subject to DC+DW+1.3L(1+I). The dead and live loads are identical to the previous design. Figure 4.2 shows the moment envelopes for a HS20 loading. The LRFD elastic design capacity for this structure is a HS15.9. Redistributing 10% of the negative pier moments to the positive moment region as is allowed for compact shapes, and scaling the HS20 live load moments by HS15.9/HS20, the resultant stress at the pier section is 47.5 ksi (=0.95F_y) and it is 42.1 ksi at the positive moment region (Hartnagel 1997). Thus, the LRFD elastic HS15.9 design load is less than the capacity of the current LRFD inelastic design specifications. Design loads for this particular bridge structure are shown in Table 4.2.

4.2.4 Proposed LRFD Inelastic Design

The proposed LRFD inelastic design provisions located in the Appendix are compared to the current LRFD inelastic design provisions. The procedures follow those presented for the design of the noncompact girder bridge in Section 5.2.1. The Service II limit controlled the design. With the compact pier section, the effective plastic moment at the Service II limit is equal to the plastic moment. For this structure, this meant that there is no redistribution of moment at the pier section due to yielding since the Service II loading of DC+DW+1.3L(1+I) did not exceed the effective plastic moment. The design check then becomes the 0.95F_y stress limit at the positive moment region. Using the dead load and HS20 live load moments shown in Figure 4.2, the stress at the positive moment region is 47 ksi (Hartnagel 1997). This results in a HS20 design

load capacity. Thus, the LRFD criteria and the current LRFD inelastic design specifications result in the same design load. Design loads for this particular bridge structure are shown in Table 4.2.

4.2.5 Design Summary

Table 4.2 shows the design load for the current LRFD inelastic design, the LFD elastic design with 10% redistribution of negative pier moments, the LRFD elastic design with 10% redistribution of negative pier moments, and the proposed LRFD inelastic design methods. The bridge structure for these design loads was determined using the current LRFD inelastic design provisions. The Service II limit state (Overload for the LFD method) controlled in all the design checks.

The proposed LRFD inelastic design and the current LRFD inelastic design methods both result in the same design load. The Service II limit for the two methods are near identical, although the proposed method has simplified the procedures greatly. The LFD and the LRFD with the redistribution of moments are slightly less. However, with bridges comprising compact sections, the designs should not differ greatly since the LFD and the LRFD with the redistribution of moments accounts for the ability of the girder to redistribute the pier moments with some inelastic action. There would be significantly lower design loads without the 10% redistribution in the LFD and LRFD methods. This is shown in Chapter 5, Table 5.2 where current codes do not allow for redistribution when sections are noncompact.

4.3 THREE-SPAN COMPOSITE GIRDER TEST

4.3.1 Girder Model and Test Set-Up

The test girder was a scaled interior girder from the prototype bridge. Structural modeling techniques were employed to determine the theoretical scale factors, S, for the fundamental measures of interest in the 1/2 scale model. Steel and concrete properties for the prototype and the model were identical. Therefore, the independent variables were chosen as the elastic modulus, E (S_E=1), and the length, L (S_L=2). A half-scale model of the deck effective width, deck thickness, deck reinforcement, shear studs, and bearing stiffeners was easily produced (Weber 1994). However, an exact half-scale model of the W30x108 rolled shape did not exist, so a W14x26 was chosen as the best alternative. Figure 4.4 illustrates the test girder section and measurement instrumentation. Using the W14x26, the actual scale factors for several

fundamental measures did not match the theoretical scale factors. A summary of important cross sectional properties is presented in Table 4.1, along with the theoretical and actual scale factors of these properties. In Table 4.1,

I^+ = positive bending section moment of inertia in positive moment regions,

I^- = negative bending section moment of inertia in negative moment regions,

$_{COMP}$ = composite section, (steel + rebar for I^-)

S_x = section modulus,

S_{actual} = P/M = actual scale factor (prototype / model scale factor),

S_{theory} = P/M = theoretical scale factor (prototype / model scale factor),

b_f = width of flange,

t_f = thickness of flange,

d = section depth, and

t_w = thickness of web.

Loading applied to the model was scaled in order to simulate equal stresses in the model and the prototype. Since scale factors for all the section modulii were approximately 8.5, as shown by the shaded portion of Table 4.1, to model equal stresses, all prototype bending moments were factored by 1 / 8.5 (Weber 1994). Also shown in Table 4.1 are scale factors computed for the plastic moment capacities at the critical sections. The actual yield stress of the test beam was 50 ksi. Therefore, no adjustments were necessary for design and test differences.

Compensatory dead load was added to accurately simulate dead load stresses since a half-scale model weighs only one-quarter of the prototype. Ten 2000 lb concrete blocks were hung from the bottom of the W-shape before the concrete deck was placed to compensate for the self-weight lost due to scaling. Additional concrete blocks were placed on top of the deck after it hardened to represent the composite dead loads (wearing surface, guard rails, etc.).

Moving live loads were simulated with four discrete loading points on the test beam as shown in Figure 4.5 Influence lines for each of the four loading points were used to determine the sequence of loads needed to simulate a moving truck. The total moment envelope produced by

the four discrete loading points is shown in Figure 4.6 along with the scaled theoretical design truck [L(1+I)] moment envelopes. The truck load sequence could be linearly adjusted to represent any percentage of the modeled truck design weight (LL).

Several different measurements were recorded for the test including deck slip, rotation, deflection, reaction, and strain gage readings. Dial gages were also used to manually measure deflections. A 200 kip compression load cell was placed under each support to measure the reactions of the beam. The locations of these measurements are shown in Figure 4.7. The girder, load actuators, compensatory dead load, and instrumentation are shown in Figure 4.8.

4.3.2 Test Sequence

The modeled live loads were applied to the test beam cyclically at various load levels. The following design load levels and collapse loads were examined rigorously due to their importance:

(1) Service I,

(2) Service II,

(3) Strength I, and

(4) Plastic Collapse Load (Strength I loads proportionally increased until failure).

The entire loading history of the test is as follows. Elastic low-level tests were carried out at 10, 20, 40, 60, 70, 80, and 90% LL, where LL represents modeled Service I design loads. These provided an opportunity to confirm elastic behavior and instrumentation performance. Service I level live loads (100% LL) were applied to examine fatigue (ratioed to 75% LL) and deflection requirements of the LRFD provisions. Increasing the loads towards the Service II level, live loads of 110 and 120% LL were applied to examine the behavior in this range of loads.

At the Service II live-load level (130% LL), the girder experienced controlled inelastic behavior. After seven cycles, deflections stabilized and the girder behaved elastically for additional cycles. The inelastic behavior is characterized by residual deflection or permanent set. Design provisions predict this residual deflection and limit stresses in positive moment portions of the structure to control the amount of permanent set. Live loads were applied at 140, 155, and 166% LL to examine the inelastic behavior above the Service II level. The last simulated moving load test was at 175% LL plus factored dead loads. This loading represents the worst possible maximum design load level applied to a bridge.

After the cyclic tests, the girder was tested to failure by monotonically increasing loads proportioned to represent the theoretical design collapse configuration. This configuration simulated a stationary truck where the center axle of the truck was located at the centerline of the middle span. The additional factored dead load was applied by adding extra simulated loads to the P1 through P4 discrete load locations.

4.3.3 Design Limit Test Results

4.3.3.1 Service I Level Behavior

The main design concerns at the Service I load level are fatigue and live-load deflection control. Fatigue stress criteria limited the allowable fatigue stress range to 5.8 ksi; the corresponding strain is 200 με. Strains (ratioed to 75% LL) at the top flange of Sections 1 and 2 (Figure 4.4 and 4.7) were 71 and 158 με, respectively. Thus, the model met the Category C fatigue stress requirement.

There was 0.08 in of permanent set measured at the bridge centerline before applying the 100% LL sequence. After four 100% LL cycles, residual deflection at the center of the bridge was 0.12 in. The largest live load deflection at 100% LL occurred in the middle span (with P2 and P3 loaded) and was measured as 1.22 in. Theoretical deflection of the model was computed as 1.16 in using a nonprismatic analysis and the actual loads at P2 and P3 (Weber 1994). This indicates that the model represented the prototype bridge live-load deflection behavior well.

4.3.3.2 Service II Level Behavior

As the load level was increased to 130% LL, strain measurements at negative bending sections were substantially higher than the theoretical elastic strains indicating that some yielding had occurred. LRFD provisions require that the stresses in positive bending regions be less than $0.95F_y$ after redistribution of moments. A maximum strain of 1449 με occurred at Section 4. The maximum strain allowed by LRFD for 50 ksi steel is 0.95×1724 με = 1638 με. Therefore, the structure met the Service II limit-state criterion.

A permanent set of 0.38 in occurred at Section 4 after seven 130% LL cycles. Theoretical residual deflections at the Service II level can be calculated from the prototype design residual moments and rotations, 34 k-ft and 0.00083 radians, respectively, previously determined using the LRFD pier moment-inelastic rotation curve. Using a nonprismatic beam with a reduced moment

of inertia for 20% of the span each side of the interior piers yielded a scaled residual deflection of 0.26 in.

4.3.3.3 Strength I Level Behavior

The Strength I mechanism test was conducted by first applying the simulated factored portion of the dead load to P1, P2, P3 and P4. Live loads were then applied to P1, P2 and P3 to recreate the prototype mechanism moment diagram. The P1 and P4 loads were set to load control for the duration of the collapse test while the P2 and P3 loads were slowly increased under stroke control until the girder failed by concrete crushing. Figure 4.9 is the total load at P2 and P3 (P2 + P3) plotted against the deflection at the girder centerline. The figure shows the Strength I factored load level in relation to the load - deflection response. The figure clearly shows that the girder had excess capacity (36%) beyond the Strength I loading in accordance with the design calculations.

4.3.4 Inelastic Behavior

4.3.4.1 Shakedown Behavior

Each modeled truck weight percentage loading was repeated until the residual deflections stabilized and the bridge experienced shakedown. Figure 4.10 shows the permanent set residual deflection at the centerline of the bridge in terms of the percent Service I design load level. This shakedown plot shows how the structure accumulated permanent set as the live load level increased. The onset of permanent set occurred at 70% LL. After the last cycle of the 175% LL + factored dead load level loads, the girder had a residual deflection at the centerline of 2.6 in.

Stabilization of residual deflections was obtained with all live load levels except for the factored dead load plus 175% LL level (Strength I). Three cycles were carried out at the Strength I load level upon which each cycle resulted in large increases in residual deflection. The cyclic live loading portion of the test concluded at this level because some web buckling at the pier sections was detected. At the Strength I load level, the structure may or may not have shaken down. However, it can be concluded that the incremental collapse load, where inelastic deflections continually grow, occurred above the 166% LL level.

The moment-inelastic rotation at the negative moment pier section is the determining relation for the current LRFD inelastic design method. From this behavior, the inelastic rotation, residual moment field, actual moments, and residual deflection are determined.

For the Service II limit, Figure 4.11 shows the moving load experimental moment-inelastic rotation for the south pier. Figure 4.12 shows the same information except with the addition of the plastic collapse test moment-rotation data. Both figures include dead loads and maximum negative moment loadings. From Figure 4.11, the inelastic rotation at the south pier (and north) is 4 mrads at the Service II level (130%LL).

Positive moment regions also show similar moment-rotation behavior as shown in Figure 4.13 for the centerline of the girder. At the Service II level, the inelastic rotation is 0.8 mrads. Even though stresses are less than $0.95F_y$, there is some nonlinear behavior. The inelastic design provisions do not explicitly incorporate positive region inelastic rotation. However, although it is small, this inelastic rotation does have an effect on permanent deflections. Chapter 3 describes methods to calculate residual deflections with positive region inelastic rotations.

The residual deflection at 130%LL (Service II limit), based on the actual inelastic rotations at the two piers and at the girder centerline, is calculated in Figure 4.14. The conjugate beam method, using a length weighted moment of inertia, is employed loaded with an unknown residual moment field and known concentrated inelastic rotations. Figure 4.14 shows the calculated residual deflection to be 0.36 in which is very close to the experimental deflection of 0.38 in. The determinate residual moment is 16.2 ft-k, which also agrees with experimental pier residual moments of 20.2 ft-k and 19.1 ft-k after the 130%LL load cycles.

Concrete cracking over the pier regions, although important for serviceability, has little effect at Service I or Service II levels as shown in Figure 4.15. At low loads, the concrete is uncracked or partially cracked and the neutral axis is high in the beam. However, at design limit loads, the concrete has cracked sufficiently such that the neutral axis has settled near the design position. At the 175%LL, the neutral axis starts to migrate towards the plastic hinge location.

4.3.4.2 Plastic Collapse Behavior

After the moving load tests, the girder was tested to failure by monotonically increasing loads proportioned to represent the theoretical design collapse configuration. The simulated factored portion of the dead load was applied to P1, P2, P3 and P4 and then P1, P2 and P3 were

loaded to simulate the truck. Figure 4.9 is the total load at P2 and P3 (P2 + P3) plotted against the deflection at the girder centerline. The figure shows the Strength I factored load level (175%LL plus factored dead load) in relation to the load-deflection response. The figure shows that the girder had excess capacity (36%) beyond the Strength I loading in accordance with the design calculations. The theoretical plastic collapse load was calculated using the effective plastic moment at the pier sections and the plastic moment capacity of the section at location P2. The actual maximum attained load was within 1% of the theoretical collapse load.

After sustaining about 14 in of deflection at the bridge centerline (in addition to the 2.6 in from the shakedown tests), the concrete crushed at the bridge centerline. Figure 4.16 illustrates the collapse test girder. Two aspects of the collapse test are worthy to note. The first is that the girder resisted 13.8 in of deflection at near maximum loads. This deflection (length / deflection = 33) shows tremendous ductility for this compact girder. The second item is that this ductility behavior was not from an ideal elastic-perfectly plastic mechanism.

In Figure 4.12 it was seen that the pier sections are unloading moment with increasing rotation throughout the test. This is primarily due to flange buckling, web buckling (started during the moving load tests) and lateral buckling. The lateral torsional buckling was very apparent with two distinct sine waves (sweep approximately 1 in) between the bracing 4 ft on each side of the pier. The flange and web buckling were visible, but seemed to stabilize early in the collapse loading.

While the pier sections were unloading, the centerline positive moment section was absorbing the redistributed moments as shown in Figure 4.13. The combination resulted in a very ductile girder.

4.4 COMPONENT TESTS

A total of four girder components were tested in a double cantilever manner to simulate the pier region of a bridge girder (Unterreiner 1995). The components represent half-scale models similar to the W30x108 three span prototype bridge girder.

Three of the components were tested subject to a monotonically increasing load as shown in Figure 4.17. Of these three, Girder A was noncomposite, Girder B was composite with the deck reinforcement, and Girder C was composite with twice the area of deck reinforcement as

Girder B. Girder C, identical to the three-span test, had enough reinforcement to satisfy the requirement (LRFD 6.10.1.2) (AASHTO 1994) that 1 percent of the gross area of the slab of reinforcement is required in the longitudinal direction. Girder B does not satisfy the 1 percent requirement. However, it does satisfy the minimum reinforcement requirements for the positive moment region. Maintaining a W14x26 steel shape, these tests represent a controlled range of slenderness variations and expected moment-rotation behaviors. Table 4.3 presents the girder component properties.

A fourth W14x26 composite component (Girder D) with the higher deck reinforcement was tested subject to variable repeated load. The loading simulated the cyclic nature of variable moment peaks, variable moment gradients, and alternating span loadings inherent in multi-span bridges. The loading scheme is illustrated in Figure 4.18. The simulated moving truck load was applied 107 times, 92 at levels at or above service level loads. This test is used to examine the possibility of stiffness and strength degradation due to cyclic strain and strain gradients at the pier section. It has been postulated that under moving loads there may be slip occurring between the concrete deck and the steel section (Barker 1990, Barker and Galambos 1992, and Leon and Flemming 1997). The properties of the fourth girder are the same as those for Girder C and are presented in Table 4.3.

Figures 4.19 through 4.21 show the moment-inelastic rotation behavior of the four component tests. The moment was determined from load cells on the hydraulic actuators and a load cell under the pier support. The inelastic rotation was calculated by subtracting elastic rotations from total rotations. Two sets (one on each side of the support) of two LVDT's spaced 18 in apart measuring horizontal movement of a vertical plate attached to the beam were used to determine total rotations.

The ascending branch, used for the current LRFD Service II design check, of the theoretical moment-inelastic curve is the same for all compact sections as shown in Figure 4.22. However, the constant or descending branch, important for the current LRFD Strength I design check, depends on the compression element slenderness. Only if all compression elements are ultra-compact can the section be expected to maintain its plastic moment capacity, M_p, to the required inelastic rotation of 63 mrads. This is evident by the ultra-compact, noncomposite section of Girder A illustrated in Figure 4.19.

The experimental curve ascends to and above M_p and maintains M_p beyond the required 63 mrads. The component, along with the others, also demonstrated large rotational capacity (not shown) beyond 63 mrads. The experimental moment reaches M_p slightly above the 5 mrads predicted by theory. This would result in a slight underestimate of the permanent deflection at the LRFD Service II limit. However, upon examining the results for all four component tests, the permanent deflection predictions should be within camber design tolerances.

Figure 4.20 shows the theoretical and experimental moment-inelastic rotation curves for Girder B. This component is compact, but it is not ultra-compact. At the required 63 mrads of inelastic rotation, the conservative estimate of the effective capacity M_{pe} available is 90 percent of the plastic capacity M_p. During large rotations, the pier section redistributes some of its moment to the positive moment regions: the pier section unloads in a moment sense.

The experimental data of Girder B also shows an unloading as inelastic rotations increase at approximately the same rate as the theoretical curve. Like Girder A, the experimental moment increases above M_p near 5 mrads and shows M_{pe} is a conservative estimate of the moment capacity at 63 mrads.

Girders C and D have ultra-compact flanges (desirable), but the web slenderness is at the limit for compact. M_{pe} is estimated to be 88 percent of the plastic moment capacity M_p. Only if the flanges exceed the ultra-compact requirements would M_{pe} be much lower than M_p since the flanges constitute the great majority of the plastic moment capacity.

Figure 4.21 shows the theoretical and experimental moment-inelastic rotation curves for the monotonically loaded Girder C. The comparison mimics that of Girder B where it attains M_p approximately at 5 mrads, climbs above M_p, and descends at a rate similar to the theoretical curve. The importance of Figure 4.21 is the comparison of Girder C with the simulated moving load test of Girder D. Except for some random variability, to be expected for the complex loading and testing, the curve closely resembles that of Girder C. If slip or degradation occurred, the moving load testing of Girder D would show increased rotation at a given moment or a reduced moment at a given rotation, especially at higher rotations where strain demands are high.

4.5 SUMMARY OF COMPACT GIRDER TESTS

The one-half scale three-span continuous composite girder was subjected to simulated moving HS20 loading. The girder was designed and modeled to represent an interior girder of the current LRFD inelastic design bridge in the design comparisons above. Figures 4.8 and 4.16 are photos of the structure during testing. After the simulated moving load tests, the girder was subjected to modeled ultimate loading to determine the load-deflection characteristics. Below is a summary of the findings during the experimental program.

The behavior of the model behaved according to elastic structural theory. The elastic deflections and stresses (strains) matched well with that predicted. The measured Service II load level stresses (strains) met the Service II stress criteria. The fatigue stresses also met design criteria. The compact pier section redistributed moments and there were permanent residual deflections approximately according to predictions, especially when considering small inelastic rotations at the positive moment region. The current and proposed LRFD inelastic design provisions refer the engineer to ways of incorporating the positive moment region in analyses if deformations are important.

The plastic collapse test showed great ductility prior to collapse. The total deflection being approximately 1/33 of the span length. Strength I loads did not control the design. However, the experimental and the theoretical collapse loads were within 1%. This means the girder could withstand the theoretical Strength I loading. The pier section suffered moment unloading during the collapse test. This is in accordance with the design specification for a section which is compact yet not ultra-compact. During the pier section moment unloading, the positive moment region had significant moment loading due to the redistribution of moments from the pier section. The positive region eventually failed by concrete crushing.

The girder components were tested to develop and verify moment-inelastic rotation relations. They were tested in a double cantilever manner to model the pier section of a continuous span girder. Chapter 4 contains moment-inelastic rotation relations for the four girder components. The experimental results are compared to the current LRFD inelastic design moment-inelastic rotation relations. Below is a summary of the findings during the experimental program.

The experimental moment-inelastic rotation relation met or exceeded that predicted by the current LRFD inelastic design relation. Also the design relation modeled the test results well in magnitude and behavior. The noncomposite component had ultra-compact flanges and web. The section was able to maintain the plastic moment capacity well into the inelastic range. The composite component had ultra-compact flanges, but only compact webs. Therefore, by theory, the moment should have, and did, decrease with increasing inelastic rotation. The slope of the moment unloading was near identical to that predicted by the current LRFD inelastic design provisions. The girder component that was tested subjected to simulated moving loads did not show any indication of slip between the concrete deck and the steel beam. This puts some concern to rest related to stiffness and strength degradation during strain reversals at the interface.

The tests performed in this project support the development and verify the procedures of the proposed inelastic design provisions for bridges comprising noncompact girders. The limit state design levels were satisfied and the overall behavior of the girders were good.

Table 4.1 Prototype and Model Girder Section Properties

Item	Prototype	Model	$P/M = S_{actual}$
$I^{+}_{LL,COMP}$ (in^4)	13,500	751.3	17.97
$I^{+}_{DL,COMP}$ (in^4)	10,400	578.5	17.98
$I^{-}_{DL\&LL,COMP}$ (in^4)	6,960	380.2	18.31
I_{STEEL} (in^4)	4,470	245	18.24
$S^{+}_{LL,COMP}$ (in^3)	461.1	54.36	8.48
$S^{+}_{DL,COMP}$ (in^3)	422.1	49.74	8.49
$S^{-}_{DL\&LL,COMP}$ (in^3)	362.7	42.58	8.52
S_{STEEL} (in^3)	299	35.3	8.47
$b_f / 2t_f$	6.9	6	1.15
d / t_w	54.7	54.5	1.004

Table 4.2 Comparison of Design Methods

Design Method	Design Load
Current LRFD Inelastic Design	HS20
LFD Elastic with 10% Redistribution	HS18.1
LRFD Elastic with 10% Redistibution	HS15.9
Proposed LRFD Inelastic Design	HS20

Table 4.3 Component Girder Section Properties

	Type	Deck Reinf.	Flange Slender.	Web Slender.	M_p	M_{pc}	M_{pc}/M_p	Remarks
Units		in^2			k-ft	k-ft		
Girder A	Noncomp.	N/A	5.98 ultra-compact	51.25 ultra-compact	147.5	147.5	1.00	Ultra-Compact
Girder B	Composite	1.10	5.98 ultra-compact	71.5 compact	202.7	181.5	0.90	Compact
Girder C Girder D	Composite	2.20	5.98 ultra-compact	93.5 ~ compact	213.2	188.6	0.88	Web at compact limit

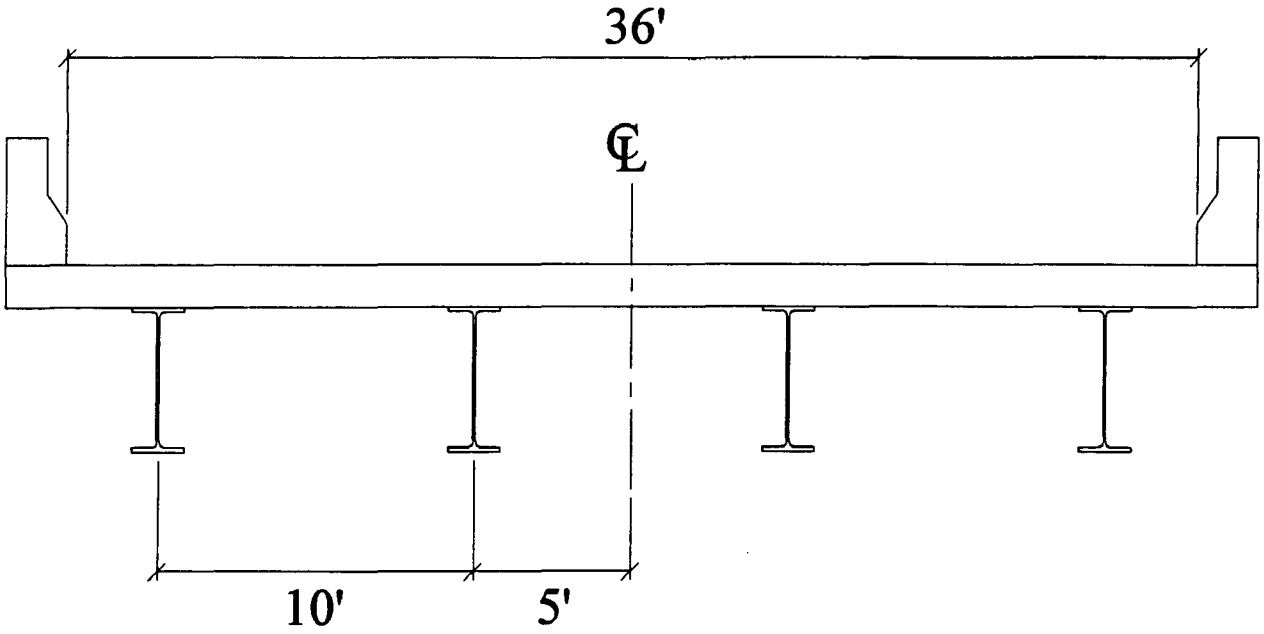

Figure 4.1 Cross Section of the Prototype Bridge

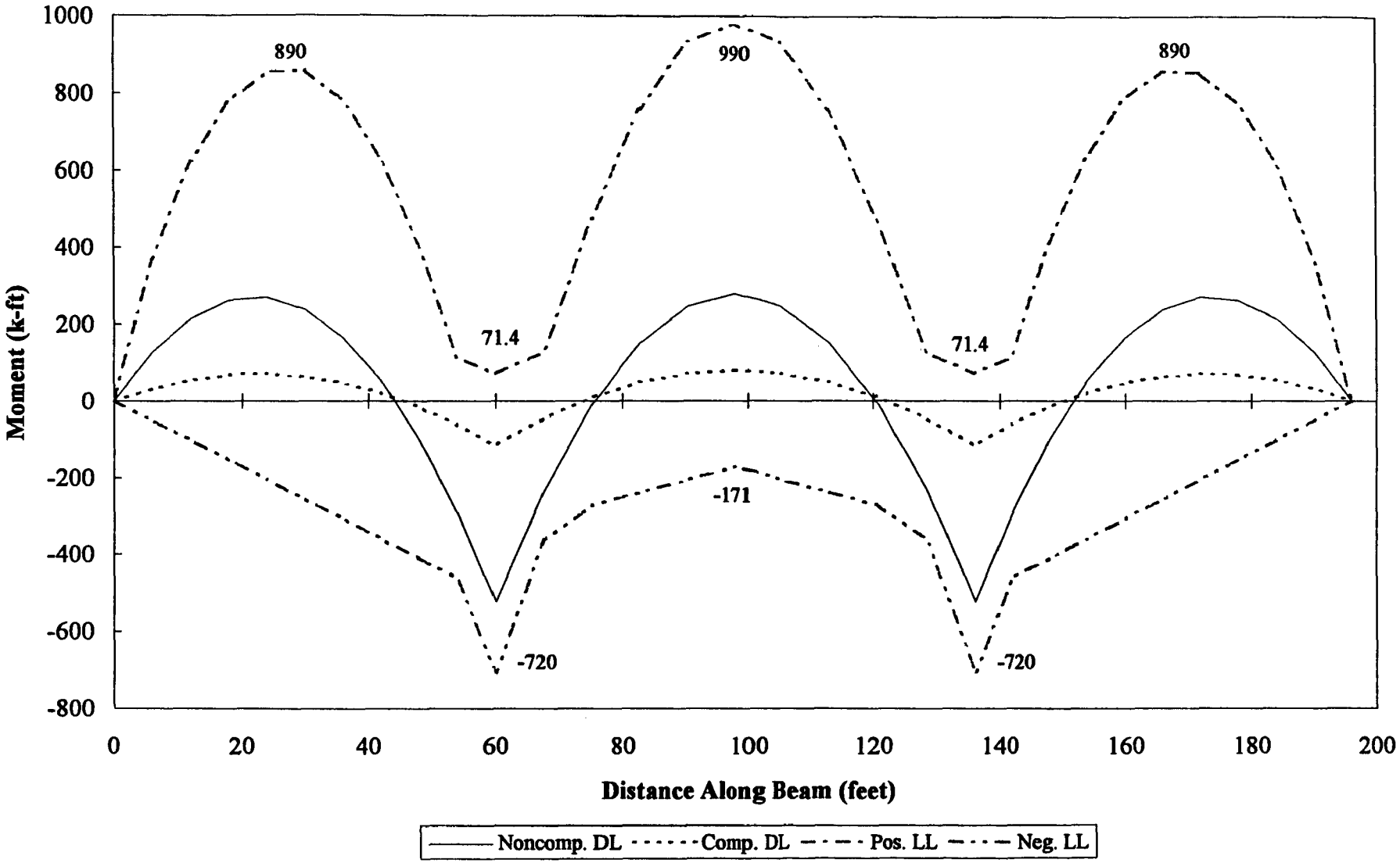

Figure 4.2 Moment Envelopes for the Prototype Girder

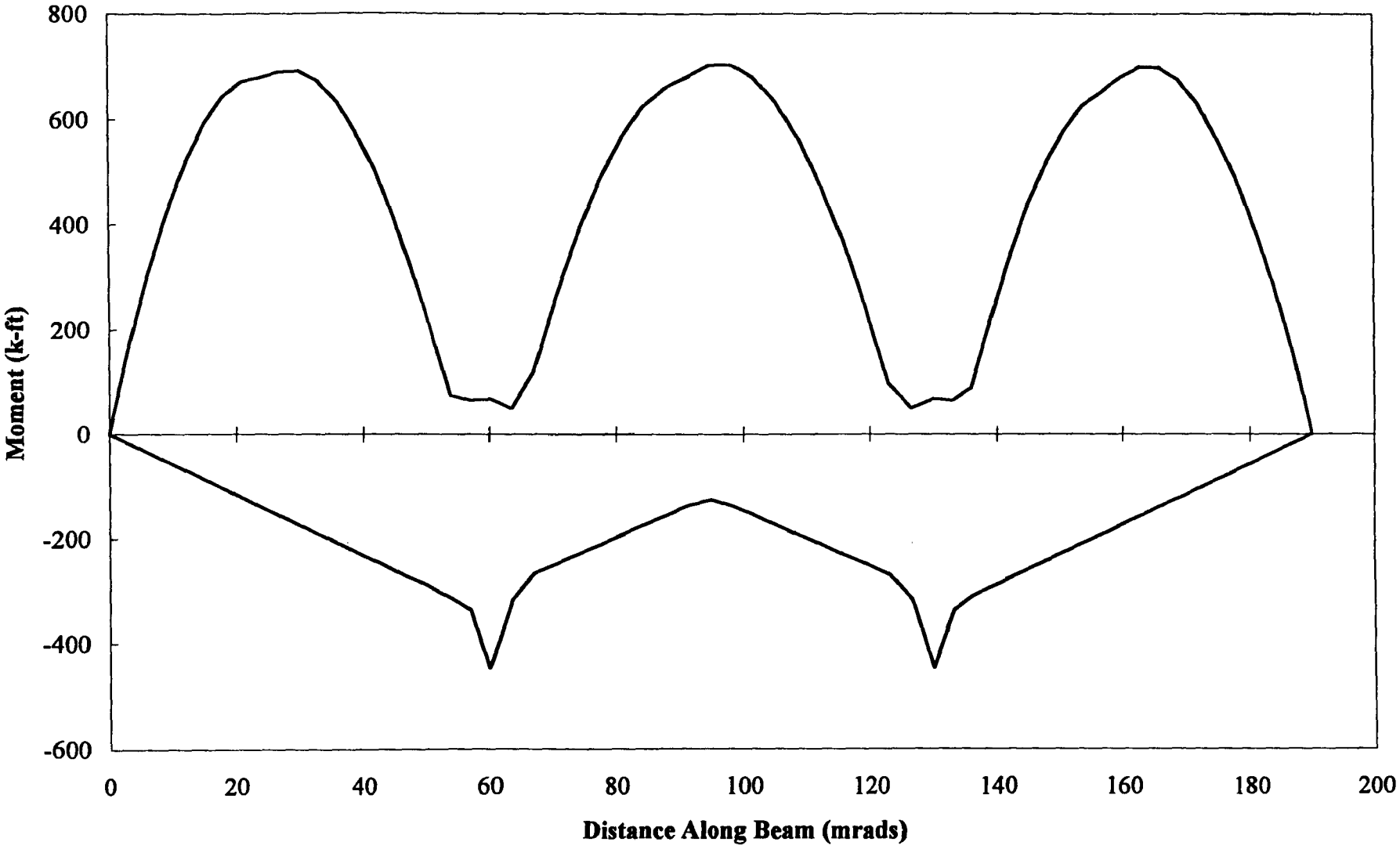

Figure 4.3 LFD Live Load Moments - HS18.1 Loading

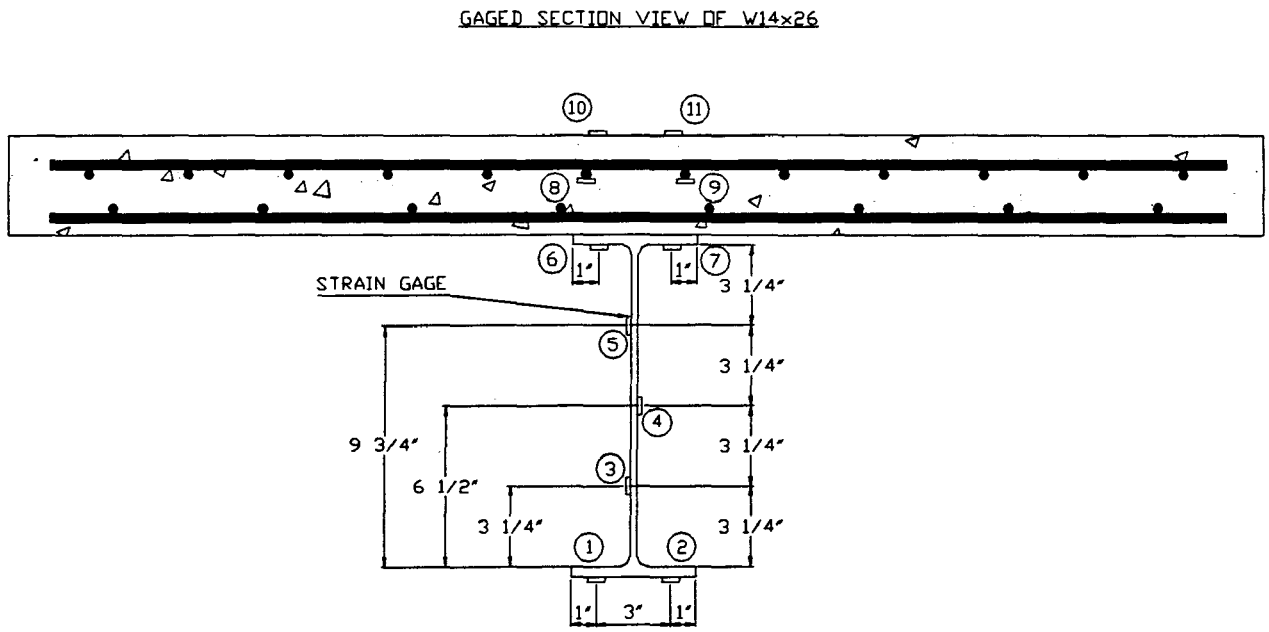

Figure 4.4 Test Girder Cross Section and Strain Gage Layout

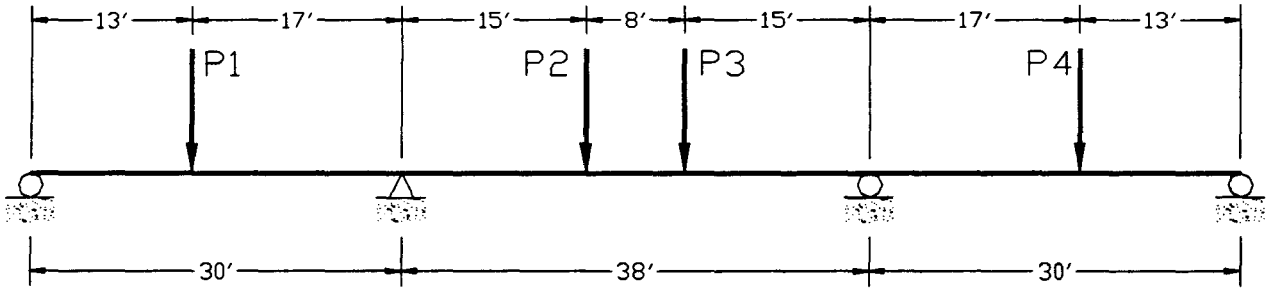

Figure 4.5 Layout of the Three Span Model Test

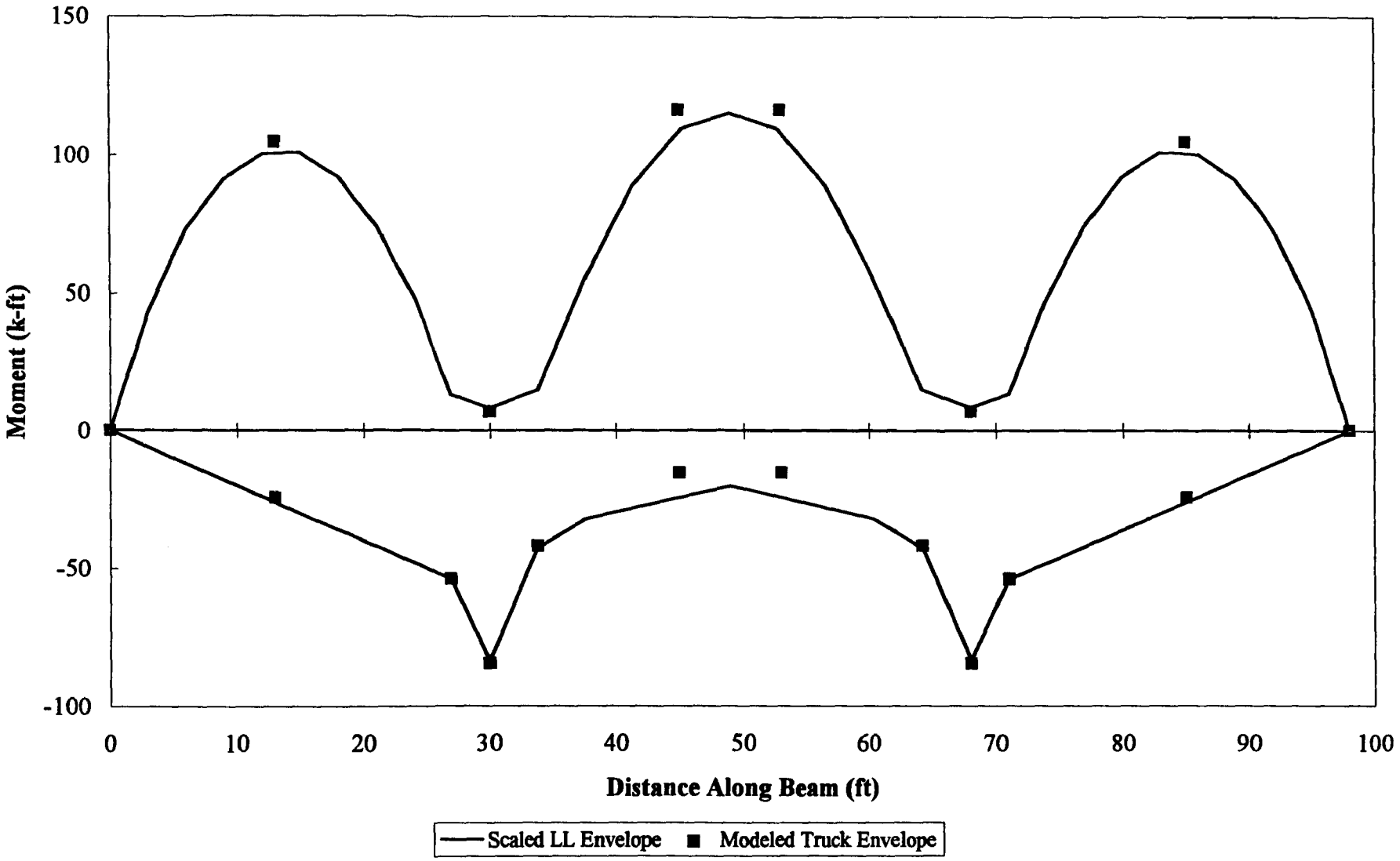

Figure 4.6 Modeled Live Load Moment Envelope

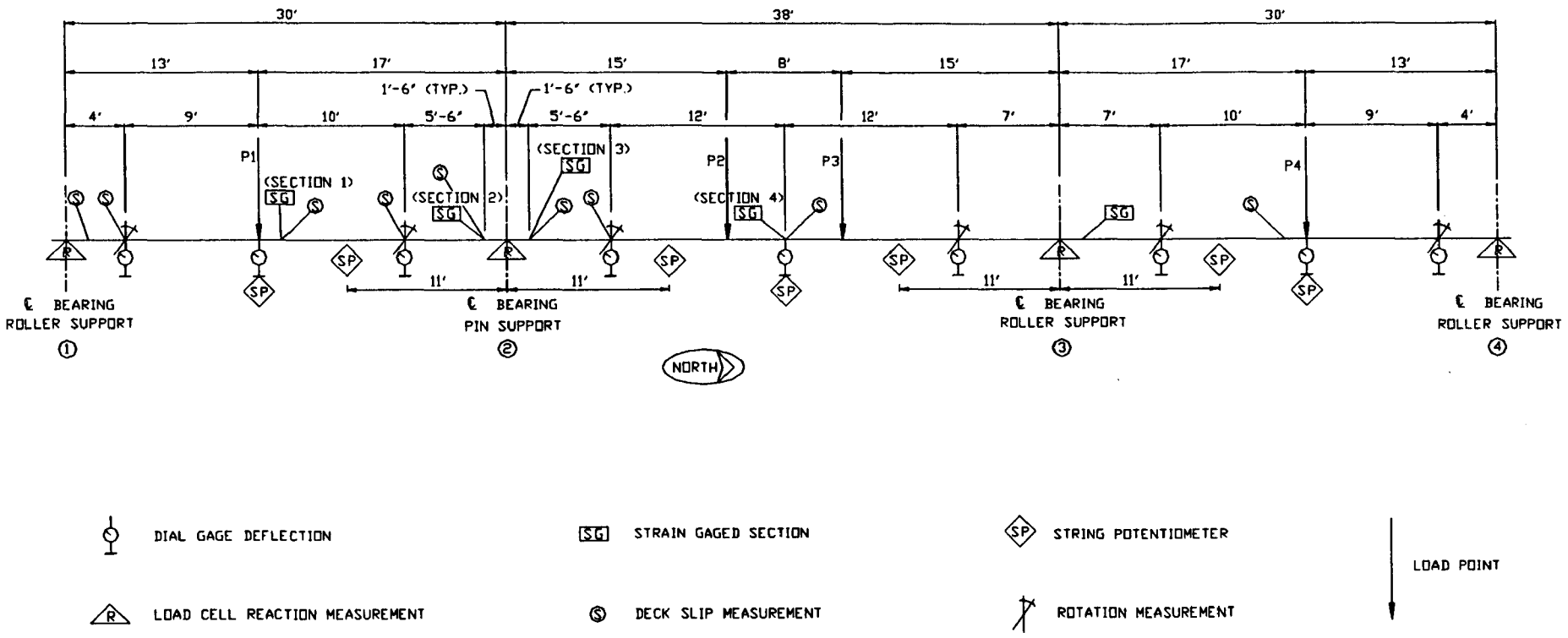

Figure 4.7 Test Measurement Layout

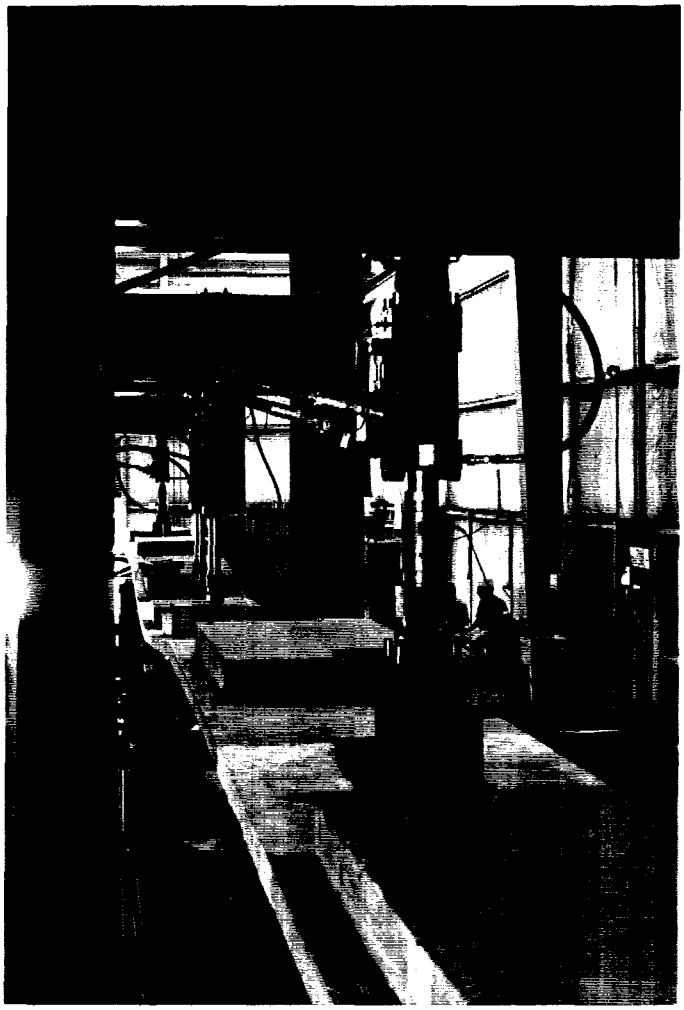

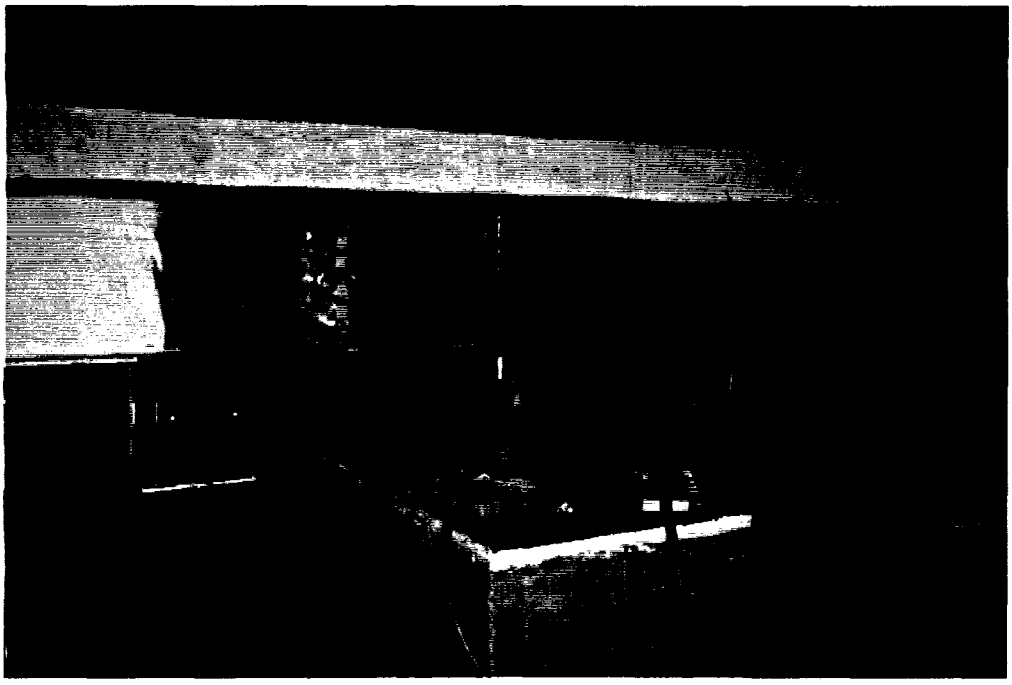

Figure 4.8 Compact Girder Photos

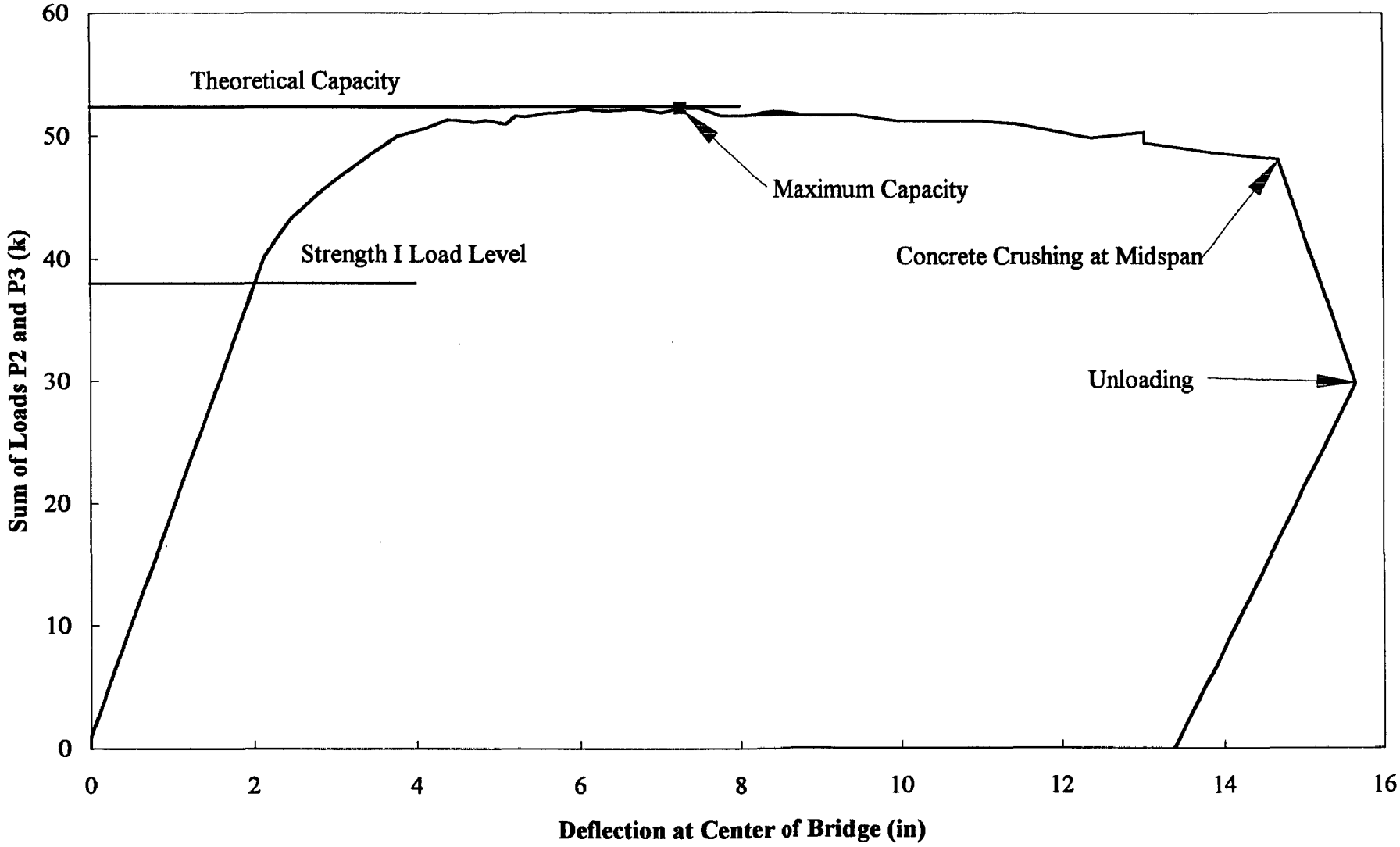

Figure 4.9 Load vs Deflection During Plastic Collapse Test

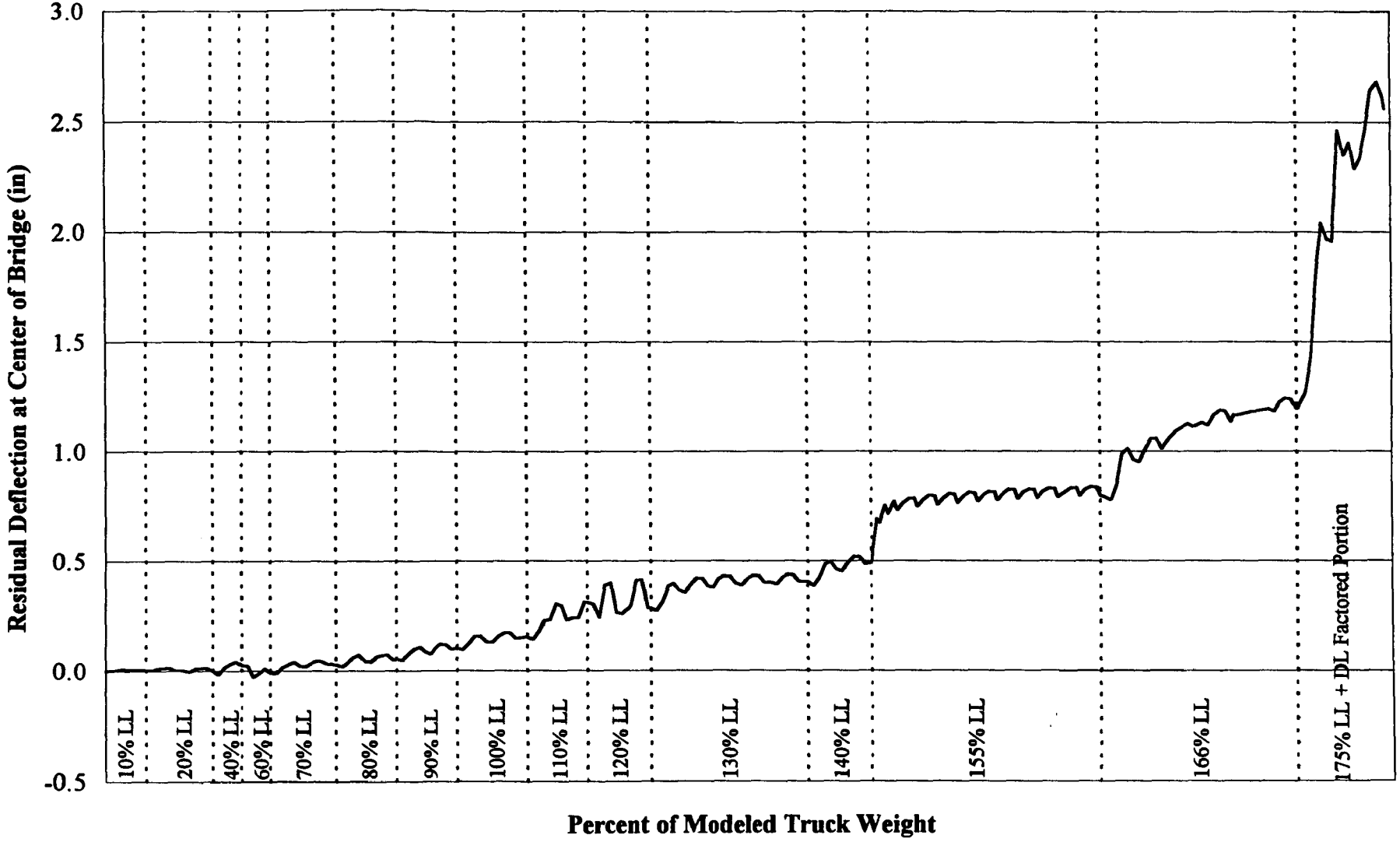

Figure 4.10 Residual Deflection vs Percent of Modeled Truck Weight

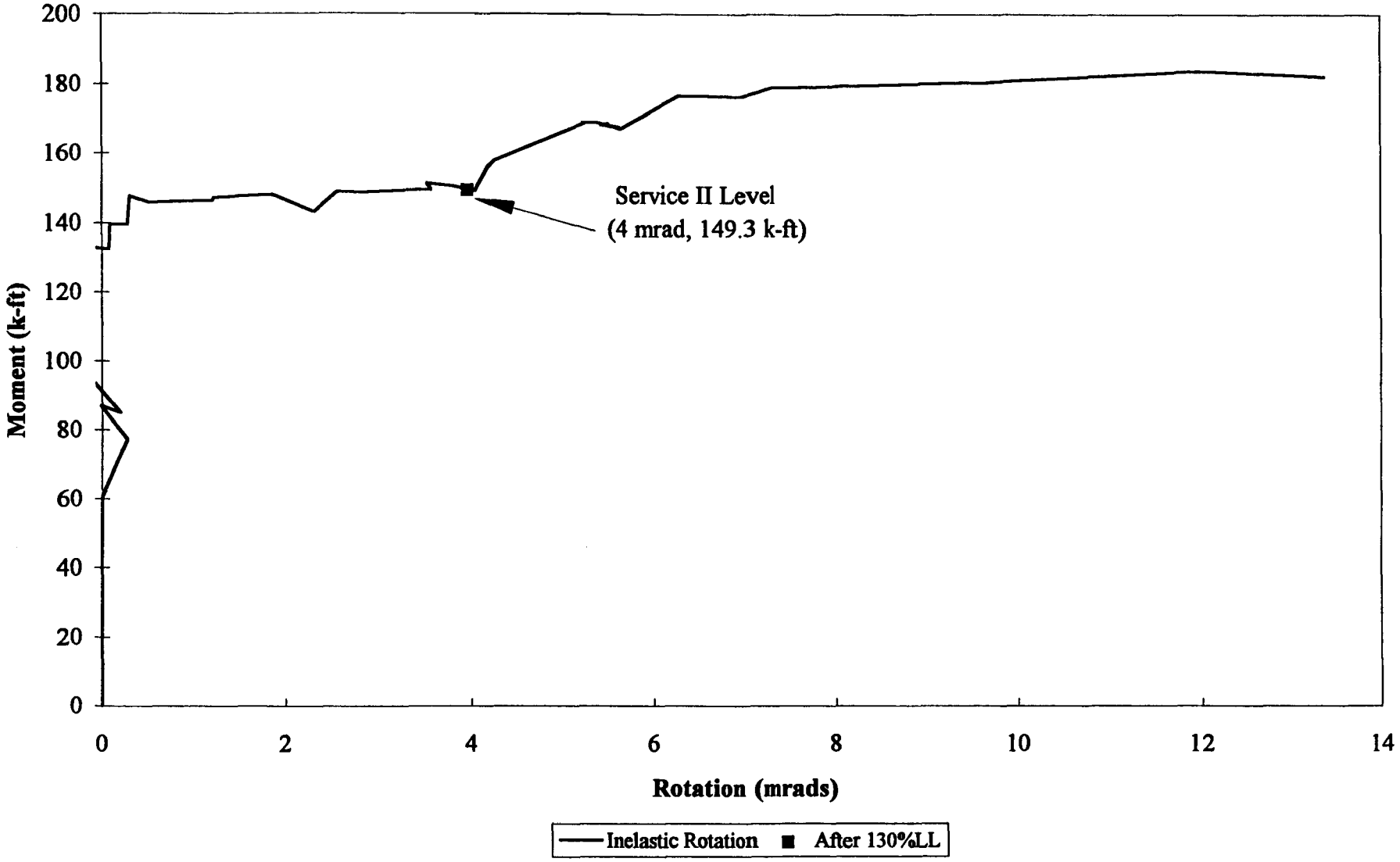

Figure 4.11 Moment vs Inelastic-Rotation for the Interior Support (Small θi)

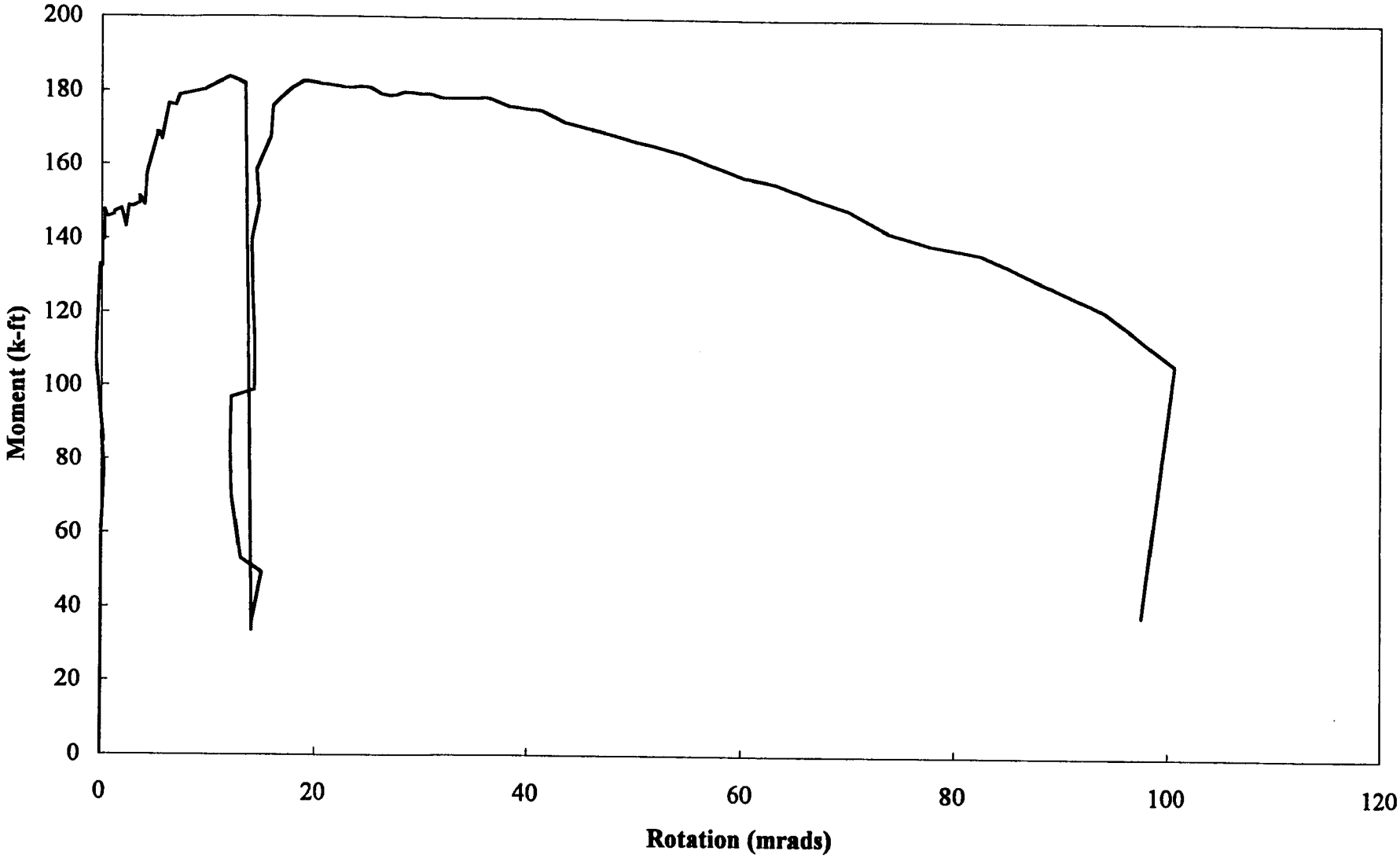

Figure 4.12 Moment vs Inelastic-Rotation for the Interior Support

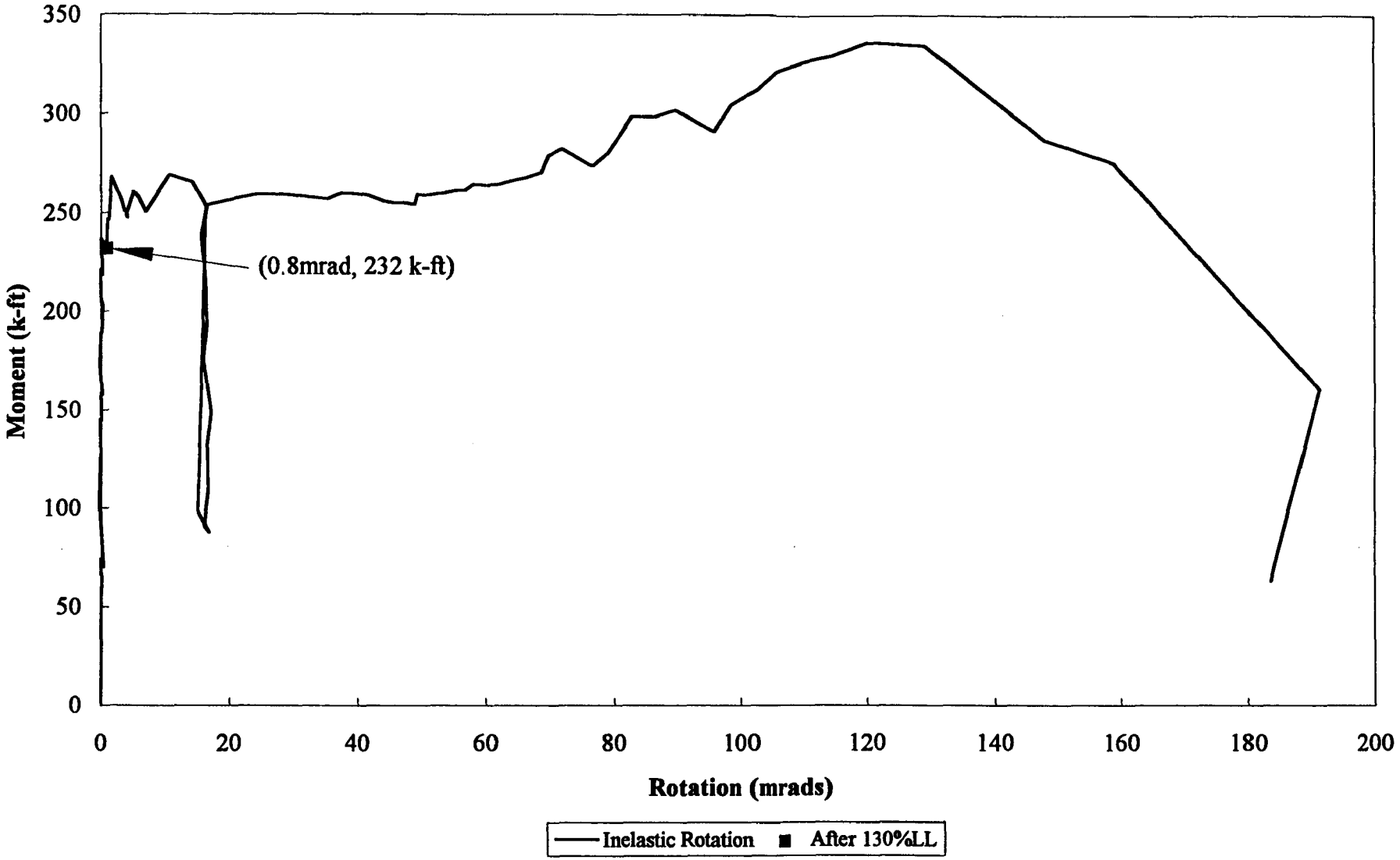

Figure 4.13 Positive Moment vs Inelastic-Rotation

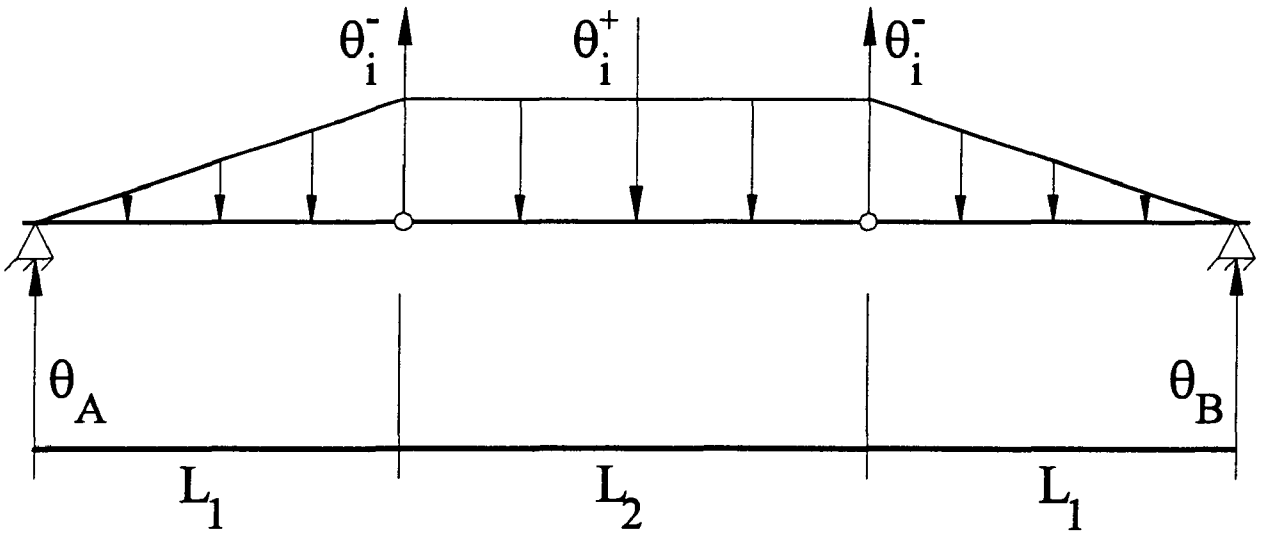

$$\theta_A = \theta_B = \frac{M_{rd}L_1}{6EI}, \quad \frac{M_{rd}}{EI} = \frac{6\theta_i^- - 3\theta_i^+}{3L_2 + 2L_1}, \quad \Delta_{CL} = \frac{\theta_i^- L_2}{2} - \frac{M_{rd}L_2}{48EI}(6L_2 + 8L_1)$$

$$\theta_i^- = 4\text{mrads}, \theta_i^+ = 0.8\text{mrads}, \text{ E} = 29{,}000\text{ksi and I} = 650\text{in}^4$$

$$\Delta_{CL} = 0.36"$$

$$M_{rd} = 16.2\text{k} - \text{ft}$$

Figure 4.14 Calculation of Residual Deflection at Centerline of Bridge

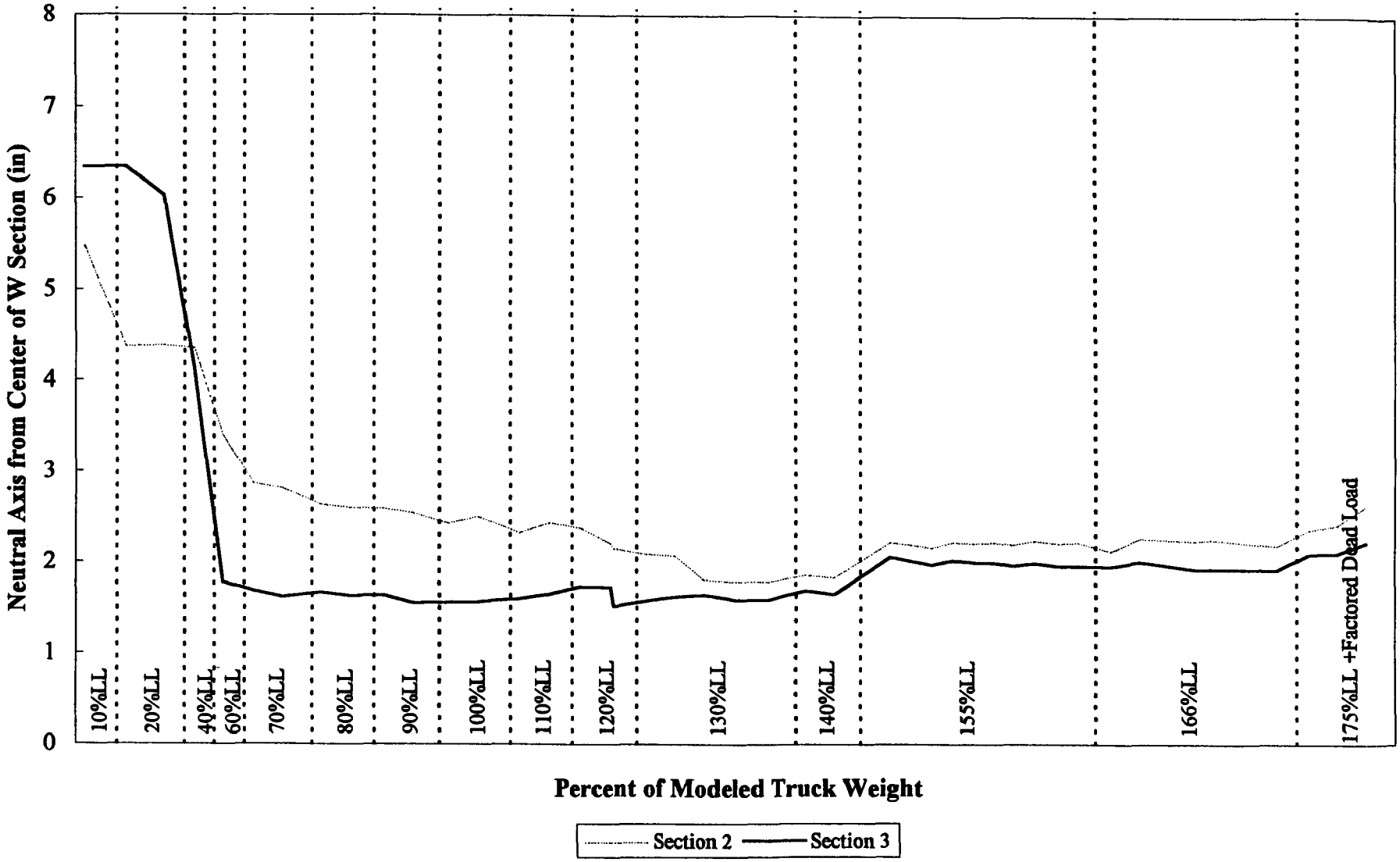

Figure 4.15 Location of Neutral Axis vs Percent of Modeled Truck Weight

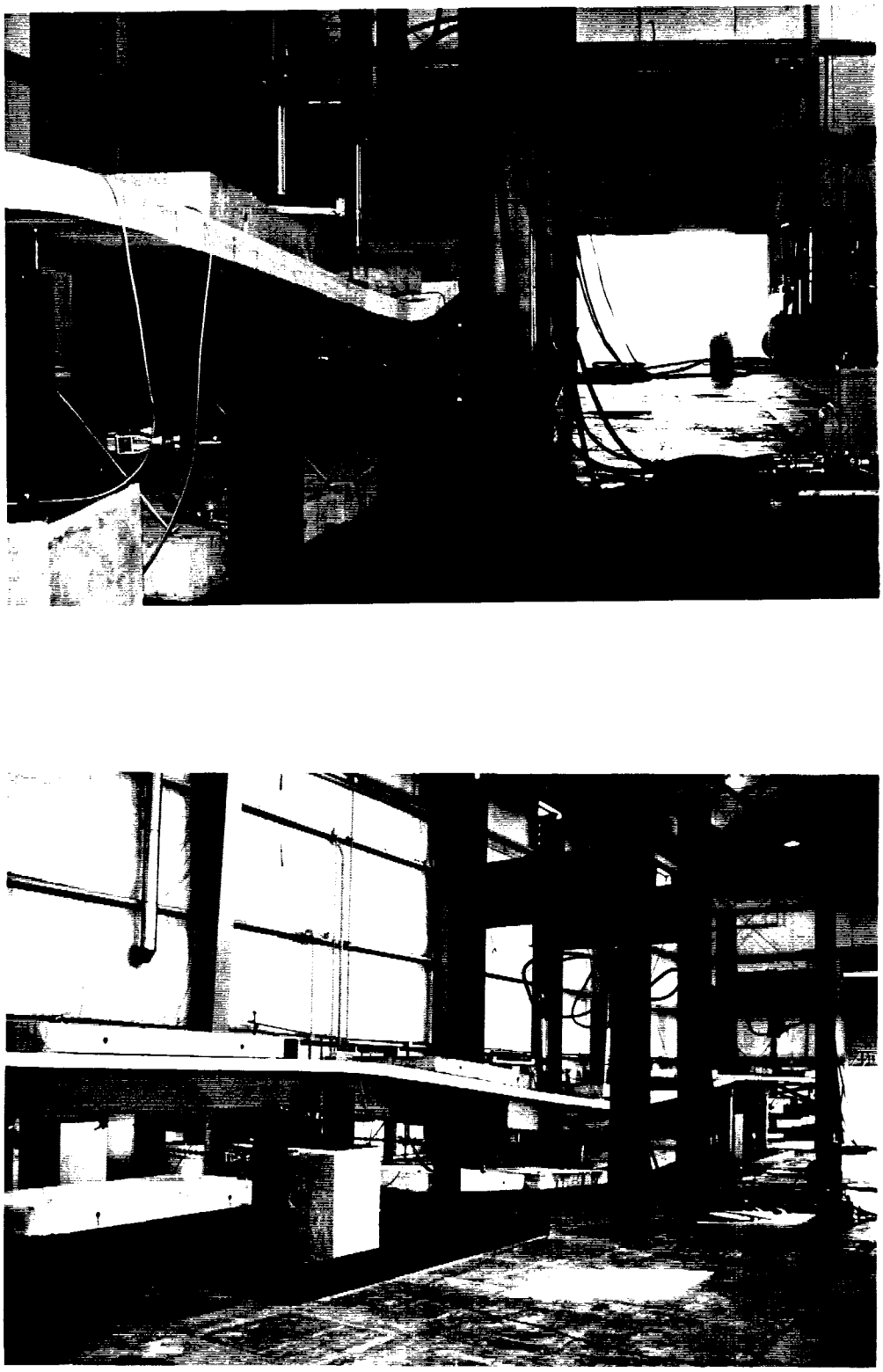

Figure 4.16 Compact Girder Collapse Photos

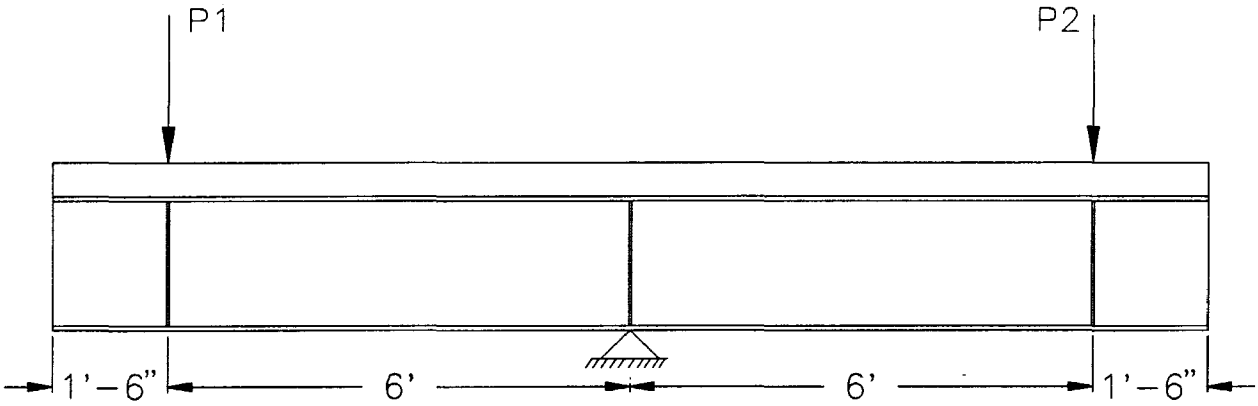

Figure 4.17 Component A, B and C Test Layout

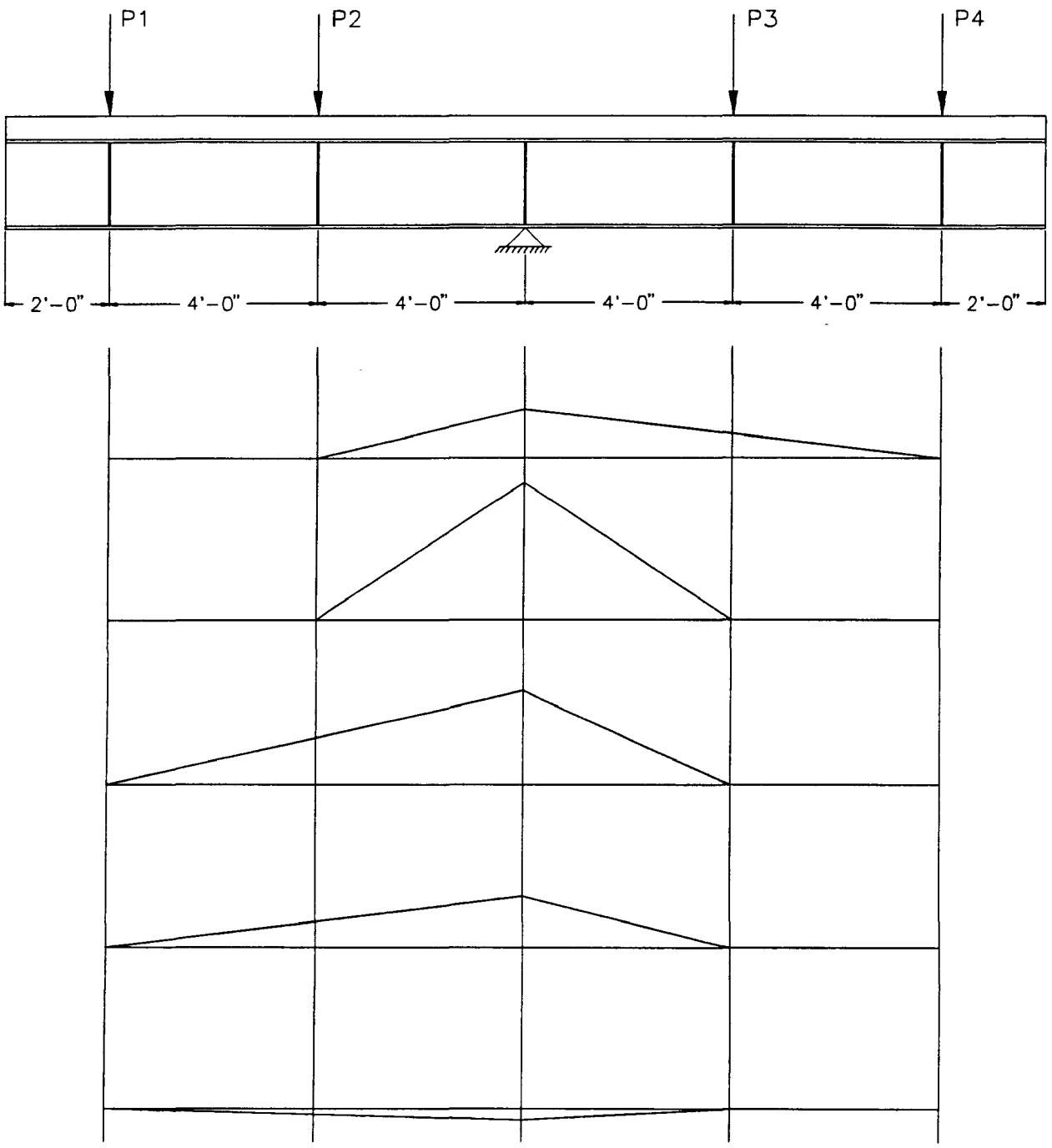

Figure 4.18 Component D Test Layout and Moving Load Moment Diagrams

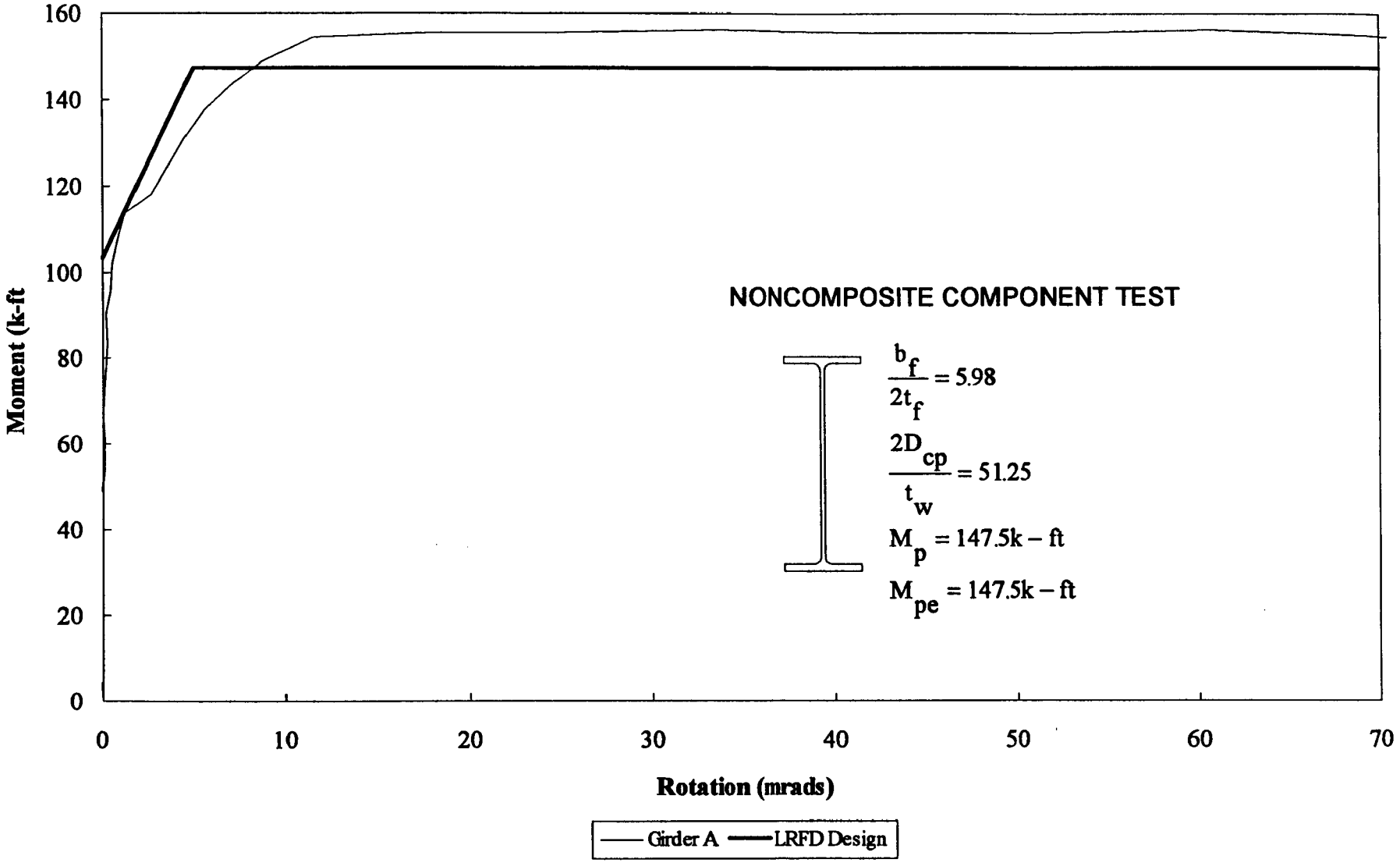

Figure 4.19 Moment vs Inelastic-Rotation for Girder A

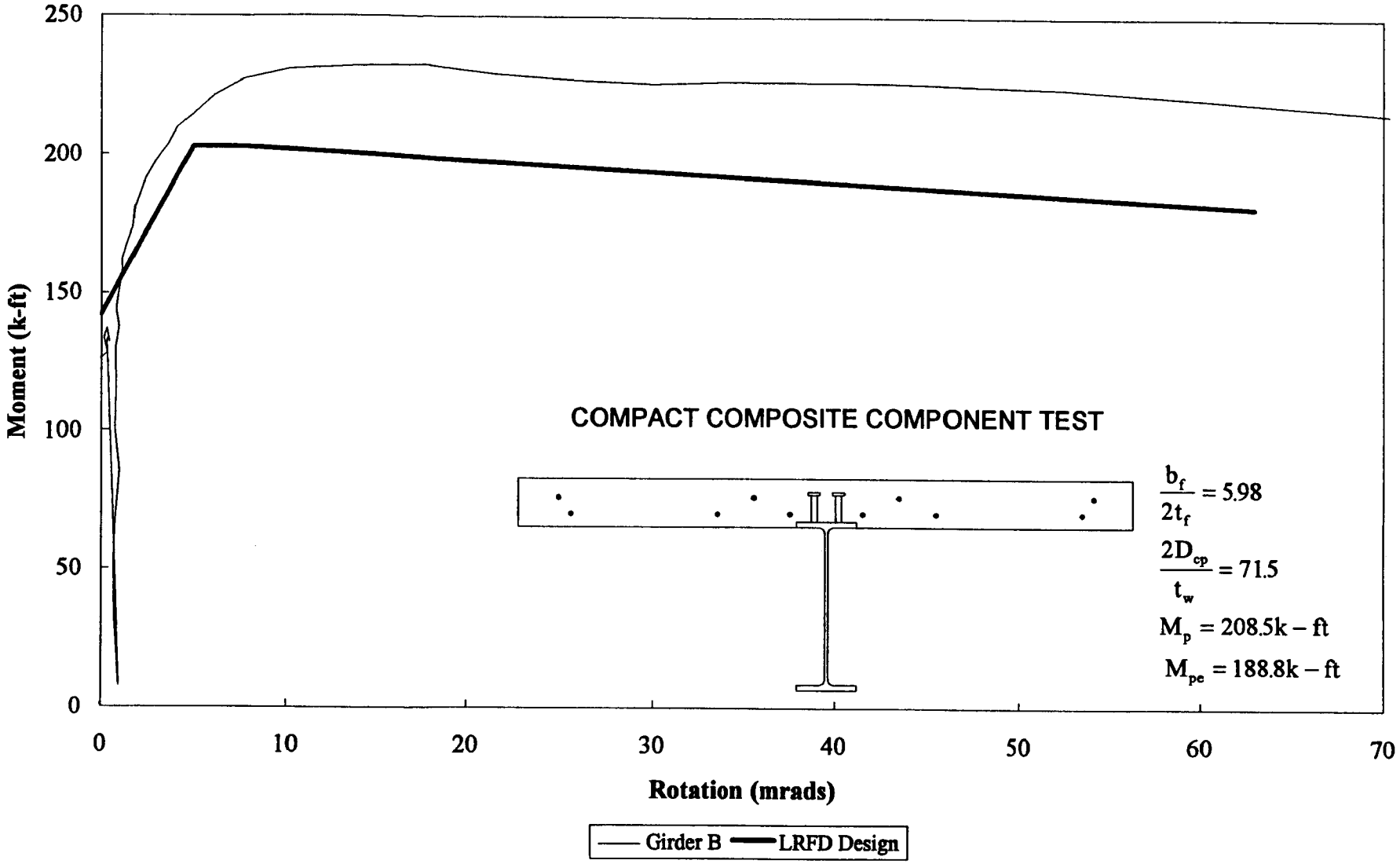

Figure 4.20 Moment vs Inelastic-Rotation for Girder B

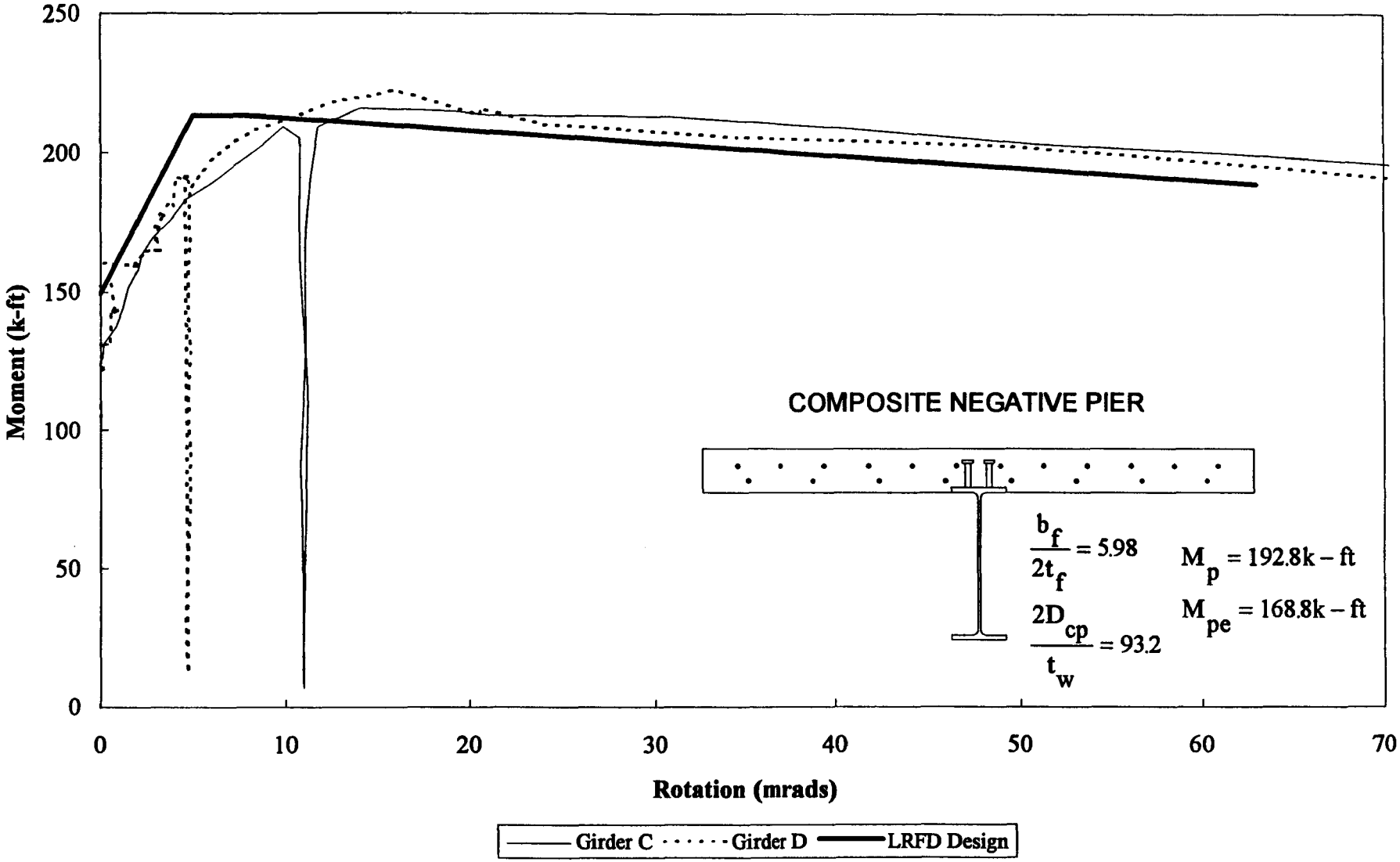

Figure 4.21 Moment vs Inelastic-Rotation for Girder C and Girder D

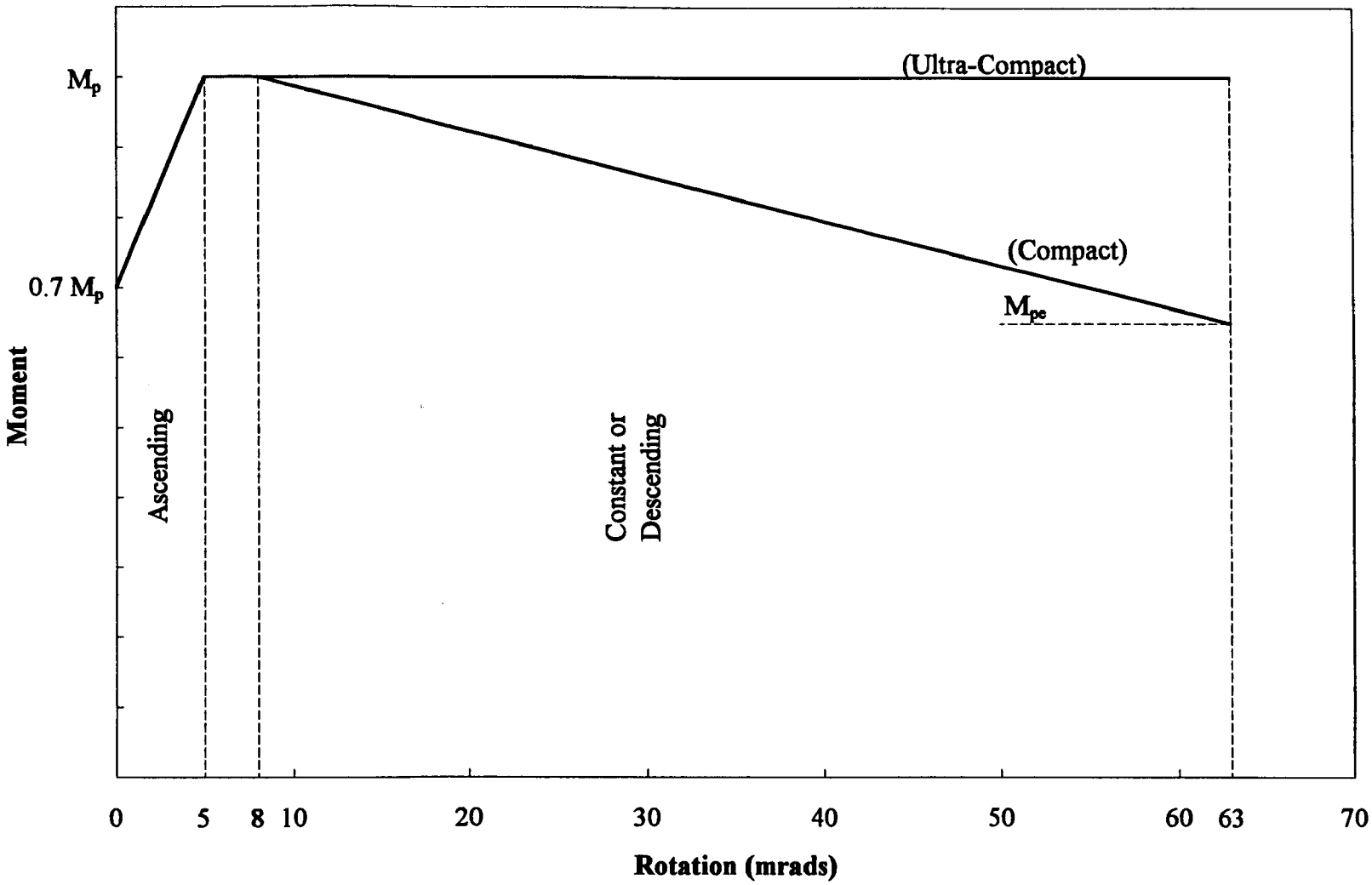

Figure 4.22 Moment vs Inelastic-Rotation Behavior

CHAPTER FIVE

GIRDER BRIDGES COMPRISING NON-COMPACT SECTIONS

5.1 INTRODUCTION

This chapter presents design provisions for steel girder bridges comprising noncompact sections. The chapter is divided into two major themes: design and experimental verification. The presentation of material is summarized herein due to length. The original and detailed information can be found in Hartnagel (1997).

Unlike for bridges comprising compact sections, currently noncompact bridges can be designed only by a couple methods according to AASHTO. The Load Factor Design (LFD - AASHTO 1992) method can be employed to design bridges using elastic limits and the Load and Resistance Factor Design (LRFD - AASHTO 1994) method can be used to design bridges using elastic limits. This report presents proposed LRFD inelastic design provisions (Appendix) meant to include bridges comprised of compact or noncompact sections. The proposed specifications are meant to replace the current LRFD inelastic design provisions.

In the first part of this chapter, a bridge is designed according to the proposed LRFD inelastic design provisions. This design is compared to the LFD elastic method and the LRFD elastic method. The design comparisons are summarized in Table 5.2. The table shows the benefits of using inelastic design procedures.

The second part of this chapter is devoted to experimental testing of a one-third scale model of an interior girder from the bridge designed by the proposed LRFD inelastic design method. The tests consisted of a two-span composite girder subjected to modeled moving truck loads and girder component tests to examine the inelastic behavior of bridge girders. This chapter examines the behavior at the design limit states and the general elastic and inelastic behavior through collapse of the test girder.

5.2 DESIGN PROVISIONS

5.2.1 Proposed LRFD Inelastic Design and Test Girder Prototype Design

5.2.1.1 General

Current LRFD design provisions do not allow the inelastic design methods to be used with non-compact cross sections. One of the objectives of the research is to allow the use of cross sections which have non-compact webs and compression flange slenderness limited by $\frac{b_c}{2t_c} \le 0.408\sqrt{\frac{E}{F_{yc}}}$. This slenderness limit is the maximum compression flange slenderness permitted for non-compact sections in the current LRFD Article 10.48.2.1 (AASHTO 1994). Inelastic behavior of girders with compression flange slenderness ratios exceeding this limit has not been adequately investigated.

The proposed LRFD inelastic design procedures limit the compression flange slenderness to the above and limit the web slenderness to $\frac{2D_c}{t_w} \le 6.77\sqrt{\frac{E}{F_{yc}}}$. The proposed procedures are limited to steel with yield strength not exceeding 50 ksi.

The proposed LRFD inelastic design provisions to replace Section 6.10.11 of the current LRFD Specifications are shown in the Appendix. The loading and limit states are the same as for the current LRFD provisions as described in Chapter 4.

5.2.1.2 Prototype Bridge Design

A non-compact plate girder bridge was designed using the proposed simplified inelastic design provisions located in Appendix A. The bridge is a two span structure with span lengths of 165 ft-165 ft. A 42 ft. wide deck was supported by four 69 in deep plate girders with a spacing of 12 ft. Figure 5.1 is a cross section of the bridge. Steel yield strength of 50 ksi was used and the 28 day compressive strength of the concrete deck was 4000 psi. Grade 60 reinforcing steel was used in the 9in thick composite concrete deck. Dead and live loadings were in accordance with the current AASHTO LRFD Specifications (AASHTO 1994). A 12 psf future wearing surface and two 305 plf barriers were also applied to the bridge. The ADTT for a single lane of 540 was used in the fatigue design.

The plate girder consisted of two different cross sections: the interior support region and the positive moment region. At the interior support, a 69 in deep plate girder with two 21 in wide flanges was used. Flange thickness was 15/16 in for the top flange and 1.5 in for the bottom flange. This cross section extended 33 ft on either side of the interior support. In the positive moment region a 69 in deep girder was used but the top flange was 15 in by 3/4 in and the bottom flange was 21 in by 15/16 in. Figure 5.2 illustrates the prototype girder elevation. The girder was designed as a single girder with live load effects approximated with the use of the current LRFD live load distribution factors. Cross sectional properties of the negative and positive moment regions are shown in Table 5.1. The effective plastic moment capacity of the section is calculated using reduced yield stresses based on the slenderness of the component (Hartnagel 1997). Effective yield stresses are determined based on the slenderness of the compression elements in accordance to the current LRFD Specification (6.10.11.1.2) or proposed (6.10.11.2.3b).

5.2.1.3 Loads

The dead load of the steel girder and the concrete deck, component dead load DC, is applied to the non-composite section. This is a result of unshored construction. A non-prismatic elastic analysis was used to determine the moments caused on the structure from the non-composite dead load. Moments from the component dead load, DC, are 2940 k-ft for the positive moment region and -6210 k-ft for the interior support. Moments for the future wearing surface and barrier curbs, DW, are 570 k-ft for the positive moment region and -1020 k-ft for the interior support. Weight of the barrier rails and a future wearing surface, DW, is applied to the composite section with a modular ratio of $3n = 24$ to take into account for creep and shrinkage of the concrete.

Live loads and impact are applied to the composite section with a modular ratio of $n = 8$ for the positive moment region. At the interior support the structural resistance was the steel section plus the contribution of the longitudinal reinforcing steel in the concrete deck. All moments and shears were computed using a non-prismatic elastic analysis. Positive moments were based on the 640 plf lane load and the HS20 truck with 33% impact included only on the truck. Negative moments were based on 90% of both the lane load and two trucks spaced 50 feet apart from front to rear with impact included only on the trucks (3.6.1.3.1). The LRFD revised distribution factors (4.6.2.2) are used to estimate the amount of live load moment and shear that is

applied to each girder. The live load moments for the girder were 3550 k-ft for the positive moment region and -2910 k-ft for the interior support region. Moment envelopes are shown in Figure 5.3.

5.2.1.4 Design Limit States

5.2.1.4.1 Service II Limit State

The Service II Limit State load combination as stated in LRFD Table 3.4.1-1 shall apply. The limit state requirement is a stress limit on the positive moment region. For the proposed LRFD inelastic design provisions, after the redistribution of moment from the interior support positive moment stresses are limited to 95% F_y for composite sections and 80% F_y for non-composite sections. There is no stress limit at the interior support regions. The redistribution moment at each interior support shall be:

$$M_{rd} = M_{pc} - M_e \geq 0 \qquad (5.1)$$

where:

M_{pc} = effective plastic moment specified in proposed Article 6.10.11.3.4, and

M_e = elastic moment at the interior support due to the factored loading, $DC + DW + 1.3L(1+I)$

At all other locations, the full redistribution moment shall be determined by connecting the moments at interior supports by straight lines and extending these lines from the first and last interior supports to points of zero moments at adjacent abutments. This ensures a self-equilibrating residual moment field.

The effective plastic moment capacity specified in proposed Article 6.10.11.3.4 of sections which satisfy the ultra-compact compression flange requirements (Equation 6.10.11.2.3a-1) or sections which satisfy the compactness requirements of Article 6.10.5.2.3 or 6.10.6.2 is:

$$M_{pc} = M_p \qquad (5.2)$$

where:

M_{pc} = effective plastic moment, and

M_p = plastic moment specified in Article 6.10.5.1.3 or 6.10.6.1.1

For all other sections:

$$M_{pe} = 0.8R_hM_y \quad (5.3)$$

where:

M_y = yield moment specifies in Article 6.10.5.1.2 or 6.10.6.1.1, and

R_h = flange-stress reduction factor specified in Article 6.10.5.4.1

If these provisions are not satisfied, a rigorous inelastic analysis shall be performed on the member as specified in proposed Article 6.10.11.2.5.

For the girder under consideration, the Service II limit state is satisfied as evidenced by the following calculations.

In Equation 5.1, M_e is calculated as:

$$M_e = 6210 + 1020 + 1.3(2910) = 11000 \text{ k-ft} \quad (5.4)$$

and

$$M_{pe} = M_p = 12800 \text{ k-ft} \quad (5.5)$$

The redistribution moment is calculated from Equation 5.1:

$$M_{rd} = M_{pe} - M_e = -12800 - (-11000) = -1800 \text{ k-ft} \geq 0 \quad (5.6)$$

Because the effective plastic moment capacity is greater than the elastic moment demand for the Service II loading there is no redistribution moment. The limit state check is a limited stress in the positive moment region. For composite sections, the stress is limited to 95% F_y. The design check is demonstrated below:

$$\frac{2940(12)}{1670} + \frac{570(12)}{2160} + \frac{1.3(3550)12}{2350} = 47.9\,\text{ksi} \approx 47.5\,\text{ksi} \quad \checkmark \text{ ok} \quad (5.7)$$

The Service II limit state is satisfied. This limit state is intended to prevent objectionable permanent deflections due to the occasionally overloaded vehicle.

5.2.1.4.2 Strength I Limit State

The proposed simplified Strength I limit state is a shakedown limit state. However, an alternative procedure where a rigorous inelastic analysis is used is still allowed (explained in Chapter 3). Schilling's unified autostress method (1989, 1991 and 1993) or the residual deformation method by Dishongh and Galambos(1992) are acceptable methods of inelastic analysis for bridges.

For the shakedown check, the flexural resistance of all sections shall satisfy:

$$M_r = \phi_{sd} M_{pe} - M_{rd} \quad (5.8)$$

where:

ϕ_{sd} = resistance factor for shake down specified in Article 6.5.4.2 (addition proposed)

M_{pe} = effective plastic moment specified in proposed Article 6.10.11.2.3 or 6.10.11.2.4

M_{rd} = redistribution moment specified in proposed Article 6.10.11.2.2

The redistribution moment at each of the interior supports shall be taken as:

$$M_{rd} = \phi_{sd} M_{pe} - M_e \geq 0 \quad (5.9)$$

where:

ϕ_{sd} = resistance factor for shake down specified in article 6.5.4.2

M_{pe} = effective plastic moment specified in Article 6.10.11.2.3 or 6.10.11.2.4

M_{rd} = redistribution moment specified in Article 6.10.11.2.2

M_e = elastic moment at interior support due to the factored loading

At all other sections, again the redistribution moment diagram shall be determined by connecting the moments at all interior supports with straight lines and extending these lines from the first and last interior supports to points of zero moment at the adjacent abutments. The effective plastic moment at the interior supports is determined from one of the following equations depending on the compression flange slenderness and the web slenderness. Proposed equation numbers are also included. For sections that satisfy:

$$\frac{b_c}{2t_c} \leq 0.291\sqrt{\frac{E}{F_{yc}}} \quad (6.10.11.2.3a\text{-}1) \quad (5.10)$$

If $\frac{2D_{cp}}{t_w} \leq 3.76\sqrt{\frac{E}{F_{yc}}}$, then:

$$M_{pe} = M_p \quad (6.10.11.2.3a\text{-}2) \quad (5.11)$$

If $3.76\sqrt{\frac{E}{F_{yc}}} < \frac{2D_{cp}}{t_w} \leq 5.05\sqrt{\frac{E}{F_{yc}}}$, then:

$$M_{pe} = R_h M_y \quad (6.10.11.2.3a\text{-}3) \quad (5.12)$$

If $\frac{2D_{cp}}{t_w} > 5.05\sqrt{\frac{E}{F_{yc}}}$, then:

$$M_{pe} = \left[1.56 - 0.111\left(\frac{2D_{cp}}{t_w}\right)\sqrt{\frac{F_{yc}}{E}}\right] R_h M_y \quad (6.10.11.2.3a\text{-}4) \tag{5.13}$$

where:

b_c = compression flange width,

t_c = compression flange thickness,

D_{cp} = depth of web in compression at the plastic moment specified in Article 6.10.5.1.4b or 6.10.6.1.2,

t_w = web thickness,

F_{yc} = specified minimum yield strength of the compression flange,

M_y = yield moment specified in Article 6.10.5.1.2 or 6.10.6.1.1,

M_p = plastic moment specified in Article 6.10.5.1.3 or 6.10.6.1.1,

M_{pe} = effective plastic moment, and

R_h = hybrid flange-stress reduction factor specified in Article 6.10.5.4.1c.

If the effective plastic moment is determined from any of the four equations above, a transverse stiffener shall be placed a distance of one-half the web depth on each side of that support. If the stiffeners are placed on only one side of the web, they shall be welded to the compression flange. Tests have shown that girders with ultra-compact compression flanges satisfying Equation 5.10, and with transverse stiffeners near the peak-moment location, provide good rotation characteristics even if the web is non-compact, Schilling and Morocos (1988).

The following calculations show the girder satisfies the proposed simplified inelastic design Strength I limit state with the exception of the transverse stiffener one-half the web depth on each side of the support. For the Strength I loading, the resistance of any cross section is determined from Equation 5.8 and the effective plastic moment capacity, M_{pe}, is determined from the above equations (5.11 - 5.13). The interior support resistance is calculated below.

$$M_r = 1.1(-10650) - M_{rd} \tag{5.14}$$

$M_{rd} = 1.1(-10650) - M_e$ (5.15)

and

$M_e = 1.25(-6210) + 1.5(-1020) + 1.75(-2910) = -14385$ k-ft (5.16)

Calculating M_{rd} and M_r as follows:

$M_{rd} = 1.1(-10650) - (-14385) = 2670$ k-ft (5.17)

$M_r = 1.1(-10650) - 2670 = -14385$ k-ft (5.18)

Once the interior support resistance is calculated, the design check is to ensure the positive moment region elastic demand is less than the positive moment region resistance. The same Equation 5.14 is used to compute the resistance with the attributed redistribution moment, M_{rd}. Figure 5.4 illustrates the total and residual moments and the design capacities at the Strength I design check. For the positive moment region:

$M_r = 1.1(12800) - 0.4(2670) = 13000$ k-ft (5.19)

The elastic moment demand on the positive moment region is computed as:

$M_e = 1.25(2940) + 1.5\ (570) + 1.75(3550) = 10750$ k-ft ≤ 13000 k-ft (5.20)

Therefore, the girder satisfies the Strength I design limit.

5.2.2 LFD Design

To compare the proposed LRFD inelastic design to past practice, the same geometry bridge with the same sections was used to determine the design capacity using the Load Factor Design provisions (AASHTO 1992). LFD has two limits: Overload and Maximum load. The Maximum case controlled the design. The Maximum limit is a limited stress at all sections of F_y subject to 1.3[D+5/3L(1+I)]. The dead loads are identical to the previous design. The live loads used in LFD differ from the LRFD specs. Figure 5.5 shows the 5/3L(1+I) moment envelopes for an equivalent HS4 loading. The pier is noncompact, therefore, there is no redistribution of negative pier moments allowed. The resultant stress at the pier section is 50 ksi (=F_y) and it is 42.2 ksi at the positive moment region (Hartnagel 1997). It is clear that the restriction on the redistribution of moments greatly reduces the efficiency of the girder. The LFD criteria does not meet the capacity of the proposed LRFD inelastic design specifications. Design loads for this particular bridge structure are shown in Table 5.2.

5.2.3 LRFD Elastic Design

To compare the proposed LRFD inelastic design to the LRFD elastic design, the same geometry bridge with the same sections was used to determine the design (AASHTO 1994). LRFD has two design limits: Service II and Strength I. The Strength I case controlled the design. The Strength I limit is a limited stress at all sections of F_y subject to 1.25DC+1.50DW+1.75L(1+I). The dead and live loads are identical to the previous design. Figure 5.3 shows the moment envelopes for a HS20 loading. The LRFD elastic design capacity for this structure is a HS4.5. The pier is noncompact, therefore, there is no redistribution of negative pier moments allowed. Scaling the HS20 live load moments by HS4.5/HS20, the resultant stress at the pier section is 50 ksi (=F_y) and it is 38.3 ksi at the positive moment region (Hartnagel 1997). The LRFD criteria does not meet the capacity of the current LRFD inelastic design specifications. It is clear that the restriction on the redistribution of moments greatly reduces the efficiency of the girder. Design loads for this particular bridge structure are shown in Table 5.2.

5.2.4 Design Summary

For bridges comprising noncompact sections, current bridge specifications do not allow for inelastic design nor redistribution of negative pier moments. The proposed LRFD inelastic design method, meant to replace the current LRFD inelastic design provisions, do allow redistribution of negative pier moments for noncompact girder sections (see Chapter 3). Table 5.2 shows the design load for the current LRFD inelastic design (not applicable), the LFD elastic design, the LRFD elastic design, and the proposed LRFD inelastic design methods. The bridge structure for these design loads was determined using the proposed LRFD inelastic design provisions. The Service II limit state controlled for the proposed LRFD inelastic design, but the Strength I (Maximum Load for LFD) controlled for the remaining methods.

The elastic methods (LFD and LRFD) have much lower capacities than the proposed LRFD inelastic design method. With bridges comprising noncompact sections, inelastic design methods should have significantly higher design capacities than bridges that are forced to remain elastic at factored loads. The ability to redistribute large negative pier moments, coupled with section capacities exceeding the yield moment, results in an efficient structure used to its limit state capacity. Elastic methods don't account for either component of this reserve strength.

However, this great difference of design load is partly due to the fact that this girder had very high dead load stresses. The available stress remaining for live load is small and, when the total stress must remain elastic, the truck capacity is low compared to an inelastic method that allows some of this live load stress to be redistributed to other areas.

Of course, inelastic methods for bridges comprising noncompact sections should only be used if the behavior is reliable. Chapter 3 justifies the use of inelastic design methods for girders with noncompact sections and the tests described below verify the ability to predict the inelastic behavior.

5.3 TWO-SPAN COMPOSITE GIRDER TEST

An interior girder from the bridge designed by the proposed LRFD inelastic provisions was used as a prototype for the test specimen. The test girder was a one-third scale model of the prototype bridge. Two 55 ft spans were used as the model. The two independent scale factors were the length scale factor, S_L, and the material scale factor, S_E. S_L was chosen as 1/3 so the model would fit in the laboratory and S_E was chosen as 1.0 because the material for the prototype and the model was steel and concrete. The plate girder was designed with length increments divisible by three to accommodate the ease of scaling. Figure 5.6 shows the test section geometries. The properties of the model can easily be adjusted by the appropriate scale factors shown in Table 5.1.

5.3.1 Girder Model & Test Set-Up

This section will cover the experimental testing of the two span girder. Special considerations were necessary in modeling the girder also to be discussed in this section. Structure load modeling and the experimental measurements made will be discussed. Finally, results from the continuous span test will be presented.

The one third scale model weighed only one ninth of the prototype girder. In order to properly scale the dead load stresses in the girder an additional amount of dead load equal to 2/9 of the weight of the prototype was required to be placed on the girder. This was accomplished by hanging one and a half 7 ft x 3.5 ft x 7 in concrete blocks weighing 3000 lb each from the bottom flange of the girder before the concrete deck was placed. It was necessary to hang the compensatory dead load blocks before the placement of the concrete to ensure the component

dead load, DC, stresses were carried entirely by the steel girder alone. This resembles the loading experienced during unshored construction. After the concrete deck was placed and allowed to cure for several days, additional dead load was applied to the girder. Steel plates 36 in x 36 in x 1 1/4 in weighing 500 pounds each were placed on top of the cured concrete deck to simulate the future wearing surface and the barrier curb dead load on the composite section.

The loads applied to the bridge represent levels of modeled design live load, design live load being 100% of an equivalent HS20 truck. However, adjustments to the specified levels were necessary due to material properties. The coupon test yield stress of the flanges, the important contributor for moment capacity, were approximately 42 ksi instead of 50 ksi. This lower yield stress had to be accounted for since the difference is significant and greatly affects the structural behavior for this particular girder.

This girder is very efficient in that the design maximizes the section capacity at both the positive and negative moment regions. In doing so, the dead load stresses are relatively large (already there and using up a large part of the available stress). Therefore, the applied live load stresses must be adjusted to recreate the limit states at the critical locations. For instance, at the positive moment region, the steel stress is limited to $0.95F_y$ at the Service II limit state. If the dead load stress is 25 ksi, there remains 22.5 ksi for live load stresses for 50 ksi material ($0.95F_y$ - 25 ksi), but only 14.9 ksi ($0.95F_y$ - 25 ksi) for the lower 42 ksi material. Thus, it is clear that significant problems would exist in assuming the 42 ksi material girder behavior would be identical to the 50 ksi material girder behavior.

For the moving load tests, the adjustments result in reducing the modeled truck loading by a factor of 0.65 (Hartnagel 1997). In other words, the experimental Service II limit state equivalent loading is 65% of 130% of the modeled design truck, or 84.5% of the modeled design vehicle loads. Using this adjusted loading, the stress and strain demand, in addition to redistribution of forces, is the same as for the original 50 ksi material subjected to the original modeled truck loading. In the following analyses, except for the Service I level check described below, only the adjusted equivalent levels are presented. The reader is referred to Hartnagel (1997) for a full description of the procedures.

The fatigue stress range and live load deflection are not dependent on the yield stress, rather, they depend only on the elastic response of the structure. Therefore, the original modeled

truck load levels are used for the Service I (fatigue and deflection) limits (Hartnagel 1997). The adjusted levels are not presented in this analysis.

Live load on the model was applied with four hydraulic actuators. Two actuators were placed in each span to simulate the maximum positive moment in the span and the maximum negative moment at the interior support. Influence lines were produced for each of the actuators and these were used to reproduce the actual live load moment envelope through the use of linear algebra. A loading scheme was developed to first apply the maximum positive moment in the first span then unload. Next, the maximum negative moment at the interior support was applied then released. Finally, maximum positive moment in the second span was applied and released.

A variety of measurements were taken during the testing of the model girder. Rotation measurements were made at 4 ft from each end of the girder and 6 ft on either side of the interior support. The measurements at the interior support location were made by two LVDT's spaced 18 in apart. Total rotation at the measurement location can then be computed by dividing the difference of the two readings by 18. Rotation near the end of the beam was made with two dial gages spaced at eight inches apart.

Strain measurements were made at four locations on the girder. Two locations were placed 18 in on either side of the interior support and the other two locations were near the middle of each span. The positive moment measurements were made 24.5 ft from the end supports. At each of the strain measurement locations, ten strain gages were used on the steel cross section. Six of the gages were attached to the web in equal spaced increments along the depth of the girder. The other four gages were attached to the top and bottom flange, two gages for each flange. At Section 1 two strain gages were attached to the steel reinforcing bars directly above the steel beam. At Section 2 and 3, four gages were attached to the steel reinforcing, two were on reinforcing directly above the steel girder and two were on the extreme reinforcing bars on either side of the steel girder. The purpose of these gages was to study the effect of shear flow in the deck slab.

A load cell measured the reaction at each of the three supports and load measurements were also made for each of the load actuators. The three support reaction load cells were 200 kip capacity. The interior support was pin supported and the two end supports were rocker supports. The supports were type "D" bridge bearings.

Several clip gages were attached to the girder to measure the slip between the concrete deck and the steel girder. A layout of all the measurements is shown in Figure 5.7.

The girder, load actuators, compensatory dead load, and instrumentation are shown in Figure 5.8.

5.3.2 Test Sequence

The two span girder was loaded in a fashion similar to that of an actual bridge girder. First, the steel girder was set on the three supports where it was subjected to structural dead load. Additional dead load was attached to the bottom flange of the girder to simulate the actual dead load stresses experienced by the prototype girder. Formwork for the concrete deck was then attached to the steel girder. The deck was placed using unshored construction techniques. Once the concrete deck hardened, the concrete forms were removed (approximately 3 days). One week after the concrete deck was placed, additional composite dead load was placed on the top of the girder. These steel plates simulated the weight of the barrier curbs and future wearing surface.

Twenty-eight days after placing the concrete composite deck, the live load testing began. Four hydraulic actuators were used to simulate the live load on the girder. Two were used in each span of the two span structure as shown in Figure 5.7. Influence lines were determined for each of the four actuators and the live load moment envelopes were approximated by use of the four actuators. The moment envelopes were modeled using a liner programming tool and the influence line diagrams for each actuator. The live load moment envelope and the modeled moment envelope are shown in Figure 5.9. After the modeled live load envelope was determined, it was applied to the girder in stages. The loading could be applied in any percentage desired as a percentage of a Service I design truck. The loading sequence consisted of three steps; each followed by an unloading step. Each step was designed to produce maximum moment in a specified portion of the girder. The first step was to load actuator P1 and P2. This produced maximum positive moment in the first span. After the load was applied, it was held for approximately 30 seconds while data was collected and then the load was returned to zero. Next, actuators P2 and P3 were loaded to produce maximum negative moment over the interior support. After the data was collected, the load was again returned to zero. Finally, actuators P3 and P4 were loaded to produce maximum positive moment in the second span. This three step cycle was applied to the girder at each load level until deflections in the spans stabilized. Load

levels started at 15.4% of a design truck and progressed through the following sequence: 15.4, 30.8, 61.5, 92.3, 107.7, 123, 138.5, 153.8, 169.2, 184.6, 200, 215.4, 238.5, 255.4, and 269. At the 269% load level, additional dead load was added with the four actuators to simulate the Strength I load factors of 1.25 DC and 1.5 DW. After the additional dead load was applied, the 269% truck was started on the bridge. With P1 and P2 on the first span suffered significant damage. Loading then progressed to P2 and P3 on where a large buckle in the web at the interior support occurred. The flange at the interior support also had a small buckle after the interior support loading. When the loading progressed to the second span the girder collapsed.

5.3.3 Design Limit Test Results

5.3.3.1 Service I Behavior

The critical Service I check for this girder was the weld detail of the composite studs to the top flange. Fatigue of this category C detail was investigated. Loadings for the Fatigue limit state are 75% of the HS20 design truck with the distance between the 32 kip axles of 30 feet. Dynamic load allowance for the Fatigue limit state is 15%. The stress limit at the flange-stud connection was calculated from Section 6.6.1.2.5-2 to be 5.8 ksi (≈200με). To ensure the girder met the Fatigue limit state, live load strains from the 107.7% live load level were ratioed to account for the 75% design truck and the difference in dynamic load allowance (1.15/1.33). For strain gage sections two and three, the determinant strains were 173 με and 162 με respectively (Hartnagel 1997). Therefore, the girder met the Fatigue limit state.

5.3.3.2 Service II Behavior

The 138.4% load level is used to check the behavior at the Service II limit. The strains are reduced by 0.93 (130/138.4), but the deformations are checked for the full 138.4% of the adjusted modeled truck load. At the Service II level, design calculations limit the positive moment region stresses to $0.95F_y$ after the redistribution of forces. For this girder, there were no redistributed stresses due to pier yielding. The calculated stress at the positive moment region (Section 1) was 39.9 ksi (Hartnagel 1997). The allowable stress is also 39.9 ksi ($0.95F_y$), resulting in an allowable strain of 1380 με. The maximum measured strain at the Service II limit is 1550 με. The experimental strain exceeds the $0.95F_y$ limit by 12%.

However, the $0.95F_y$ Service II limit criterion does not incorporate the small amount of yielding due to locked in sectional residual stresses that occurs in all bridges. The purpose of the limit is to limit the steady state summation of stresses that occur from the separate dead, live and residual moments. The locked in sectional residual stress yielding adjusts itself after a few cycles of load. Examining the live load stress range and the dead load stresses, the maximum measured elastic strains at the Service II limit are 1380 με (835 με dead load and 545 με live load). Although measured strains exceed Service II limits, the difference is small and elastic strains are within $0.95\ F_y$.

The proposed LRFD inelastic design provisions used to design this girder do not require a deflection check at the Service II limit. However, the proposed provisions do refer the reader to methods to determine these deflections (Chapter 3). Following is a method that can predict permanent set at the limit (as was done in Chapter 4) using moment-inelastic rotation curves for the girder sections. The moment-rotation curves used here are the actual curves determined from the test. The moment-inelastic rotation curve for the pier section is shown in Figure 5.10 and Figure 5.11 illustrates the relationship for the positive moment region.

A permanent set of 0.22 in occurred at Section 1 after 3 cycles at the 138.4% load level. The measured inelastic rotation at the pier was 4.7 mrads and at the positive moment region it was 2.7 mrads. Using a conjugate beam analysis (shown in Figure 5.12), the calculated residual moment at the pier was 22 ft-k and the calculated permanent set at Section 1 was 0.18 in. These compare well to the measured residual moment at the pier of 15 ft-k and a measured permanent set at Section 1 of 0.22 in.

Although a permanent set prediction is not required by the proposed provisions at the Service II limit, knowing the expected deformation may be useful to the engineer.

5.3.3.3 Strength I Behavior

Unlike the current LRFD inelastic design procedures that require a mechanism check at Strength I level loads, the proposed provisions use a shakedown limit state at the Strength I limit. The design procedures are greatly simplified compared to a mechanism check as was done in Chapter 4.

The Strength I limit load is 1.25DC+1.50DW+1.75L(1+I). This is represented by the 184.6% load level: 175% plus extra for the factored dead loads. The requirement is that the

structure shakes down at this load. Figure 5.13 shows the residual permanent set after cycles of loading for the girder. Shakedown is demonstrated by stabilization of these permanent deflections. As can be seen, the girder definitely shakes down at the 184.6% level. In fact, the girder achieved shakedown at load levels well above the Strength I limit. This is expected since the Strength I limit did not control the design. Figure 5.14 shows the test girder during the heavier moving load tests.

5.3.4 Inelastic Behavior

5.3.4.1 Shakedown Behavior

Each adjusted modeled truck weight loading was repeated until the residual deflections stabilized and the bridge achieved shakedown. Figure 5.13 shows the permanent set deflection at the positive moment region in the first span (Section 1) in terms of the percent of the design vehicle. The onset of the permanent set occurred very early. This is due to the high dead load stresses in relation to the yield stress. With such high dead load stresses, the available live load stress prior to yielding is relatively small, especially considering locked in sectional residual stresses.

Stabilization of residual deflections was obtained up to the 255.3% load level. The theoretical shakedown capacity of the girder is at the 253% level (Hartnagel 1997). The response at the 255.3% level of Figure 5.13 shows large incremental deformations that stabilize (shakedown). However, at the 269.2% plus factored dead level, it is clear that the structure is severely damaged and did, in fact, collapse during the application of the first cycle.

The moment-inelastic rotation curve at the negative pier section is important for determining the Strength I limit design capacity. The ability for the noncompact girder to maintain a reliable moment capacity during sufficient rotations is essential for the redistribution of moments. Figure 5.10 shows the moment-inelastic rotation for the pier section during the cyclic tests. At the Strength I limit, the measured moment was 413 ft-k at a measured inelastic rotation of 8 mrads. This corresponds to a calculated design moment of M_{pc} = 318 ft-k. The pier section behaved better than that predicted by the design provisions. The maximum usable moment according to the proposed design provisions is M_{pc} where M_{pc} equals 425 ft-k for the Service II

check and 318 ft-k for the Strength I check. As usual, and for the better, the beam surpassed these levels.

Examining the theoretical shakedown limit (the maximum Strength I limit case) at the 255.3% level, the measured pier moment was 459 ft-k at an inelastic rotation of 9.6 mrads, which exceeds the proposed Strength I moment capacity of M_{pc} = 318 ft-k. The pier section was able to retain more moment than expected, not redistributing the moment to the positive moment regions. At the positive section, the measured moment was 335 ft-k while the theoretical moment was 400 ft-k assuming the pier section shed moment. This illustrates reserve that will be inherent in the inelastic design provisions.

5.3.4.2 Plastic Collapse Behavior

Stabilization of residual deflections was obtained up to the 255.3% load level. At the 269.2% plus factored dead load level, the girder failed during the first cycle by plastic collapse. The theoretical collapse load with the additional factored dead loads was at the 208% load level. Therefore, the girder was able to withstand loads well above the theoretical collapse load. The reason for this excess capacity is that the pier section was able to maintain a much higher than predicted moment capacity at rotations necessary to collapse the girder. The pier section did not unload moment to the positive moment region and, therefore, the girder could withstand loads above the theoretical collapse level assuming M_{pc} at the pier.

5.4 COMPONENT TESTS

Two additional components were tested in a double cantilever manner (similar to Chapter 4 component tests) to simulate the pier region of the test girder. The components were one-third scale models of the plate girder design discussed above. Component properties are shown in Table 5.3.

A composite component identical to the above girder test (see Figure 5.6) was monotonically loaded to produce the complete moment-inelastic rotation curve shown in Figure 5.15. On the plot, it is shown that indeed the section performs better than the predicted moment capacities for both the Service II limit and the Strength I limit.

The second component test was built with the same steel section as above, but was noncomposite. This girder had ultra-compact flanges and a compact web. According to the

proposed LRFD inelastic design provisions, the girder should be able to maintain M_p well beyond inelastic rotation necessary at the Strength I limit state. Figure 5.16 illustrates the moment-inelastic rotation curve for the noncomposite component test. It is clear that the component exceeds the design capacity requirements.

5.5 SUMMARY OF NON-COMPACT GIRDER TESTS

The one-third scale two-span continuous composite girder was subjected to (adjusted) simulated moving HS20 loading. The girder was designed and modeled to represent an interior girder of the proposed LRFD inelastic design bridge in the design comparisons above. Figures 5.8 and 5.14 are photos of the structure during testing. During large simulated moving load tests, the girder suffered plastic collapse. Chapter 5 presents experimental results at the design limit states and during inelastic loading. Below is a summary of the findings during the experimental program.

The behavior of the model behaved according to elastic structural theory. The elastic deflections and stresses (strains) matched well with that predicted. The measured Service II load level stresses (strains) nearly met (within 12%) the Service II stress criteria. This bridge was a very efficient design where both the pier and positive moment region were at design limits. Thus, the 12% overstress is deemed adequate, especially considering design philosophy. The fatigue stresses met design criteria. The noncompact pier section redistributed moments and there were permanent residual deflections approximately according to predictions, although the simplified proposed LRFD inelastic design procedures do not require the determination of deflections. The current and proposed LRFD inelastic design provisions refer the engineer to ways of calculating deformations if deemed important.

The experimental moment at the Service II and Strength I levels exceeded the predicted. The proposed LRFD inelastic design provisions use a M_{pc} at each limit state and there is no need to relate moment to inelastic rotation. M_{pc} depends on the web and flange slenderness ratios. The girder obtained shakedown above the theoretical incremental collapse level. The pier section maintained higher than predicted moments at large rotations. The girder resisted well above theoretical collapse loads during the last cycle of loads. Again, the pier section maintained higher than predicted moments at large rotations.

Rotations at the limit states were within the boundaries necessary for redistribution according to Chapter 3.

The girder components were tested to develop and verify moment-inelastic rotation relations. They were tested in a double cantilever manner to model the pier section of a continuous span girder. Chapter 5 contains moment-inelastic rotation relations for the two girder components. The experimental results are compared to the proposed LRFD inelastic design effective moment capacities at the different limit states. Below is a summary of the findings during the experimental program.

The experimental moment-inelastic rotation relations met or exceeded the effective plastic moments predicted by the proposed LRFD inelastic design procedures. The noncomposite component had ultra-compact flanges and web. The section was able to maintain the plastic moment capacity well into the inelastic range. The composite component had ultra-compact flanges, but noncompact webs. Therefore, by theory, the moment should have, and did, decrease with increasing inelastic rotation. However, the moment exceeded the expectations from the design predictions.

The tests performed in this project support the development and verify the procedures of the proposed inelastic design provisions for bridges comprising noncompact girders. The limit state design levels were satisfied and the overall behavior of the girders were good.

Table 5.1 Prototype and Model Girder Section Properties

Property	Scale Factor	Prototype		Model	
Non-Composite		Midspan	Pier	Midspan	Pier
I_x (in^4)	1/81	51900	76650	640	950
S_t (in^3)	1/27	1310	1910	49	71
S_b (in^3)	1/27	1660	2450	62	91
Composite n=8					
I_x (in^4)	1/81	140400	103100	1730	1270
S_b (in^3)	1/27	2350	2720	87	100
Composite n=24					
I_x (in^4)	1/81	103800		1280	
S_b (in^3)	1/27	2160		80	
Plastic Moment					
M_p (k-ft)[1]	1/27	12,800	12,800	474	474
M_{pe} (k-ft)[1]	1/27		10,500		389

[1] Moment properties for model girder are not adjusted to account for yield strength of material. This will be explained in the text Section 5.3.1.

Table 5.2 Comparison of Design Methods

Design Method	Design Load
Current LRFD Inelastic Design	Not Applicable
LFD Elastic No Redistribution	HS4.0
LRFD Elastic No Redistibution	HS4.5
Proposed LRFD Inelastic Design	HS20

Table 5.3 Component Girder Section Properties

Type	Deck Reinf.	Flange Slender.	Web Slender.	Strength I M_{pe}	Service II M_{pe}	Remarks
Units	in^2			k-ft	k-ft	
Noncomp.	N/A	7.0 ultra-compact	51.25 ultra-compact	312	312	Web Compact
Composite	1.44	7.0 ultra-compact	134.6 non-compact	425	318	Web non-compact

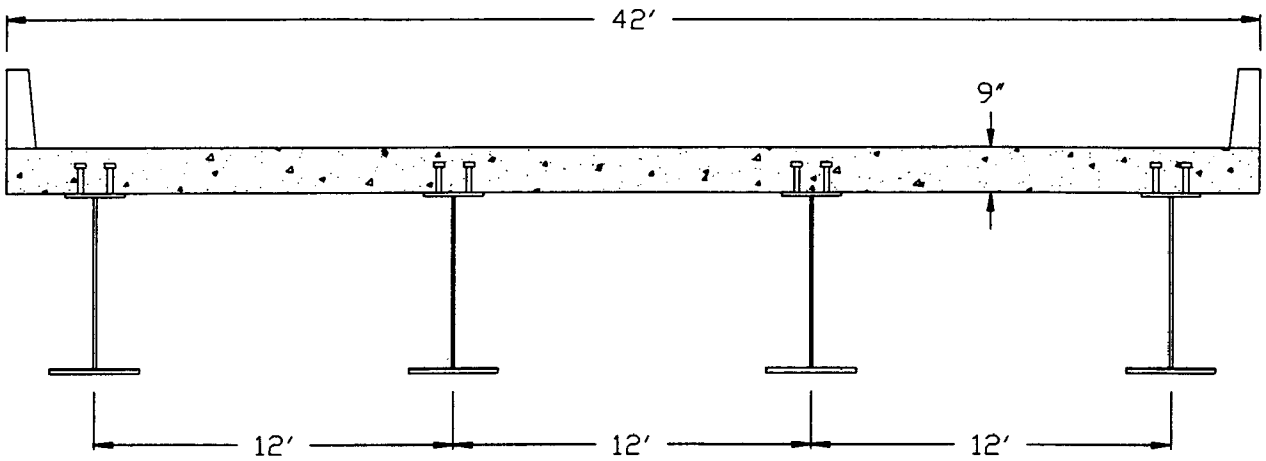

Figure 5.1 Prototype Bridge Cross Section

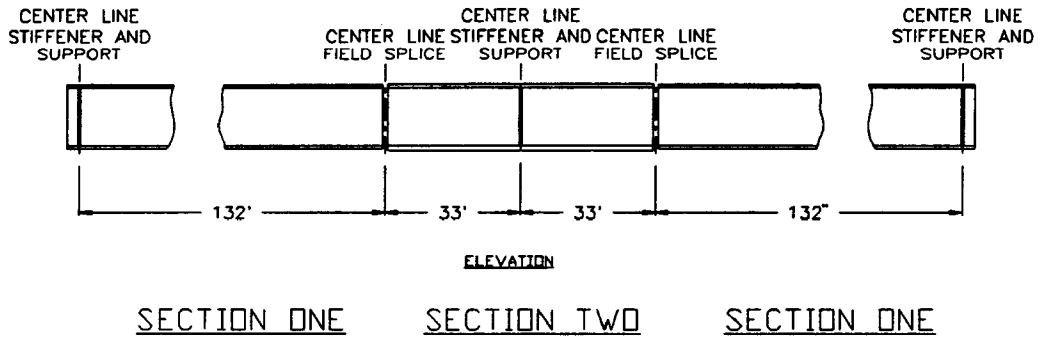

Figure 5.2 Prototype Girder Elevation

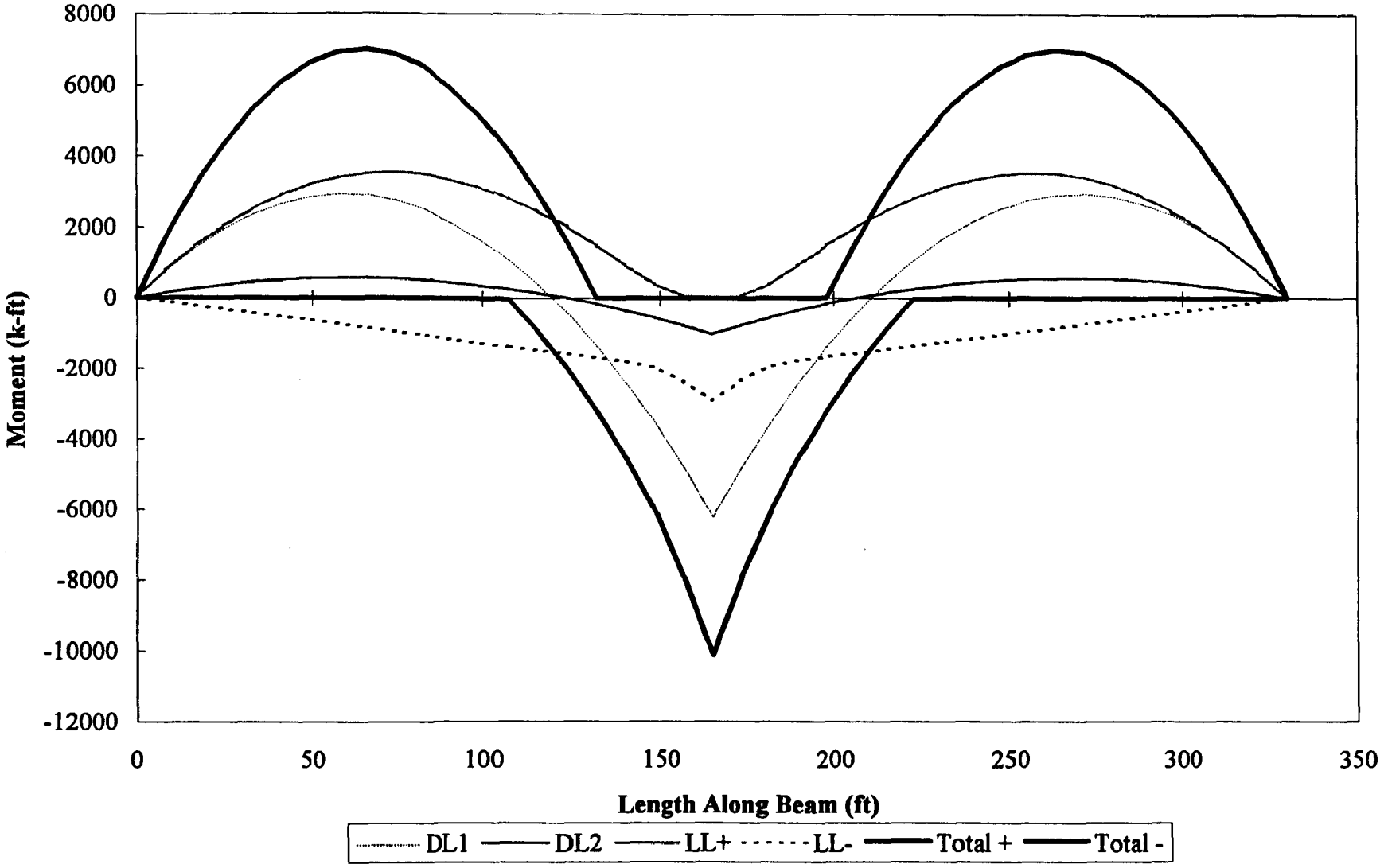

Figure 5.3 Moment Envelopes for the Prototype Girder

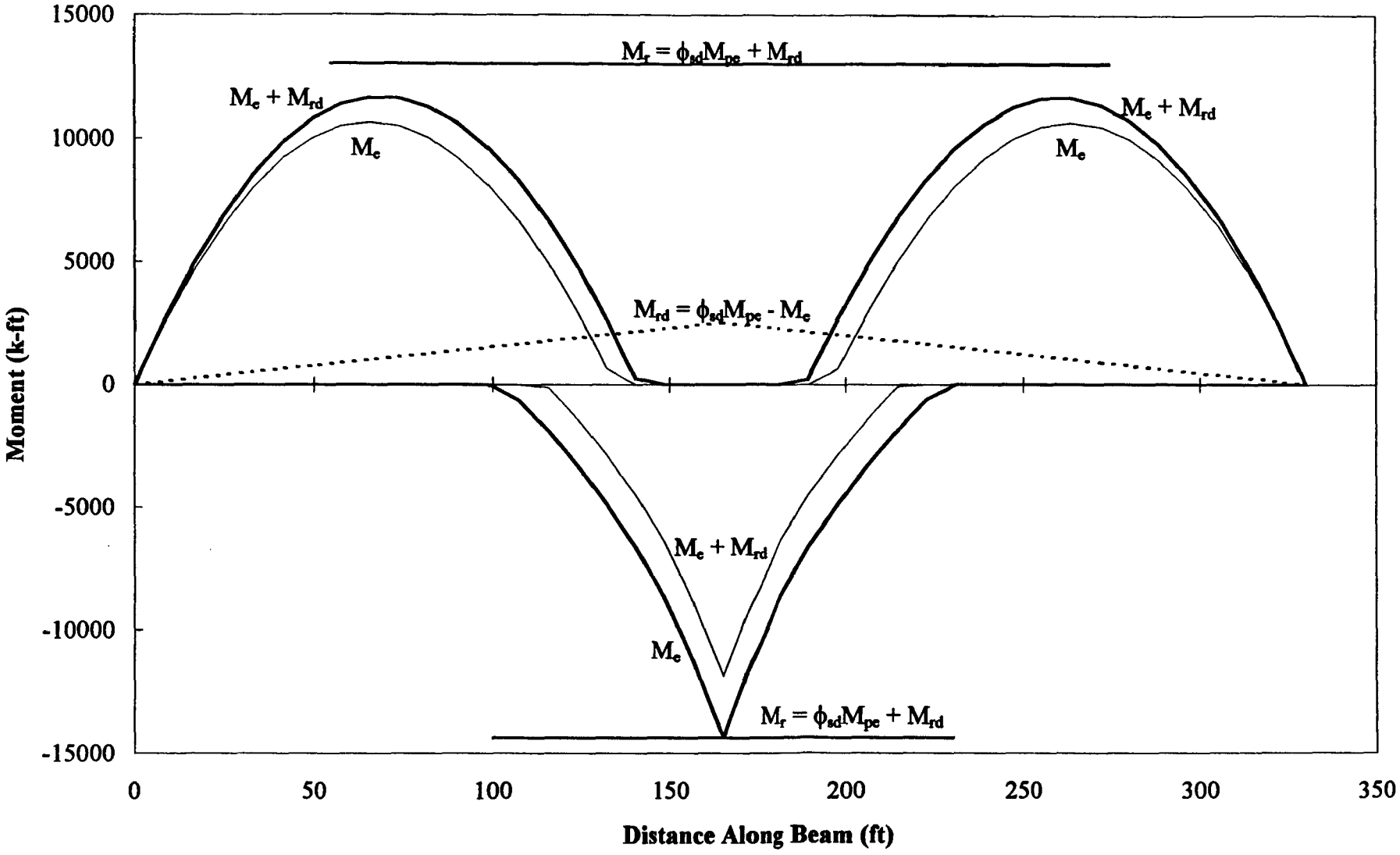

Figure 5.4 Strength I Design Limit Moments

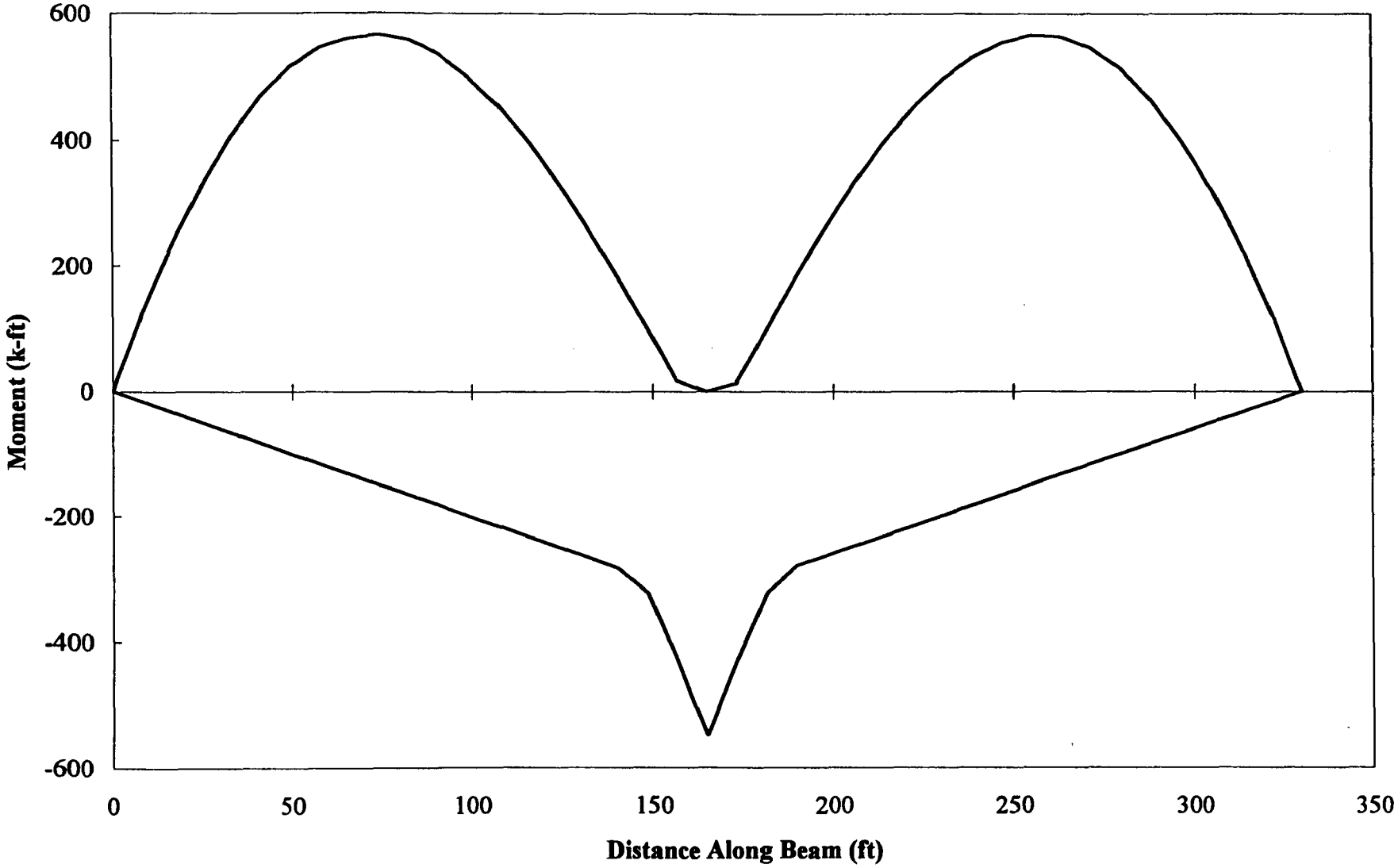

Figure 5.5 LFD Live Load Moments - HS4 Loading

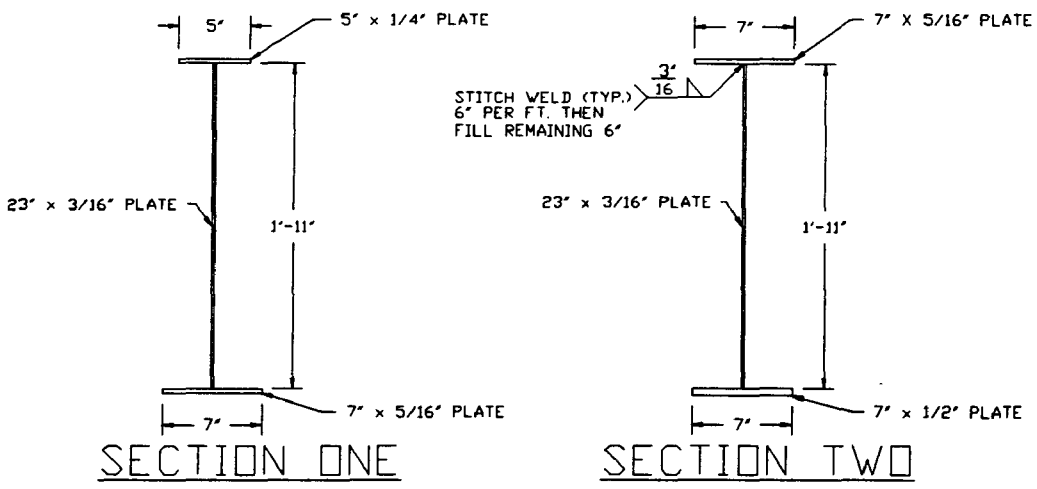

Figure 5.6 Model Girder Cross Sections

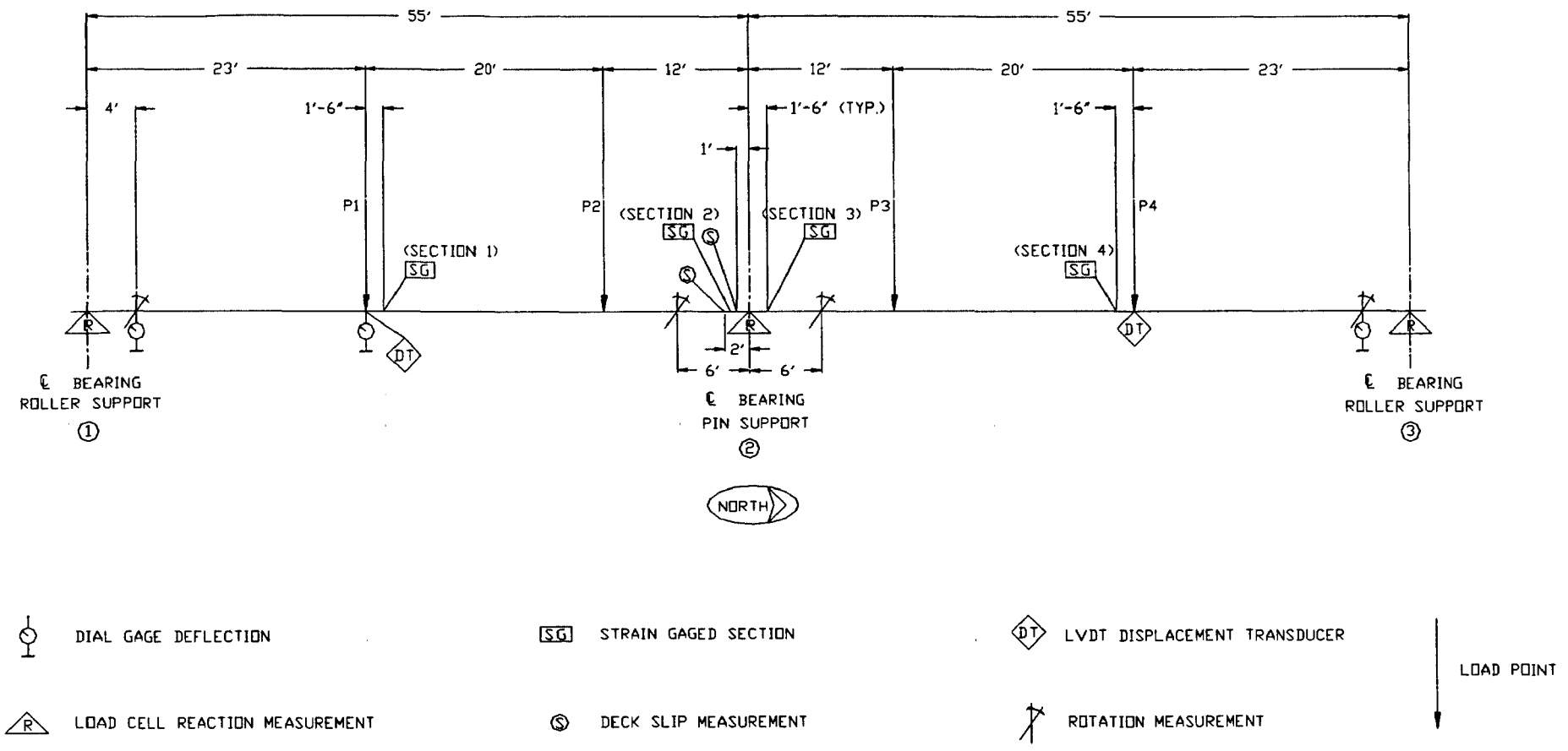

Figure 5.7 Test Measurement Layout

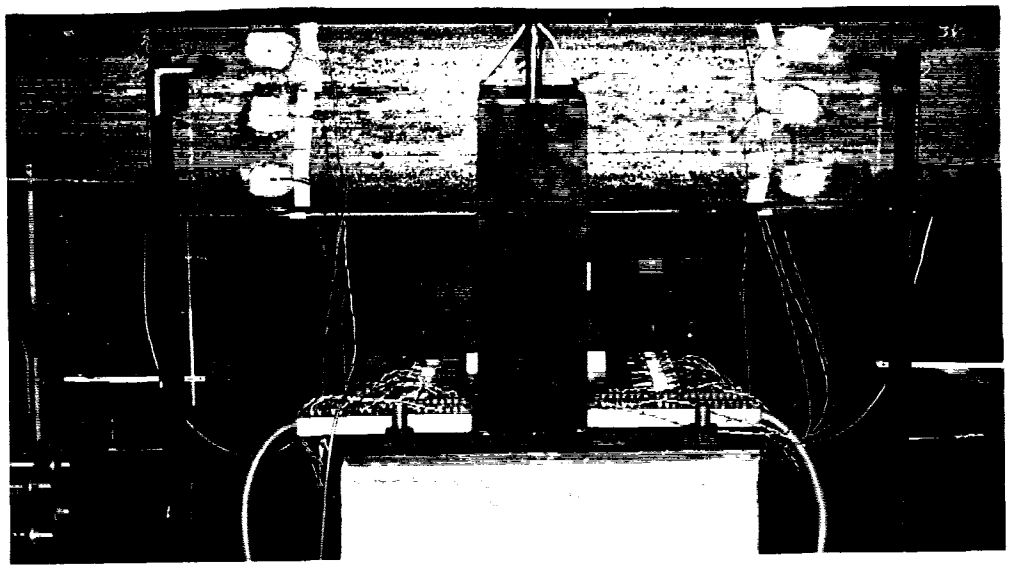

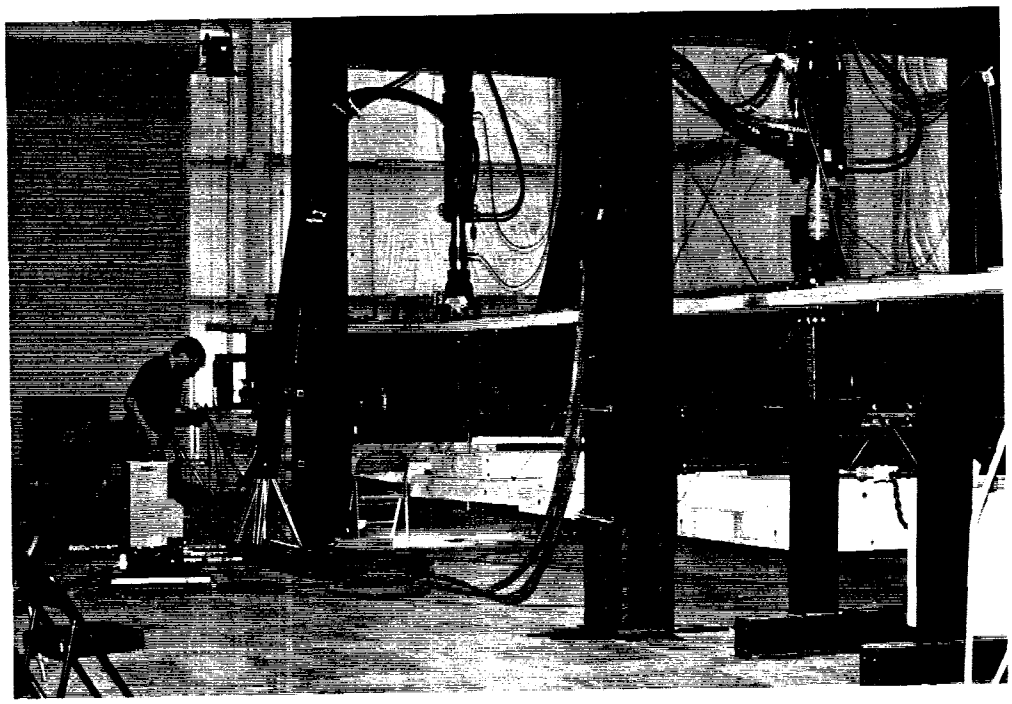

Figure 5.8 Noncompact Girder Photos

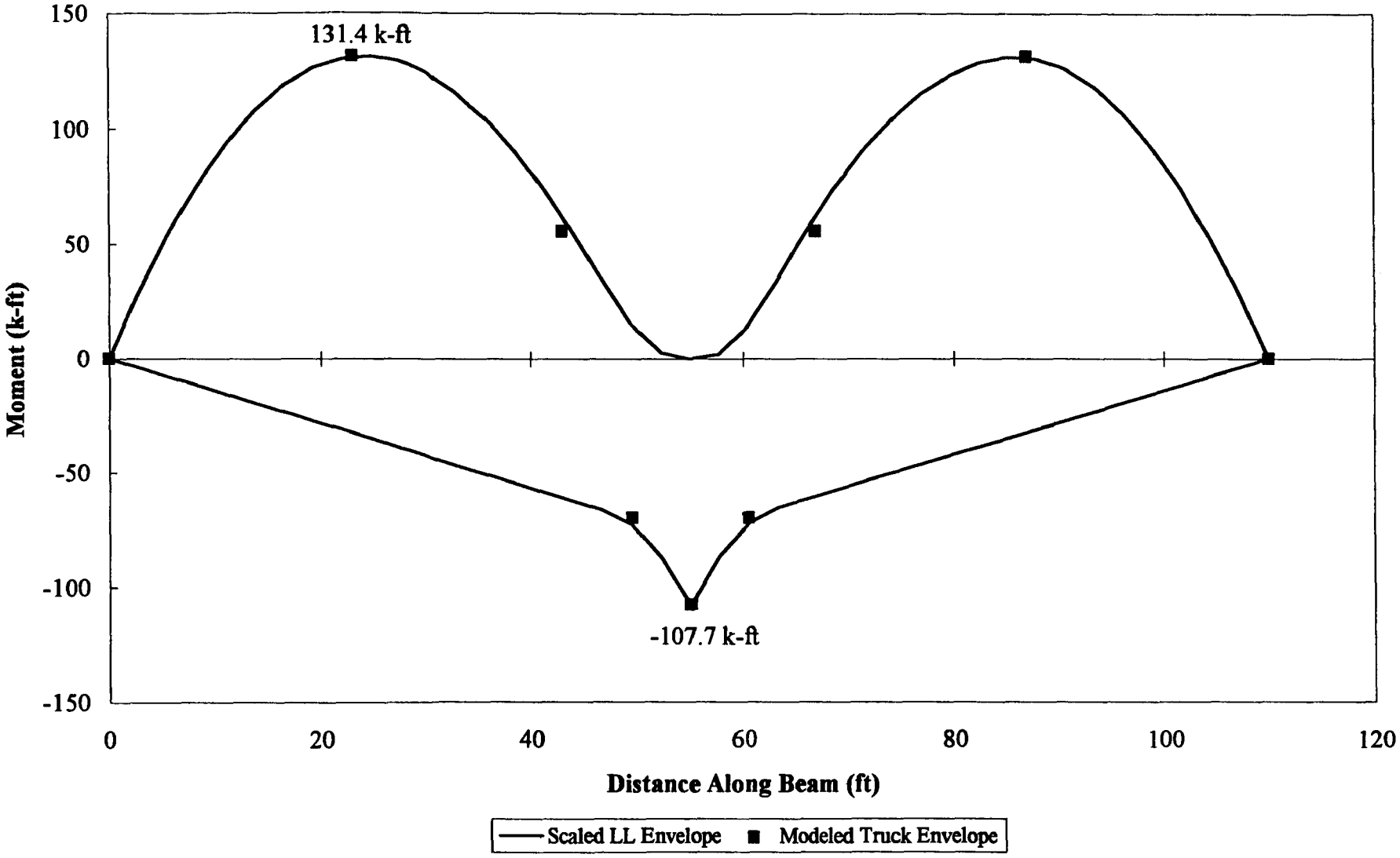

Figure 5.9 Modeled Live Load Moment Envelope

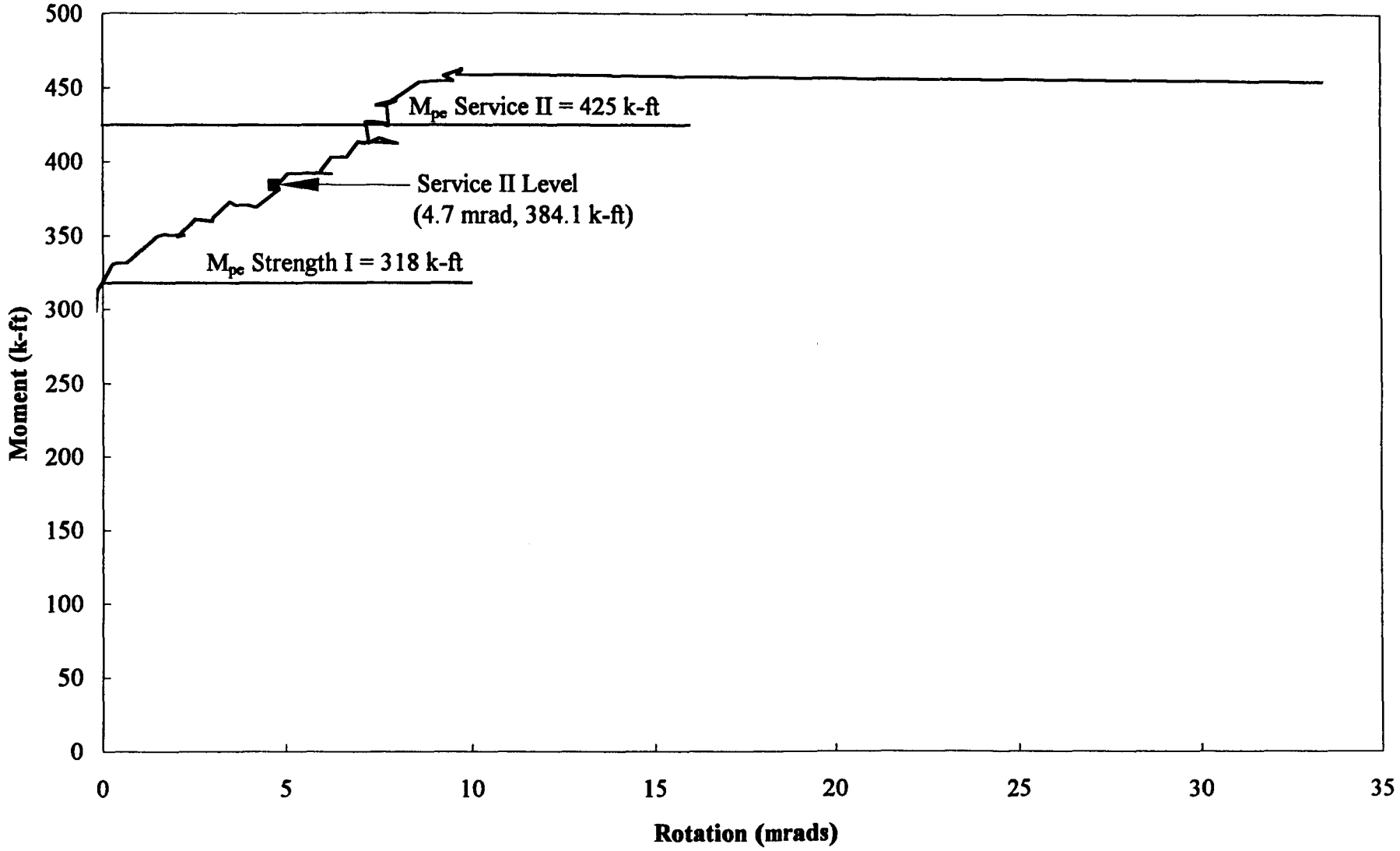

Figure 5.10 Moment vs Inelastic-Rotation for the Interior Support

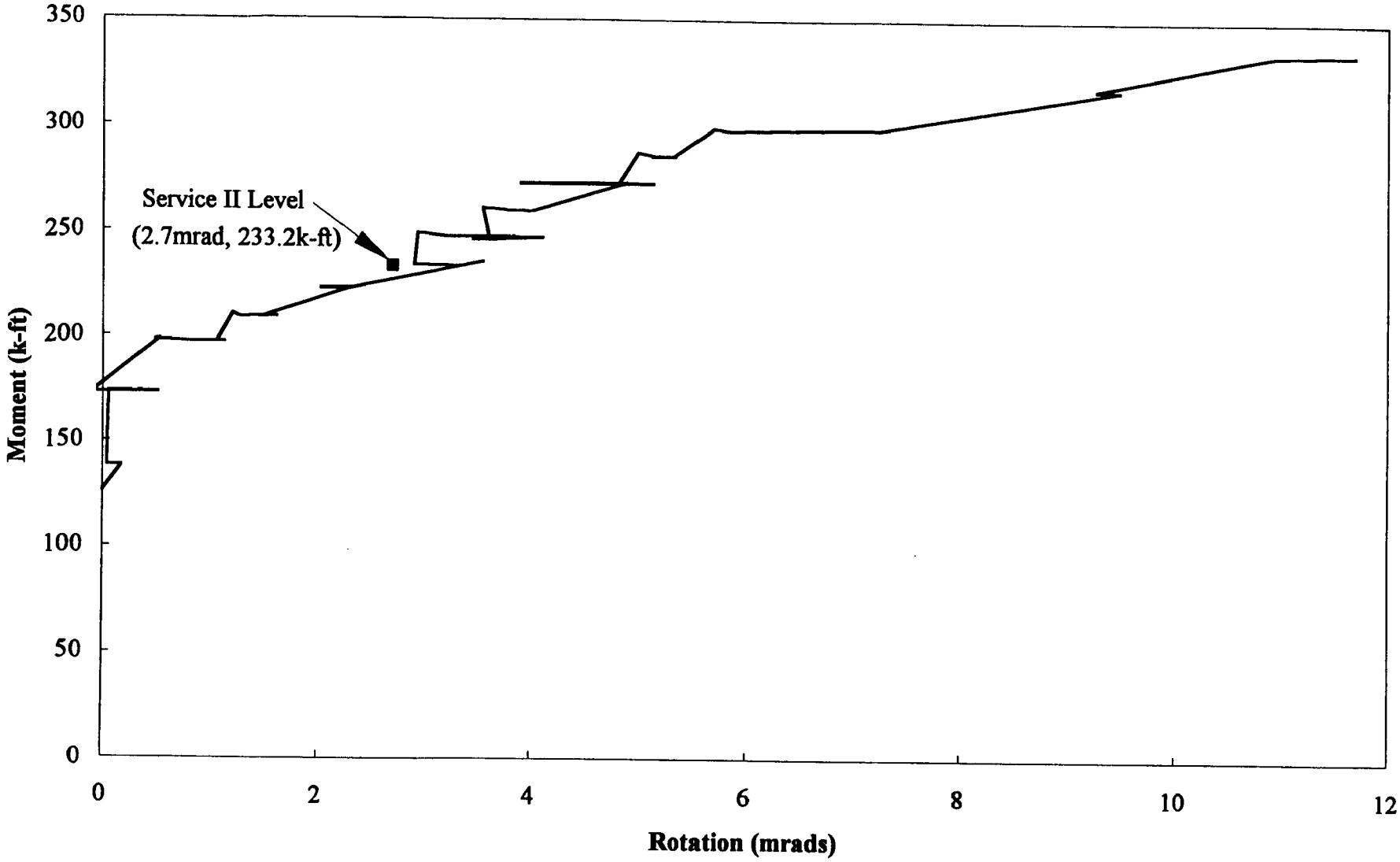

Figure 5.11 Positive Moment vs Inelastic-Rotation

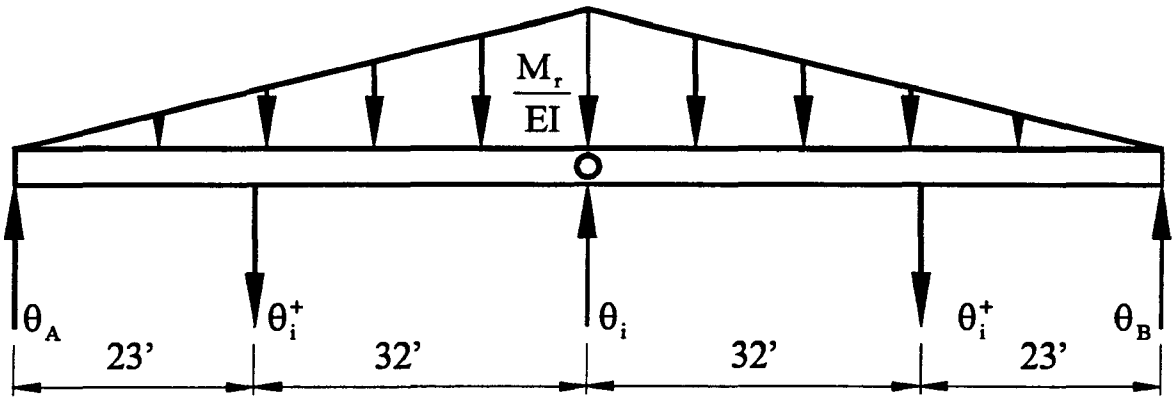

$$\theta_A = \theta_B = \frac{32}{55}\theta_i^+ + 9.167\frac{M_{rd}}{EI}, \qquad \Delta_{23'} = 13.38\theta_i^+ + 173.97\frac{M_{rd}}{EI}$$

$$\theta_i^- = 4.7\text{mrads}, \theta_i^+ = 2.7\text{mrads}, \text{ E} = 29{,}000\text{ksi and I} = 164\text{in}^4$$

$$\Delta_{23'} = 0.36"$$

$$M_{rd} = 14.9\text{k} - \text{ft}$$

Figure 5.12 Calculation of Residual Deflection at Positive Span

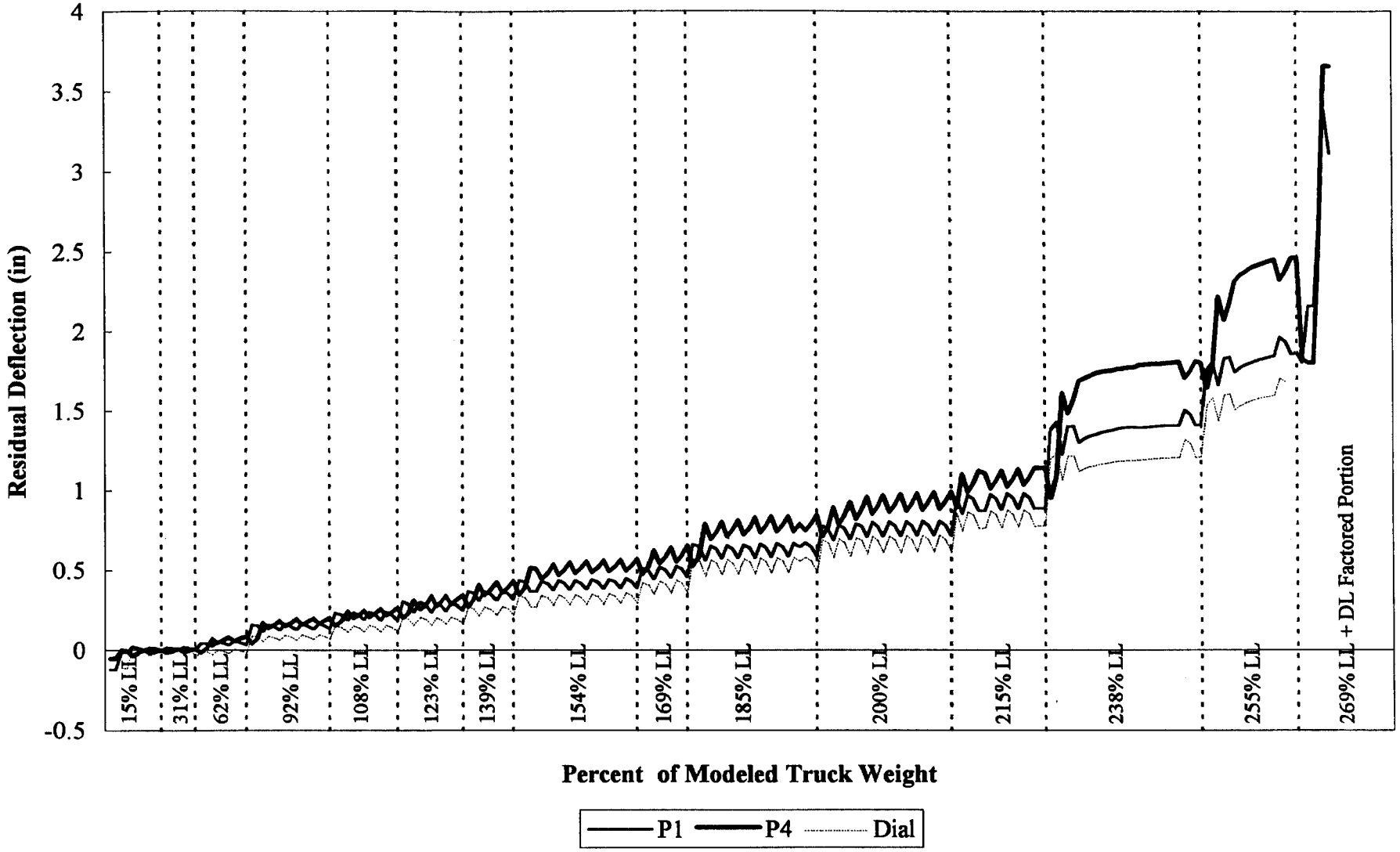

Figure 5.13 Residual Deflection vs Percent of Modeled Truck Weight

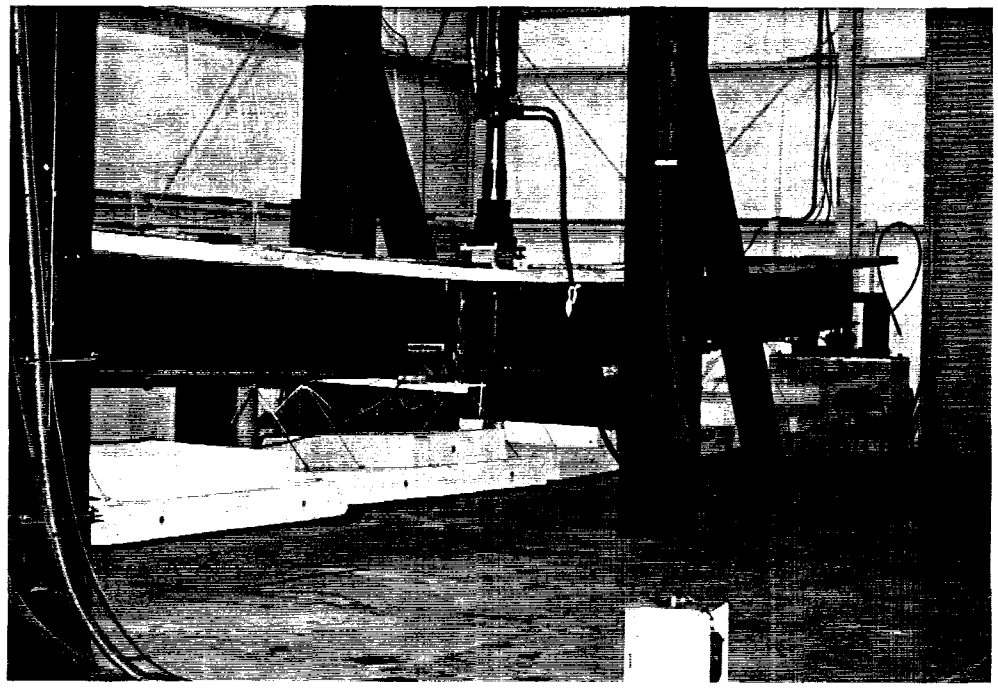

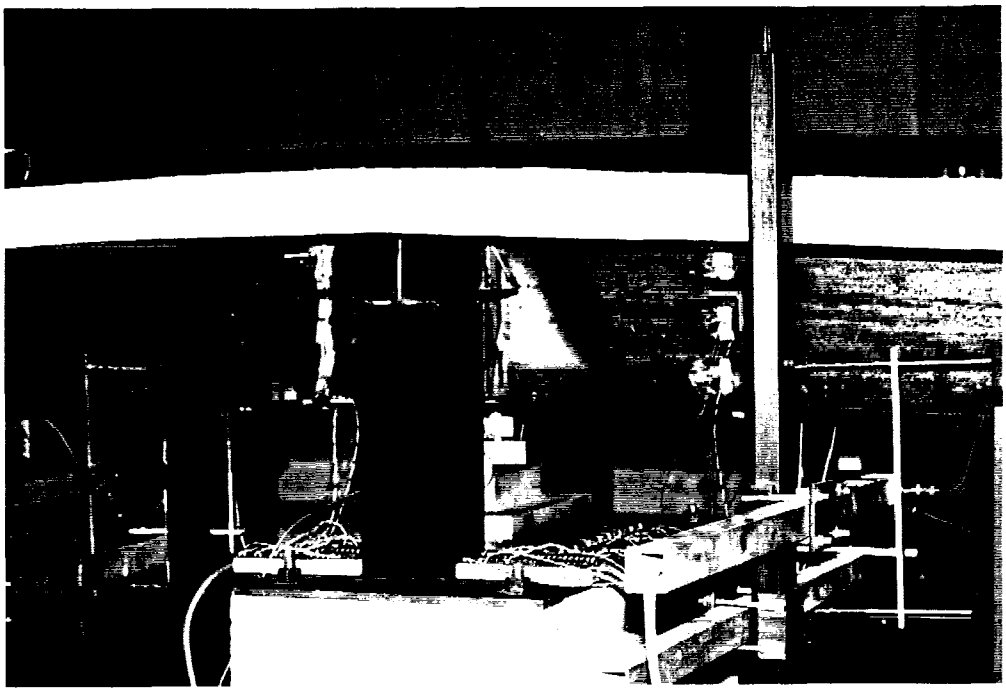

Figure 5.14 Noncompact Girder Heavy Load Photos

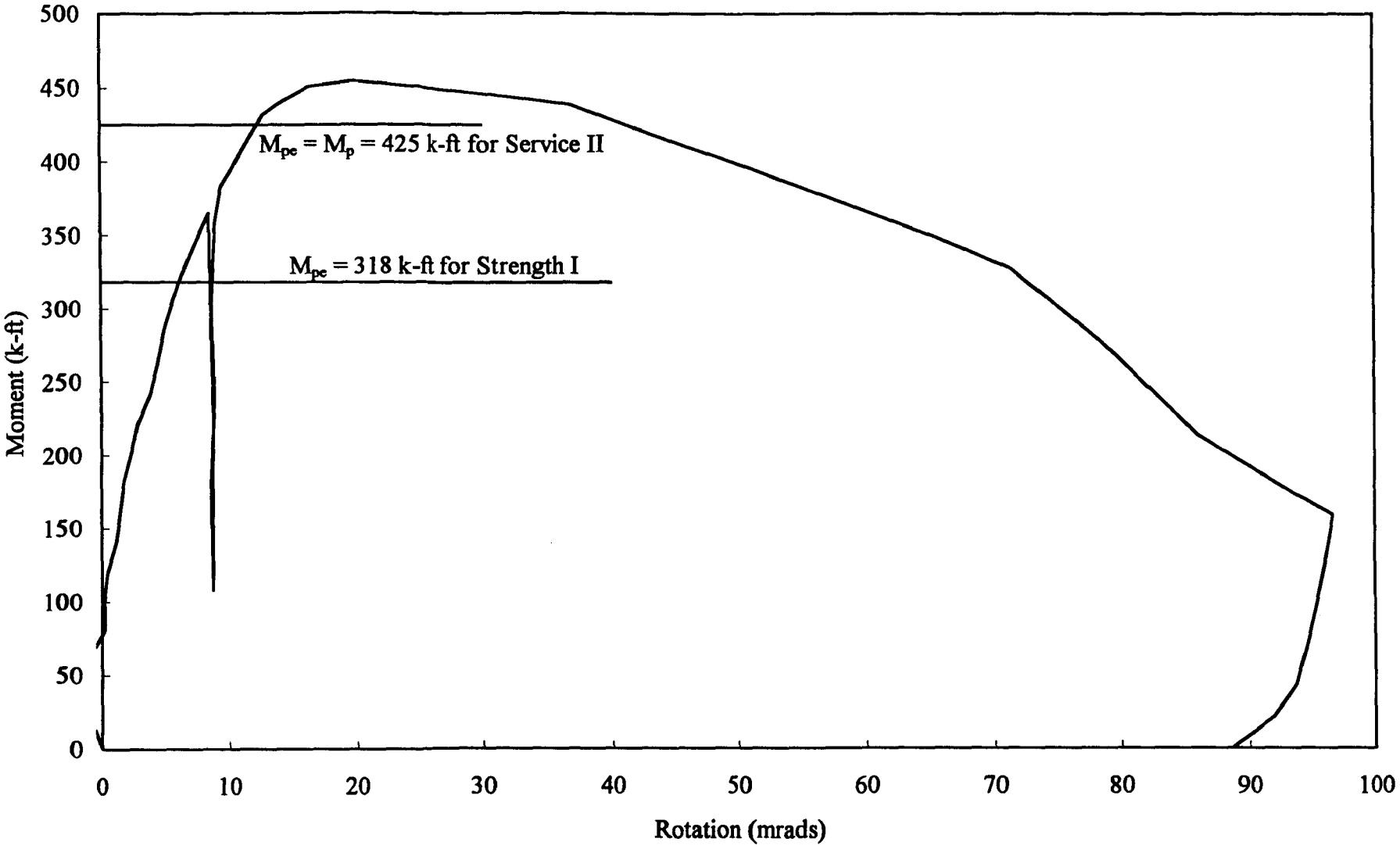

Figure 5.15 Moment vs Inelastic-Rotation for the Composite Component

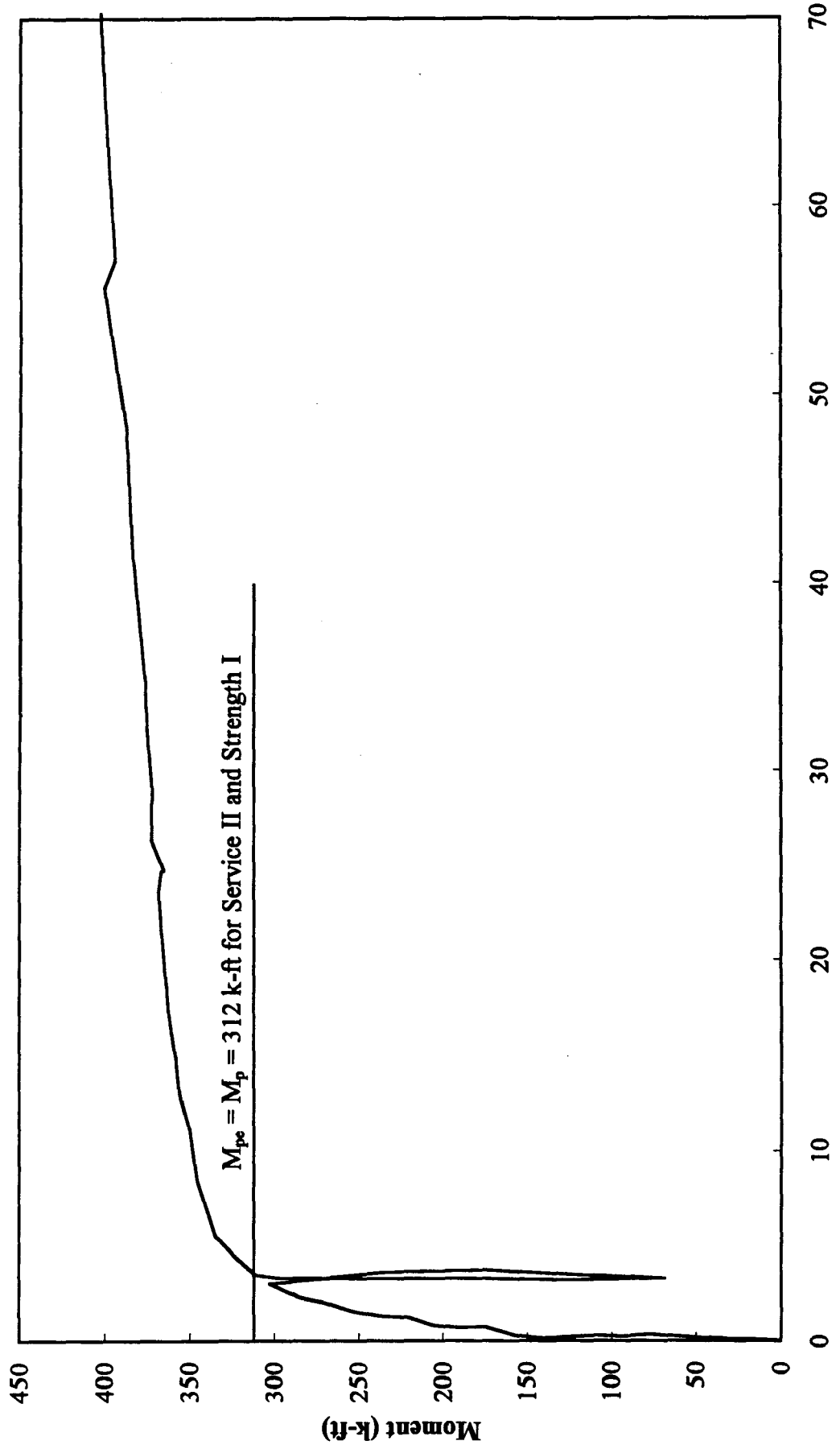

Figure 5.16 Moment vs Inelastic-Rotation for the Noncomposite Component

REFERENCES

The following organizational abbreviations are used in these references:

AASHO: American Association of State Highway Officials, Washington, DC (predecessor to AASHTO)

AASHTO: American Association of State Highway and Transportation Officials, Washington, DC

AISI: American Iron and Steel Institute, Washington, DC

AISC: American Institute of Steel Construction, Chicago, IL

ASCE: American Society of Civil Engineers, New York, NY

FHWA: Federal Highway Administration, Washington, DC

IABSE: International Association of Bridge and Structural Engineers, Zurich, Switzerland

NCHRP: National Cooperative Highway Research Program, Washington, DC

TRB: Transportation Research Board, Washington, DC

AASHTO, [1973] "Standard Specifications for Highway Bridges," 11th ed.

AASHTO, [1986] "Guide Specifications for Alternate Load Factor Design Procedures for Steel Beam Bridges Using Braced Compact Sections."

AASHTO, [1989] "Guide Specifications for Strength Evaluation of Existing Steel and Concrete Bridges. "

AASHTO, [1991] "Guide Specifications for Alternate Load Factor Design Procedures for Steel Beam Bridges Using Braced Compact Sections."

AASHTO, [1992] "Standard Specifications for Highway Bridges," 15th ed.

AASHTO, [1994] "AASHTO LRFD Bridge Design Specifications," 1st ed.

AISC, [1978] "Specification for the Design, Fabrication and Erection of Structural Steel for Buildings," and Commentary, Nov.

AISC, [1993] "Load and Resistance Factor Design (LRFD) Specification for Structural Steel Buildings."

Ansourian, P., [1982] "Plastic Rotation of Composite Beams," Journal of the Structural Division, ASCE, Vol. 108, No. ST3, March.

ASCE, [1971] "Plastic Design in Steel - A Guide and Commentary," Manuals and Reports on Engineering Practice No. 41, 2nd. ed.

ASCE-AASHO, [1968] "Design of Hybrid Steel Beams," by the Joint ASCE-AASHO Subcommittee on Hybrid Beams and Girders, C. G. Schilling, Chmn., Journal of the Structural Division, ASCE, Vol. 94, No. ST6., June.

Axhag, F., [1995] "Plastic Design of Composite Bridges Allowing for Local Buckling," Technical Report 1995:09T, Lulea University of Technology, Lulea, Sweden, April.

Barker, M. G., [1990] "The Shakedown Limit State of Slab-on-Girder Bridges," Ph.D. Thesis Submitted to the University of Minnesota, Minneapolis, MN, June.

Barker, M. G., & Galambos, T. V., [1992] "Shakedown Limit State of Compact Steel Girder Bridges," Journal of Structural Engineering, ASCE, Vol. 118, No. 4, April.

Barker, M. G., [1995] "Inelastic Design of Steel Girder Bridges," Engineering Journal, AISC, Vol. 32, No. 1, First Quarter.

Barth, K. E., White, D. W., & Ramirez, J. A., [1994] "Summary of Progress on Moment-Rotation Relationships for Non-Compact Steel Bridge Girders," School of Civil Engineering, Purdue University, West Lafayette, IN, May 4.

Beedle, L. S., [1958] "Plastic Design of Steel Frames," John Wiley and Sons, New York, NY.

Carskaddan, P. S., & Grubb, M. A., [1991] "Improved Autostress Procedure," AISC Marketing, Pittsburgh, PA, Oct. 18.

Carskaddan, P. S., [1976] "Autostress Design of Highway Bridges, Phase 1: Design Procedure and Example Design," Research Laboratory Report, United States Steel Corporation, Monroeville, PA, March 8.

Carskaddan, P. S., [1980] "Autostress Design of Highway Bridges, Phase 3: Interior-Support-Model Test," Research Laboratory Report, United States Steel Corporation, Monroeville, PA, Feb. 11.

Carskaddan, P. S., [1991] "Concrete Cracking in the Autostress Method," Memo, AISC Marketing, Pittsburgh, PA, Oct. 2.

Carskaddan, P. S., Haaijer, G., & Grubb, M. A., [1982] "Computing the Effective Plastic Moment," Engineering Journal, AISC, Vol. 19, No. 1, First Quarter.

Carskaddan, P. S., Haaijer, G., & Grubb, M. A., [1984] "Adjusting the Beam-Line Method for Positive-Moment Yielding," Engineering Journal, AISC, Vol. 21, No. 4, Fourth Quarter.

Csagoly, P. F., & Jaeger, L. G., [1979] "Multi-Load Path Structures for Highway Bridges," Transportation Research Record 711, TRB.

Dishongh, B. E., & Galambos, T. V., [1992] "Residual Deflection Analysis for Inelastic Bridge Rating," Journal of Structural Engineering, ASCE, Vol. 118, No. 6., June.

Dishongh, B. E., [1990] "Residual Damage Analysis: A Method for the Inelastic Rating of Steel Girder Bridges," Ph.D. Thesis Submitted to the Faculty of the University of Minnesota, Minneapolis, MN, Jan.

Dishongh, B. E., [1992] "Residual Deformation Analysis for Bridges," Louisiana Department of Transportation and Development, Baton Rouge, LA, Nov.

Disque, R. O., [1964] "Wind Connections with Simple Framing," Engineering Journal, AISC, Vol. 1, No. 3, July.

Eyre, D. G., & Galambos, T. V., [1969] "Variable Repeated Loading - A Literature Survey," Bulletin No. 142, Welding Research Council, July.

Eyre, D. G., & Galambos, T. V., [1970] "Shakedown Tests on Steel Bars and Beams," Journal of the Structural Division, ASCE, Vol. 96, No. ST7, July.

Eyre, D. G., & Galambos, T. V., [1973] "Shakedown of Grids," Journal of the Structural Division, ASCE, Vol. 99, No. ST10, Oct.

Frangopol, D. M., & Nakib, R., [1991] "Redundancy in Highway Bridges," Engineering Journal, AISC, Vol. 28, No. 1, First Quarter.

Frost, R. W., & Schilling, C. G., [1964] "Behavior of Hybrid Beams Subjected to Static Loads," Journal of the Structural Division, ASCE, Vol. 90, No. ST3, June.

Fukumoto, Y., & Yoshida, H., [1969] "Deflection Stability of Beams Under Repeated Loads," Journal of the Structural Division, ASCE, Vol. 95, No. ST7, July.

Galambos, T. V., & Ellingwood, B., [1986] "Serviceability Limit States: Deflections," Journal of the Structural Division, ASCE, Vol. 112, No. 1, Jan.

Galambos, T. V., et al., [1993] "Inelastic Rating Procedures for Steel Beam and Girder Bridges," NCHRP Report 352.

Gaylord, E. H., & Gaylord, C. N., [1979] "Structural Engineering Handbook," 2nd. ed., McGraw-Hill, New York, NY.

Ghosn, M., & Moses, F., [1991] "Redundancy in Highway Bridge Superstructures," Interim Report, NCHRP Project 12-36, Department of Civil Engineering, City College of New York, NY, Dec.

Grubb, M. A., & Carskaddan, P. S., [1979] "Autostress Design of Highway Bridges, Phase 3: Initial Moment-Rotation Tests," Research Laboratory Report, United States Steel Corporation, Monroeville, PA, April 18.

Grubb, M. A., & Carskaddan, P. S., [1981] "Autostress Design of Highway Bridges, Phase 3: Moment-Rotation Requirements," Research Laboratory Report, United States Steel Corporation, Monroeville, PA, July 6.

Grubb, M. A., [1985] "Design Example: A Two-Span Continuous Highway Bridge Designed by the Autostress Method," Report on Project 188, AISI, May 10.

Grubb, M. A., [1987] "The AASHTO Guide Specification for Alternate Load-Factor Design Procedures for Steel Beam Bridges," Engineering Journal, AISC, First Quarter.

Grubb, M., [1989] "Autostress Design Using Compact Welded Beams," Engineering Journal, AISC, Vol. 26, No. 4, Fourth Quarter.

Grundy, P., [1976] "Bridge Design Criteria," Nov. 25 to 26, 1976, Australian Metal Structures Conference held in Adelaide, Australia.

Grundy, P., [1983] "The Application of Shakedown Theory to the Design of Steel Structures," Instability and Plastic Collapse of Steel Structures, L. J. Morris (edition), Granada Publishing, London, UK.

Gurley, C. R., [1981] "Plastic Design of Two-Way Structures and Elements," Journal of Constructional Steel Research, Vol. 1, No. 3, May.

Gurley, C. R., [1982] "Plastic Analysis of Advanced Grillage and Plate Problems with Nodal Forces," Journal of Constructional Steel Research, Vol. 2, No. 1, Jan.

Gutkowski, R. M., [1990] "Structures - Fundamental Theory and Behavior," Second Edition, Van Nostrand Reinhold, New York, NY.

Haaijer, G., & Carskaddan, P.S., [1970] "Autostress Design of Continuous Steel Bridge Members," Proceedings of the Canadian Structural Engineering Conference, held at Montreal, Canada.

Haaijer, G., [1993] "Objectives and Early Research of Autostress Design," Transportation Research Record 1380, TRB.

Haaijer, G., Carskaddan, P. S., & Grubb, M. A., [1987] "Suggested Autostress Procedures for Load Factor Design of Steel Beam Bridges," Bulletin No. 29, AISC, April.

Hall, J. C., & Kostem, C. N., [1981] "Inelastic Overload Analysis of Continuous Steel Multi-girder Highway Bridges by the Finite Element Method," Fritz Engineering Laboratory Report 432.6, Lehigh University, Bethlehem, PA, June.

Hartnagel, B. A., [1997] "Experimental Verification of Inelastic Load and Resistance Factor Design Limits," PhD. Thesis Submitted to the Faculty of the University of Missouri, (in progress).

Heins, C. P., & Kuo, J. T. C., [1973] "Live Load Distribution on Simple Span Steel I-Beam Composite Highway at Ultimate Load," Civil Engineering Department, University of Maryland, MD, April.

Heins, C. P., & Kuo, J. T. C., [1975] "Ultimate Live Load Distribution Factor for Bridges," Journal of the Structural Division, ASCE, Vol. 101, No. ST7, July.

Ho, H. S., [1972] "Shakedown in Elastic-Plastic Systems Under Dynamic Loading," Journal of Applied Mechanics, Vol. 39.

Holtz, N. M., & Kulak, G. L., [1975] "Web Slenderness Limits for Non-Compact Beams," Structural Engineering Report No. 51, University of Alberta, Edmonton, Alberta, Canada, Aug.

Hourigan, E. V., & Holt, R. C., [1987] "Design of a Rolled Beam Bridge by New AASHTO Guide Specification for Compact Braced Sections," Engineering Journal, AISC, First Quarter.

HRB, [1962a] "The AASHO Road Test," proceedings of the May 16-18, 1962, Conference held in St. Louis, MO, Special Report 73, National Research Council, Washington, DC.

HRB, [1962b] "The AASHO Road Test, Report 4, Bridge Research," Highway Research Board Special Report 61D, National Research Council, Washington, DC.

Idriss, R., & White, K., [1991] "Secondary Load Paths in Bridge Systems," March 1991 Third TRB Bridge Engineering Conference held in Denver, CO.

Kostem, C. N., [1984] "Further Studies on the Inelastic Overload Response of Multi-Girder Bridges," Fritz Engineering Laboratory Report 435.2, Lehigh University, Bethlehem, PA.

Kubo, M., & Galambos, T. V., [1988] "Plastic Collapse Load of Continuous Composite Plate Girders," Engineering Journal, AISC, Vol. 25, No. 4, Fourth Quarter.

Kulicki, J. M., & Mertz, D. R., [1991] "A New Live Load Model for Bridge Design," Proceedings of the 8th Annual International Bridge Conference, June.

Leon, R. T., [1997] "Experimental Verification of Shakedown Approaches for Bridge Design," To be published by TRB.

Loveall, C. L., [1986] "Advances in Bridge Design and Construction," Proceedings of the June 12-14, 1986, AISC National Engineering Conference held at Nashville, TN.

Moses, F., Ghosn, M., & Khedekar, N., [1993] "Development of Redundancy Factors for Highway Bridges," Paper No. IBC-93-58, 10th Annual International Bridge Conference held in Pittsburgh, PA, on June 14 to 16.

Moses, F., Schilling, C. G., & Raju, K. S., [1987] "Fatigue Evaluation Procedures for Steel Bridges," NCHRP Report 299, Nov.

Newmark, N. M., [1942] "Numerical Procedure for Computing Deflections, Moments, and Buckling Loads," Proceedings, ASCE, Vol. 68.

Nowak, A. S., & Hong, Y. K., [1991] "Bridge Live-Load Models," Journal of Structural Engineering, ASCE, Vol. 117, No. 9, Sept.

Nowak, A. S., [1993] "Live Load Model for Highway Bridges," Journal of Structural Safety, Vol. 13, No. 1, Jan.

Nowak, A. S., [1995] "Calibration of LRFD Bridge Code," Journal of Structural Engineering, ASCE, Vol. 121, No. 8, Aug.

Ohtake, A., & Iwamuro, F., [1982] "Load-Deformation Characteristics of Light-Gage I-Shaped Members, Part 1," Research Report 6104, Research Institute of Sumitomo Metal Industry, Japan, March, (in Japanese).

Roeder, C. W., & Eltvik, L., [1985] "An Experimental Evaluation of Autostress Design," Transportation Research Record 1044, TRB.

Rotter, J. M., & Ansourian, P., [1979] "Cross-Section Behavior and Ductility in Composite Beams," Proceedings of the Institution of Civil Engineers, London, England, Part 2, Vol. 67, June.

Schilling, C. G., & Morcos, S. S., [1988] "Moment-Rotation Tests of Steel Girders with Ultracompact Flanges," Report on Project 188, AISI, July.

Schilling, C. G., [1984] "Highway Structures Design Handbook, Chapter I/6 - Fatigue, Section III - Fatigue Behavior," United States Steel Corporation, Pittsburgh, PA, Jan.

Schilling, C. G., [1985] "Moment-Rotation Tests of Steel Bridge Girders," Report on Project 188, AISI, April 15.

Schilling, C. G., [1986] "Exploratory Autostress Girder Designs," Report on Project 188, AISI, July.

Schilling, C. G., [1988] "Moment-Rotation Tests of Steel Bridge Girders," Journal of Structural Engineering, ASCE, Vol. 114, No. 1, Jan.

Schilling, C. G., [1989] "A Unified Autostress Method," Report on Project 51, AISI, Nov.

Schilling, C. G., [1989] "Chapter Two - Safety and Serviceability Criteria for Highway Bridges, Bridge Overstress Criteria," Interim Report of FHWA Project, Dept. of Civil Engineering, City College of New York, New York, NY, May.

Schilling, C. G., [1990] "Moment-Rotation Tests of Steel Girders with Ultracompact Flanges," Proceedings of the April 9-11, Conference of the Structural Stability Research Council held in St. Louis, MO.

Schilling, C. G., [1990] "Variable Amplitude Load Fatigue, Task A - Literature Review, Volume I - Traffic Loading and Bridge Response," Publication FHWA-RD-87-059, FHWA, July.

Schilling, C. G., [1991] "Unified Autostress Method," Engineering Journal, AISC, Vol. 28, No. 4, Fourth Quarter.

Schilling, C. G., [1993] "Unified Autostress Method," Transportation Research Record 1380, TRB.

Schilling, C. G., Barker, M. G., Dishongh, B. E., and Hartnagel, B. A., [1997] "Inelastic Design Procedures and Specifications," Final Report submitted to AISI for study on Development and Experimental Verification of Inelastic Design Procedures for Steel Bridges Comprising Noncompact Sections, Jan.

Toridis, T. G., & Wen, R. K., [1966] "Inelastic Response of Beams to Moving Loads," Journal of the Engineering Mechanics Division, ASCE, Vol. 92, No. EM6, Dec.

Unterriener, K. C., [1995] "Moment-Rotation Behavior of Composite and Non-Composite Steel Bridge Girders in Negative Bending," M.S. Thesis Submitted to the Faculty of the University of Missouri, Aug.

Vasseghi, A., & Frank, K. H., [1987] "Static Shear and Bending Strength of Composite Plate Girders," PMFSEL Report No. 87-4, Department of Civil Engineering, University of Texas Austin, TX, June.

Vincent, G. S., [1969] "Tentative Criteria for Load Factor Design of Steel Highway Bridges," Bulletin No. 15, AISI, New York, NY, March.

Weber, D. C., [1994] "Experimental Verification of Inelastic Load and Resistance Factor Design Limits," M.S. Thesis Submitted to the Faculty of the University of Missouri, Aug.

White, D. W., & Dutta, A., [1992] "Numerical Studies of Moment-Rotation Behavior in Steel and Composite Steel-Concrete Bridge Girders," Preprint 921026, 71st Annual Meeting of the TRB held in Washington, DC on Jan. 12-16.

White, D. W., & Dutta, A., [1992] "Numerical Studies of the Inelastic Moment-Rotation Behavior of Non-Compact Bridge Girders," Report CE-STR-92-1, School of Civil Engineering, Purdue University, West Lafayette, IN, Jan.

White, D. W., [1994] "Analysis of the Inelastic Moment-Rotation Behavior on Non-Compact Steel Bridge Girders," Report CE-STR-94-1, School of Civil Engineer, Purdue University, West Lafayette, IN, Feb.

Wright, R. N., & Walker, W. H., [1971] "Criteria for the Deflection of Steel Bridges," Bulletin 19, AISI, Nov.

GLOSSARY

Abutment: An end support for a bridge superstructure.

Actual Rotation Capacity: The plastic rotation corresponding to the plastic moment, or to an effective plastic moment, on the plastic-rotation curve for the section; the plastic-rotation curve is above this plastic moment, or effective plastic moment, for a plastic rotation equal to the actual rotation capacity.

Alternating Plasticity: Yielding in both directions when a section is subjected to large reversals of moments.

Automoment: Moment that develops as a result of local yielding at one or more locations in a continuous-span member and remains after all loading has been removed; this is also called redistribution moment.

Beam: A member whose primary purpose is to support loads applied perpendicular to its length; this term usually refers to rolled shapes.

Beam-Line Method: A method of calculating the redistribution moments and plastic rotations due to yielding at a section by plotting on a single graph the plastic-rotation curve for the section and a straight line defining the angular discontinuity at the section as a function of moment; this is a special case of the unified autostress and residual-deformation methods.

Bending Strength: The maximum bending moment that can be applied to a section without violating applicable specification requirements.

Classical Plastic-Design Assumptions: Assumptions normally made in the plastic design of buildings; the main ones are that plastic rotations are concentrated at single cross sections so that the rest of the structure is elastic and that the total rotation curve for all sections is linear to the plastic moment and thereafter remains at the plastic moment for a sufficient rotation to form a mechanism.

Compact Compression Flange: A compression flange that can sustain sufficient strains so that the entire cross section can be assumed to be at the yield stress when calculating its bending strength; the flange must satisfy specified slenderness and bracing-spacing requirements to qualify as compact.

Compact Section: A section that has a compact web and compression flange; the bending strength of the section is equal to its plastic-moment capacity.

Compact Web: A web that can sustain sufficient bending strains so that the entire cross section can be assumed to be at the yield stress when calculating the bending strength; the web must satisfy a specified slenderness limit to qualify as compact.

Composite Beam or Girder: A steel beam or girder connected to a concrete slab so that the steel element and the slab, and/or the longitudinal rebars within the slab, respond to bending loads as a unit; in positive-bending regions, both the slab and rebars participate in this unit, but in negative-bending regions only the rebars participate.

Compression-Flange Bracing Spacing: Distance between supports resisting lateral deflection of the compression flange.

Conjugate Beam: A conceptual beam used to represent a real bending member when calculating member distortions.

Continuity Relationship: A relationship between the moments at all pier locations in a continuous-span member and the plastic rotations at all yield locations; this relationship is based on the fact that the member must be continuous with all plastic rotations in place and involves the variation of stiffness along the member.

Cracked Section: A composite section in which the slab is assumed to carry no stress because of tensile cracking.

Cross Frame: A transverse truss framework connecting adjacent longitudinal bending members.

Deflection Stability: Stabilization of permanent deflection after progressive increases due to sequential loading; this is also called shakedown.

Deflection-Stability Loading: The highest sequential loading that results in deflection stability; this is also call shakedown loading.

Design: Proportioning and detailing the components and connections of a bridge to satisfy the requirements of specifications.

Design Lane: A width of bridge assumed to carry the full specified truck or lane loading; the width of the design lane may differ from that of the traffic lane.

Diaphragm: A transverse bending member connecting adjacent longitudinal bending members.

Dummy-Load Method: A method of deflection analysis in which the work done by a unit dummy (conceptual) load as a structure deforms due to the actual loading is equated to the internal energy generated by the dummy-load moments to get the deflection at the dummy-load location.

Dynamic Yield Stress or Strain: The yield stress or strain for a given or assumed strain rate; the dynamic yield stress or strain is higher than the static yield stress or strain.

Dynamic Yielding: The time dependence of yielding in a steel member; after any increment of load or deflection imposed in the inelastic range, a short time (usually a few minutes) is required for the resulting deflections and loads to stabilize.

Effective Plastic Moment: The moment corresponding to a specified required rotation on the plastic-rotation curve for the section; the plastic-rotation curve is above this moment for a plastic rotation equal to the required value.

Elastic Analysis: An analysis in which the moments and/or deflections caused by applied loads are calculated without considering yielding.

Elastic Design: Design based on an elastic analysis; in such a design, the elastic moments are sometimes limited to values above the yield moment even though this implies that yielding will occur.

Elastic Moment: Moment from an elastic analysis.

Elastic Moment Envelope: A plot of the maximum positive and negative elastic moments that can occur at all locations along a member as a result of a given sequential loading; this plot is made by successively placing specified live loads at the positions that cause the highest moments at each location and combining these moments with concurrent dead load moments.

Elastic Rotation: An elastic change in slope over a length of member.

Engineer: The engineer directly responsible for the design of the bridge.

Factored Loading: The service live load and/or the nominal dead load times a load factor specified for various load combinations.

Finite-Element Method: A method of analysis in which the structure is discretized into elements connected at nodes, the shape of the element displacement field is assumed, and partial or complete compatibility is maintained among the element interfaces, and nodal displacements are determined by using energy variational principles or equilibrium methods.

Flange Slenderness: One half the width of a flange divided by its thickness.

Girder: A member whose primary purpose is to support loads applied perpendicular to its length; this term usually refers to fabricated members.

Grillage Method: A method of analysis in which all or part of the superstructure is discretized into orthotropic components that represent the characteristics of the structure.

Hybrid Girder: A fabricated steel girder with a web that has a lower specified minimum yield stress than one or both flanges.

Incremental Collapse: A progressive increase without limit of permanent deflection due to sequential loading.

Indeterminate Analysis: An analysis that utilizes stiffness properties to calculate moments that cannot be determined by statics.

Inelastic Analysis: An analysis in which the moments and/or deflections caused by applied loads are calculated by considering yielding.

Inelastic Design: Design based on an inelastic analysis.

Inelastic Lateral Redistribution of Moments: A redistribution of elastic moments among the individual girders in a multigirder bridge due to local yielding at one or more locations in the girders.

Inelastic Redistribution of Moments: A change in the elastic moments in a continuous-span beam or girder due to local yielding at one or more locations; usually the

negative moments at piers are reduced and the positive moments elsewhere are increased.

Inelastic Region: The phase of an analysis that involves yielding.

Lateral Bracing: A truss placed in a horizontal plane between two main members to resist lateral loads and deflections.

Lateral Buckling: Buckling of the compression flange of a bending member by lateral deflection and twist.

Limit State: A design limit related to the usefulness of a structure.

Mechanism: A system of member segments and real and/or plastic hinges that offers no resistance to deformation.

Mechanism Method: A method of calculating the ultimate strength of a beam, girder, or frame in which the loading required to cause each possible mechanism is determined; the lowest loading is the ultimate strength.

Negative-Bending Region: Any length in which the member is subjected to negative moment under the loading condition being considered.

Negative-Bending Section: Any section that is subjected to negative moment under the loading condition being considered; this section may be a positive-bending section under a different loading condition.

Negative Moment: Moment producing tension at the top edge of the member.

Noncompact Compression Flange: A compression flange that does not qualify as compact, but can reach the yield stress without local or lateral buckling; the flange must satisfy specified slenderness and bracing requirements to qualify as noncompact.

Noncompact Section: A section that has a noncompact compression flange and web; the bending strength of the section is usually equal to its yield-moment capacity.

Noncompact Web: A web that does not qualify as compact, but can sustain sufficient bending strain so that the stress in the compression flange can reach the yield stress; the web must satisfy a specified slenderness requirement to qualify as noncompact.

Permanent Deflection: Deflection that remains in a member after all the loading has been removed.

Pier: An interior support for a bridge superstructure.

Plastic Design: A design based on an inelastic analysis; this term usually refers to the classical inelastic procedures used in building design.

Plastic Hinge: A yield location at which the moment is assumed to remain constant at the plastic moment, or the effective plastic moment, while plastic rotation occurs.

Plastic Moment: A moment calculated by assuming that the entire cross section is at the yield stress in either tension or compression; this moment approximates the bending strength of a compact section.

Plastic Rotation: A permanent change in slope that occurs over a length of member due to yielding; usually, the yielding occurs over a short length and is assumed to be concentrated in an angular discontinuity at a single cross section for plastic-design calculations.

Positive-Bending Region: Any length in which the member is subjected to positive moment under the loading condition being considered.

Positive-Bending Section: Any section that is subjected to positive moment under the loading condition being considered; this section may be a negative-bending section under a different loading condition.

Positive Moment: Moment producing tension at the bottom edge of the member.

Proportional Loading: A set of individual concentrated and/or distributed loads applied in specified directions at specified locations and interrelated by specified ratios; the magnitude of the proportional loading is defined by a single factor that applies to all individual loads.

Redistribution Moment: Moment that develops as a result of local yielding at one or more locations in a continuous-span member and remains after all loading has been removed; this is also called automoment.

Reliability Index: A measure of safety equal to the difference between the mean resistance, or strength, and a corresponding mean load effect divided by the combined standard deviation; values of the reliability index correspond to the probabilities of failure as listed below:

Reliability Index	Probability of Failure
0	0.500
1	0.159
2	0.0228
3	0.00135
4	0.0000317

Required Rotation Capacity: The amount of plastic rotation required at a plastic-hinge location to permit formation of a mechanism involving that hinge; no plastic rotation is required at the last hinge to form.

Residual-Deformation Method: An inelastic method of calculating the redistribution moments and permanent deflections by satisfying continuity and rotation relationships at yield locations; the unified autostress method utilizes these same relationships, but different computational procedures.

Residual Stress: Internal stress created during the manufacture, fabrication, or subsequent loading of a member; such stresses are in equilibrium at each cross section.

Rotation Curve: A plot of applied moment vs. the plastic, elastic, or total rotation over a length of member.

Rotation Relationship: A relationship between the total moment (elastic moment plus redistribution moment) and plastic rotation at a section; this is the plastic-rotation curve for the section.

Sequential Loading: A series of proportional loadings applied sequentially in any order including repeats of some or all of the individual loadings; the magnitude of the sequential loading is defined by a single factor that applies to all individual loads.

Shakedown: Stabilization of permanent deflection after progressive increases due to sequential loading; this is also called deflection stability.

Shakedown Loading: The highest sequential loading that results in shakedown; this is also called deflection-stability loading.

Shape Factor: Ratio of the plastic moment to the yield moment.

Slab: The concrete deck of a bridge superstructure.

Slope-Deflection Method: A method of deflection analysis in which equations that interrelate the slopes and moments at the ends of a beam segment are used to calculate deflections and angular discontinuities.

Static Yield Stress or Strain: The yield stress or strain corresponding to a zero strain rate; these quantities are determined from a tensile test by stopping the imposed deformation several times within the inelastic range and allowing the stress and deformation to stabilize after each stop.

Statical Method: A method of calculating the strength of a mechanism by treating the portion of the member within the mechanism as a simple span, applying the known plastic moments at both ends, and varying the applied loads and corresponding moment diagram to make the combined moments equal to the plastic moment at the critical location within the span.

Stress Range: The algebraic difference between the extreme values in a stress cycle.

Three-Moment Equation: An equation that interrelates the moments and slopes at three adjacent supports of a continuous-span member and can be used in an indeterminate analysis.

Total Rotation: The sum of the elastic and plastic rotations that occur over a length of member.

Traffic Lane: A width of bridge designated to carry one lane of traffic and marked on the bridge.

Ultimate Strength: The highest proportional loading that can be carried by a member.

Uncracked Section: A composite section in which the slab is assumed to be fully effective because no tensile cracking has occurred.

Unified Autostress Method: An inelastic method of calculating the redistribution moments and permanent deflections due to a given stationary or sequential loading by satisfying continuity and rotation relationships at yield locations; the residual-deformation method utilizes these same relationships, but different computational procedures.

Web Slenderness: Twice the depth of the web in compression divided by the web thickness.

Yield Moment: The lowest moment that causes yielding in a section if residual stresses are ignored; for composite sections, it is the sum of moments applied before and after the slab has hardened to cause yielding in a steel flange.

Yield Strain: The strain corresponding to the yield stress.

Yield Stress or Strain: The lowest stress or strain at which yielding occurs if residual stresses are ignored.

APPENDIX - PROPOSED LRFD INELASTIC DESIGN SPECIFICATIONS

6.10.11 Inelastic Analysis Procedures

6.10.11.1 GENERAL

6.10.11.1.1 Scope

Inelastic analysis procedures shall apply only to composite or non-composite continuous-span I-section members that have a specified minimum yield strength not exceeding 50 KSI.

C6.10.11.1.1

Development of these new inelastic provisions is documented in a comprehensive report, Schilling, et al, (1997). The new provisions apply to both compact and non-compact sections and are simpler than the previous (1994) provisions. They utilize elastic moment envelopes and do not require successive loadings, iterative procedures, or simultaneous equations. At present (1997), inelastic procedures are not permitted for steels with yield strengths exceeding 50 KSI because sufficient research on inelastic behavior of girders of such steels has not yet been conducted.

6.10.11.1.2 Web Slenderness

The web slenderness of all sections shall satisfy:

$$\frac{2D_c}{t_w} \le 6.77\sqrt{\frac{E}{F_{yc}}} \qquad (6.10.11.1.2\text{-}1)$$

where:

D_c = depth of web in compression for elastic moment (IN)

F_{yc} = specified minimum yield strength of compression flange (KSI)

t_w = web thickness (IN)

C6.10.11.1.2

This is the maximum web slenderness permitted in Article 6.10.5.3.2b for webs without longitudinal stiffeners. Sufficient information to permit inelastic design of girders with longitudinal stiffeners is not available.

6.10.11.1.3 Compression Flange Slenderness

The compression flange slenderness at all sections shall satisfy:

$$\frac{b_c}{2t_c} \le 0.408\sqrt{\frac{E}{F_{yc}}} \qquad (6.10.11.1.3\text{-}1)$$

where:

b_c = compression flange width (IN)

t_c = compression flange thickness (IN)

C6.10.11.1.3

This is the maximum compression flange slenderness permitted for non-compact sections in Article 10.48.2.1 of the previous bridge specifications, AASHTO (1992). The inelastic behavior of girders with compression flange slenderness ratios exceeding this limit has not been adequately investigated.

6.10.11.2 STRENGTH LIMIT STATE

6.10.11.2.1 Flexural Resistance

Unless the alternative requirements of Article 6.10.11.2.5 are satisfied, the factored flexural resistance of all sections shall be taken as:

$$M_r = \phi_{sd} M_{pe} - M_{rd} \qquad (6.10.11.2.1\text{-}1)$$

where:

ϕ_{sd} = resistance factor for shakedown specified in Article 6.5.4.2

M_{pe} = effective plastic moment specified in Article 6.10.11.2.3 or 6.10.11.2.4 (K-IN)

M_{rd} = redistribution moment specified in Article 6.10.11.2.2 (K-IN)

C6.10.11.2.1

This provision assures that the girder will shakedown to an equilibrium condition after repeated passages of the factored live loads in combination with the factored dead load, Schilling, et al, (1997). Repeated passages of heavier loads would theoretically cause incremental collapse, that is, progressively increasing permanent deflections, ASCE (1971). Thus, shakedown is the appropriate strength requirement for bridges subject to moving loads, Galambos, et al, (1993).

A resistance factor of 1.1 is justified for this limit state because the shakedown loading is generally lower than the ultimate strength and because the progressively increasing permanent deflections give ample warning of pending failure, Schilling, et al, (1997).

For composite sections, the total moment due to factored loadings applied before and after the slab has hardened must not exceed M_r.

6.10.11.2.2 Redistribution Moment

6.10.11.2.2a At Interior Supports

At each interior support, the redistribution moment shall be taken as:

$$M_{rd} = \phi_{sd} M_{pe} - M_e \geq 0 \qquad (6.10.11.2.2a\text{-}1)$$

where:

ϕ_{sd} = resistance factor for shakedown specified in Article 6.5.4.2

M_{pe} = negative-flexure effective plastic moment specified in Article 6.10.11.2.3 (K-IN)

M_e = elastic moment at interior support due to the factored loading (K-IN)

C6.10.11.2.2a

The redistribution moments, sometimes called automoments, are caused by yielding at peak-moment locations and remain if all loading is removed. At interior supports, the redistribution moments are equal to the difference between the plastic moment capacity of the section and the elastic moment.

For composite sections, this elastic moment is the total due to loadings applied before and after the slab has hardened.

The redistribution moments are always positive.

6.10.11.2.2b At All Other Sections

The full redistribution-moment diagram shall be determined by connecting the moments at interior supports with straight lines and extending these lines from the first and last interior supports to points of zero moment at adjacent abutments.

C6.10.11.2.2b

After all loading has been removed from the girder, redistribution moments are held in equilibrium by the reactions. Therefore, redistribution moments must vary linearly between supports.

6.10.11.2.3 Effective Plastic Moment for Negative Flexure

6.10.11.2.3a Ultra-compact Compression Flange Sections

For sections that satisfy:

$$\frac{b_c}{2t_c} \le 0.291\sqrt{\frac{E}{F_{yc}}} \qquad (6.10.11.2.3a\text{-}1)$$

If $\frac{2D_{cp}}{t_w} \le 3.76\sqrt{\frac{E}{F_{yc}}}$, then:

$$M_{pe} = M_p \qquad (6.10.11.2.3a\text{-}2)$$

If $3.76\sqrt{\frac{E}{F_{yc}}} < \frac{2D_{cp}}{t_w} \le 5.05\sqrt{\frac{E}{F_{yc}}}$, then:

$$M_{pe} = R_h M_y \qquad (6.10.11.2.3a\text{-}3)$$

If $\frac{2D_{cp}}{t_w} > 5.05\sqrt{\frac{E}{F_{yc}}}$, then:

$$M_{pe} = \left[1.56 - 0.111\left(\frac{2D_{cp}}{t_w}\right)\sqrt{\frac{F_{yc}}{E}}\right] R_h M_y \qquad (6.10.11.2.3a\text{-}4)$$

where:

b_c = compression flange width (IN)

t_c = compression flange thickness (IN)

D_{cp} = depth of web in compression at the plastic moment specified in Article 6.10.5.1.4b or 6.10.6.1.2 (IN)

t_w = web thickness (IN)

F_{yc} = specified minimum yield strength of the compression flange (KSI)

M_y = yield moment specified in Article 6.10.5.1.2 or 6.10.6.1.1 (K-IN)

M_p = plastic moment specified in Article 6.10.5.1.3 or 6.10.6.1.1 (K-IN)

M_{pe} = effective plastic moment (K-IN)

R_h = hybrid flange-stress reduction factor specified in Article 6.10.5.4.1c

C6.10.11.2.3a

Test showed that girders with ultra-compact compression flanges satisfying Equation 6.10.11.2.3a-1, and with transverse stiffeners near the peak-moment location, provide good rotation characteristics even if the web is non-compact, Schilling and Morcos, (1988). Therefore, this type of section is efficient for inelastic designs.

An equation defining M_{pe}/M_{max} for a plastic rotation of 30 MRAD as a function of the web slenderness was developed from the test results and was combined with equations defining M_{max} to get Equations 6.10.11.2.3a-2 to 4, Schilling, et al, (1997). A plastic rotation of 30 MRAD is considered sufficient to allow shakedown, Schilling, et al, (1997).

Equations 6.10.11.2.3a-2 to 4 generally provide higher values of M_{pe} than the procedures specified in Article 6.10.11.2.3b for sections without ultra-compact compression flanges and transverse stiffeners near interior supports.

Transverse stiffeners are required near interior supports, but not near negative-flexure splices because smaller rotation capacities are required at the splice locations.

If the effective plastic moment at an interior support is determined from Equation 6.10.11.2.3a-2, 6.10.11.2.3a-3, or 6.10.11.2.3a-4, a transverse stiffener shall be placed a distance of one-half the web depth on each side of that support. If the stiffeners are placed on only one side of the web, they shall be welded to the compression flange.

6.10.11.2.3b All Other Sections

The effective plastic moment shall be calculated as specified in Article 6.10.5.1.3 or 6.10.6.1.1 using the following effective yield strengths:

$$F_{yec} = 0.0845E(2t_c/b_c)^2 \le F_{yc} \qquad (6.10.11.2.3b\text{-}1)$$

$$F_{yet} = F_{yec} \le F_{yt} \qquad (6.10.11.2.3b\text{-}2)$$

$$F_{yew} = 5.28E\left(t_w/2D_{cp}\right)^2 \le F_{yw} \qquad (6.10.11.2.3b\text{-}3)$$

$$F_{yer} = F_{yr} \qquad (6.10.11.2.3b\text{-}4)$$

where:

F_{yc} = specified minimum yield strength of the compression flange (KSI)

F_{yec} = effective yield strength of the compression flange (KSI)

F_{yt} = specified minimum yield strength of the tension flange (KSI)

F_{yet} = effective yield strength of the tension flange (KSI)

F_{yw} = specified minimum yield strength of the web (KSI)

F_{yew} = effective yield strength of the web (KSI)

F_{yr} = specified minimum yield strength of the longitudinal reinforcement (KSI)

F_{yer} = effective yield strength of the longitudinal reinforcement (KSI)

t_c = compression flange thickness (IN)

b_c = compression flange width (IN)

t_w = web thickness (IN)

D_{cp} = depth in web in compression at the

C6.10.11.2.3b

The specified empirical procedures for calculating the effective plastic moment were originally developed for compact sections, Grubb and Carskaddan (1981) and Haaijer, et al, (1987). It was later shown that these procedures could also be applied to non-compact sections and provide a plastic rotation capacity of at least 30 MRAD, which is considered sufficient to develop shakedown, Schilling, et al, (1997).

A section is fully effective and $M_{pe}=M_p$ if:

$$\frac{b_c}{2t_c} \le 0.291\sqrt{\frac{E}{F_{yc}}} \qquad (C6.10.11.2.3b\text{-}1)$$

and

$$\frac{2D_{cp}}{t_w} \le 2.30\sqrt{\frac{E}{F_{yw}}} \qquad (C6.10.11.2.3b\text{-}2)$$

plastic moment specified in Article 6.10.5.1.4b or 6.10.6.1.2 (IN)

6.10.11.2.4 Effective Plastic Moment for Positive Flexure

6.10.11.2.4a Composite Sections

Composite sections in positive flexure shall satisfy:

$$\frac{2D_{cp}}{t_w} \le 3.76\sqrt{\frac{E}{F_{yc}}} \qquad (6.10.11.2.4a\text{-}1)$$

For such sections:

$$M_{pe} = M_p \qquad (6.10.11.2.4a\text{-}2)$$

where:

M_{pe} = effective plastic moment (K-IN)

M_p = plastic moment specified in Article 6.10.5.1.3 (K-IN)

C6.10.11.2.4a

Composite sections in positive flexure are compact if they satisfy the specified web slenderness requirement since the compression flange is supported by the deck slab. For such compact sections, the plastic-rotation capacity at M_p is sufficient to permit the development of shakedown since considerably less rotation capacity is required in positive flexural regions than at interior supports.

Most composite sections in positive flexure easily satisfy the specified web slenderness requirement because only a small portion of the web is in compression.

6.10.11.2.4b Non-composite Sections

The effective plastic moment shall be calculated as specified in Article 6.10.11.2.3b.

6.10.11.2.5 Alternative Procedure

6.10.11.2.5a General

Unless the requirements of Article 6.10.11.2.1 are satisfied, a rigorous inelastic analysis shall be performed on the member; if a solution can be found, the member shall be considered to satisfy the strength limit state.

C6.10.11.2.5a

The unified autostress method, Schilling (1993), and the residual deformation method, Dishongh and Galambos (1992), are acceptable methods of inelastic analysis for bridges. These methods will not provide a valid solution if the shakedown loading is exceeded; therefore, a girder satisfies the strength limit state if a solution can be found for the specified factored loading, Schilling, et al, (1997).

6.10.11.2.5b Elastic Moment Envelope

The elastic moment envelope for the factored loading shall be used in the analysis.

C6.10.11.2.5b

If the elastic moment envelope, instead of the moment diagram for a particular loading, is used in the inelastic analysis, the solution gives the permanent deflections and redistribution moments after repeated passages of the live load across the bridge and, therefore, checks shakedown, Schilling, et al, (1997).

6.10.11.2.5c Continuity Relationship

In the analysis, a continuity relationship that interrelates the moments at all interior supports with the plastic rotations at all yield locations shall be satisfied at each interior support.

6.10.11.2.5d Rotation Relationship

In the analysis, the moment and corresponding plastic rotation at each yield location shall fall on the factored plastic-rotation curve for the section at that location. The factored curve shall be obtained by increasing the moments in the unfactored curve by the factor ϕ_{sd} specified in Article 6.5.4.2.

6.10.11.2.6 Compression Flange Bracing

In negative flexural regions:

$$L_b \le \left[0.124 - 0.0759\left(\frac{M_l}{M_h}\right)\right]\left[\frac{r_y E}{F_{yc}}\right] \qquad (6.10.11.2.6\text{-}1)$$

$$M_t = M_e + M_{rd} \qquad (6.10.11.2.6\text{-}2)$$

where:

L_b = unbraced length (IN)

r_y = minimum radius of gyration of the steel section, with respect to the vertical axis in the plane of the web, within the unbraced length (IN)

M_t = total moment calculated for the factored loading by inelastic procedures (K-IN)

M_e = elastic moment due to the factored loading (K-IN)

M_{rd} = redistribution moment specified in Article 6.10.11.2.2 (K-IN)

M_l = value of M_t at the lower-moment end of the unbraced length (K-IN)

M_h = value of M_t at the higher-moment end of the unbraced length (K-IN)

F_{yc} = specified minimum yield strength of the compression flange at the section

C6.10.11.2.5c

Possible yield locations include peak-moment locations, splice locations, and cover-plate end locations.

C6.10.11.2.5d

Typical rotation curves for various types of sections have been developed from test results, Schilling, et al, (1997). More-refined curves that more precisely account for various pertinent parameters are being developed from sophisticated computer analyses and further tests, White (1994) and Barth, et al, (1994).

Typical rotation curves must be scaled by ϕ_{sd} to be consistent with the simplified design approach specified in Article 6.10.11.2.1.

C6.10.11.2.6

This lateral buckling equation was included in the previous (1994) inelastic provisions and is also applied to compact sections in elastic design as specified in Article 6.10.5.2.3d. M_{rd} is always positive and therefore subtracts from M_e in negative flexural regions.

A check of compression flange bracing is not required in positive flexural regions because it is assumed that the deck provides adequate support to that flange.

where r_y is calculated (KSI)

The ratio M_l/M_h shall be taken as negative if the portion of the member within the unbraced length is bent in reverse curvature.

6.10.11.2.7 Bearing Stiffeners

A bearing stiffener designed by the provisions of Article 6.10.8.2 shall be placed at each interior support.

6.10.11.2.8 Wind Effects on Girder Flanges

If the girder flanges are designed to transfer wind loads according to the provisions of Article 4.6.2.7, the provisions of Article 6.10.5.7.1 shall apply.

C6.10.11.2.8

Article 6.10.5.7.1 specifies that the portion of the flange required to carry lateral wind loading be deducted from that available to carry vertical loadings.

6.10.11.2.9 Shear Resistance

The shear resistance specified in Article 6.10.7 shall apply. In Article 6.10.7.3.3a, M_u shall be taken as:

$$M_u = M_e + M_{rd} \qquad (6.10.11.2.9\text{-}1)$$

where:

M_u = maximum moment in the panel under consideration after inelastic redistribution of moments (K-IN)

M_e = elastic moment in the panel under consideration due to the factored loading (K-IN)

M_{rd} = redistribution moment in the panel under consideration specified in Article 6.10.11.2.2 (K-IN)

C6.10.11.2.9

The shear resistance for inelastic design is the same as that for elastic design except that moments used in the interaction relationships for combined moment and shear must be those occurring after inelastic redistribution of moments.

M_{rd} is always positive and, therefore, subtracts from M_e in negative flexural regions and adds M_e in positive flexural regions.

6.10.11.3 SERVICE LIMIT STATE CONTROL OF PERMANENT DEFLECTION

6.10.11.3.1 Loading

Load combination Service II in Table 3.4.1-1 shall apply.

6.10.11.3.2 Stress Limit

6.10.11.3.2a At Interior Supports

The stresses in negative flexural lengths of the girder extending from each interior support to the nearest splice location or point of dead-load contra-flexure, whichever is closest, on

C6.10.11.3.2a

In the inelastic permanent-deflection check, yielding is permitted at interior supports and results in redistribution of moments. Permanent deflections are controlled by

both sides of the support shall not be limited.

6.10.11.3.2b At All Other Locations

Unless the alternative requirements of Article 6.10.11.3.5 are satisfied, the stresses in both steel flanges at all other locations due to the factored loadings shall satisfy:

$$|f_{ef} + f_{rd}| \le |\alpha R_h F_{yf}| \qquad (6.10.11.3.2b\text{-}1)$$

where:

f_{ef} = elastic stress in the flange due to the factored loading (KSI)

f_{rd} = redistribution stress in the flange due to the redistribution moment specified in Article 6.10.11.3.3; for composite sections, the redistribution moment shall be applied to the short-term composite section (KSI)

R_h = flange-stress reduction factor specified in Article 6.10.5.4.1

F_{yf} = specified minimum yield strength of the flange (KSI)

α = 0.95 for composite sections and 0.80 for non-composite sections

6.10.11.3.3 Redistribution Moment

6.10.11.3.3a At Interior Supports

At each interior support, the redistribution moment shall be:

$$M_{rd} = M_{pe} - M_e \ge 0 \qquad (6.10.11.3.3a\text{-}1)$$

where:

M_{pe} = effective plastic moment specified in Article 6.10.11.3.4 (K-IN)

M_e = elastic moment at the interior support due to the factored loading (K-IN)

6.10.11.3.3b At All Other Locations

The full redistribution-moment diagram shall be determined by connecting the moments at interior supports by straight lines and extending these lines from the first and last interior supports to points of zero moment at adjacent abutments.

imposing stress limits at positive flexural sections after redistribution of moments has occurred.

C6.10.11.3.2b

This article limits the positive flexural stresses after redistribution of moments to the same percentages of the yield strength as are applied in the elastic permanent-deflection check. It also conservatively applies these limits at splice locations in negative flexural regions.

For composite sections, f_{ef} is the total for factored loadings applied before and after the slab has hardened. f_{rd} has the same sign as f_{ef} in positive flexural regions, but the opposite sign in negative flexural regions.

C6.10.11.3.3a

Redistribution moments are caused by yielding at interior supports as discussed in Article C6.10.11.2.2a.

C6.10.11.3.3b

Redistribution moments vary linearly between supports as discussed in Article C6.10.11.2.2b.

6.10.11.3.4 Effective Plastic Moment at Interior Supports

6.10.11.3.4a Compact Sections or Ultra-compact Compression Flange Sections

For ultra-compact compression flange sections satisfying the requirements of Equation 6.10.11.2.3a-1 or compact sections satisfying the requirements of Article 6.10.5.2.3 or 6.10.6.2:

$$M_{pe} = M_p \qquad (6.10.11.3.4a\text{-}1)$$

where:

M_{pe} = effective plastic moment (K-IN)

M_p = plastic moment specified in Article 6.10.5.1.3 or 6.10.6.1.1 (K-IN)

C6.10.11.3.4a

Compact sections, and ultra-compact compression flange sections, can reach the full plastic moment and sustain sufficient plastic rotation to allow the amount inelastic redistribution of moments required at this limit state, which is conservatively taken as 9 MRAD, Schilling, et al, (1997).

6.10.11.3.4b All Other Sections

$$M_{pe} = 0.8R_hM_y \qquad (6.10.11.3.4b\text{-}1)$$

where:

M_y = yield moment specified in Article 6.10.5.1.2 or 6.10.6.1.1 (K-IN)

R_h = flange-stress reduction factor specified in Article 6.10.5.4.1

C6.10.11.3.4b

Experimental data show that the effective plastic moment corresponding to a plastic rotation of 9 MRAD can be conservatively taken as $0.8M_y$ for non-compact sections, Schilling (1988) and Schilling, et al, (1997).

6.10.11.3.5 Alternative Procedure

Unless the requirements of Article 6.10.11.3.2b are satisfied, a rigorous inelastic analysis shall be performed on the member as specified in Article 6.10.11.2.5 and:

$$\delta \le \frac{L}{300} \qquad (6.10.11.3.5\text{-}1)$$

where:

δ = maximum permanent deflection within a span due to the factored loading (IN)

L = length of that span (IN)

C6.10.11.3.5

The specified limit is the maximum above which the permanent deflection becomes visually noticeable, Galambos and Ellingwood (1986), and was suggested as the highest limit suitable for inelastic rating, Galambos, et al, (1993).

In the analysis, unfactored rotation curves could be used instead of the factored curves specified in Article 6.10.11.2.5d since ϕ is usually taken as 1.0 for service limit states. Using the unfactored curves, however, is less conservative than using the factored curves.